

UNCLASSIFIED

AD NUMBER

AD881749

LIMITATION CHANGES

TO:

Approved for public release; distribution is unlimited.

FROM:

Distribution authorized to U.S. Gov't. agencies and their contractors; Critical Technology; 31 JUL 1970. Other requests shall be referred to Air Force Flight Dynamics Laboratory, FDV, Wright-Patterson AFB, OH 45433. This document contains export-controlled technical data.

AUTHORITY

affdl ltr, 22 dec 1971

THIS PAGE IS UNCLASSIFIED

AD881749

AFFDL-TR-70-124

10.
CPD

Boeing Company
Vertol Division

Final Report, Phase II

DETAIL DESIGN OF CRITICAL COMPONENTS
FOR A
PROP/ROTOR AIRCRAFT

TECHNICAL REPORT AFFDL-TR-70-124

JULY 1970

DAVID A. RICHARDSON
JAAN LIIVA
RICHARD R. PRUYN, et al

DDC
RECEIVED
MAR 26 1971
RECEIVED
A

AD No
DDC FILE COPY

This document is subject to special export controls and each transmittal to foreign governments or foreign nationals may be made only with prior approval of AFFDL (FDV), Wright-Patterson Air Force Base, Ohio 45433.

AIR FORCE FLIGHT DYNAMICS LABORATORY
AIR FORCE SYSTEMS COMMAND
WRIGHT-PATTERSON AIR FORCE BASE, OHIO

390

NOTICE

When Government drawings, specifications, or other data are used for any purpose other than in connection with a definitely related Government procurement operation, the United States Government thereby incurs no responsibility nor any obligation whatsoever; and the fact that the Government may have formulated, furnished, or in any way supplied the said drawings, specifications, or other data, is not to be regarded by implication or otherwise as in any manner licensing the holder or any other person or corporation, or conveying any rights or permission to manufacture, use, or sell any patented invention that may in any way be related thereto.

This document is subject to export controls and each transmittal to foreign governments or foreign nationals may be made only with prior approval of AFFDL (FDV), Wright-Patterson Air Force Base, Ohio 45433.

Copies of this report should not be returned unless return is required by security considerations, contractual obligations, or notice on a specific document.

APPROVED FOR	
DATE	
BY	
REASON	
REMARKS	
2	

DETAIL DESIGN OF CRITICAL COMPONENTS
FOR A
PROP/ROTOR AIRCRAFT

DAVID A. RICHARDSON
JAAN LIIVA
RICHARD R. PRUYN, ET AL

Details of illustrations in
this document may be better
studied on microfiche



FOREWORD

This report was prepared by The Boeing Company, Vertol Division, Philadelphia, Pennsylvania for the Air Force Flight Dynamics Laboratory, Wright-Patterson Air Force Base, Ohio under contract F33615-69-C-1570, Project No. 698BT, "US/FRG V/STOL Technology Program". This contract is for a multiphase effort of parametric studies, detail design, model tests and analyses. This report only covers Phase II, detail design of critical prop/rotor components. Phase I, configuration design analysis, was reported in AFFDL-TR-70-44. The effort was terminated on completion of Phase II.

The contract was administered by the Air Force Flight Dynamics Laboratory with Mr. Daniel E. Fraga (FDV) as project engineer. This report covers the Phase II work conducted from 15 August 1969 to 31 July 1970, Boeing Document No. D215-10001-1.

The principal investigators for The Boeing Company were Mr. David A. Richardson and Mr. Jaan Liiva. Acknowledgement is made of the following contributors to this report: Mr. R. R. Pruyn, Mr. R.W. Sandford, Mr. G. Miliziano, Mr. F. Renola, Mr. D. G. Prichard, Mr. N. Miller and Mr. L. DeLarm in Technology and Mr. N. Weir and Mr. K. Smith in Design.

This technical report has been reviewed and is approved.



ERNEST J. CROSS, JR.
Lt. Colonel, USAF
Chief, V/STOL Technology Division

ABSTRACT

Detail design studies of critical prop/rotor aircraft components are summarized in this interim report as a second phase of the four-phase USAF Contract F33615-69-C-1570. The program objective is to determine design criteria and demonstrate the adequacy of technology by designing a full-scale prop/rotor aircraft and by designing, manufacturing and testing scaled models. Thirty percent of the weight empty components of the aircraft consisting of the wing, nacelle support and tilt mechanism, nacelle truss, prop/rotor hub, controls and blades has been designed in this phase. The weight empty of the aircraft has decreased by one to five percent from the target value established in the Phase I studies. Weight increases in the nacelle and tilting mechanism components were offset by substantial weight decreases in the rotor and hub components. Supporting technology studies in the areas of stability and control and aeroelastic stability requirements are also included. Discussed are the primary control system, rotor feedback system and power management system and aircraft flutter and vibration suppression considerations.

TABLE OF CONTENTS

<u>SECTION</u>		<u>PAGE</u>
I.	INTRODUCTION	I-1
II.	SUMMARY	II-1
III.	GENERAL STRUCTURAL CRITERIA	III-1
	1. Introduction	III-1
	2. Flight Mode Definition	III-1
	3. Basic Design Parameters	III-1
	4. Factor of Safety	III-3
	5. Rotor Torque Factor	III-3
	6. Airplane Flight Design Speed	III-3
	7. V-n Diagram	III-3
	8. Limit Load Design Conditions	III-6
	9. Hover Control Requirements	III-6
	10. Fatigue Design Considerations	III-6
	11. Material Allowables	III-11
IV.	WING DESIGN	
	1. Introduction	IV-1
	2. Objective	IV-2
	3. Design Criteria	IV-2
	4. Wing Geometry	IV-5
	5. Description of Wing Primary Structure	IV-6
	5.1 Wing-Nacelle Attachment Structure	IV-17
	5.2 Wing Associated Systems	IV-17

SECTIONPAGE

5.2.1	Fuel System (A)	IV-23
5.2.2	Fuel System (B)	IV-23
5.2.3	Cross Shafting	IV-26
6.	Structural Analysis	IV-28
6.1	Design Loads	IV-29
6.2	Stress Analysis	IV-29
6.2.1	Load Paths	IV-29
6.2.2	Material Selection	IV-33
6.2.3	Wing Structure Summary	IV-33
6.3	Wing Stiffness and Deflections	IV-33
7.	Weight Analysis	IV-37
7.1	Basic Wing Weight	IV-41
7.2	Wing Tip and Nacelle Support	IV-47
7.3	Provisions for Wing Tip Attachment	IV-47
8.	Survivability	IV-49
9.	Conclusions and Recommendations	IV-49
V.	ROTOR NACELLE AND TILTING MECHANISM DESIGN	
1.	Introduction	V-1
2.	Objective	V-7
3.	Design Criteria	V-7
4.	Nacelle Geometry	V-9
5.	Nacelle and Actuating System Design Description	V-9
5.1	Wing-Nacelle Attachment Structure	V-9
5.1.1	Wing-Nacelle Attachment System A	V-9
5.1.2	Wing-Nacelle Attachment System B	V-12
5.2	Actuator System Design	V-12
5.2.1	Actuator Design A	V-12
5.2.2	Actuator Design B	V-16
5.3	Space Frame Primary Structure Design	V-16
6.	Structural Analysis	V-17

SECTION

PAGE

6.1	Design Loads	V-17
6.2	Material Selection	V-17
6.3	Stress Analysis	V-27
6.3.1	Wing-Nacelle Attachment Stress	V-27
6.3.2	Tilt Actuator Stress	V-27
6.3.3	Nacelle Primary Structure Stress	V-29
7.	Weight Analysis	V-29
7.1	Wing Tip and Nacelle Support Weight	V-35
7.2	Nacelle Tilt Actuator Weight	V-35
7.3	Nacelle Primary Structure Weight	V-36
8.	Survivability	V-36
9.	Conclusions and Recommendations	V-37
VI.	ROTOR BLADE DESIGN	
1.	Introduction	VI-1
2.	Objective	VI-1
3.	Design Criteria	VI-1
3.1	Dynamics	VI-1
3.2	Design Conditions	VI-2
4.	Rotor Geometry	VI-4
5.	Rotor Blade Design Description	VI-4
5.1	Introduction	VI-4
5.2	Design Description of Root Retention and Spar Assembly	VI-6
5.2.1	Root Retention	VI-6
5.2.2	Spar	VI-15
5.2.3	Failure Detection	VI-15
5.3	Design Description of Blade Fairing and Balance Provisions	VI-19
5.3.1	Blade Sections	VI-19
5.3.2	Core Assemblies	VI-19
5.3.3	Nose Balance Weights	VI-19
5.3.4	Tip Hardware	VI-20
5.3.5	Leading Edge Erosion Strip	VI-20
5.3.6	Material Selection	VI-20
6.	Structural Analysis	VI-21

SECTIONPAGE

6.1	Preliminary Calculation of Root Flexure Properties	VI-21
6.2	Rotor Blade Physical Properties	VI-25
6.3	Rotor Blade Natural Frequency Calculation and Flutter Evaluation	VI-25
6.3.1	Stall Flutter	VI-32
6.3.2	Conventional Flutter	VI-32
6.4	Rotor Blade Loads Calculation	VI-37
6.4.1	Required Aircraft Trim and Inertia Moments	VI-37
6.4.2	Required Rotor Forces and Moments	VI-38
6.4.3	Rotor Hub Forces and Moments Produced by Cyclic Pitch	VI-39
6.4.4	Ultimate Loads	VI-41
6.5	Stress Analysis	VI-51
6.5.1	Rotor Blade Loads and Stresses	VI-51
7.	Weight Analysis	VI-63
8.	Survivability	VI-69
9.	Conclusions and Recommendations	VI-69
VII.	ROTOR HUB AND CONTROLS DESIGN	
1.	Introduction	VII-1
2.	Objective	VII-1
3.	Design Criteria	VII-1
4.	Description of Rotor Hub Assembly	VII-2
4.1	Introduction	VII-2
4.2	Hub Assembly	VII-3
4.3	Rotor Controls	VII-9
4.3.1	Swashplate Assembly	VII-9
4.3.2	Rotor Control Actuators	VII-17
4.4	Lubrication	VII-18
4.5	Spinner Assembly	VII-19
5.	Structural Analysis	VII-20
5.1	Introduction	VII-20
5.2	Design Loads	VII-20
5.3	Stress Analysis of Blade Retention	VII-20
5.3.1	Blade Retention Components	VII-20
5.3.2	Blade Root Assembly C.F. Stresses	VII-20

<u>SECTION</u>	<u>PAGE</u>
5.3.3 Blade Root Assembly Socket Analysis	VII-28
5.3.4 Spar Root Stress	VII-30
5.3.5 Elastomeric Bearing Analysis	VII-34
5.3.6 Tie Bar Analysis	VII-37
5.3.7 Blade Root Torsion Reaction	VII-39
5.4 Stress Analysis of Hub Assembly	VII-46
5.4.1 Introduction	VII-46
5.4.2 Pitch Change Bearing Analysis	VII-46
5.4.3 Hub Mounting to Transmission Ring Analysis	VII-52
5.4.4 Spider Fitting Analysis	VII-59
5.5 Rotor Control System Stress Analysis	VII-69
5.6 Material Selection	VII-69
5.6.1 Hub Assembly	VII-69
5.6.2 Rotor Controls	VII-69
6. Weight Analysis	VII-70
6.1 Hub Assembly	VII-70
6.2 Rotor Controls	VII-70
7. Survivability	VII-73
8. Conclusions and Recommendations	VII-73
 VIII. SUPPORTING TECHNOLOGY	
1. Summary	VIII-1
2. Flight Control Requirements	VIII-2
2.1 Criteria	VIII-2
2.2 Control System	VIII-3
2.2.1 Description	VIII-3
2.2.2 Control Response and Power	VIII-3
2.3 Dynamic Stability	VIII-8
2.3.1 Introduction	VIII-8
2.3.2 Stability Derivatives	VIII-8
2.3.3 Results of the Stability Analysis in Hover	VIII-8
2.3.4 Results of Stability Analysis for Low-Speed Flight	VIII-13
2.4 Gust and Turbulence Response	VIII-13
2.5 Control Mixing in Transition	VIII-19
2.6 Power Management System	VIII-22
2.7 Wing Torsional Effects	VIII-25
2.8 Rotor Feedback System	VIII-25
3. Aeroelastic Stability	VIII-28

SECTION

PAGE

3.1 Whirl Flutter	VIII-28
3.2 Air/Ground Resonance	VIII-36
3.3 Classical Flutter	VIII-39
3.4 Stall Flutter	VIII-39
3.5 Pitch-Lag Stability	VIII-40
4. Vibration Suppression Considerations	VIII-40

REFERENCES

APPENDIX 1

APPENDIX 2

LIST OF ILLUSTRATIONS

<u>FIGURE</u>		<u>PAGE</u>
I-1	Boeing Model 215 USAF 5-Ton Payload Tilt Rotor Transport	I-3
III-1	V-n Diagram for Sea Level, Basic Design Gross Weight	III-4
III-2	V-N Diagram for Sea Level, Minimum Flying Gross Weight	III-5
IV-1	Model 215 Wing Plan View	IV-7
IV-2	Model 215 Wing Airfoil Geometry	IV-9
IV-3	Model 215 Wing Hinge and Closure Rib	IV-11
IV-4	Model 215 Wing-Fuselage Splice	IV-13
IV-5	Model 215 Wing Splice Rib and Access Door	IV-15
IV-6	Model 215 Wing Flight Control Layout	IV-16
IV-7	Model 215 Wing-Nacelle Attachment Beam	IV-21
IV-8	Fuel Tankage System B	IV-25
IV-9	Cross Shaft Power Transfer Schematic	IV-27
IV-10	Model 215 Wing Ultimate Bending Moments	IV-30
IV-11	Model 215 Wing Ultimate Torsion	IV-31
IV-12	Model 215 Wing Stiffness	IV-36
IV-13	Model 215 Wing Deflections and Twist for Helicopter Flight Mode	IV-38

<u>FIGURE</u>		<u>PAGE</u>
V-1	Model 215 Nacelle Structural Layout - Elevation	V-3
V-2	Model 215 Nacelle Structural Layout - Plan View	V-5
V-3	Wing/Nacelle Attachment Beam	V-10
V-4	Nacelle Actuator Kinematics	V-14
V-5	Actuator for Twin Actuator Installation	V-15
V-6	Single Actuator	V-19
V-7	Idealized Nacelle Structure	V-21
V-8	Loads for 2.5g Takeoff in Hover	V-24
V-9	Loads for Maximum Cyclic Condition in Hover	V-25
V-10	Loads for Maximum Positive Gust Condition	V-26
VI-1	Model 215 Blade Characteristics	VI-5
VI-2	Model 215 Blade Assembly Layout TRB215-2B	VI-7
VI-3	Model 215 Inboard Blade Section, Design 2B	VI-9
VI-4	Model 215 Outboard Blade Section, Design 2B	VI-11
VI-5	Model 215 Alternate Blade, Design 3A	VI-13
VI-6	Titanium Root Retention Fitting Detail	VI-17
VI-7	Comparison of Materials on Fatigue Strength/ Stiffness Basis	VI-22

<u>FIGURE</u>		<u>PAGE</u>
VI-8	Flow Chart of Blade Stress Calculation	VI-23
VI-9	Margin of Safety Vs. Blade Span	VI-24
VI-10	Blade Design TR-2B Weight Distribution	VI-26
VI-11	Blade Design TR-2B Flapwise Stiffness Distribution	VI-27
VI-12	Blade Design TR-2B Chordwise Stiffness Distribution	VI-28
VI-13	Blade Design TR-2B Polar Mass Distribution	VI-29
VI-14	Blade Design TR-2B Torsional Stiffness Distribution	VI-30
VI-15	Blade Design TR-2B Chordwise Neutral Axis Distribution	VI-31
VI-16	Blade Design TR-2B Hover Natural Frequency Spectrum	VI-34
VI-17	Blade Design TR-2B Cruise Natural Frequency Spectrum	VI-35
VI-18	Blade Design TR-2B Stall Flutter Evaluation	VI-36
VI-19	Blade Design TR-2B Centrifugal Force Distribution	VI-42
VI-20	Blade Design TR-2B Vibratory Flap Bending Moment	VI-43
VI-21	Blade Design TR-2B Vibratory Chord Bending Moment	VI-44

<u>FIGURE</u>		<u>PAGE</u>
VI-22	Blade Design TR-2B Steady Flap Bending Moment	VI-45
VI-23	Blade Design TR-2B Steady Chord Bending Moment	VI-46
VI-24	Blade Design TR-2B Vibratory Torsional Moment	VI-47
VI-25	Blade Design TR-2B Steady Torsional Moment	VI-48
VI-26	Positive Sign Convention for Blade Loads	VI-52
VI-27	Resolution of Blade Moments and Shears	VI-56
VII-1	Rotor Assembly	VII-5
VII-2	Hub Assembly	VII-7
VII-3	Swashplate Assembly	VII-11
VII-4	Cyclic Pitch Mechanism	VII-13 & 13a
VII-5	Actuator Assembly Rotor Control	VII-15
VII-6	Stress Analysis of Blade Retention Spanwise Hoop Pressure Distribution Due to Centrifugal Force	VII-25
VII-7	Stress Analysis of Blade Retention Spanwise Hoop Stress Distribution in the Spar Due to Centrifugal Force	VII-26
VII-8	Stress Analysis of Blade Retention Spanwise Hoop Stress Distribution in the Retention Fitting Due to Centrifugal Force	VII-27
VIII-1	Hover Control Power in Pitch	VIII-5

<u>FIGURE</u>		<u>PAGE</u>
VIII-2	Hover Control Power in Roll	VIII-6
VIII-3	Hover Control Power in Yaw	VIII-7
VIII-4	Hovering Response to Collective Pitch Input	VIII-9
VIII-5	Vertical Control Response Criteria	VIII-10
VIII-6	Hovering Pitch Dynamic Stability Requirements	VIII-11
VIII-7	Hovering Roll Dynamic Stability Requirements	VIII-14
VIII-8	Low-Speed Flight Short Term Pitch Response Requirements - Helicopter Mode	VIII-15
VIII-9	Low-Speed Flight Short Term Lateral-Directional Response Requirements - Helicopter Mode	VIII-16
VIII-10	Model 215 Gust Sensitivity and Response - Longitudinal and Lateral Gust - CG Acceleration	VIII-17
VIII-11	Model 215 Gust Sensitivity and Response - Lateral Gust, Yaw and Roll Acceleration	VIII-18
VIII-12	Effects of Gust Loading on the Model 215 Aircraft	VIII-20
VIII-13	Effect of Turbulence Encounter on the Model 215 Aircraft in the Cruise Mode	VIII-21
VIII-14	Roll Control Mixing in Transition	VIII-23
VIII-15	Model 215 Power Management System	VIII-24
VIII-16	Effect of Wing Torsion on Short Period Frequency	VIII-26

<u>FIGURE</u>		<u>PAGE</u>
VIII-17	Rotor Analog Schematic	VIII-27
VIII-18	Damping of 215 Aircraft Whirl Flutter Modes at Sea Level with 207 rpm	VIII-29
VIII-19	Adequate Stability Margins at Low Power Settings with Cyclic Feedback System Inoperative	VIII-31
VIII-20	Sketch of Damage to Wing Considered in Whirl Flutter Analysis	VIII-32
VIII-21	Loss of Wing Stiffness of Damaged Wing	VIII-33
VIII-22	Wing Damage Does Not Cause Whirl Flutter	VIII-37
VIII-23	Frequency Spectrum of Rotor Air/Ground Resonance Modes Relative to Uncoupled Wing Modes	VIII-38
VIII-24	Vibration Isolation Provided by 215 Wing Design for 3/Rev Rotor Forces	VIII-42
A-1	Description of ISIS	
A-2	ISIS Indicator Assembly	

LIST OF SYMBOLS*

A_q	Propeller crossflow due to pitch or yaw = $\frac{\alpha}{2} \rho V^2$, = degrees - psf
b	Number of rotor blades
c	Blade chord at .75 radius, feet
$C_{T/\sigma}$	Prop/rotor thrust coefficient $T/\rho \pi R^2 V_T^2$
\bar{I}_θ	Blade first torsion mode inertia, slugs-ft ²
R	Prop/rotor radius, ft
V	Aircraft forward velocity, ft/sec
V	Prop/rotor tip speed, ft/sec
α	Aircraft angle of attack, degrees
α_N	Nacelle angle of attack, 90 degrees in hover, 0 degrees in cruise
ξ	Critical damping ratio
ρ	Air density, slugs/ft ²
ρ_0	Air density at sea level, standard day, slugs/ft ²
σ	Rotor solidity = $bc/\pi R$
ω_n	Natural frequency of mode, radians/second
ω_θ	First blade torsion mode natural frequency including control system stiffness, radians/second

*All structural and weights symbols are defined in the test

LIST OF TABLES

<u>TABLE</u>		<u>PAGE</u>
II-1	Summary of Aircraft Design Weights	II-2
III-1	Basic Design Parameters for Model 215	III-2
III-2	Limit Design Conditions for Helicopter Flight	III-8
III-3	Limit Design Conditions for Transition Flight	III-9
III-4	Limit Design Conditions for Airplane Flight	III-10
IV-1	Limit Wing Design Conditions for Helicopter Flight Mode	IV-4
IV-2	Cross Shaft Design Conditions	IV-26
IV-3	Summary of Skin-Stringer Requirements	IV-34
IV-4	Summary of Spar Requirements	IV-35
IV-5	Summary of Wing Weights	IV-39
IV-6	Basic Wing Weight	IV-42
IV-7	Provisions for Wing Tip Attachments	IV-48
V-1	Summary of Design Conditions - Nacelle Structure and Tilting Mechanism	V-8
V-2	Summary of Ultimate Nacelle Hinge Moments, Actuator and Bearing Loads	V-18
V-3	Summary of Wing-Nacelle Support Structure - Web, Skins and Flanges	V-28
V-4	Summary of Nacelle Truss Member Stresses	V-31

<u>TABLE</u>		<u>PAGE</u>
V-5	Summary of Wing Tip and Nacelle Support Weight	V-33
V-6	Summary of Tilt Mechanism and Attachments	V-34
VI-1	Blade Natural Frequencies for Blade Design TR-2B	VI-33
VI-2	Rotor Blade Loads: Hover 3.54° Cyclic Condi- tion	VI-53
VI-3	Rotor Blade Loads: Maximum Cyclic Condition (11.8°)	VI-54
VI-4	Rotor Blade Loads: 2.5g Vertical Takeoff Condition	VI-55
VI-5	Fatigue Analysis for 3.54° Cyclic (Moments)	VI-57
VI-6	Ultimate Analysis for Maximum Cyclic Condi- tion (Moments)	VI-58
VI-7	Ultimate Analysis for 2.5g Vertical Takeoff Condition (Moments)	VI-59
VI-8	Fatigue Analysis for 3.54° Cyclic Condition (Shears)	VI-60
VI-9	Ultimate Analysis for Maximum Cyclic Condi- tion (Shears)	VI-61
VI-10	Ultimate Analysis for 2.5g Vertical Takeoff Condition. (Shears)	VI-62
VI-11	Blade Section Properties	VI-64
VI-12	Summation of Fatigue Condition	VI-65

<u>TABLE</u>		<u>PAGE</u>
VI-13	Summary of Ultimate Condition	VI-66
VI-14	Summary of Margins of Safety	VI-67
VI-15	Rotor Blade Weight	VI-68
VII-1	Rotor Hub Assembly Minimum Margins of Safety	VII-21
VII-2	Hub Forces	VII-22
VII-3	Blade Loads at 7.5% Radius	VII-23
VII-4	Design Loads for Blade Retention	VII-24
VII-5	Weight Summary Rotor Hub	VII-71
VII-6	Weight Summary Upper Rotor Controls	VII-72
VIII-1	Stability Derivatives for Model 215 Aircraft (1)	VIII-12
VIII-2	Aircraft Geometric Parameters Used in Prop Whirl Analysis	VIII-34
VIII-3	Uncoupled Free-Free Wing Mode Natural Frequencies of the 215 Aircraft	VIII-35

SECTION I

INTRODUCTION

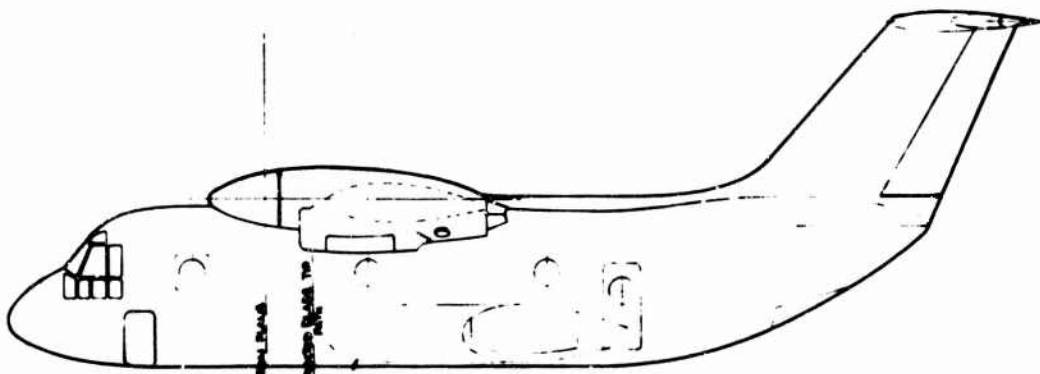
The detailed designs of a prop/rotor, hub, nacelle, tilting mechanism, wing and associated controls for a tilting prop/rotor aircraft are documented in this report. This report satisfies the requirements of Phase II of AFSC Flight Dynamics Laboratory Contract Number F33615-69-C-1570, "Determination of Design Criteria and Demonstration of Technology of a Prop/Rotor Aircraft."

Phase I of this contract (Reference I-1) provided the preliminary design, performance and weight parameters of the 67,000-pound transport aircraft shown in Figure I-1. A preliminary look at the dynamic stability of the aircraft, flying qualities and structural design criteria was also presented in Reference I-1.

Phase II carries the preliminary design parameters into detailed designs in order to verify the weight predictions of Phase I quantitatively and to determine problem areas which can be resolved by testing in Phase III or further design optimization in Phase IV.

The fuselage, empennage and landing gear are not designed since, apart from testing the fuselage and empennage for vibration minimization and choosing the landing gear stiffness for ground resonance stability, these designs will be conventional and the technology for these tasks is available as presented in Reference I-2.

Each section in this report provides the design objectives, structural analysis, weight analysis and ends with conclusions and recommendations for further work.

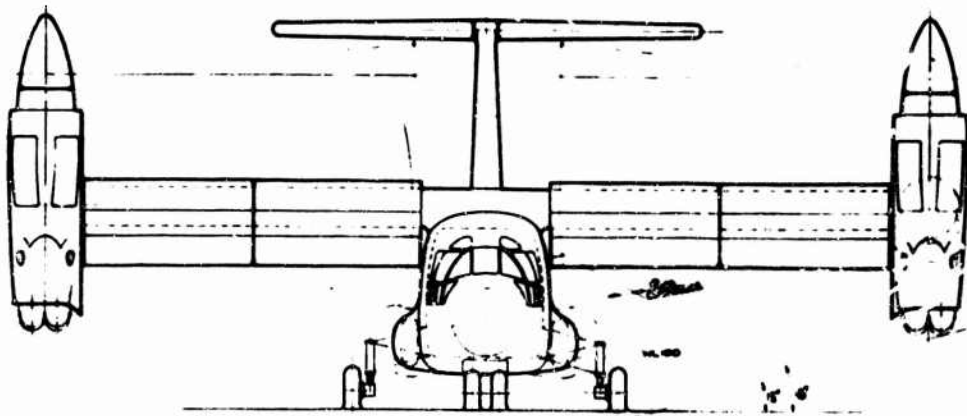


BASE NORMAL PLANE

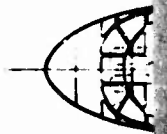
RESCUER PLANE TO

RESCUER POD
DETACHABLE FULL
POD

AIRCRAFT IN CRUISE MODE



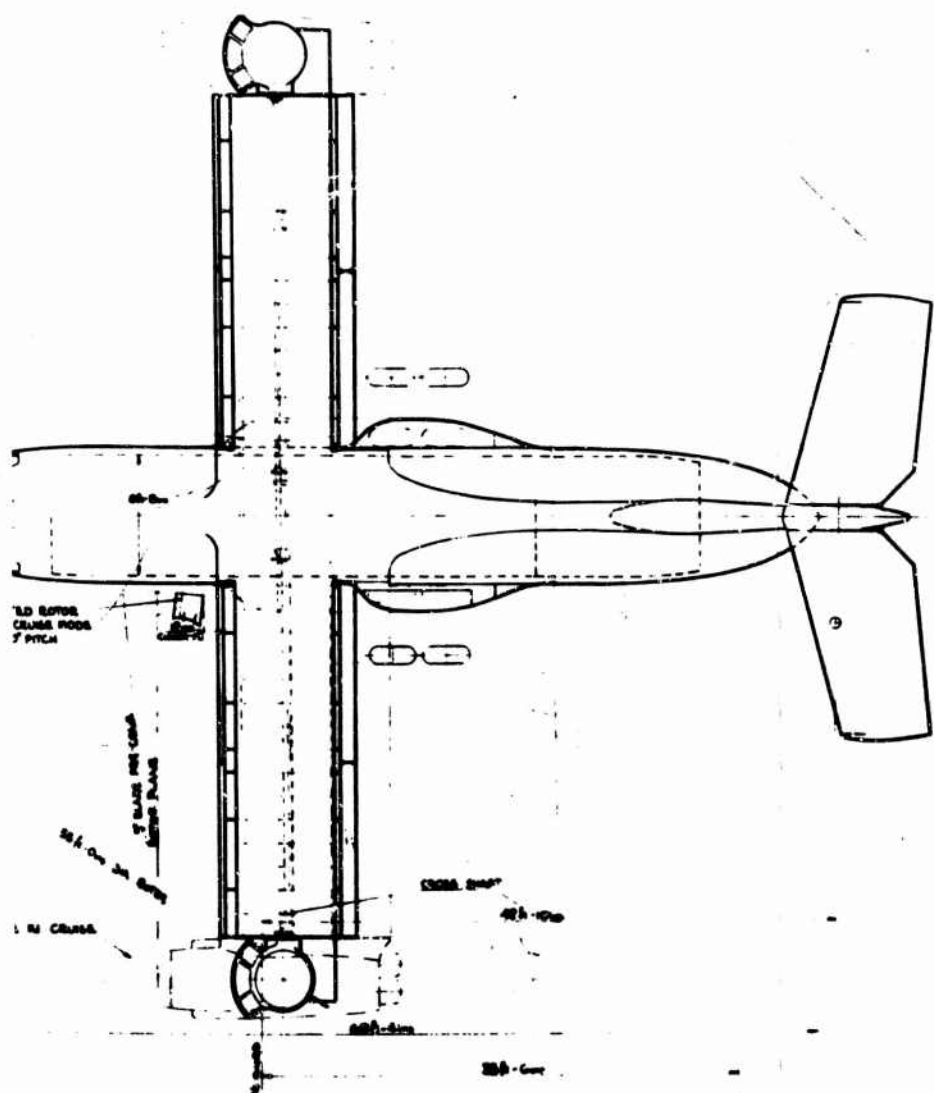
300
300-000
00
300
300-000
(TRACK)



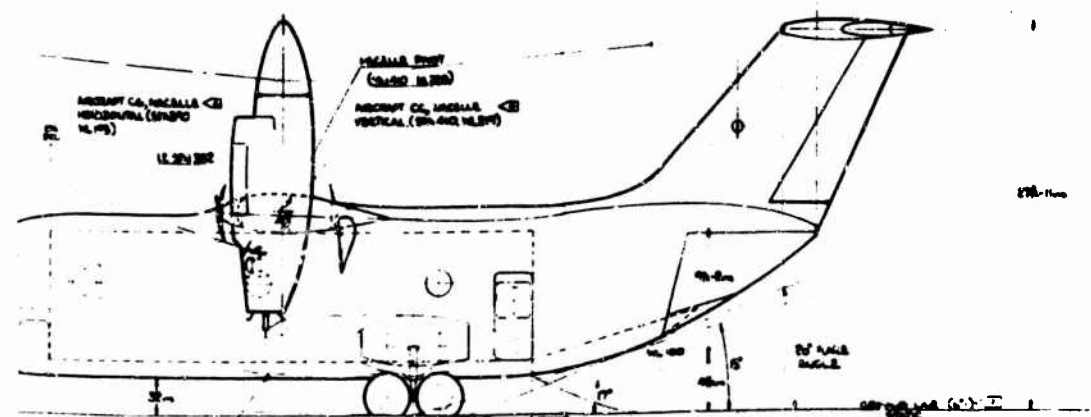
DETAIL
TO A1
WITH 6

DETAIL
POD





FUSELAGE		PAYLOAD COMPARTMENT SIZE	
	LENGTH	524 - 0.00	
	WIDTH	84 - 0.00	
	HEIGHT	48 - 2.00	
OVERALL SIZE			
	LENGTH	484 - 0.00	
	WIDTH	48 - 0.00	
	HEIGHT	118 - 0.00	
WING			
	SPAN	554 - 0.00	
	MEAN CHORD	154 - 0.00	
	AREA	85000	
	ASPECT RATIO	5.16	
	TAPER C RATIO	1.0	
	THICKNESS CHORD RATIO	0.01	
	WING LOADING	800 LBS/WT	
HORIZONTAL TAIL			
	SPAN	224 - 0.00	
	MEAN CHORD	64 - 0.00	
	AREA	14200	
	ASPECT RATIO	4.0	
	TAPER C RATIO	0.7	
	THICKNESS CHORD RATIO	0.15	
	TAIL VOLUME	1.04	
VERTICAL TAIL			
	SPAN	134 - 0.00	
	MEAN CHORD	124 - 0.00	
	AREA	16700	
	ASPECT RATIO	1.02	
	TAPER C RATIO	0.64	
	THICKNESS CHORD RATIO	0.18	
	TAIL VOLUME	1.04	
ROTOR			
	DIAMETER	564 - 0.00	
	SOLIDITY	0.041	
	DISC LOADING	145 LBS/WT	
	UP BLADES	5	
WEIGHTS			
	DESIGN GROSS WT	21,000 LBS	
	FUEL CAPACITY	12,000 LBS	
	MAXIMUM TAKEOFF WEIGHT	33,000 LBS	
	MAXIMUM LIFTING CAPACITY	910 LBS	
ENGINES			
	NUMBER	4	
	TYPE	TURBO-PROP	
	HP	1750 HP	
	PERCENT EFFICIENCY	80%	
LANDING GEAR			
MAIN WHEELS			
	NUMBER	4	
	ARRANGEMENT	TWO MAIN	
	WHEEL	24x8-10 - 5000	
	FLATION	80 PSI	
NOSE WHEELS			
	NUMBER	2	
	ARRANGEMENT	ONE	
	WHEEL	24x8-10 - 1000	
	FLATION	70 PSI	
RESCUE MISSION WEIGHTS			
	VTOL - GROSS WT	22,000 LBS	
	FUEL CAPACITY	12,000 LBS	
	STOL - GROSS WT	21,000 LBS	
	FUEL CAPACITY	12,000 LBS	



- GROUND LBS. DISTRIBUTION PER FIG. I-1-1
- ① GROUND LBS. WITH AIRCRAFT IN THREE POINT ATTITUDE WITH TIEES & SHOCKS ADJUSTED STATICALLY DEFLECTED
- ② GROUND LBS. WITH MAIN GEAR SHOCK ADJUSTED & TIEES STATICALLY DEFLECTED WITH GEAR SHOCK ADJUSTMENT FULLY COMPENSATED WITH WHEEL TIRE TILT
- ③ FOR THE SHOWN GROUND LBS. MAIN GEAR SHOCK ADJUSTED & TIEES STATICALLY DEFLECTED
- ④ GROUND GROSS WEIGHT CENTER OF GRAVITY

THE BOEING COMPANY	
PHILADELPHIA, PA.	
USAF 5-TON PAYLOAD	
VTOL TILT ROTOR AC.	
1771	SK 215-21585

BOEING MODEL 215 USAF 5-TON PAYLOAD TILT ROTOR TRANSPORT

FIGURE I-1

SECTION II

SUMMARY

Detail design of the critical components of a prop/rotor aircraft has been conducted to accomplish the following objectives:

- a. verify weight predictions obtained in preliminary design, Reference I-1.
- b. identify areas where additional design, analysis and/or testing is required.

The preliminary design estimates of the weight of the critical components to satisfy the aircraft maneuver and mission requirements with adequate stress margins are verified. This effort shows the weight empty of the baseline aircraft to be 112 pounds less than the preliminary design value. Distribution of this change in weight is summarized on the following page.

The small overall change in weight results from an increase in the tilt mechanism weight being offset by a reduction in weight of the rotor and hub.

Further work by testing, analyses and design are recommended in the following areas:

- a. The 2.5g hover takeoff structural design condition needs re-examination. The achievement of this load factor is believed to be beyond the capability of rotor system designed to the required hover and cruise thrust and power

TABLE II-1
SUMMARY OF AIRCRAFT DESIGN WEIGHTS

	ORIGINAL WEIGHT REF.	COMPONENT WEIGHT STUDIES			
		BASELINE DESIGN		REVISED DESIGN	
		WEIGHT	ΔWEIGHT	WEIGHT	ΔWEIGHT
Rotor	(5,455)	(3,870)	(-1,585)	(3,870)	(-1585)
Hubs	2,375	1,440	- 935	1,440	- 935
Blades	2,880	2,238	- 642	2,238	- 642
Spinners	200	192	- 8	192	- 8
Wing	(4,945)	(5,191)	(+ 246)	(5,148)	(+ 203)
Basic Wing	4,445	4,837	+ 392	4,837	+ 392
Provisions for Wing Tip	500	354	- 146	311	- 189
Flight Controls	(5,399)	(6,626)	(+1,227)	(6,128)	(+ 729)
Upper Rotor Controls	2,367	2,442	+ 75	2,442	+ 75
Tilt Mechanism	(1,005)	(2,157)	(+1,152)	(1,659)	(+ 654)
Nacelle Support	450	989	+ 539	751	+ 301
Mechanism	555	1,168	+ 613	908	+ 353
Others	(2,027)	NOT STUDIED			
Remaining Groups	30,062	NOT STUDIED			
Weight Empty	45,861	45,749	- 112	45,208	- 653
Weight of Compon- ents Studied	13,772	13,660	- 112	13,119	- 653
% of Weight Empty Verified by Component Design	30.0				

criteria.

- b. A complete fatigue loading spectrum is required for the prop/rotor aircraft missions. It should include gusts/turbulence and ground handling.
- c. Fail safety/damage tolerance criteria should be established.
- d. Full scale blade root fatigue tests to determine the endurance limits under combined loadings.
- e. Establish through model testing the blade vibratory control moments when operating in the maximum thrust and control condition.
- f. Verification of the wing stiffness selected for minimum vibration by dynamic model testing.
- g. The pilot-control system-airframe elastic couplings need investigation in a moving base simulation of flight in turbulent air.
- h. Determine stability and control characteristics in and out of ground effect by model testing.
- i. Determine dynamic stability derivatives of the rotor through transition by dynamic model rotor tests.

In summary then, while the Model 215 prop/rotor transport designed in Phase I is structurally sound and within the established weight targets as verified in Phase II, there are areas in both technical analysis, test and structural design that can be improved by additional work. The design is based on conservative assumptions and the weight empty can be reduced by additional design and analysis efforts.

SECTION III

GENERAL STRUCTURAL CRITERIA

1. INTRODUCTION

This section contains criteria for the structural design of the prop/rotor aircraft rotor blades, hub, wing and nacelle structure. Limit load and fatigue conditions are included. Specifications MIL-A-8860 and MIL-S-8698 were used to guide the selection of conditions and only those which are critical are considered for design purposes.

2. FLIGHT MODE DEFINITION

- a. Helicopter flight: lift is provided only by the rotor.
- b. Transition flight: lift is provided by the rotor and wing. This regime ends at V_{CON} .
- c. Airplane flight: lift is provided only by the wing. The regime starts at V_{CON} and is limited at V_L .
- d. V_{CON} is the airspeed at which $n_z = 1.2$ can be achieved with the flaps retracted.

3. BASIC DESIGN PARAMETERS

The basic design parameters for the three flight modes are listed in Table III-1.

4. FACTOR OF SAFETY

The yield factor of safety shall be 1.0. The ultimate factor of safety shall be 1.5.

TABLE III-1
BASIC DESIGN PARAMETERS FOR MODEL 215

PARAMETER	DESIGN VALUE
<u>HELICOPTER FLIGHT</u>	
Basic Design Gross Weight	67,000 lb.
Minimum Flying Gross Weight	47,798 lb.
Landing Gross Weight at 8 Feet Per Second Sink Speed	68,888 lb.
Most Aft C.G. Position	F.S. 421.6 in.
Most Forward C.G. Position	F.S. 398.7 in.
Limit Load Factor at Basic Design Gross Weight (n_z)	2.5, -1.0
Normal Rotor Speed, Power On	295 RPM
Rotor Speed Limit Factor	1.25
Nacelle Axle	F.S. 410
<u>TRANSITION FLIGHT</u>	
Basic Design Gross Weight	67,000 lb.
Maximum Design Gross Weight	74,000 lb.
Limit Load Factor at Basic Design Gross Weight (n_z)	3.0, -1.0
Normal Rotor Speed, Power On	295 RPM
Rotor Speed Limit Factor	1.25
<u>AIRPLANE FLIGHT</u>	
Basic Design Gross Weight	67,000 lb.
Maximum Design Gross Weight	74,000 lb.
Minimum Flying Gross Weight	47,798 lb.
Most Aft C.G. Position	F.S. 402.5 in.
Most Forward C.G. Position	F.S. 379.5 in.
Limit Load Factor at Basic Design Gross Weight	3.0, -1.0
Normal Rotor Speed	207 RPM

5. ROTOR TORQUE FACTOR

The limit torque factor shall be 1.5.

6. AIRPLANE FLIGHT DESIGN SPEED

- a. Maximum level flight speed V_H equal to 360 knots (transmission torque limit) at sea level.
- b. The limit speed V_L shall be 450 knots (1.25 V_H) at sea level.
- c. The maximum speed for a 66 fps gust V_G shall be 260 knots (S.L.) for the basic design gross weight and 240 knots (S.L.) for the minimum flying gross weight, $V_G = \sqrt{n}V_S$ where n is the maximum gust load factor determined at V_H and V_S is the stalling speed for level flight at sea level in the basic configuration with power off. Prop/rotor normal forces have been neglected in the calculation of gust limit load factor.

7. V-n DIAGRAM

Composite V-n diagrams for the three flight modes at the basic design gross weight and the minimum flying gross weight are shown in Figures III-1 and III-2. The diagrams for airplane flight (solid lines) were constructed as specified in MIL-A-8861 for maneuver and gust load factors.

The limit load factors for helicopter and transition flight (dashed lines) are shown as the sum of the helicopter (2.5) and the airplane load factor at a given speed, the maximums being 3.0 and -1.0.

COMPOSITE MANEUVER AND GUST DIAGRAM
IS BOUNDED BY THE HEAVY LINE.

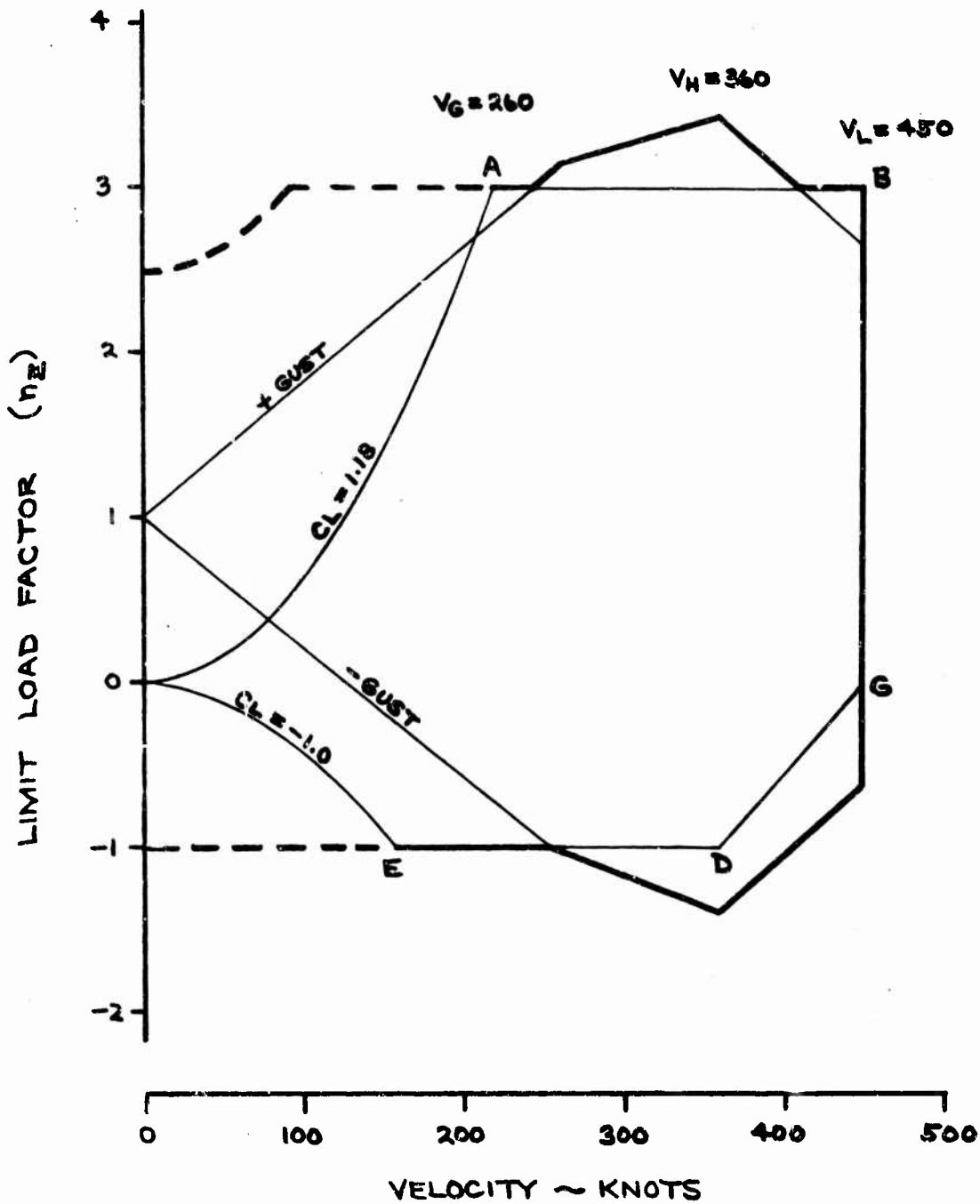


FIGURE III-1. V-n DIAGRAM (SEA LEVEL)
BASIC DESIGN GROSS WEIGHT = 67000 LB

COMPOSITE MANEUVER AND GUST DIAGRAM
IS BOUNDED BY THE HEAVY LINE.

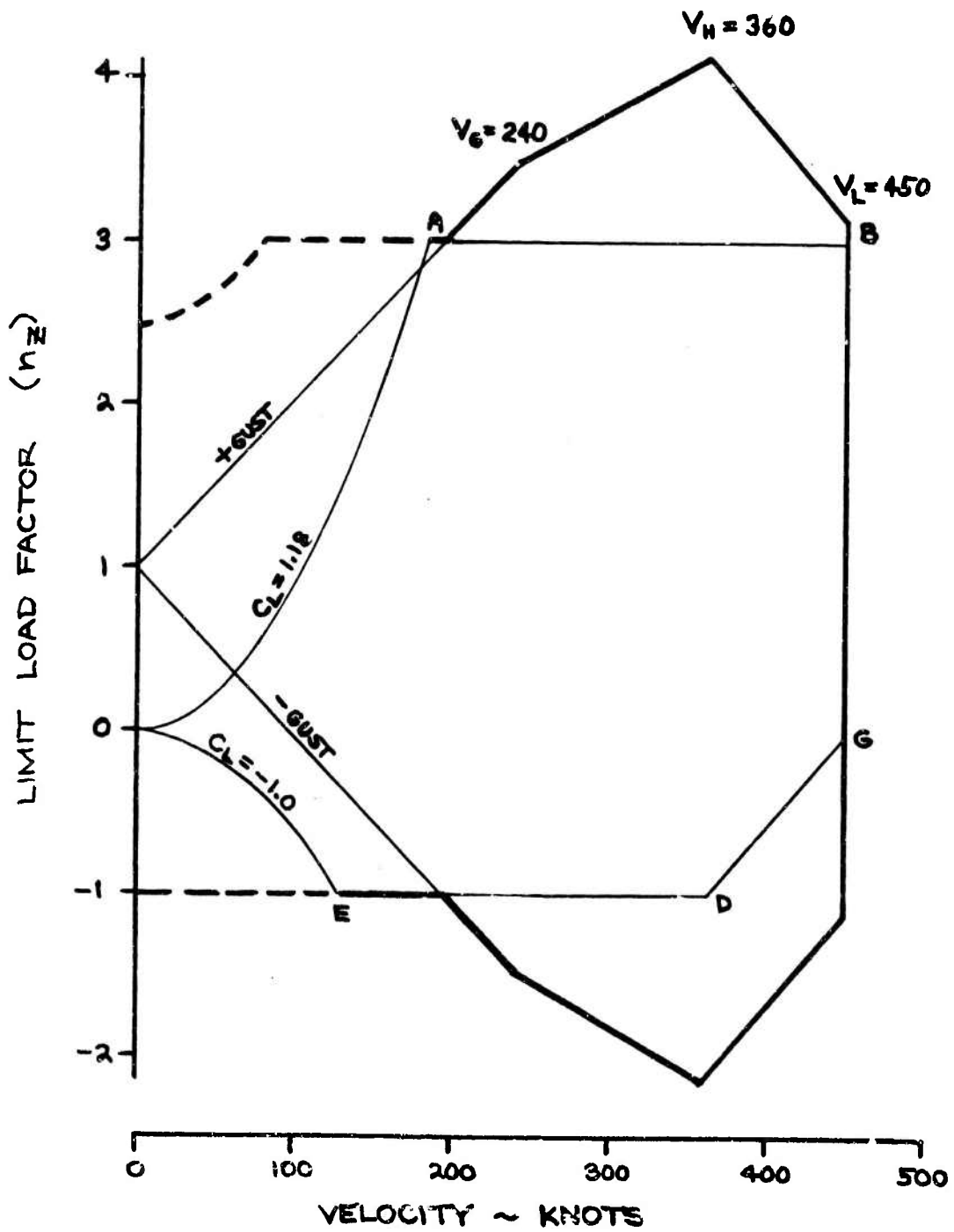


FIGURE II-2. V-n DIAGRAM (SEA LEVEL)

MINIMUM FLYING GROSS WEIGHT = 47798 LBS.

8. LIMIT LOAD DESIGN CONDITIONS

Limit load design conditions for helicopter, transition and airplane flight are contained in Tables III-2, III-3, and III-4, respectively. The conditions listed have been selected for investigation.

9. HOVER CONTROL REQUIREMENTS

The required angular acceleration capabilities of the aircraft in the helicopter mode are as follows:

Roll	1.0 rad/sec ²
Yaw	.5 rad/sec ²
Pitch	.6 rad/sec ²

10. FATIGUE DESIGN CONSIDERATIONS

The service usage for definition of structural design requirements shall be in accordance with the basic fatigue schedule in Reference I-1, Section VII, paragraph 10.

The significant conditions affecting the fatigue performance of the wing are the repeated maneuvers and atmospheric turbulence at low altitudes and the relatively large number of ground-air-ground cycles. As in conventional aircraft, the material allowable stress for preliminary design is chosen to be compatible with fatigue design requirements. A complete wing fatigue analysis must be performed at a later date when the full fatigue loading spectrum for the aircraft is developed in detail, based on the combinations of missions and cargo. This analysis should not affect the weight

of the aircraft to any extent since some consideration of fatigue effect has been included in the non-optimum weight factors.

The prop/rotor blade, hub and controls shall be designed for the various flight conditions defined in Reference I-1, Section VII, paragraph 13.

Critical fatigue loads on the rotor blade are produced by cyclic pitch control. For preliminary design, the following cyclic conditions are considered in the evaluation of the fatigue strength of the rotor blade.

- a. The rotor system shall be analyzed to determine its fatigue performance under the following conditions:
 - (1) Alternating loads due to rotor cyclic control, in the helicopter mode, equal to the cyclic required to trim the aircraft level plus 25% of the maximum cyclic for pitch control shall not exceed the fatigue endurance limits of rotor system components.
 - (2) Alternating loads due to rotor cyclic control, in the helicopter mode, equal to the cyclic required to trim the aircraft level plus 25% of the maximum cyclic for yaw control shall not exceed the fatigue endurance limits of rotor system components.
 - (3) Alternating loads due to "Aq" equal to 1,500 psf - degrees shall not exceed the fatigue endurance limits of rotor system components.

TABLE III-2 LIMIT DESIGN CONDITIONS FOR HELICOPTER FLIGHT

Cond. No.	Condition	Gross Weight LB.	Limit Load Factor	Air Speed Knots	Resulting Rate Radians/Sec	Acceleration Radians/Sec ²
1	Vertical Take-Off - NOTE 1	67,000	2.5	0	0	0
2	Vertical Take-Off with Pitch	67,000	2.5	0	NOTE 2	NOTE 2
3	Rolling	67,000	2.0	0	1.5 (Roll) NOTE 4	1.0 (Roll) NOTE 3
4	Yawing	67,000	1.0	0	1.0 (Yaw) NOTE 5	.5 (Yaw) NOTE 3
5	Pushdown (Collective Dump) - NOTE 1	67,000	-1.0	0	0	0
6	Maximum Cyclic - NOTE 6	67,000	1.0	0	NOTE 7	NOTE 7

1118

NOTE 1: Cyclic Control shall be applied to eliminate pitching motion.

2: Pitching motion due to thrust offset from aircraft c.g.

3: Maximum control input.

4: Maximum acceleration held until attitude is 60 degrees.

5: Maximum acceleration held until attitude change is 60 degrees.

6: The maximum of (a) cyclic for pitch control plus half cyclic for yaw control or (b) maximum cyclic for yaw control plus half cyclic for pitch control.

7: Pitch and yaw motion resulting from control application.

8: The rotor speed for the above conditions shall be the normal rotor speed. Except that the centrifugal force shall be for limit rotor speed.

TABLE III-3 LIMIT DESIGN CONDITIONS FOR TRANSITION FLIGHT

Cond. No.	Condition	Gross Weight lb.	Limit Load Factor	Airspeed Knots	Resulting Rate Radians/Sec (z)	Acceleration Radians/Sec ²
7	Symmetrical Pull- Out	67,000	3.0	90	0.8 (Pitch)	0.6 (Pitch)
8	Rolling Pull Out	67,000	2.4	90	1.5 (Roll)	1.0 (Roll)
9	Yawing	67,000	1.0	90	1.0 (Yaw)	.5 (Yaw)

III-9

NOTE 1: The rotor speed for the above conditions shall be the limit rotor speed.

2: This rate results from control application.

TABLE III-4 LIMIT DESIGN CONDITIONS FOR AIRPLANE FLIGHT

Cond No.	Condition	Gross Weight	Limit Load Factor	Airspeed Knots	Remarks
10	Balanced Symmetrical Maneuver	67,000	3.0	215	V-n Diagram Point "A"
			3.0	V_L	
			-1.0	155	V-n Diagram Point "E"
			-1.0	V_H	
			0	V_L	
11	Symmetrical Maneuver with Pitch	67,000			Control Displacement as Specified in MIL-A-8861, Paragraph 3.2.2.2.
12	Rolling Pull Out	67,000			Control Displacement as Specified in MIL-A-8861, Paragraphs 3.3.1 and 3.3.1.1.
13	Vertical Gust	67,000			As specified in MIL-A-8861, Paragraph 3.5.
		47,798			

These preliminary design criteria have been found to be conservative against conditions including hover in cross-wind, gusts at 250 knots and full pitch control in hover.

11. MATERIAL ALLOWABLES

Material strength properties will be based upon the following:

- a. Anticipated design allowables for new materials consistent with 1977 technology.
- b. MIL-HDBK-5, "Metallic Materials and Elements for Flight Vehicles". Column "B" allowable stresses will be used where failure of an individual element would result in the applied load being safely distributed to other load carrying members. In all other applications, the Column "A" values will be used.
- c. MIL-HDBK-17, "Plastics for Flight Vehicles".
- d. MIL-HDBK-23, "Composite Construction for Flight Vehicles".
- e. Boeing-Vertol Structural Design Manual (Reference III-1).
- f. Boeing-Vertol Report SRR-7, "Reinforced Composite Material Allowables". This document contains design strength and mechanical properties used at Boeing-Vertol for boron and S-glass composites (Reference III-2).

SECTION IV

WING DESIGN

1. INTRODUCTION

In this section the detailed design of the primary wing structure and associated systems are described. Included are the primary wing box, the wing to fuselage attachment, fuel system and cross shafting. The details of the wing tip box and the nacelle attachment structure are considered a part of the nacelle structure and are described in Section V.

The wing torque box was designed in detail because the design loads on a Prop/Rotor aircraft wing are unique and conventional aircraft weight trends are not directly applicable. The total weight of the wing and end tip provisions is 5191 pounds. This is 5% greater than the weight allocated in Reference I-1. Control surface structure, hinges, actuators, fuel system and rotor to rotor cross shaft are designed in less detail because the loads and requirements are conventional.

From this study the baseline wing design has machined tapered skin and stringers (design B) and self-sealing bag type fuel system (design A).

This wing design provides an adequate stability margin from classical flutter, whirl flutter and divergence, air/ground resonance and fuselage vibration attenuation as discussed in Section VIII.

2. OBJECTIVE

Design a wing primary structure based on the geometry and criteria, determined in Reference I-1, in order to verify the weight prediction and satisfy the structural requirements discussed below.

3. DESIGN CRITERIA

The wing design criteria based on the Phase I program are as follows:

- a. The wing structural components shall be designed and sized to accommodate the ultimate static strength requirements of the loading conditions investigated.
- b. Multiple load path structure shall be provided for the primary wing loads.
- c. Access to the wing shall be provided by nonstructural doors.
- d. Reinforcements around the nonstructural door opening shall be designed to maintain torsional continuity.
- e. All aircraft fuel shall be carried in the wing.
- f. The cross shaft shall be retained in such a manner that a shaft failure will not cause a secondary failure.
- g. Wing-nacelle support structure shall be designed to a nonbuckling criteria at 100% of design limit loads.

The limit load conditions selected for the design of the wing are listed in Table IV-1. These loading conditions are taken from the General Design Criteria presented in Section III. The conditions selected represent three helicopter flight mode conditions that are critical for the wing. Conditions investigated for the design of the wing-nacelle support structure are shown in Section V.

TABLE IV-1
SUMMARY OF LIMIT DESIGN CONDITIONS
HELICOPTER FLIGHT MODE

CONDITION NUMBER	DESCRIPTION	G.W. (LBS)	AIR SPEED (KTS)	LIMIT LOAD FACTOR	VEL. (RAD/SEC)	ACCEL. (RAD/SEC ²)
①	Vertical Takeoff	67,000	0	2.5	0	0
②	Maximum Cyclic	67,000	0	1.0	0	0
③	Rolling	67,000	0	2.0	1.5	1.0

4. WING GEOMETRY

The wing geometry defined in Reference I-1 is summarized here.

Span	65 ft - 9 in.
Chord	12 ft - 9 in.
Area	838 ft ²
Aspect Ratio	5.16
Taper Ratio	1.0
T/C Ratio	0.21
Flap	30%
L.E. Umbrella	15%
Front Spar	15%
Center Spar	40%
Rear Spar	63%
Nacelle Pivot	38%
Wing Section	NACA 64 ₄ -221 (Modified)
Fuel Volume	231 ft ³
Normal Fuel Capacity	10,224 lb
Max Fuel Capacity	18,324 lb

5. DESCRIPTION OF WING PRIMARY STRUCTURE

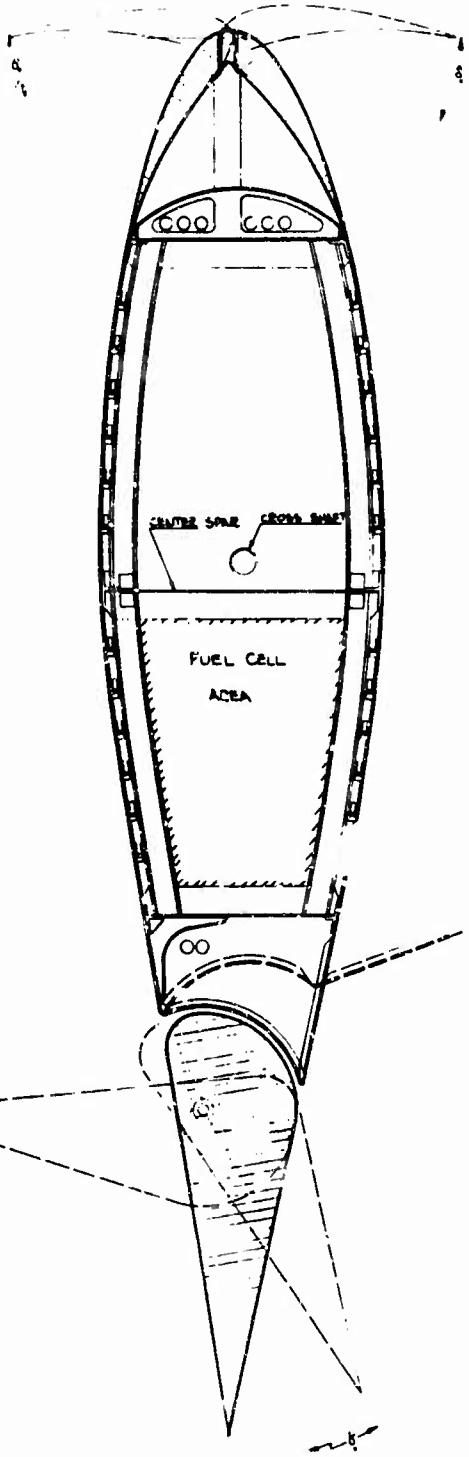
The wing has a rectangular plan form (Figure IV-1) and has a NACA 64-221 (Mod.) airfoil section (Figure IV-2). The construction is all metal conventional skin and stringer type. This method of construction was used to utilize the failsafe characteristics provided by the multi load paths of this type of structure. A secondary consideration is that production costs are generally lower for this type of manufacture.

The primary structure is a two cell torque box consisting of a front spar, center spar, rear spar, and top and bottom covers machined to a taper and stiffened with machined tapered stringers. The stringers are clipped to ribs, spaced at 19.0 in. intervals. Ribs are basically of two types, open and closed. The open ribs are of the channel and shear skirt construction and are used in fuel bay areas. The closed type ribs are of similar construction to the open and have a shear resistant panel to close the rib. The closed ribs are used as fuel bay closers and at the flap hinge positions (Figure IV-3). The wing structure is continuous over the fuselage (Figure IV-4) and is attached to the fuselage by means of a shear tied forged rib which also acts as a wing splice joint (Figure IV-5). This type of construction was used to facilitate field repair splices and spares transportation.

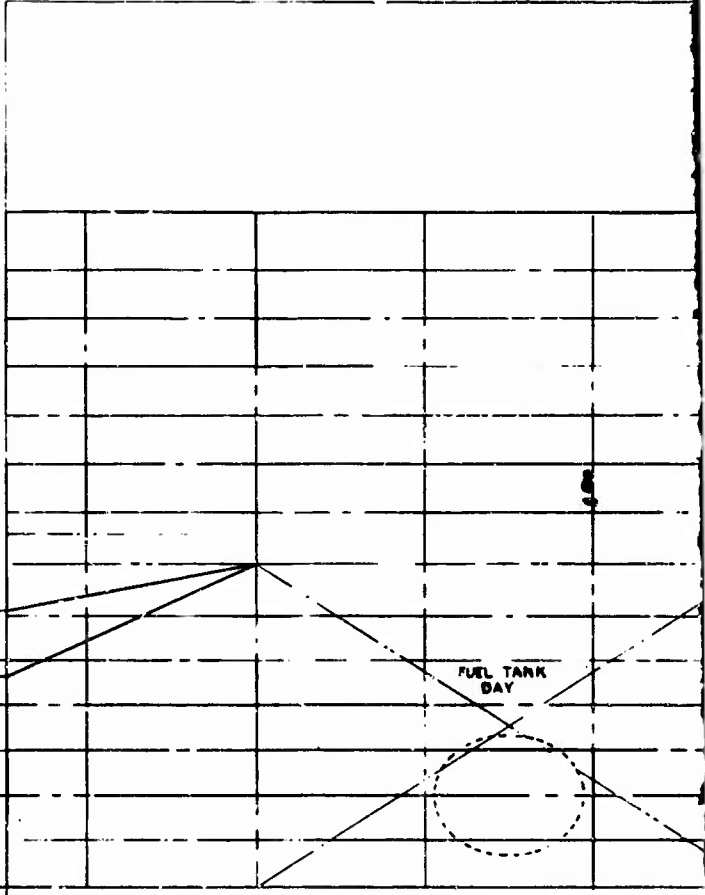
A

WING STA 32.5

UPPER RIB



WING STA 32.5



FUEL TANK BAY

FOR DETAIL OF THIS AREA SEE SHEET 6

WING STA 32.50

UPPER RIB

WING STA 32.50

13

WING STA 237.5

UMBRELLA HOOD

WING STA 237.5

UMBRELLA HOOD

2.0 AMP

ACCESS DOOR (4%)

ACCESS DOOR

ACCESS DOOR (4%)

FUEL TANK BAY

FUEL TANK BAY

FUEL TANK BAY

FUEL TANK BAY

ACCESS DOOR (4%)

ACCESS DOOR

NO TYPICAL SHOWN

RAMPON CHARGE

WING STA 237.5

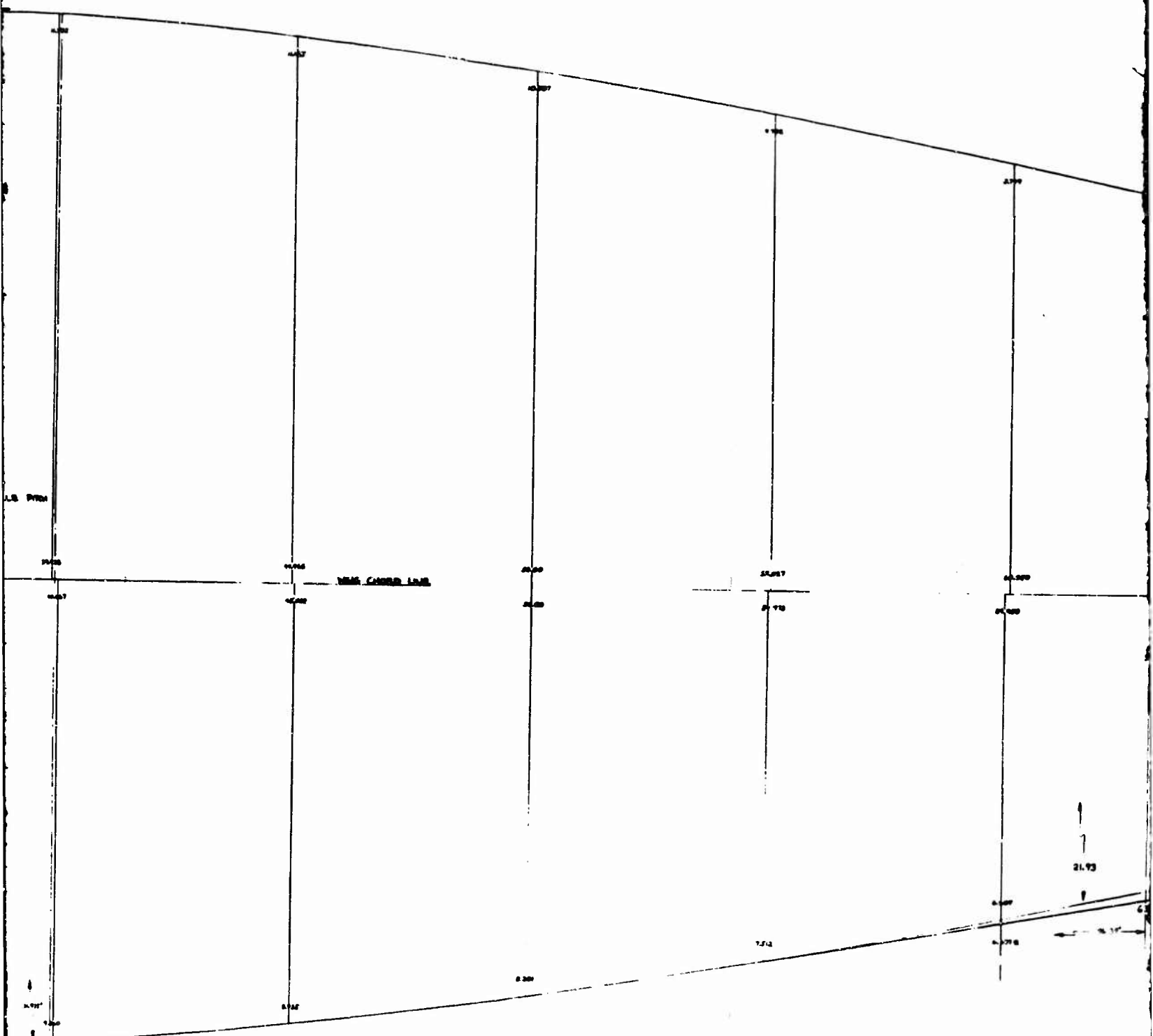
RAMPON CHARGE

WING STA 237.5

(NOT TYPICAL)

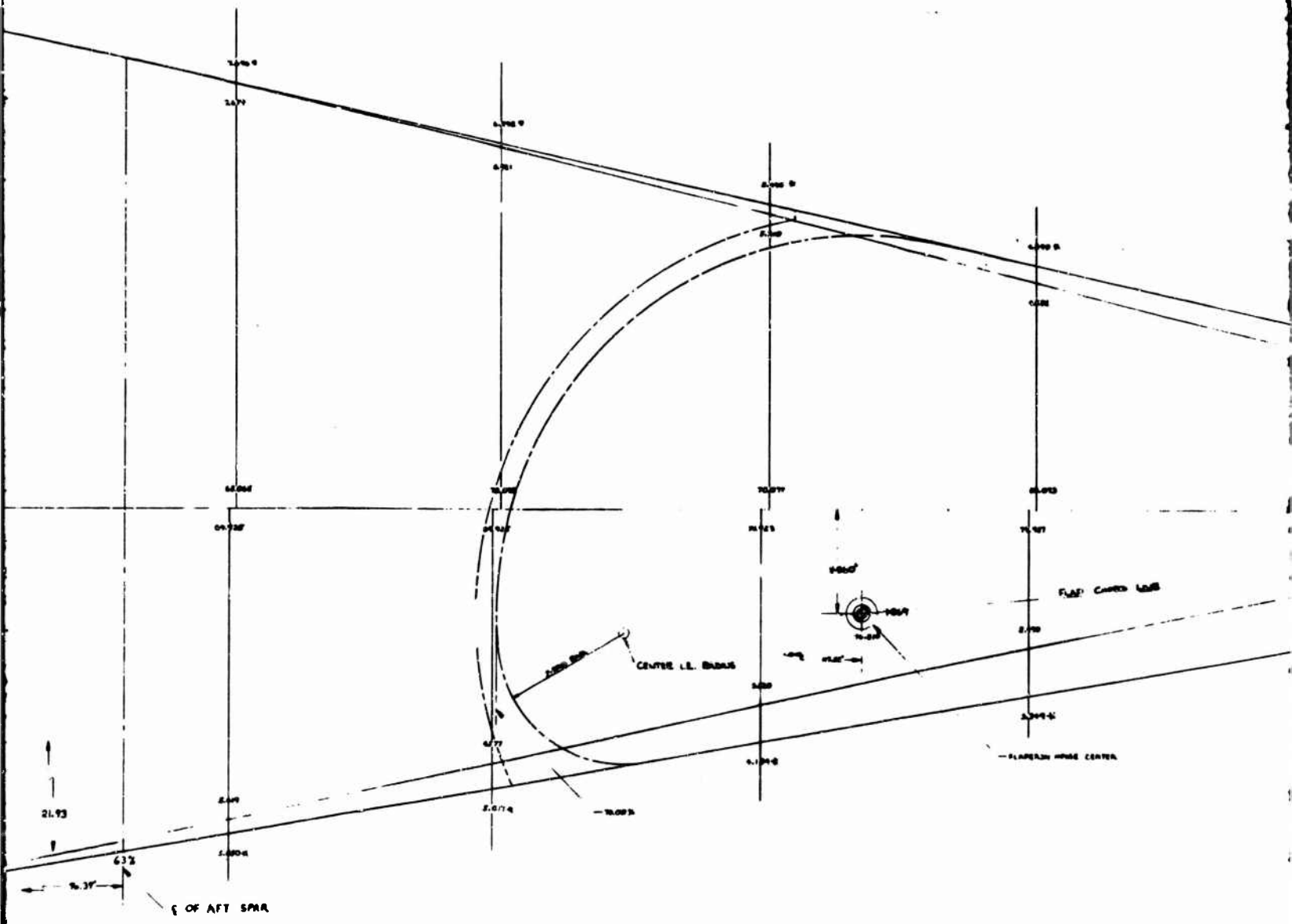
WING STA 237.5

5



OF CENTER LINE
SLOPE 10.00%

D

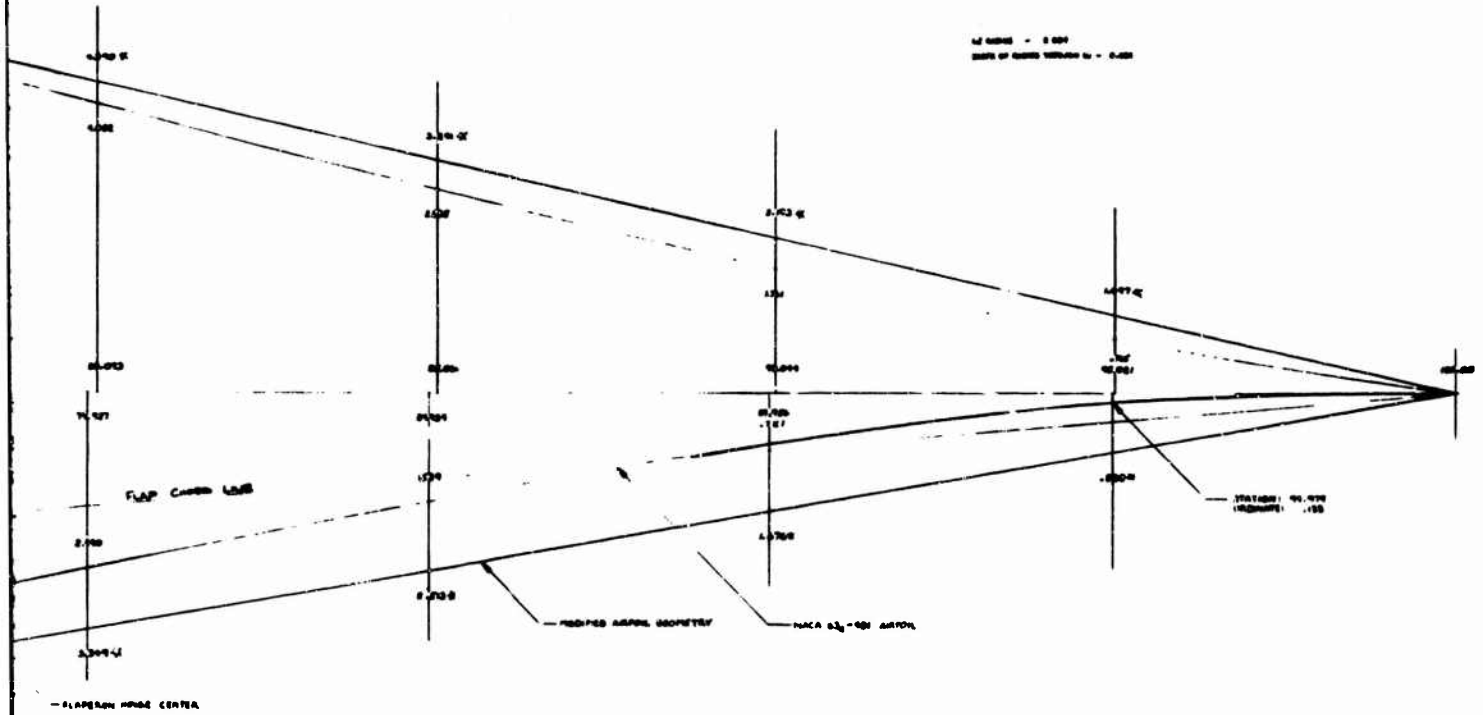


E

SECTION 1000 - 1000
 DATE OF REVISION 10-1-50

REV.	DESCRIPTION	DATE
1	INITIAL DESIGN	10-1-50
2	REVISIONS	10-1-50
3	REVISIONS	10-1-50
4	REVISIONS	10-1-50
5	REVISIONS	10-1-50
6	REVISIONS	10-1-50
7	REVISIONS	10-1-50
8	REVISIONS	10-1-50
9	REVISIONS	10-1-50
10	REVISIONS	10-1-50

SECTION 1000 - 1000
 DATE OF REVISION 10-1-50



NOTE: DIMENSIONS UNLESS OTHERWISE SPECIFIED ARE IN INCHES.

ALL FIGURES ARE PERCENTAGES UNLESS FOLLOWED BY AN INCH SYMBOL.

THE DRIVE COMPANY	
VENTNOR DIVISION PHILADELPHIA, PA.	
MODEL 215 WING	
7/57	SK-215-10000

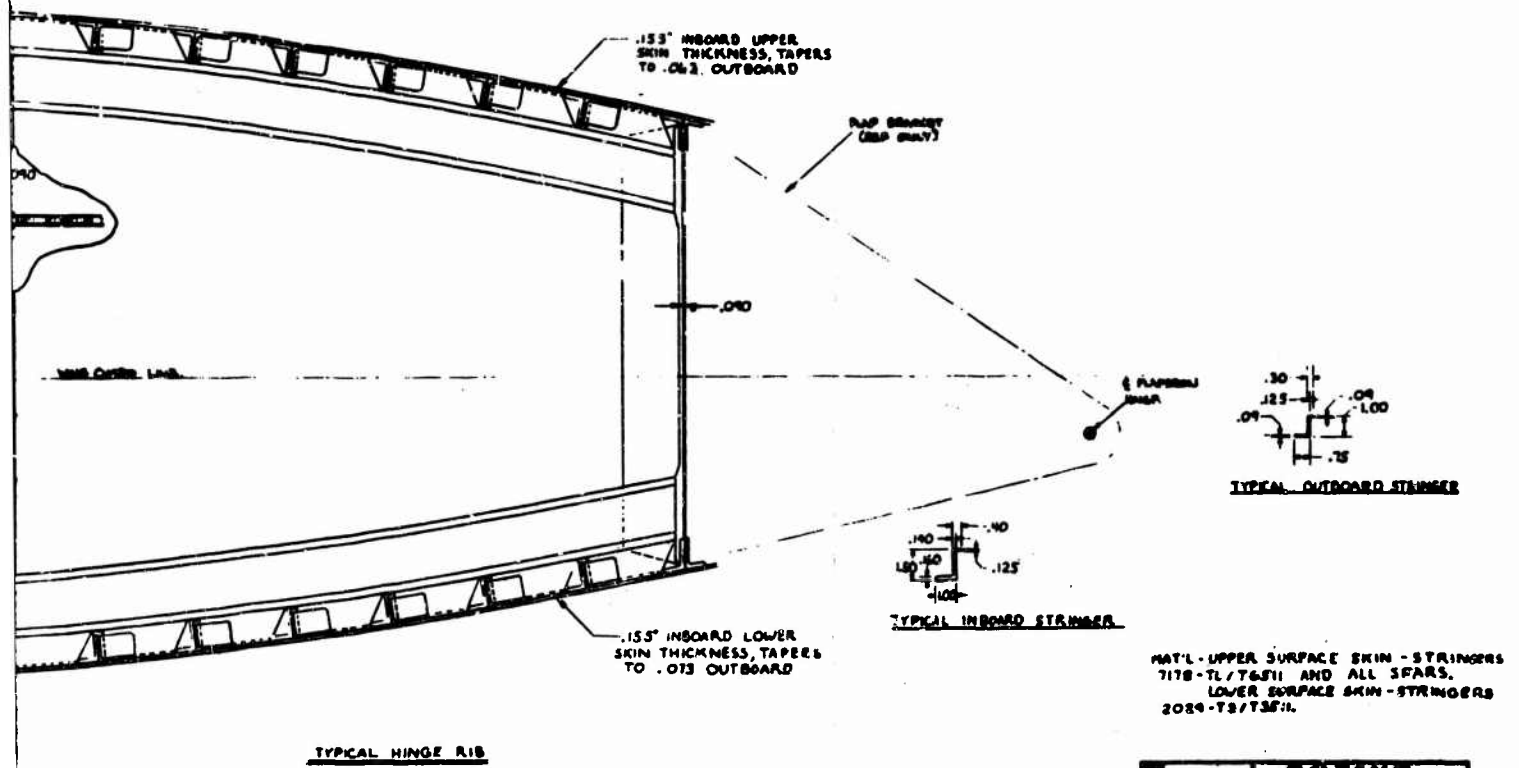
WING AIRFOIL GEOMETRY

WING AIRFOIL GEOMETRY

FIGURE IV-2

13

7



TYPICAL HINGE RIB

HINGE & CLOSURE RIB

WING HINGE AND CLOSURE RIB

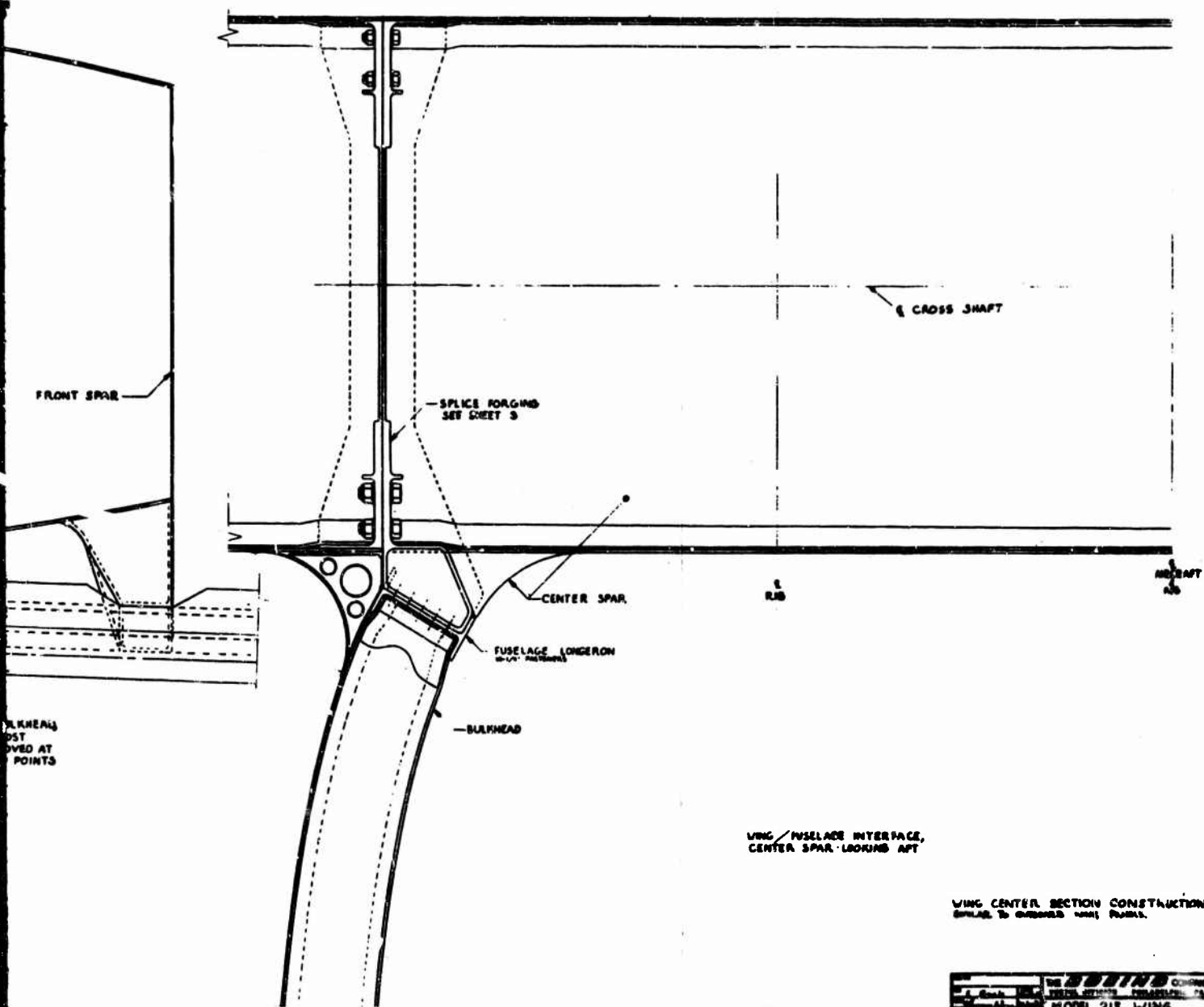
FIGURE IV-3

IV-11

DR. W. L. B. COMPANY	
DESIGNER	W. L. B. COMPANY - CHICAGO, ILL.
MODEL	WING
SK215-10000	

B

STA 24



WHEELS
MOUNTED AT
POINTS

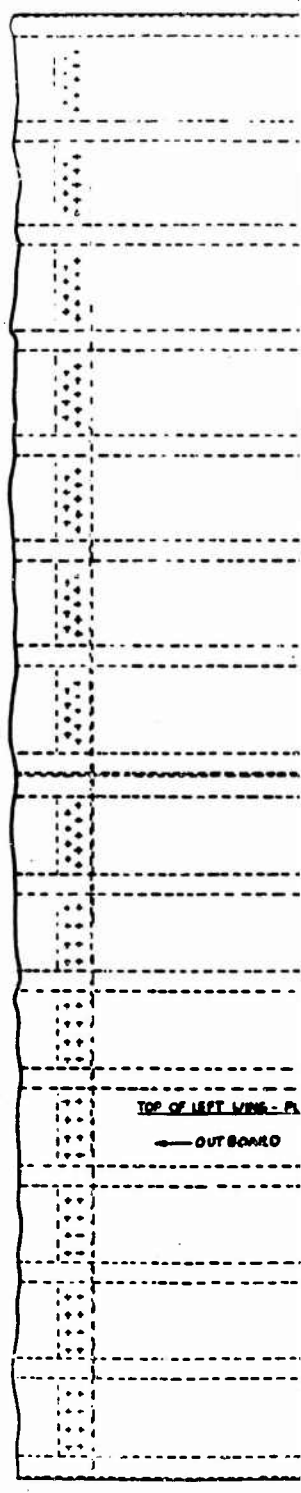
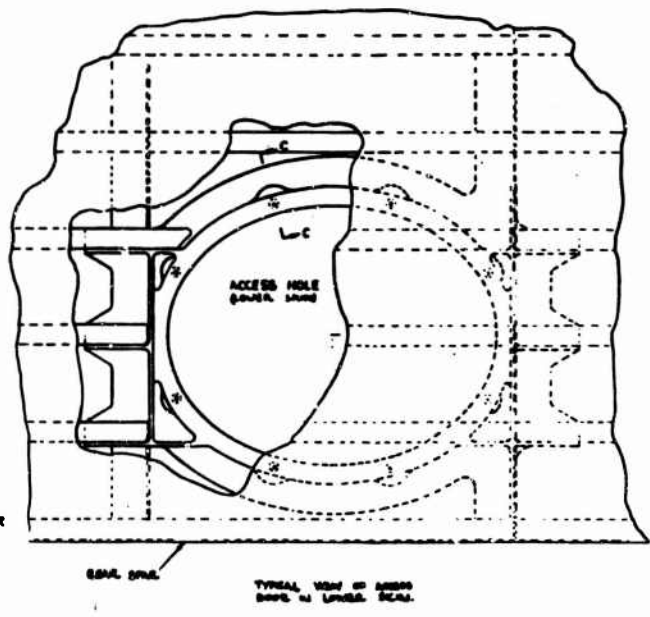
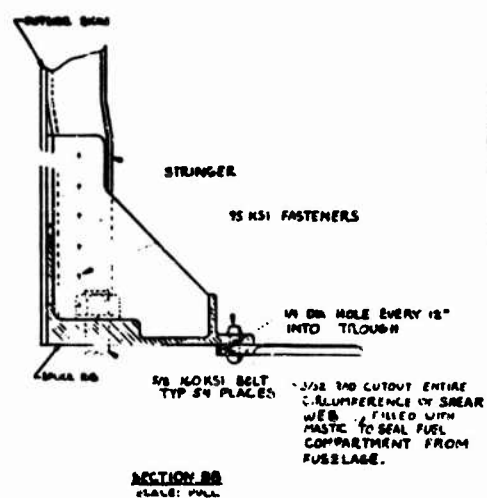
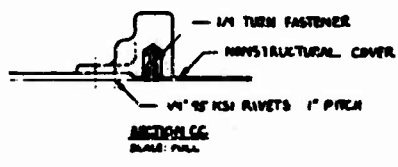
WING-FUSELAGE SPLICE

THE SK215 COMPANY	
DESIGN OFFICE: PHOENIX, ARIZONA	
MODEL 215 WING	
SK215-10000	

WING FUSELAGE SPLICE

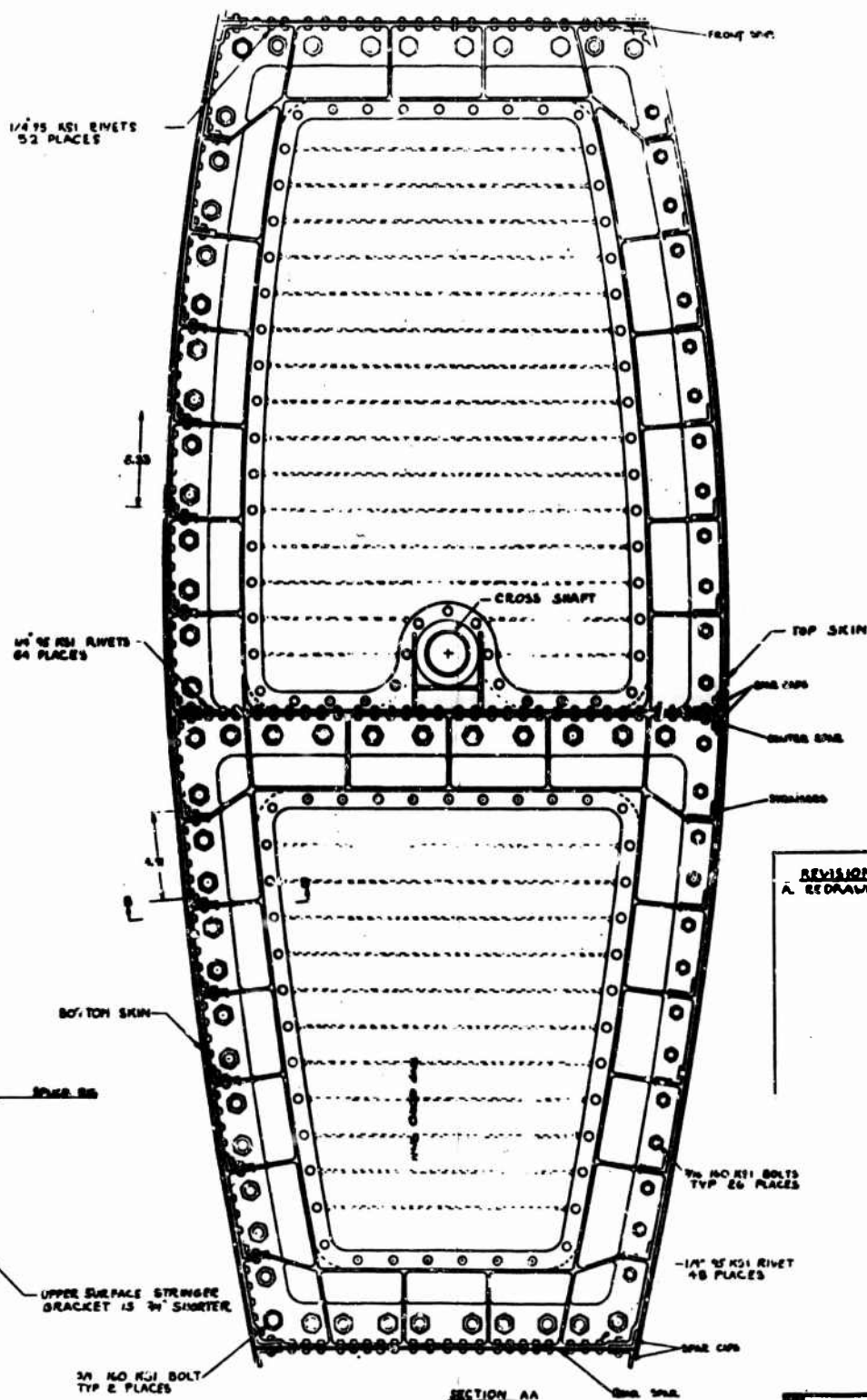
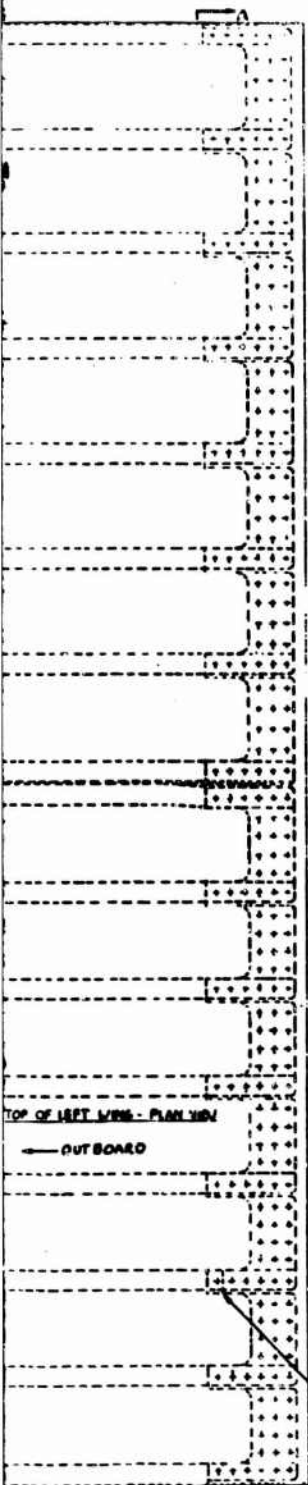
FIGURE IV-4

A



NOT REPRODUCIBLE

B



REVISIONS
A. REDRAWN 11-1-57

SPLICE RIB & ACCESS DOOR
WING SPLICE RIB AND ACCESS DOOR
FIGURE IV-5

DATE	BY	CHKD	APP'D	COMP
THE BELL CO. COMPANY 1000 BELL CO. BUILDING PHOENIX, ARIZONA, U.S.A. MODEL 816 WING SK26-10000 4-11-57				

IV-15

The area between center and rear spars is used for fuel. The fuel area extends spanwise from inboard splice rib to the first rib after the tip close-out-rib. No fuel is carried in the wing area over the fuselage and in the immediate tip area. Each fuel tank bay is provided with a non-structural access door (Figure IV-5) to allow for servicing of tanks and system.

Control surfaces are attached to primary structure by means of multi load path hinges which will prevent loss of any surface due to a single failure. The control surface actuators and the control system (Figure IV-6) are fully redundant and do not encroach upon primary structure area.

5.1 WING TO NACELLE ATTACHMENT STRUCTURE

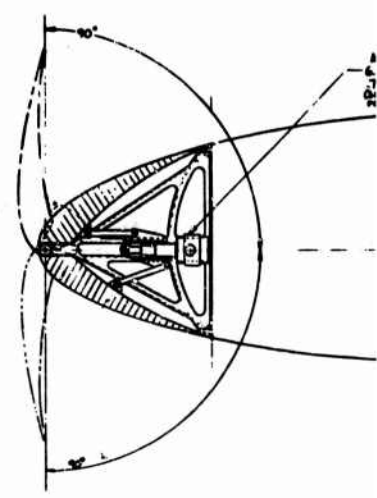
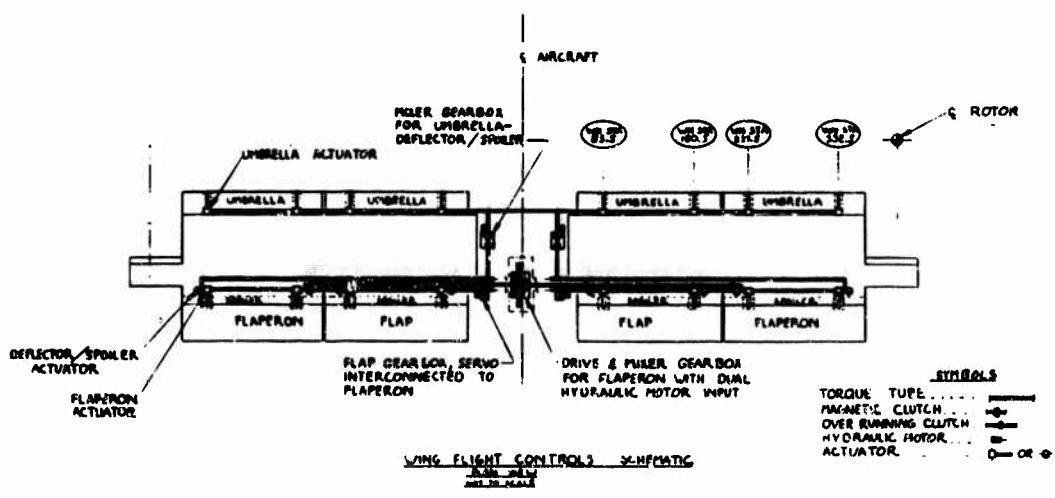
The wing to nacelle attachment beam is considered part of the nacelle structure and is described in Section V. The local re-inforcement required at the wing tip inboard of Station 360.5 however, is considered part of the wing and is shown in Figure IV-7.

5.2 WING ASSOCIATED SYSTEMS

In this section the fuel system and nacelle to nacelle interconnect shafting are described.

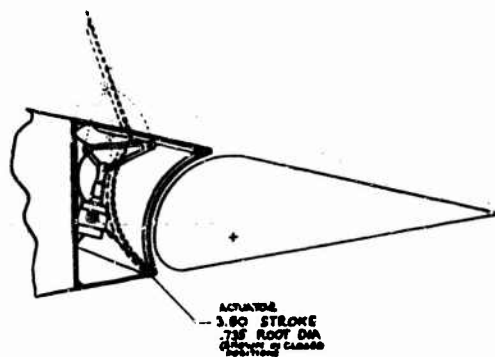
Two conceptual designs of the fuel system have been included, a conventional self-sealing bag type and an improved system to enhance

A

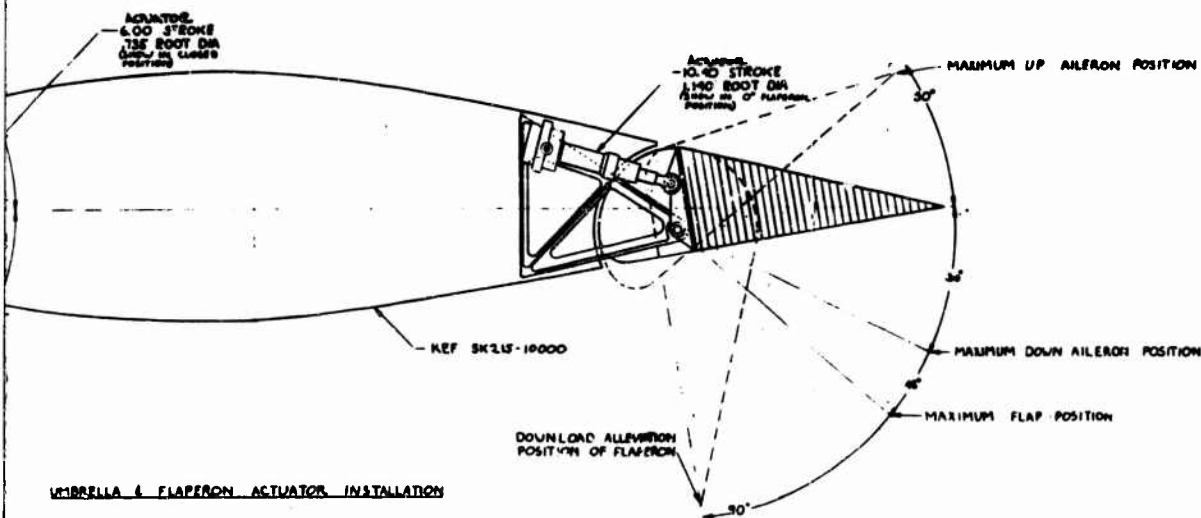


NOT REPRODUCIBLE

B



VARIABLE GEOMETRY DEFLECTOR ACTUATOR INSTALLATION



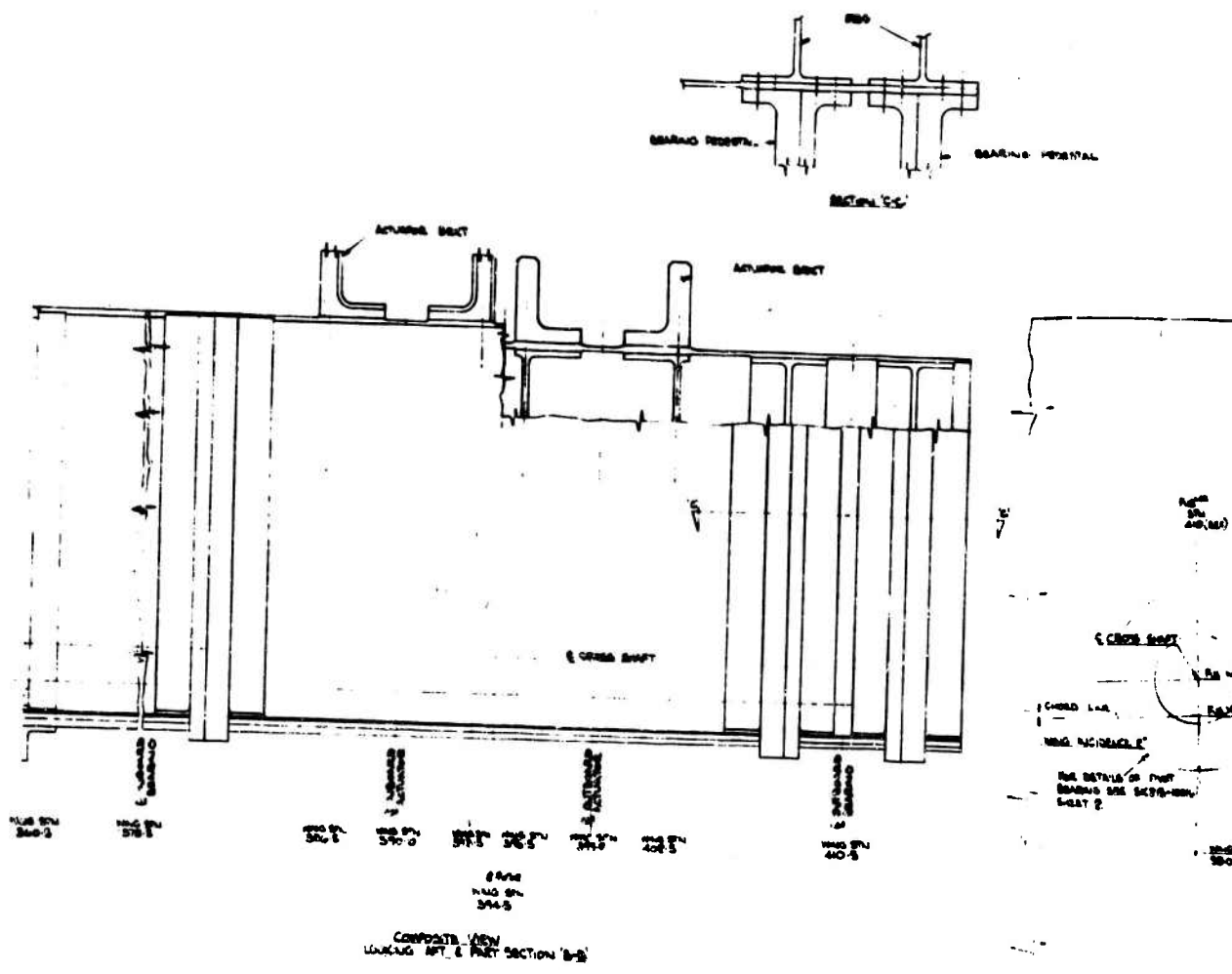
UMBRELLA & FLAPERON ACTUATOR INSTALLATION

WING FLIGHT CONTROL LAYOUT

FIGURE IV-6

NO.	REV.	DATE	BY	CHKD.	DESCRIPTION
THE BUSHNIP COMPANY 1000 N. 10TH ST., PHILADELPHIA, PA.					
MODEL 24 WING FLIGHT CONTROL LAYOUT					
SK215-10017					

A



NOT REPRODUCIBLE

survivability. No choice between the systems has been made because the wing basic structure is not affected by the difference between the systems, and further studies in survivability must be made in order to make the selection.

5.2.1 Fuel System (A)

Fuel system A, the baseline system has conventional self-sealing bag type fuel cells located in the wing between the mid and aft spar. The use of bags will reduce the leakage problems associated with wet wings coupled with skin and stringer construction.

5.2.2 Fuel System (B)

This system is designed to increase the survivability of the aircraft by providing means to eliminate fires and explosions of the fuel by enemy ground fire. This can be achieved by,

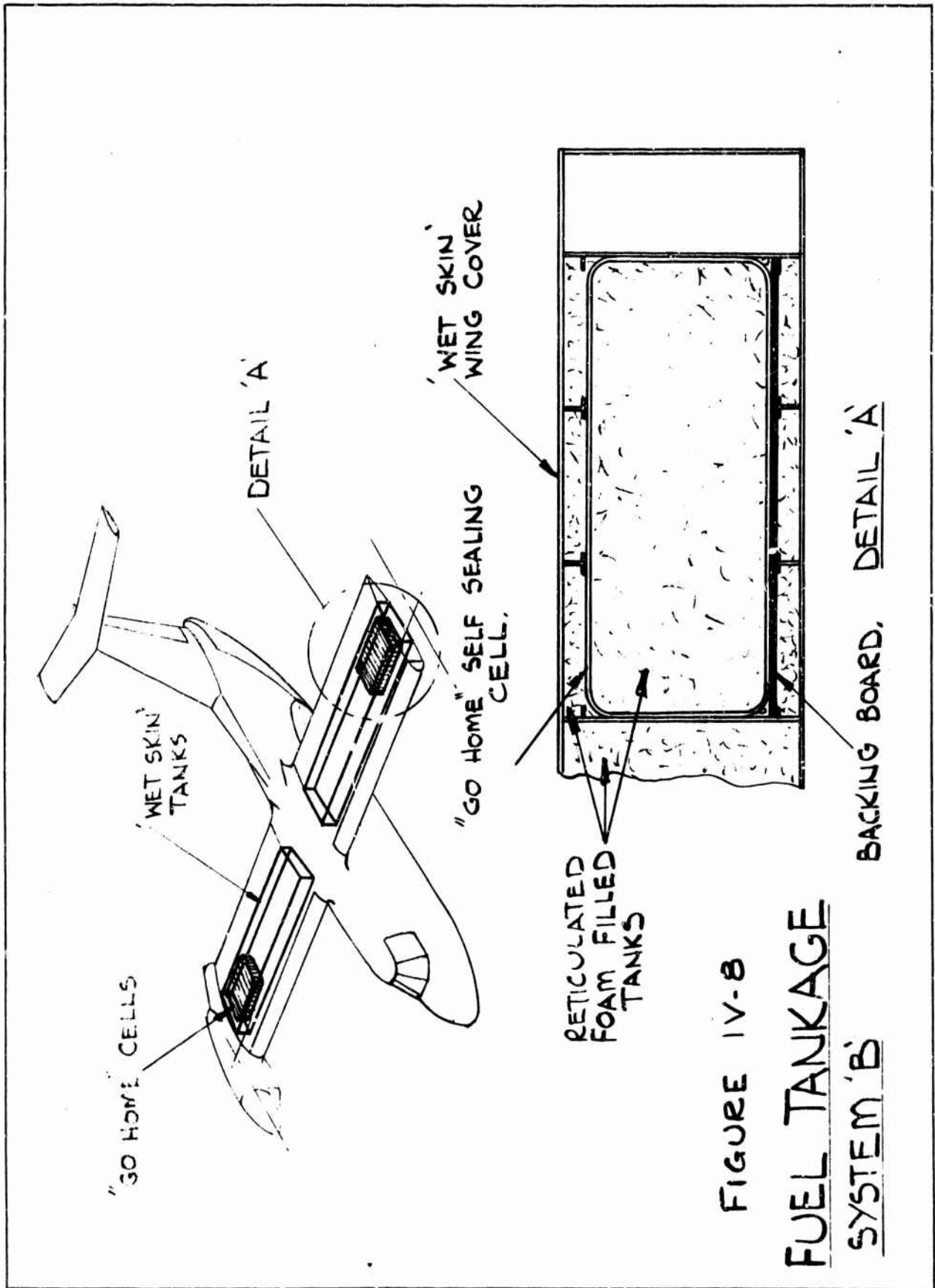
- a) correct fuel placement
- b) improved methods of fuel containment
- c) an effective vapor space ignition suppressor

These objectives can be attained by using simple, low cost, reliable systems incorporating equipment familiar to USAF ground and flight crews as described below.

All the fuel is placed in the wing to take advantage of the available aircraft structure for shielding and to keep the fuel isolated from major ignition sources such as engines.

Fuel containment will be improved by designing an integral "wet skin" tank (Figure IV-8) inside of which is contained a "go home" self sealing cell submerged within the wetted area of the integral tank. This method of fuel containment completely eliminates the potentially explosive air filled areas which are normally present on the tank periphery of conventional bag type containers. Incendiary projectiles penetrating the tank surface, which in this case is the airplane wing skin, immediately enter the liquid and are quenched, fuel will then leak directly to the aircraft exterior and cannot collect in pockets in the aircraft structure.

An effective vapor space ignition suppressor will be achieved by completely filling the interior of all tankage with voided, reticulated foam to suppress fires and explosions occurring in the vapor space above the fuel level. Reticulated foam is preferred to a nitrogen gas inerting system because the nitrogen system introduces an additional active subsystem containing moving parts which are themselves vulnerable to gunfire. System effectiveness is also dependent on a logistical supply of liquid nitrogen.



FORM 46294 (2/66)

5.2.3 Cross Shafting

The cross shaft evaluation was based on Reference IV-1. This report also gave the information required to define the space envelope to contain the system.

The super-critical cross shaft traverses the entire wing at 38% wing chord on the center of chord thickness. The design conditions are as shown in Table IV-2.

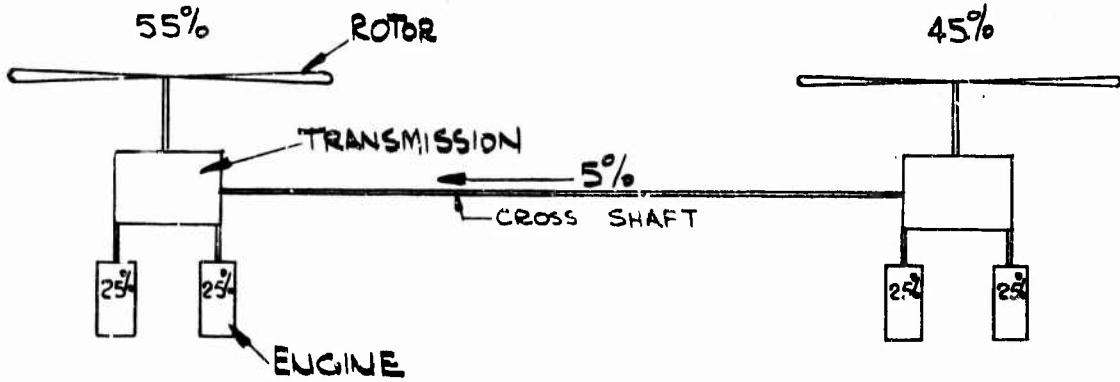
TABLE IV-2. CROSS SHAFT DESIGN CONDITIONS

	FLIGHT ^① CONDITION	NO. ENG. AVAILABLE	CROSS SHAFT TRANSFER HP (LIMIT)	SHAFT	ULT. LOAD FACTOR	FIGURE
400 kt	Dash	4	759	8420	7.34	IV-9a
358 kt	Cruise	3	2466	8420	2.25 ^②	IV-9b
290 kt	Cruise	2	4173	8420	1.46	IV-9c
	①	10,000 Ft Std Day				
	②	Design Condition				

The shaft design condition is the ultimate load condition for a single engine out, (Figure IV-9b) with a 10% (power available) power split to the engine out side. This would give a dynamic life in excess of 3,600 hours under normal operating conditions, with the ability to withstand the loss of two engines in a single nacelle (Figure IV-9c) and still complete the mission.

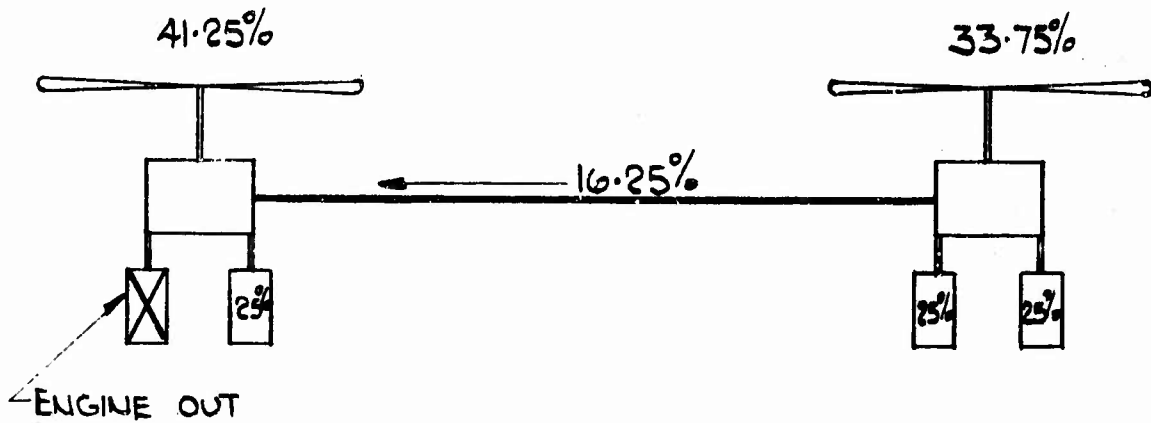
FIGURE IV-9 CROSS SHAFT POWER TRANSFER SCHEMATIC

ALL PERCENTAGES ARE RELATIVE TO A
FLAT RATED POWER OF 15,175 HP.



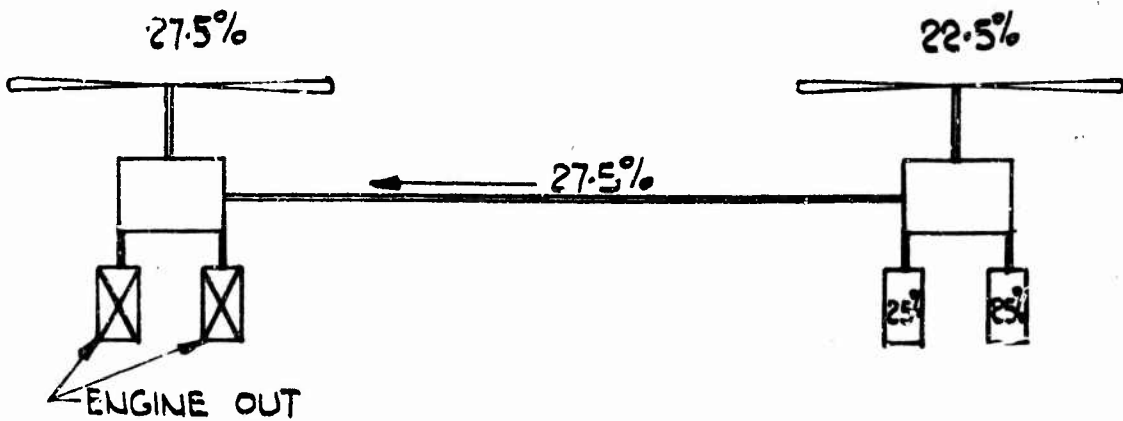
FOUR ENGINES WITH 10% POWER SPLIT

a.



THREE ENGINES WITH 10% POWER SPLIT.

b.



TWO ENGINES WITH 10% POWER SPLIT

c.

The shaft is of aluminum and is fitted with viscous shear dampers for stability. Toroidal shatter guards enclose the shaft at spaced intervals such that any shaft break will not cause a secondary failure.

The cross shaft is installed and serviced through non-structural doors on the lower wing surface.

6. STRUCTURAL ANALYSIS

In this section the design loads, stress analysis and stiffness and deflection characteristics of the primary wing structure and wing to nacelle support structure are described. Material selection is also discussed.

As in conventional aircraft practice, the material allowable stress is chosen to be compatible with fatigue design requirements. A complete wing fatigue analysis must be performed at a later date when the full fatigue loading spectrum for the aircraft is developed based on the combination of missions and cargo. This analysis should not affect the weight of the aircraft to any extent since some consideration of fatigue effect has been included in the non-optimum weight factors.

6.1 DESIGN LOADS

The bending moments, shears and torsions imposed on the wing by the loading conditions 1 and 2 of Table IV-1 are shown in Figures IV-10 and IV-11. Condition 3 is critical for the maximum shear in the wing box section between the fuselage and wing and is equal to 170,000 pounds (ultimate). Condition 1 is the maximum vertical bending and vertical shear condition. Condition 2 produces the maximum torsion on the wing. The curves represent the net results of inertia loads combined with rotor hub loads. The reference axis for wing torsion is at 40 percent of the chord at any wing station and is assumed as the elastic axis of the wing box.

For any helicopter mode flight condition, all of the lift is provided by the rotor and is applied to the wing at the centerline of the rotor. Symmetric maneuvers are performed by applying cyclic pitch control. Wing and fuel masses are applied as concentrated load at several points throughout the wing. Nacelle mass is applied as a concentrated mass at its respective center of gravity.

6.2 STRESS ANALYSIS

6.2.1 Load Paths

Basic wing box skin-stringers, spar caps and webs sizes are calculated at four wing stations (stations 360.5, 250, 150 and 50). Wing

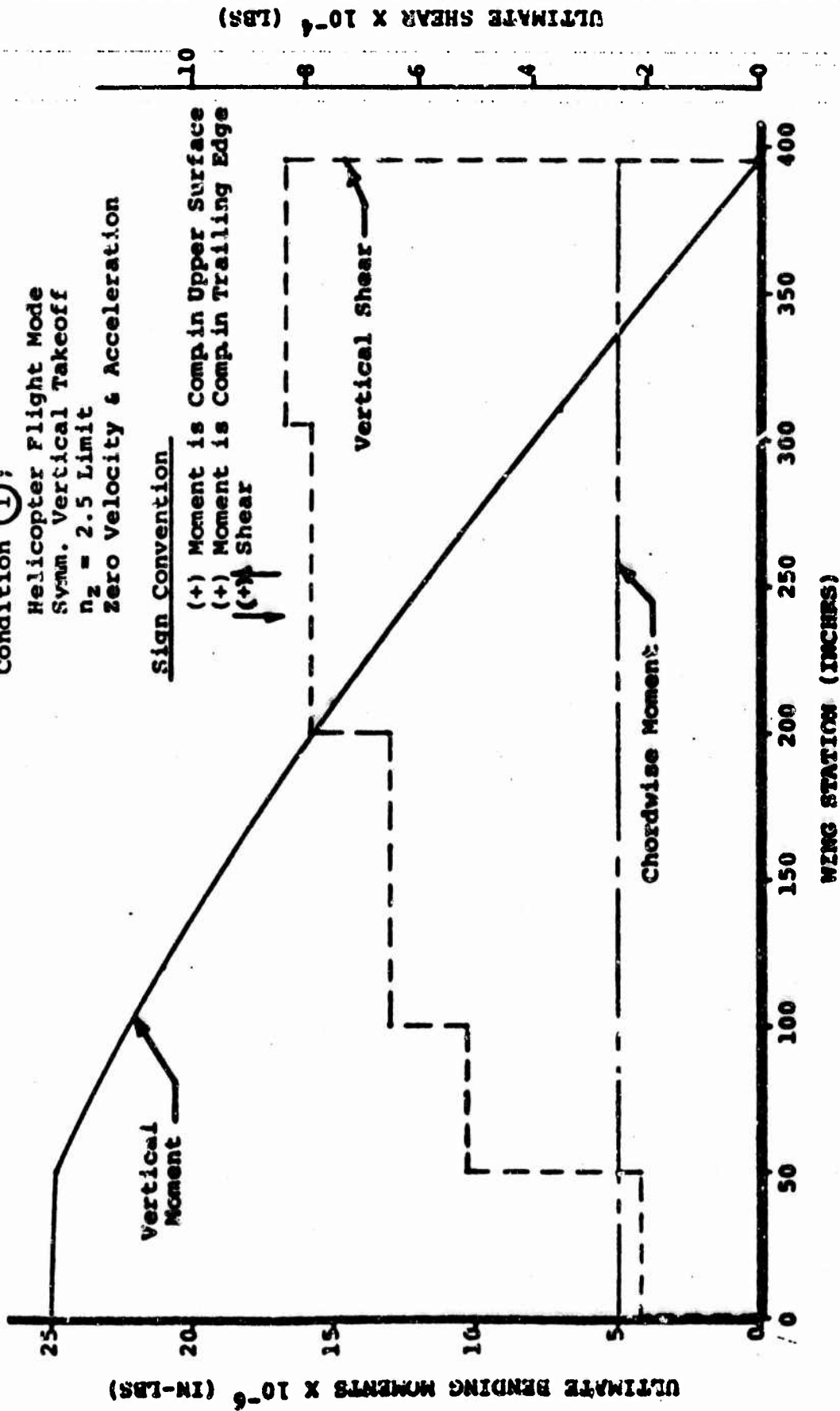
USAF MODEL 215

Condition (1):

Helicopter Flight Mode
 Symm. Vertical Takeoff
 $n_z = 2.5$ Limit
 zero Velocity & Acceleration

Sign Convention

(+) Moment is Comp in Upper Surface
 (+) Moment is Comp in Trailing Edge
 (+) Shear



MODEL 215 WING
 ULTIMATE SHEAR AND BENDING MOMENTS

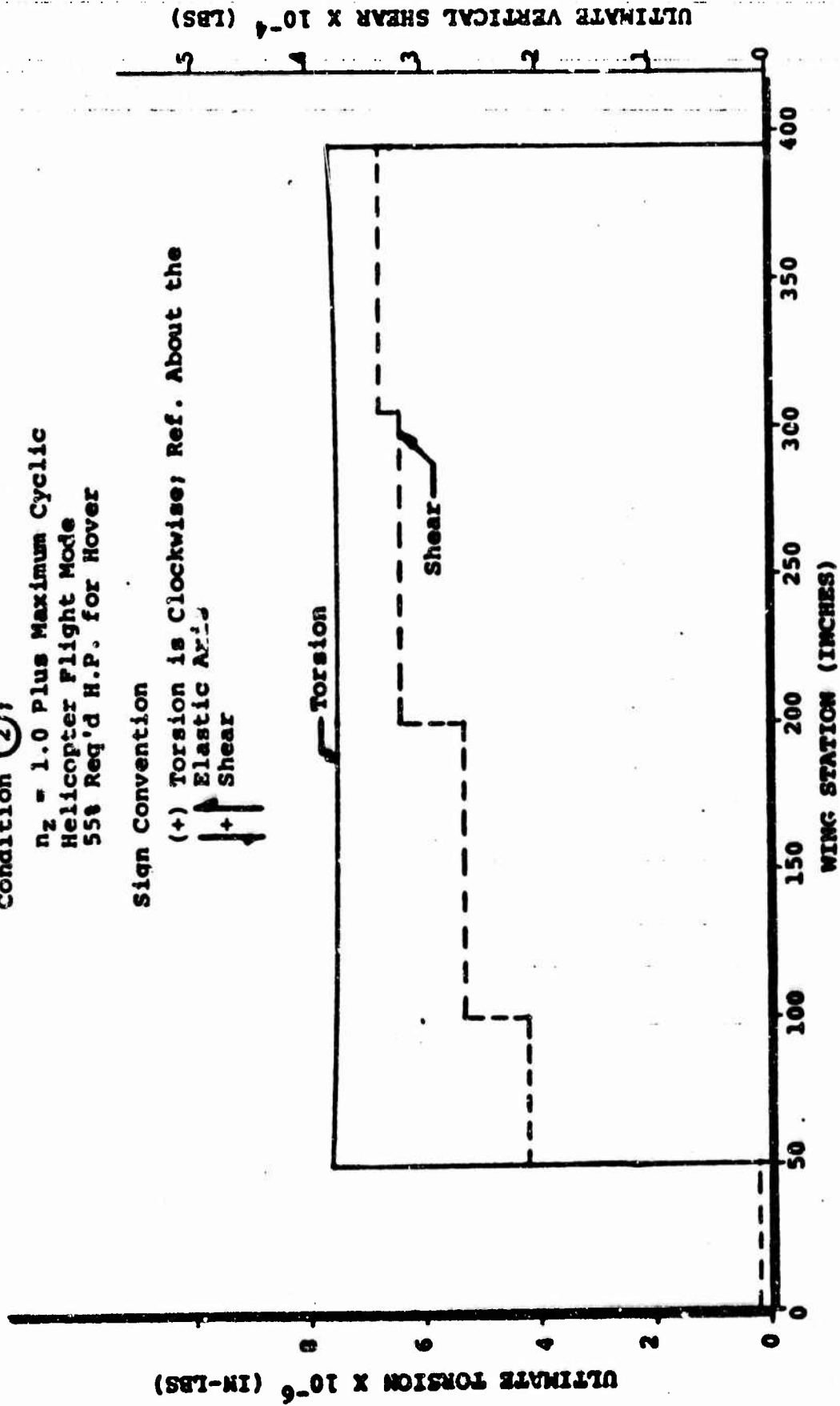
USAF MODEL 215

Condition (2)

$n_z = 1.0$ Plus Maximum Cyclic
Helicopter Flight Mode
55% Req'd H.P. for Hover

Sign Convention

(+) Torsion is Clockwise; Ref. About the
Elastic Axis



MODEL 215 WING
ULTIMATE VERTICAL SHEAR AND TORSION

FIGURE IV-11

torsion is reacted by the wing box, vertical shear by the spar webs and bending by the stringers and spar caps. For this study, the wing box is assumed as a single cell and the area requirements due to bending equally divided into stringers and spar caps.

The bending material requirements are based on a heavy-flanged beam theory (M/h). The effective depth of the beam is the area of the airfoil between front and rear spars divided by the distance between these two spars and further reduced by the centroids of the reacting flanges. 30 times the skin thickness is considered effective as additional area for each stringer in compression.

The tension surface minus rivet hole areas is considered to be fully effective. Stringer compression allowables are based on column strength. Spar web thickness is based on all the vertical shear reacted by the spars in addition to shear flow produced by torsion. Relieving shear flows were neglected and the maximum due to vertical or torsional shear is used for design.

At station 360.5, area in which the wing changes from a full section to a smaller box section, the intermediate spar is designed to react most of the vertical load.

6.2.2 Material Selection

Material selection for the basic wing box primary load structure is 2024-T3 lower skin, 2024-T3511 extruded stringers and caps, 7075-T6 upper skins, 7075-T6511 extruded stringers and caps and 7075-T73 forgings.

The 2024 alloy was chosen because of its superior fatigue properties and low crack propagation. The 7075 alloy was chosen for its high compressive yield strength and the -T73 temper in forgings is exceptionally resistant to stress corrosion.

6.2.3 Wing Structure Summary

Table IV-3 presents the summary of the basic wing box skin gauges, stringer sizes and material. Table IV-4 presents the summary of the spar web gauges and material.

6.3 WING STIFFNESS AND DEFLECTIONS

The representative stiffness, EI and GJ, are shown in Figure IV-12 and are based on wing ultimate strength requirements. Spanwise and chordwise EI values from wing station 330 to 360.5 are modified to adjust for shear lag due to the abrupt change in the wing box section at station 360.5. The torsional stiffness (GJ curve) is calculated as a single cell except that it is modified to include the effects of the intermediate spar length and thickness.

TABLE IV-3
SUMMARY OF SKIN-STRINGER REQUIREMENTS

STATION	SKIN THICKNESS		STRINGER SIZE		TYPE MBR
	UPPER	LOWER	UPPER	LOWER	
360.5	.063 ↑↓	.073 ↑	3/4 x 1 x .3 .090, 1.25, .090	3/4 x 1 x .3 .080, 1.25, .080 ↑	ZEE ↑ ↓ ZEE
284.0	.063 ↓	↑↓	3/4 x 1 x .3 .090, .125, .090	↓	
250.0	.098 ↓	.073 ↓	↓	3/4 x 1 x .3 .080, .125, .080	
150.0	.141 ↓	.122 ↓	↓	↓	
50.0	.166 ↑↓	.166 ↑↓	7/8 x 1.07 x .3 .160, .125, .090	7/8 x 1.07 x .3 .160, .125, .090	
0	.166	.166	7/8 x 1.07 x .3 .160, .125, .090	7/3 x 1.07 x .3 .160, .125, .090	

- NOTES: 1. ZEE stringer dimensions: first line, first number is skin flange, second number is vertical flange, third number is inside flange; second line, respective flange thickness
2. Material: upper surface skin-stringer, 7075-T6/T6511; lower surface skin-stringer, 2024-T3/T3511
3. ↑↓ indicates constant
↓ indicates linear variation

TABLE IV-4

SUMMARY OF SPARS REQUIREMENTS

SPAR	STATION	WEB THICKNESS	STIFFENER SIZE & THICKNESS	STIFFENER SPACING
Front	0-50	.080	1 x 1 x 7/8 x .080	6.0
	50-360.5	.063	3/4 x 1 x 5/8 x .063	6.0
Intermediate	0-320.5	.080	1 x 1 x 7/8 x .090	5.5
	320.5-360.5	.090	1 x 1 x 7/8 x .090	5.5
Rear	0-360.5	.080	1 x 1 x 7/8 x .080	5.5

Material - 7075-T6/T6511

USAF - MODEL 215

WING STIFFNESS - THICK SKIN DESIGN

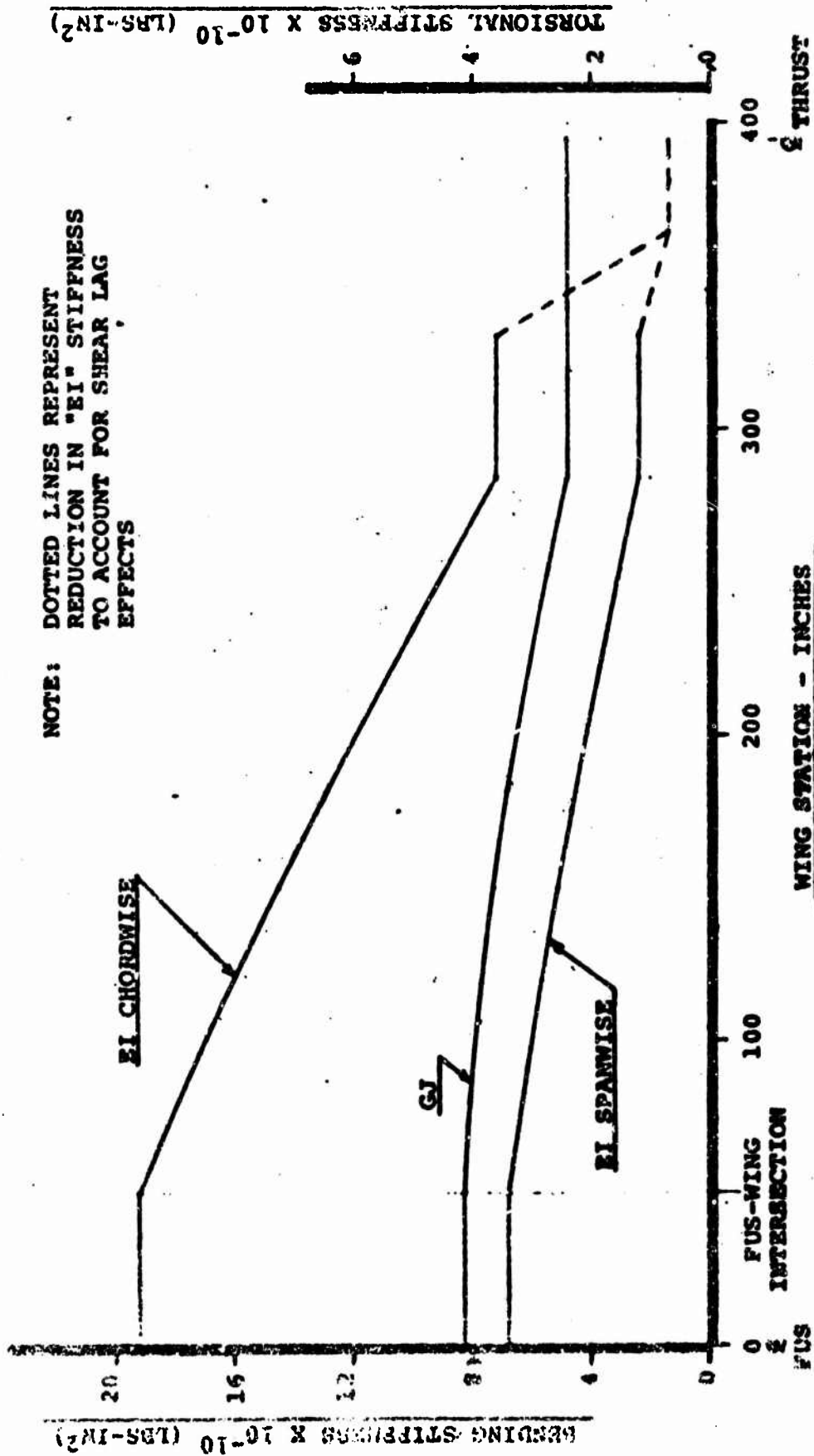


FIGURE IV-12 WING STIFFNESS CURVES

NOT REPRODUCIBLE

Figure IV-13 contains plots of torsion due to a unit load (1.0 inch-pound) and wing deflection due to 1.0g lift applied at station 394.5 which is the centerline of the nacelle. Also included is the deflection due to weight of the wing-nacelle combination for the design gross weight of 67,000 pounds. These data are used in Section VIII to calculate dynamic stability and vibration of the aircraft.

7. WEIGHT ANALYSIS

A summary of wing weights is provided in Table IV-5. The weight of the wing as quoted in Reference I-1 was derived by VASCOMP, a computerized airplane sizing and weight determination program. The detailed design as described in Part 4 of this section and the Structural Analysis in Part 5 provide the necessary data for the weight evaluation of the torque box, constructed of conventional, built-up skins, stringers, etc. This wing design is called wing A and would be the simplest to manufacture. Since the weight of wing A is 12% above the VASCOMP target weight, a new design, B the present baseline design, was derived based on built-up structure with machined skin, stringers and spar caps. The weight of the secondary structure was determined by using empirical relations which are described later.

Further reductions in weight can be achieved for 1972 technology by using composite substitution such as boron-epoxy as described

USAF - MODEL 215
WING DEFLECTIONS AND TWIST
HELICOPTER FLIGHT MODE

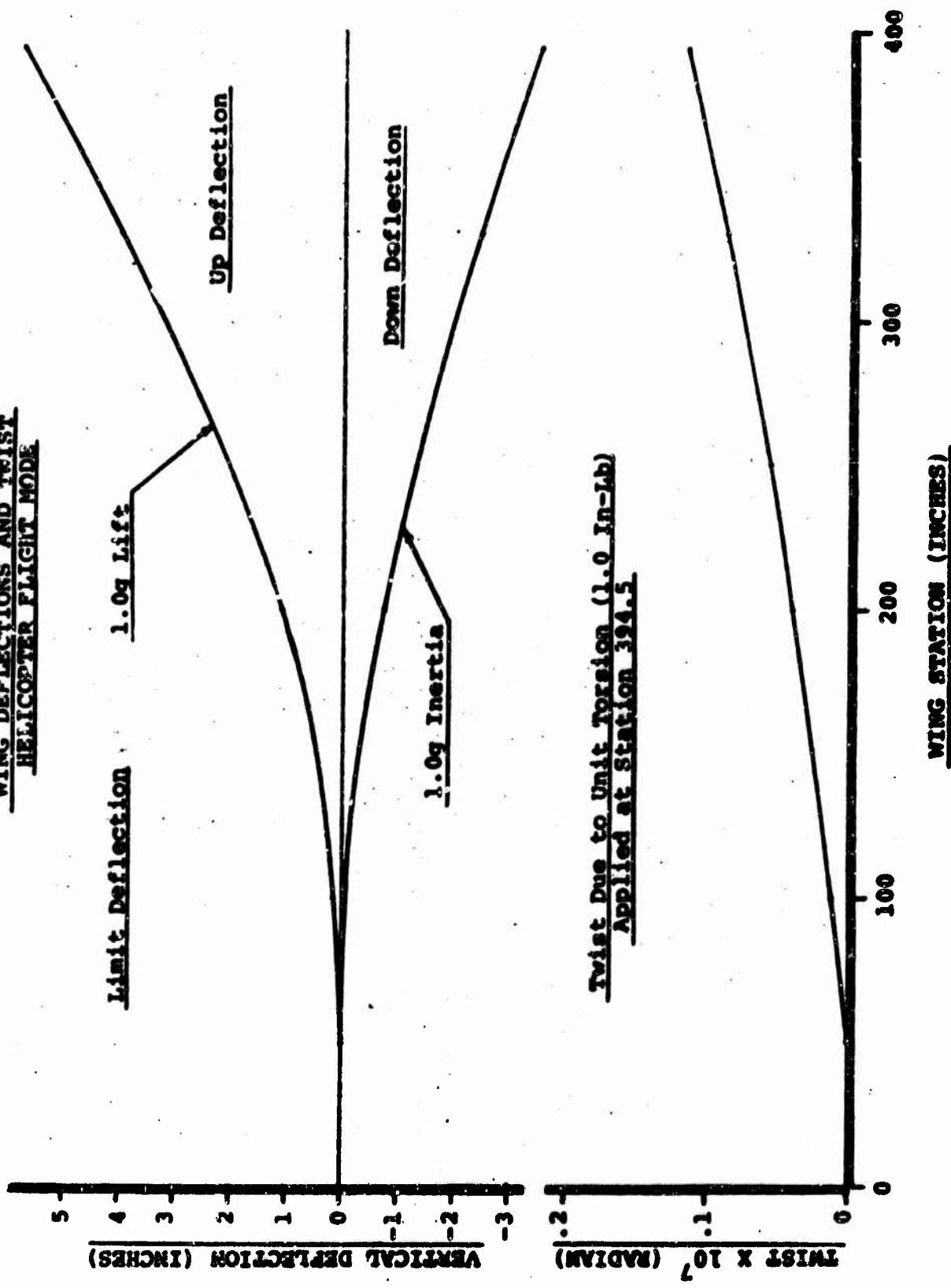


FIGURE IV-13 WING DEFLECTION AND TWIST

TABLE IV-5
SUMMARY OF WING WEIGHTS

	ORIGINAL ESTIMATE (TARGET)	BASIC DESIGN		PROPOSED DESIGN	
		BUILT-UP SKINS, STRINGERS ETC.	MACHINED INTEGRAL SKIN AND STRINGERS	BUILT-UP SKINS, STRINGERS ETC.	MACHINED INTEGRAL SKIN AND STRINGERS
Basic Wing (1970 Technology)	5077	5800	5528	5800	5528
Provisions for Wing Tip (1970 Technology)	500	422	405	362	355
Total Wing (1970)	5577	6222	5933	6162	5883
1972 Technology Reduction - Wing	-632	-725	-691	-725	-691
1972 Technology Reduction - Tip Provisions		-53	-51	-45	-44
Total Wing (1972 Technology)	4945	5444	5191	5392	5148

in Reference I-1. Existing component studies indicate that this substitution technique can be employed by the 1972 time frame. The structural design and manufacturing remain essentially conventional but boron-epoxy replaces aluminum. A conservative estimate of 12.5% group weight reduction can be achieved by using boron-epoxy substitution. Wing design C with 1972 technology is thus shown to be 5% heavier than the target weight in Table IV-5.

A Boeing-Vertol value engineering study made of another VTOL aircraft wing box showed a 14.6% weight savings achieved by the use of a combination of titanium and boron and also for a combination of titanium and carbon. This was a weight saving over the weight of an all aluminum alloy riveted structure with extruded stringers and constant thickness sheets.

The carbon titanium structure achieved the weight reduction at a lower cost than for the boron titanium structure. Material costs used were \$6/lb for aluminum (no machining), 100 \$/lb for boron, 100 \$/lb for titanium and 40 \$/lb for carbon (estimated 1970 prices). The cost of a pound of fabricated carbon and titanium structure was \$100 and the cost of a pound saved using carbon and titanium was \$266. The cost of a pound of fabricated boron and titanium structure was \$149 and the cost per pound saved was \$549.

Integrally machined skin and stringers structures cost approximately \$93/lb. Machined stringers riveted to non-constant thickness skins cost \$56/lb.

These data show the potential of lower cost weight reduction as composites such as carbon used with titanium are adapted in production.

A review of the design conditions that dictate the weight of the wing has revealed that condition 1 in Table IV-1, the vertical takeoff at 2.5g is by far the most critical from a design point of view. This requirement is not compatible with present helicopter practice and needs further definition through testing in Phase III. It is expected that when the vertical takeoff requirement has been better defined, the resulting wing weight will be less than or equal to the target weight.

7.1 BASIC WING WEIGHT

The basic wing weight consists of the torque box and the secondary structure weight. The basic wing weights are summarized in Table IV-6. Basic torque box weight consists of upper and lower covers; front, center and rear spars; ribs and miscellaneous items such as sealants, small fittings and paint. Provisions for self-sealing fuel tanks are also included in torque box weight. Non-optimum factors which account for additional material required for inter-

TABLE IV-6
BASIC WING WEIGHT

	ORIGINAL ESTIMATED WEIGHT (TARGET)	CALCULATED WEIGHT	
		DESIGN A BUILT-UP SKIN STRINGERS	DESIGN B MACHINED SKIN AND STRINGERS
Torque Box		4299	4027
	Non-Optimum Factor		
Upper Cover	1.30	1114	982
Lower Cover	1.26	1010	870
Front Spar	2.20	356	356
Center Spar	2.20	544	544
Rear Spar	2.20	415	415
① Ribs		688	531
② Miscellaneous		172	170
Leading Edge (Movable)		367	367
Inboard		178	178
Outboard		189	189
Trailing Edge		240	240
Fixed		150	150
Movable		185	185
Flaps		292	292
Flaperons		507	507
Basic Wing Weight (1970 Technology)	5077	5800	5528
1972 Technology Reduction (12.5%)	-632		-691
Basic Wing Weight (1972 Technology)	4445		4837 3

- ① 20% of cover and spar weight
- ② 5% of cover and spar weight
- 3 Design C

acting loads, splices, standard gauges, access doors, etc. were applied to obtain the final weight. Rib weight was determined as 20% and miscellaneous items as 5% of the cover and spar weights. The calculated weight for the torque box, modified by the non-optimum factor are summarized for design A, the built-up skin and stringer and design B, the built-up machined skin and machined stringer in Table IV-6. Design B torque box is 272 pounds or 6.3% lighter.

The secondary structure consists of leading edges, trailing edges, flaps and flaperons. The weights of these components are based on empirical equations and are derived below.

Leading Edge: The leading edge of this wing is hinged at the nose and opens forward during hover to decrease the download area of the wing.

$$\text{Leading Edge } W_{LE} = S_{LE} (0.003) \left[\frac{N W_g \cos^2 \Lambda_{BOX}}{b (t/c)} \right]^{0.693}$$

W_{LE} = weight of leading edge

S_{LE} = projected area

$$S_{LE} \text{ (inboard)} = 45.2 \text{ ft}^2$$

$$S_{LE} \text{ (outboard)} = 48.0 \text{ ft}^2$$

n = ultimate load factor = 4.5

w_g = design gross weight = 67,000 lbs

Λ_{BOX} = sweep angle of box = 0

b = wing span = 65.8'

t/c = thickness ratio = .21

Leading Edge Supports

$$W_{SLE} = 0.091 (W_{LE})^{1.25}$$

Therefore:

weight of inboard leading edge = 132

weight of inboard leading edge supports = 42

total inboard leading edge = 178 lbs.

weight of outboard leading edge = 144

weight of outboard leading edge supports = 45

total outboard leading edge = 189 lbs.

Trailing Edge: The trailing edge consists of a fixed section and a movable section which folds during hover to reduce the download area. For purposes of weight estimating, the movable section is treated as a spoiler.

Trailing Edge - Fixed

$$W_{TE} = S_{TE} (0.000349) \left[\frac{N W_q \cos^2 \Lambda_{BOX}}{b (t/c)} \right]^{0.89}$$

$$S_{TE} = 60 \text{ ft}^2$$

Therefore:

weight of trailing edge = 150 lbs.

Trailing Edge - Movable

$$W_{MTE} = 0.558 (V_D)^{0.25} S_{MTE}$$

$$S_{MTE} = (\text{inboard}) = 17.8 \text{ ft}^2$$

$$S_{MTE} = (\text{outboard}) = 18.8 \text{ ft}^2$$

Therefore:

weight of inboard movable trailing -

inboard = 90

outboard = 95

185 lbs.

Flaps: The flaps are the single slotted type and are on the inboard wing only.

Flaps

$$W_F = S_F (0.253) (V_D)^{0.375}$$

$$S_F = 90.8 \text{ ft}^2$$

Flap Supports

$$W_{SF} = 0.0885 (W_F)^{1.25}$$

Therefore:

flaps weight = 218

supports weight = 74

total = 292 lbs.

Flaperons:

The flaperons are considered basically as a flap, counter balanced similar to an aileron.

Flaperon

$$W_F = S_F (0.253) (V_D)^{1.25} + W_{BW}$$

$$S_F = 95.8 \text{ ft}^2$$

Supports

$$W_{SF} = 0.0885 (W_F)^{1.25}$$

Therefore:

flaps weight	=	230
balance weights	=	<u>196</u>
total	=	426
flaperon support weight	=	<u>81</u>
total flaperons	=	507 lbs.

Table IV-6 is a summary of the basic wing weights as discussed in the previous paragraphs. It shows the target weight and calculated weight for both the built-up skin and stringer and the machined skin and stringer designs. Design C shows the anticipated reduction for 1972 technology.

7.2 WING TIP AND NACELLE SUPPORT

The wing tip and nacelle support outboard of wing station 360.5 is covered in the nacelle and tilting mechanism, Section V.

7.3 PROVISIONS FOR WING TIP ATTACHMENT

The weight for the provisions for wing tip attachment summarized in Table IV-7 is that which is required for the transfer of the rotor load between the wing tip and the basic wing. This structure extends inboard into the wing for approximately two feet.

The basic design is such that the lower cover of the wing tip and that of wing do not coincide; therefore, the diagonal shelf must be provided to transfer the loads into the lower cover.

The forward spar of the wing tip also does not coincide with the wing center spar, and an additional diagonal spar must be provided to transfer the loads. An effort to redesign the wing tip so that the lower skins coincide showed a decrease of approximately forty pounds in the wing tip attachment provision weight.

1972 technology would use boron-epoxy substitution for aluminum where possible for a total saving of 29.2%.

TABLE IV-7

WEIGHT PROVISIONS FOR WING TIP ATTACHMENT

	ORIGINAL ESTIMATE (TARGET)	BASIC DESIGN		PROPOSED DESIGN	
		BUILT-UP SKIN STRINGERS ETC.	MACHINED INTEGRAL SKIN AND STRINGERS	BUILT-UP SKIN STRINGERS ETC.	MACHINED INTEGRAL SKIN AND STRINGERS
Upper Cover		35	31	25	22
Lower Shelf		48	41		
Lower Shelf/Skin Interconnect		42	36		
Lower Cover				27	23
Center Spar		151	151	160	160
Rear Spar		146	146	150	150
Total (1970 Technology)		422	405	362	355
1972 Technology Reduction (12.5%)		-53	-51	-45	-44
Total (1972 Technology)	500	369	354	317	311

8. SURVIVABILITY

A survivability analysis was not part of the basic contract but the following aspects of design and material choice contribute to survivability:

- a. plate and stringer type construction gives multipath load carrying capability.
- b. the three spar, two cell torque box provides freedom from divergence and whirl flutter with one of the spars cut as discussed in Section VIII.
- c. the 7075-T6 material is not as good as the 2024 from a fatigue and notch sensitivity viewpoint, but the plate and stringer construction used for the Model 215 wing will allow its use. The weight penalty of using 2024 for the upper cover needs to be investigated.
- d. fuel system B reduces the vulnerability of an aircraft loss due to a fuel tank hit.
- e. the cross-shaft gives protection from the loss of engine/ engines on one side of the aircraft.

9. CONCLUSIONS AND RECOMMENDATIONS

The basic design proposed for the Model 215 wing is structurally sound but is 246 pounds (5%) over the target weight. The following design aspects and criteria need to be investigated to

determine if the weight can be reduced.

- a. The design condition of 2.5g vertical takeoff in hover is beyond the thrust capability of a rotor designed for the normal hover condition. The thrusting capability of a rotor in hover must be determined to change the criterion.
- b. The wing tip nacelle attachment box accommodations need to be re-examined to determine if more efficient load paths can be established for less weight.
- c. The use of composites with high modulus and high strength must be evaluated for the wing design, since a major saving in weight can be predicted from similar studies referenced in Reference I-1, weights section.
- d. The fatigue spectrum for the wing must be established and the details of fatigue design worked.

SECTION V

ROTOR NACELLE AND TILTING MECHANISM DESIGN

1. INTRODUCTION

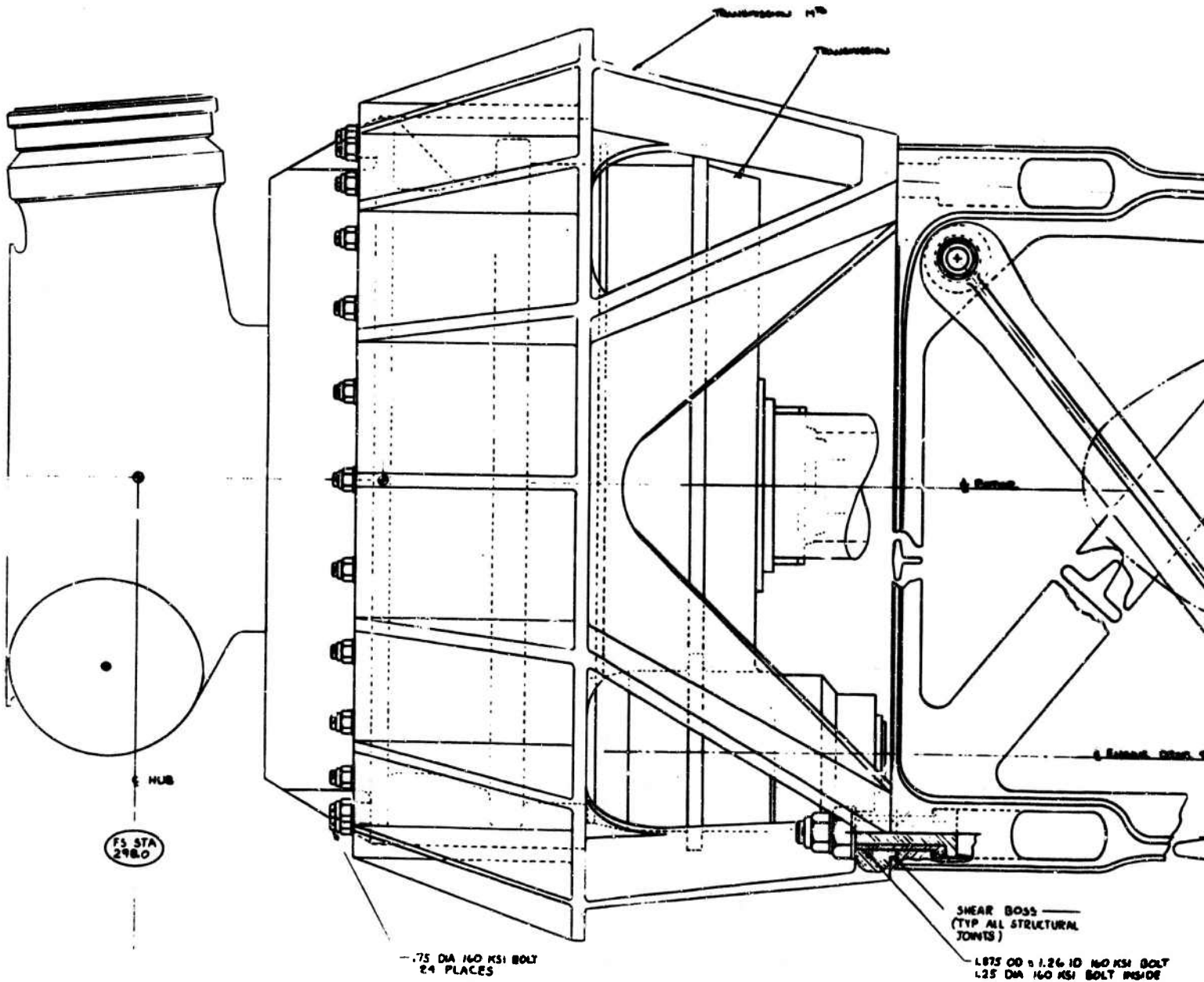
In this section the design of the wing tip nacelle support, tilting mechanism and nacelle primary structure are described. No attempt has been made to further define the other systems in the nacelle such as the oil cooler and engines since their impact on weight are small. These systems have been allocated space as shown in Figure I-1 and Figures V-1 and V-2.

The target weight from Reference I-1 for the wing tip nacelle support and the tilting mechanism is 1005 pounds per aircraft. The designs in this study vary from 1659 to 2157 which is 165 to 214% of the target weight. A thorough review of the criteria as well as the design are required in this area.

The stresses in the nacelle primary structure show that most of the members are lightly loaded. This truss needs considerably more design effort. Criteria defining the failure modes of the nacelle are required.

As shown in Section VIII the dynamics of the Tilt Rotor aircraft are significantly affected by the combined wing-nacelle stiffnesses. In the present study it has been estimated that the nacelle torsional stiffness is 73×10^6 ft lb/rad. The stiffnesses in the vertical and chord bending modes have been assumed to be large in comparison to the wing stiffnesses.

A



B

FS STA 370.62
FS WL 243.8

ACTUATOR

FRONT BRACING MEMBER

CHINA SHIPT BRNLL. Bolt

HYDRAULIC MOTOR

SEE SHEET 10000 SHG FOR FURTHER DETAILS

NACELLE PINOT

.625 DIA 160 KSI BOLT

CHINA SHIPT BRNLL. SHIPT

1.25" DIA 160 KSI BOLT (TYP)

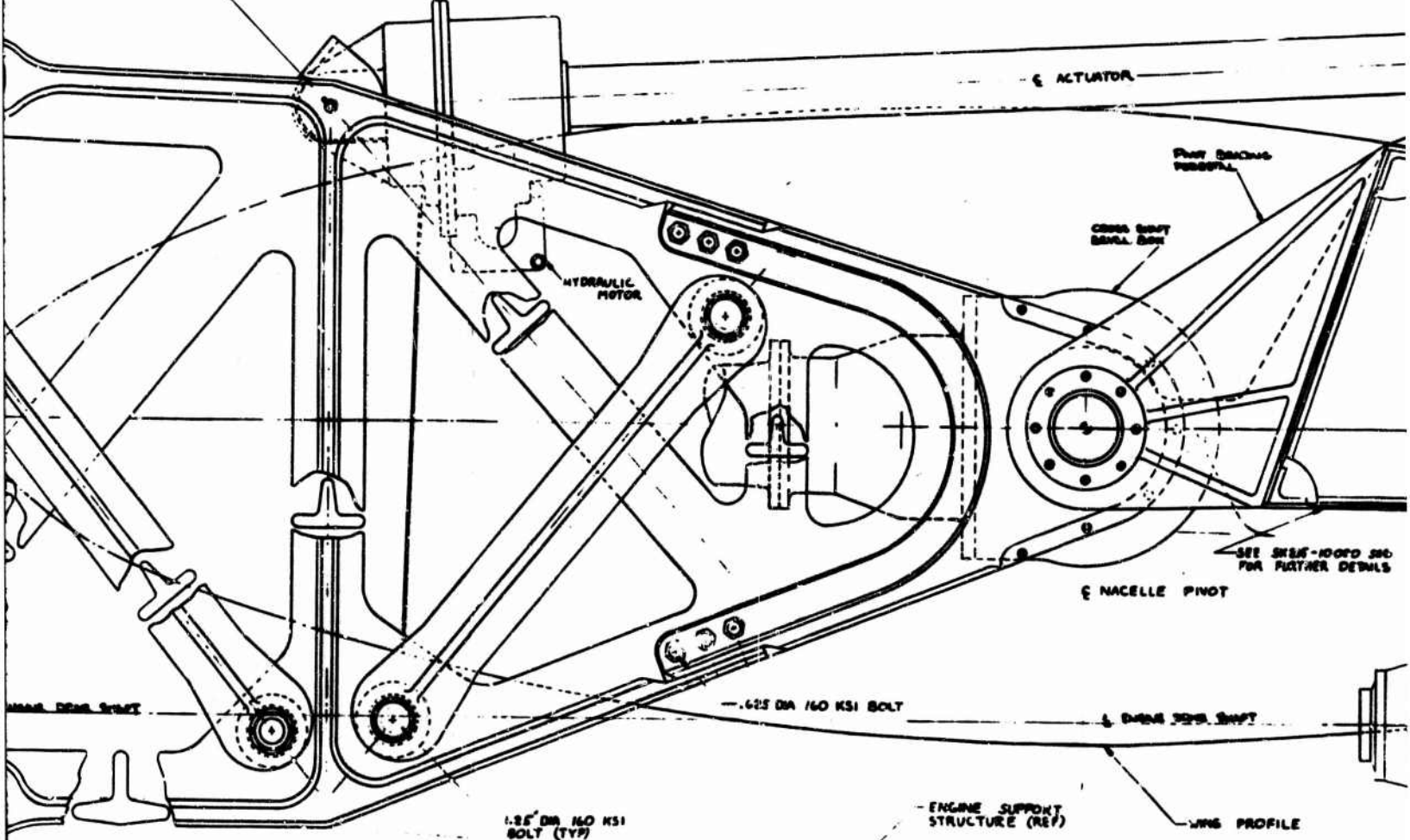
ENGINE SUPPORT STRUCTURE (REF)

WING PROFILE

ELEVATION VIEW

FS STA 370.0

160 KSI BOLT INSIDE



C

FS STA 145.4
FS WL 247.4

SEE DRAWING
10000

FS WL
228.0

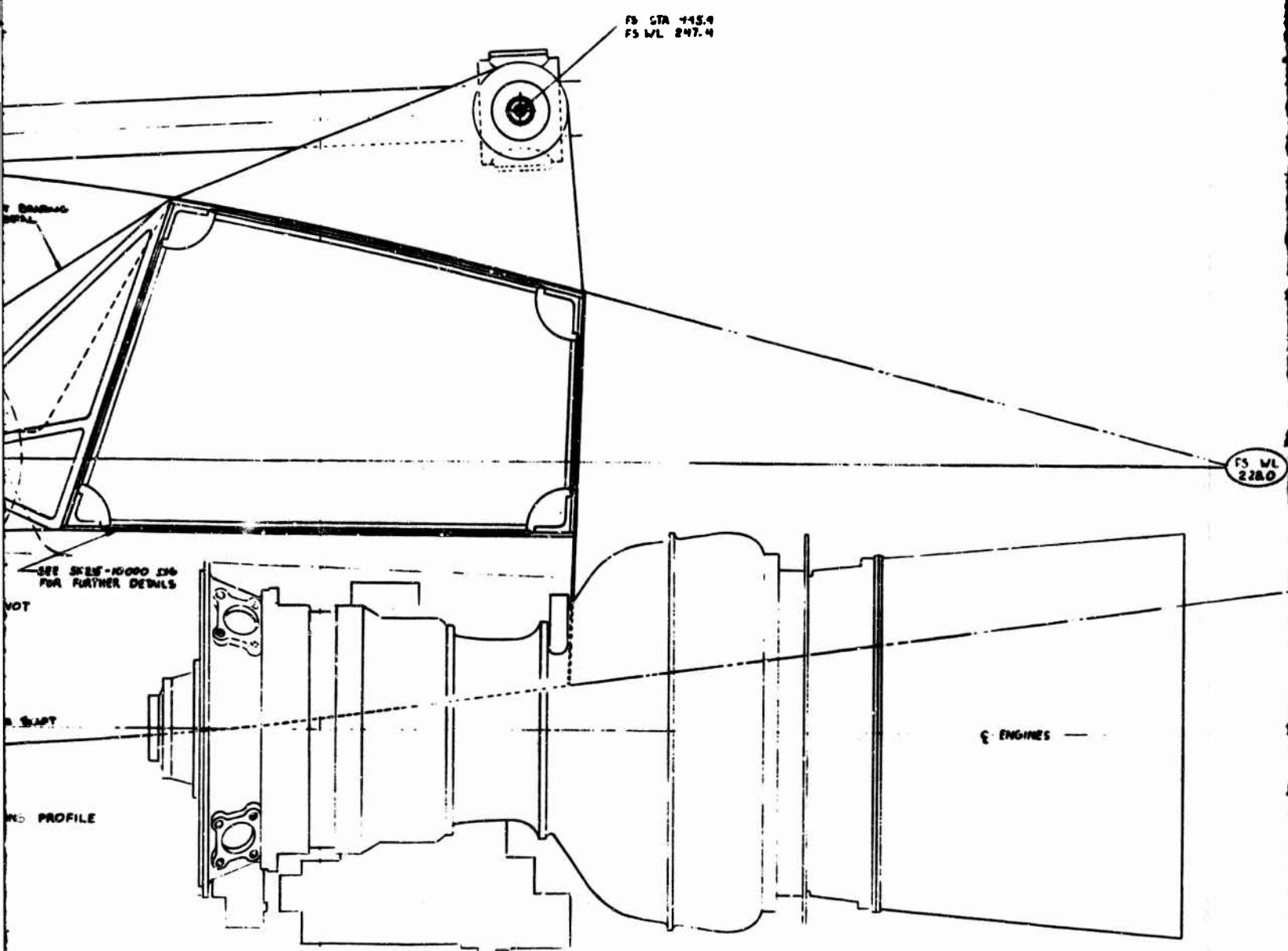
SEE SKETCH 10000 100
FOR FURTHER DETAILS

NOT

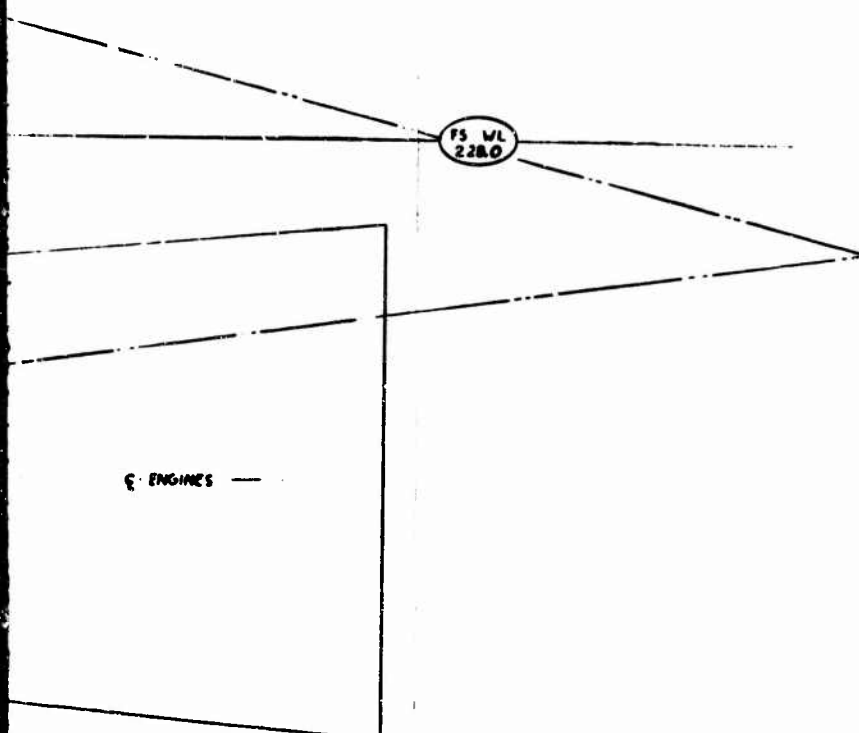
SHIPT

PROFILE

ENGINES



D



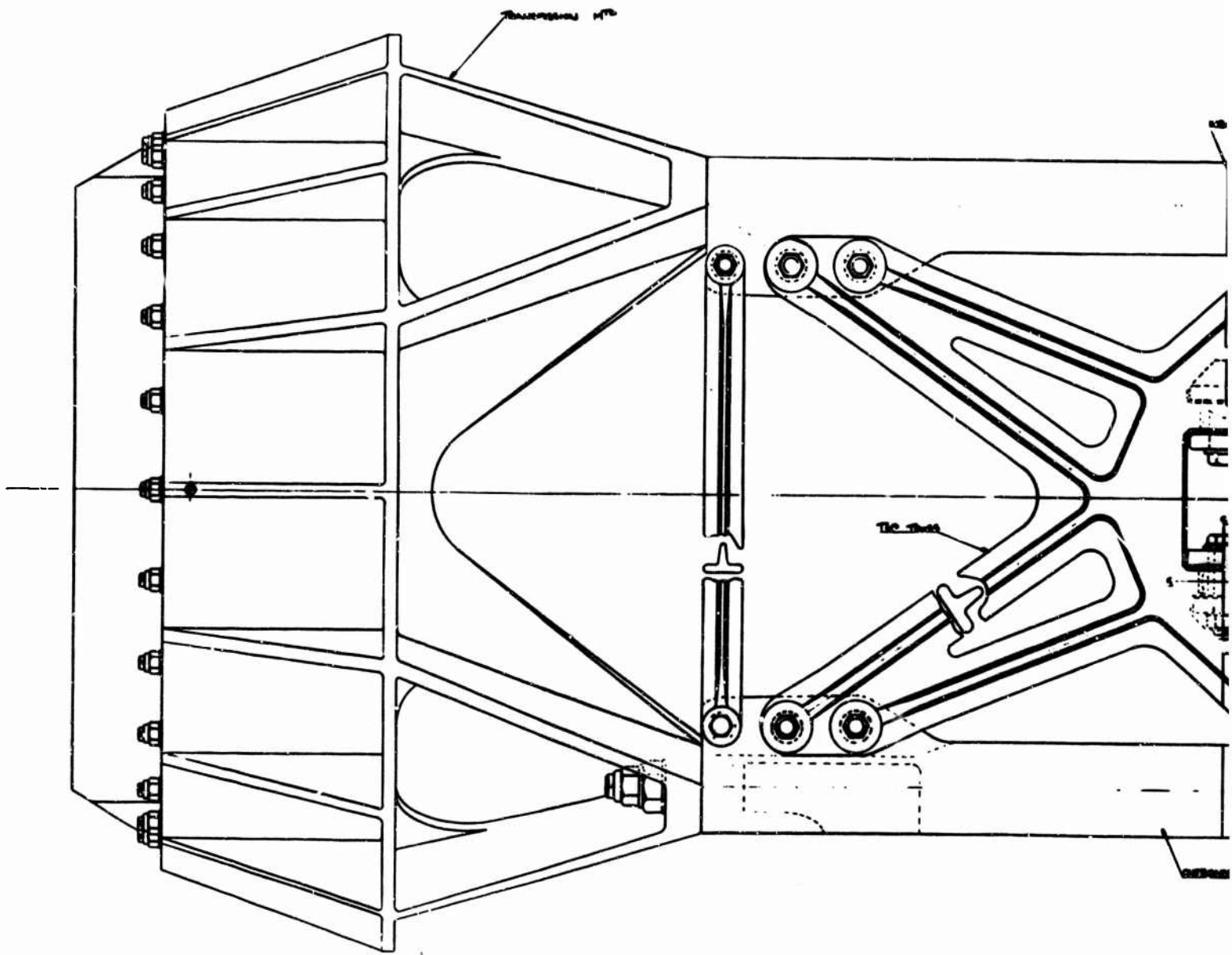
**NACELLE-STRUCTURAL
LAYOUT-ELEVATION**

FIGURE V-1

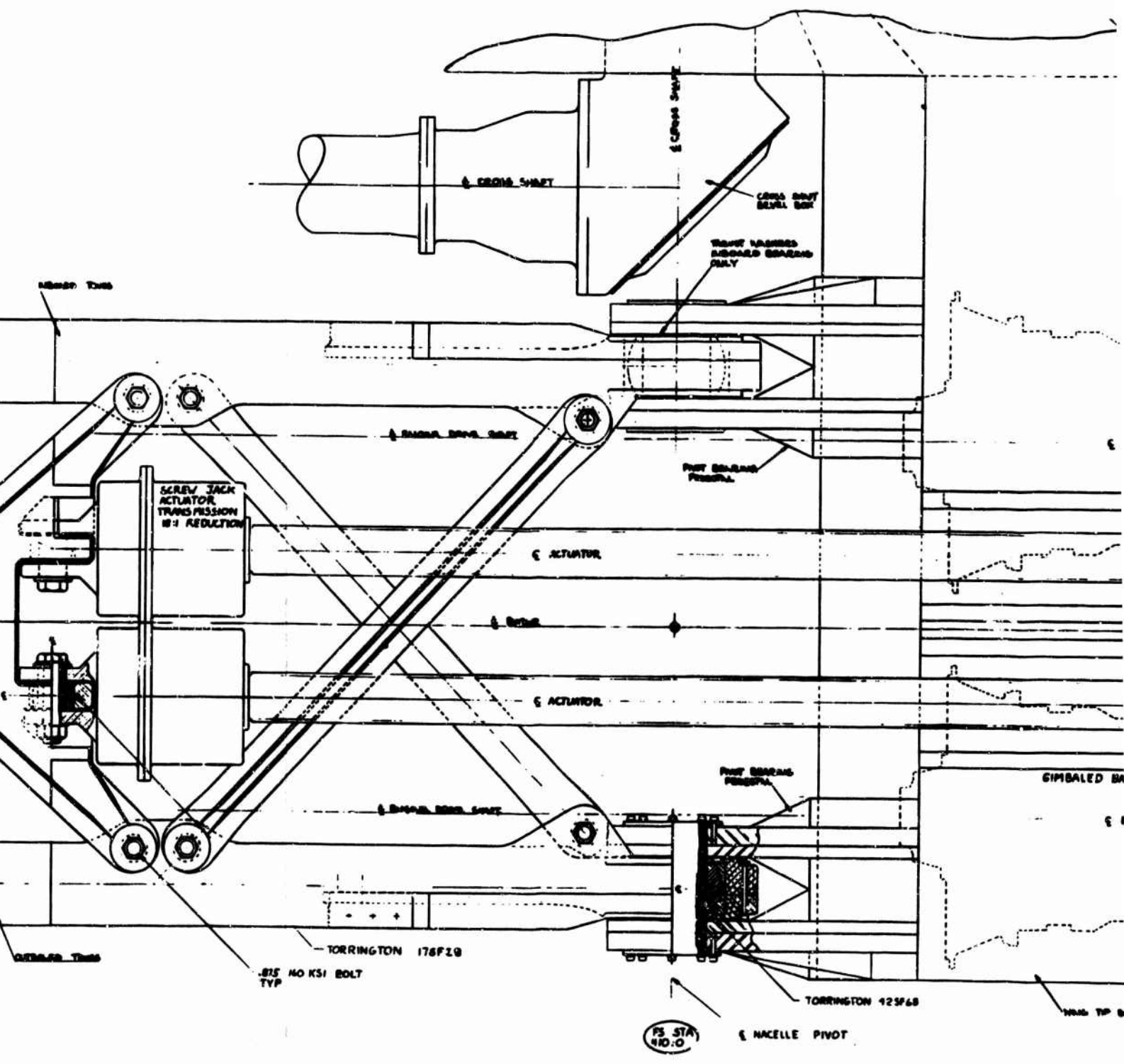
V-3

NO.	1	THE WILCOX COMPANY
DATE	10/15/54	PHILADELPHIA, PA.
BY	W. J. ...	MODEL 215 NACELLE
CHKD.	...	STRUCTURAL LAYOUT
APPROVED	...	1954 SK 215-10016

A



B



PLAN VIEW

5

WING STA 360.5

ENGINE

WING STA 370.5

← NOELLE

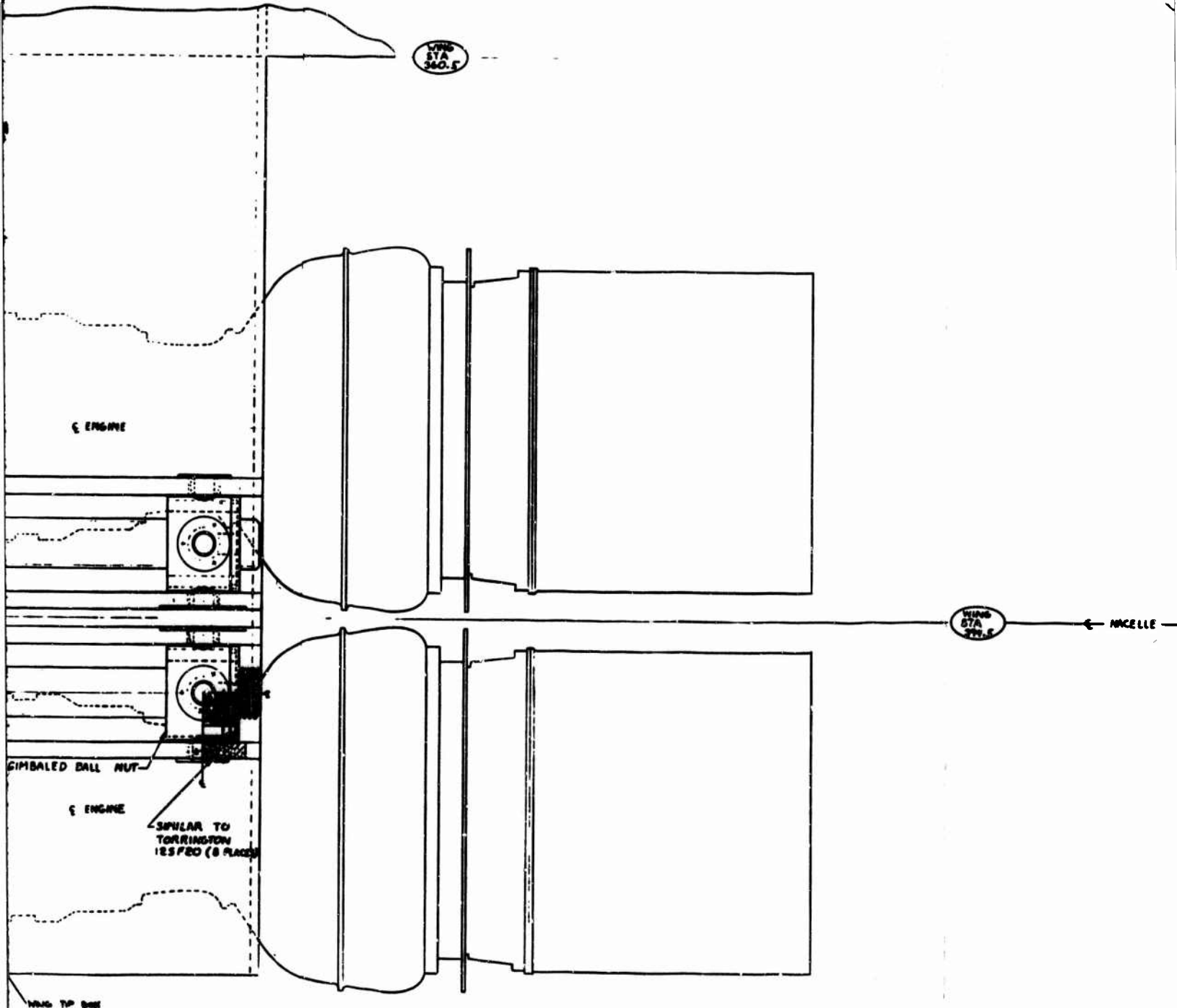
GIMBALED BALL NUT

ENGINE

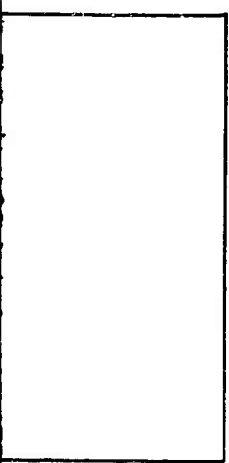
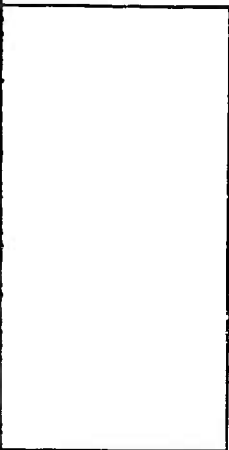
SIMILAR TO TORRINGTON 125 FPO (8 PLACES)

WING TIP BOX

NACEL
LAYCU
F



D



NACELLE STRUCTURAL LAYOUT - PLAN VIEW

FIGURE V-2

V-5

THE BOEING COMPANY	
SEATTLE, WASHINGTON, PHILADELPHIA, PA.	
PROJECT	MODEL 215 NACELLE
DESCRIPTION	STRUCTURAL LAYOUT
DATE	7/21/54
BY	SK 215-10016
CHECKED	
APPROVED	

2. OBJECTIVE

Design a nacelle primary structure and nacelle tilting mechanism based on the geometry and criteria determined in Reference I-1, in order to verify the weight prediction and satisfy the structural requirements discussed below.

3. DESIGN CRITERIA

The limit load conditions selected for the design of the actuator, bearings and nacelle structure are listed in Table V-1 and are basically the same as those shown in Section III, General Design Criteria. Rotor torque for the respective conditions is based on a 55% distribution of 15,300 horsepower; the aircraft is horsepower limited to this value. This applies to all conditions except condition ② where the required horsepower is used.

- a. Limit horsepower is defined as 55% of 15,300 times a 1.5 factor
- b. Ultimate horsepower is 1.5 times limit
- c. Multiple load paths shall be provided for the nacelle primary structure, bearings and actuator fittings
- d. Gyroscopic effects shall be conservatively based on rigid propeller mass theory
- e. Conditions with velocities and accelerations shall be combined to produce maximum effects
- f. Maximum c.g. offset shall be used for trim
- g. Ultimate load is 1.5 times limit load

TABLE VI

SUMMARY OF CONDITIONS - NACELLE STRUCTURE AND TILTING MECHANISM

CONDITION NUMBER	DESCRIPTION	GROSS WEIGHT (LBS.)	n_z	$\dot{\theta}$ RAD/SEC	$\ddot{\theta}$ RAD/SEC ²	$\dot{\phi}$ RAD/SEC	$\ddot{\phi}$ RAD/SEC ²	$\dot{\psi}$ RAD/SEC	$\ddot{\psi}$ RAD/SEC ²	FLIGHT MODE	ROTOR TORQUE PER WING
①	Max. Vertical Load Factor Plus Trim	67,000	+2.5	0	0	-	-	-	-	H	2.76 x 10 ⁶ (in-lb)
②	Level Flight Plus Trim	67,000	+1.0	-	-	-	-	-	-	H	2.19 x 10 ⁶
③	1.0g Flight Plus Max. Cyclic	67,000	+1.0	0.4	0.3	0	0	1.0	0.5	H	2.76 x 10 ⁶
④	Max. Pitch Plus Trim	67,000	+2.5	0.8	0.6	0	0	0	0	H	2.76 x 10 ⁶
⑤	Max. Rolling Plus Trim	67,000	+2.0	0	0	1.5	1.0	0	0	H	2.76 x 10 ⁶
⑥	Level Flight - Max. Speed	67,000	+1.0	0	0	0	0	0	0	A/C	3.87 x 10 ⁶
⑦	-1.0g Max. Speed	67,000	-1.0	0	0	0	0	0	0	A/C	3.87 x 10 ⁶
⑧	Max. Positive Load Factor - Sea Level	47,798	+4.15	-	-	-	-	-	-	A/C	3.87 x 10 ⁶
⑨	Max. Negative Load Factor - Sea Level	47,798	-2.15	-	-	-	-	-	-	A/C	3.87 x 10 ⁶
⑩	Max. Yawing	67,000	1.0	-	-	-	-	-	-	A/C	3.87 x 10 ⁶

H - Helicopter Flight Mode; A/C - Aircraft Flight Mode

Rotor Torque - 55% of the aircraft limited value Conditions ①, ③ through ⑩; condition ② rotor torque is 55% of required

- h. The actuator motor must be capable of tilting the nacelle 105° in 25 seconds during gusts and maneuvers. This criterion requires a dynamic loading of 65,000 pounds on the actuator.

4. NACELLE GEOMETRY

Nacelle geometry based on Figures I-1 and V-1 and 2 is as follows:

- a. Rotor ζ to nacelle pivot 112 in.
- b. Rotor ζ intersects nacelle pivot
- c. Nacelle tilt angle 0-105° (from cruise position)

5. NACELLE AND ACTUATING SYSTEM DESIGN DESCRIPTION

The design aspects of the wing tip and nacelle support, the nacelle tilting system and the nacelle primary space-frame are discussed.

5.1 WING-NACELLE ATTACHMENT STRUCTURE

Two versions of the wing-nacelle attachment beam were designed. System A, the baseline system, is shown in Figures IV-7 and V-3 and consists of a shallower beam than System B shown in Figure V-3. The two systems are compared in this Section.

5.1.1 WING-NACELLE ATTACHMENT - SYSTEM A

The wing-nacelle attachment is a built up beam shown in Figure IV-7 with step tapered top and bottom covers, a rear spar and an auxiliary spar. Multi load path pedestals for actuator and pivot bearing load points are internally supported by ribs which act as load distributors (as shown in Section C-C, Figure IV-7). The beam is attached to the

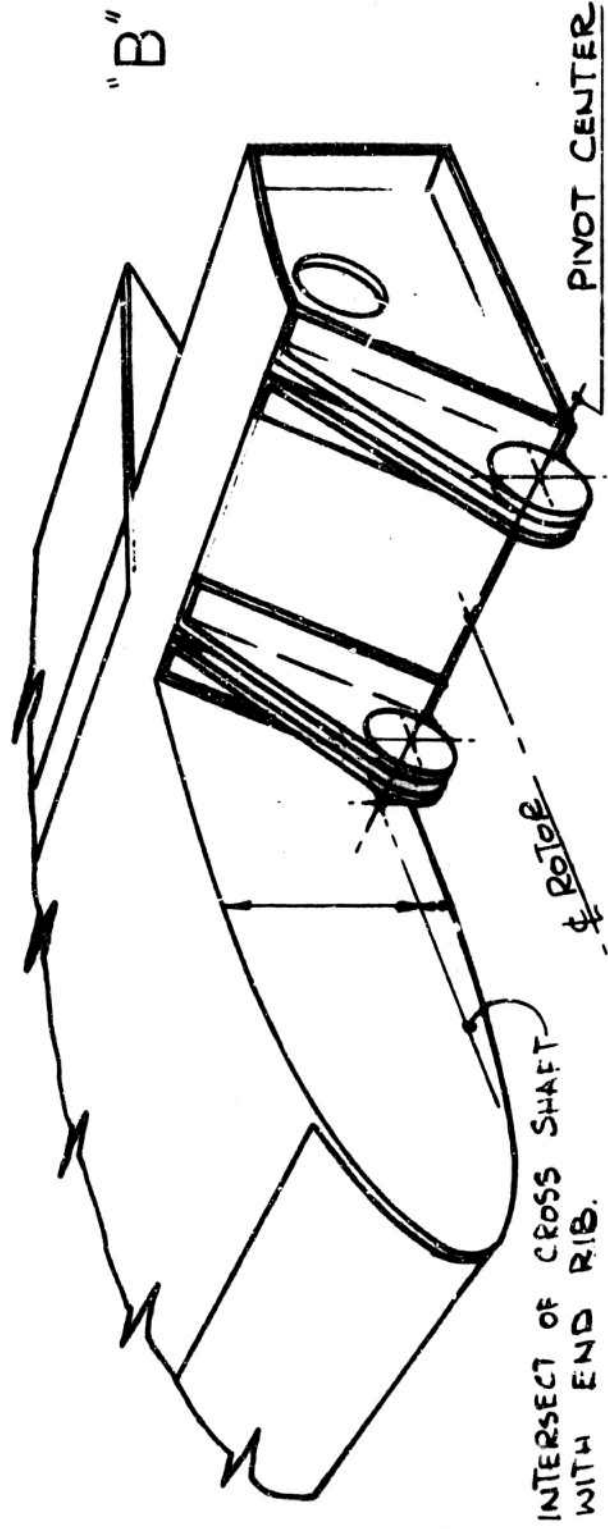
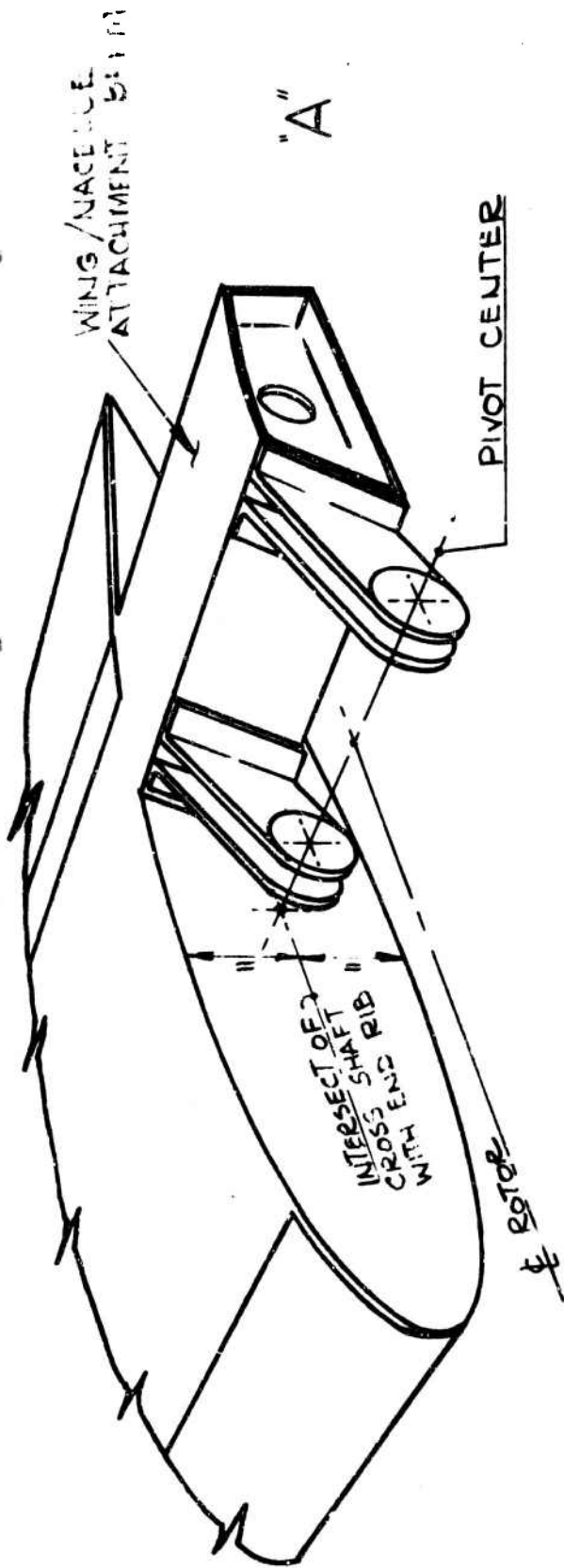


FIGURE V-3 WING/NACELLE ATTACHMENT BEAM

wing and the loading is redistributed by tapered splice plates. The cross sectional size and shape of the beam is dictated by the following geometric criteria:

- a. The cross shaft is positioned on the wing neutral vertical bending axis to give minimum superimposed loads due to wing deflection
- b. The nacelle pivot center is located at the intersection of the wing neutral axis and the hover nominal c.g. position, this gives minimum trim cyclic
- c. The engine centerline is offset from the rotor axis by the bull gear/input pinion sizing which is optimized to give minimum weight
- d. The angle required to the front face of the attachment beam is positioned by the clearance required to allow the nacelle structure to rotate 105° from cruise position for aircraft deceleration with level fuselage in the helicopter mode
- e. The rear face of the attachment beam is positioned to be continuous with the rear spar
- f. The top surface of the attachment beam is positioned to be continuous with the top wing cover
- g. The bottom surface of the attachment beam is positioned by the clearance required by the engine

The nacelle pivot center was chosen by the following procedure:

- a. A nacelle package was assembled of all component parts required and a c.g. for the package was established

- b. The nacelle package was located on the wing in the cruise mode so that rotor to wing leading edge clearance is at least one foot at all structural design loading conditions. The c.g. of total wing/nacelle package was calculated.
- c. The wing/nacelle package was located on the fuselage such that the combined c.g. was located at 25% wing chord in the cruise mode.
- d. The pivot axis is now located at the c.g. of the aircraft with the rotors tilted up for the hover mode.

5.1.2 WING-NACELLE ATTACHMENT - SYSTEM B

In an effort to reduce weight it was decided to provide an increase in depth and torque box area of the attachment beam as shown in Figure V-3. The bottom surface of the wing/nacelle attachment beam is fixed by the proximity of the engines, so, to increase the box depth the engines must be lowered and tilted. A weight review carried out on configuration B shows that approximately 103 pounds can be saved over configuration A.

5.2 ACTUATOR SYSTEM DESIGN

Two actuator systems were designed. System A consists of a pair of actuators each capable of taking the most critical ultimate load independently. Since system A is heavy, system B was designed in an effort to decrease the weight.

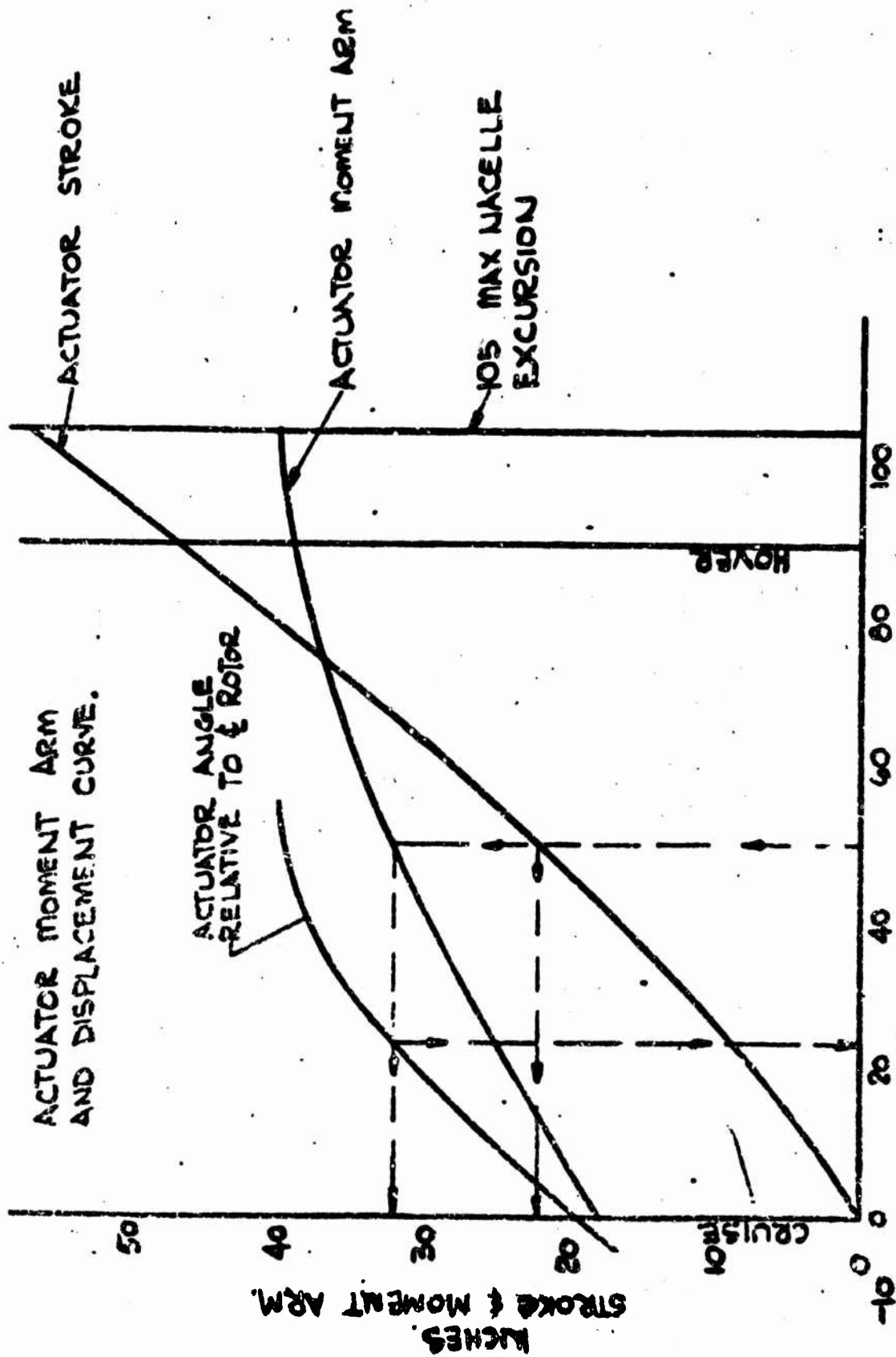
5.2.1 ACTUATOR DESIGN A

The maximum load condition for the actuators was determined by

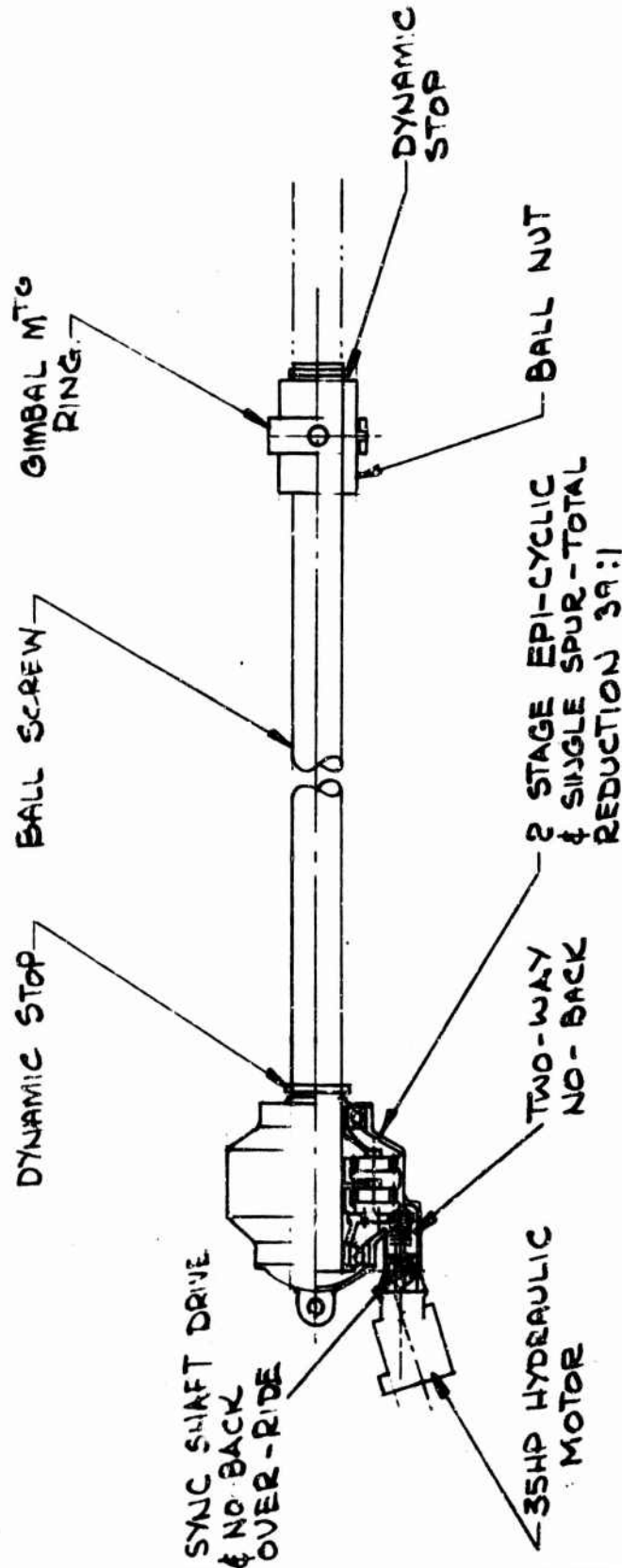
calculating the hinge moment distribution for a number of critical conditions. A number of actuator geometries were then evaluated to match moment arm distribution to hinge moment distribution. The geometry which gave the lightest actuator as a structural element was chosen. The actuator kinematics are shown as a function of nacelle tilt angle in Figure V-4.

The actuators are of the ball screw type, pre-loaded for zero backlash with dual acting no-backs. Hydraulic motors provide drive power through an epicyclic reduction box (Figure V-5). The pair of actuators mounted in each nacelle are coupled together by a differential drive synchronizing shaft which enters on the motor side of the no-back. This allows the no-back to be unlocked in the event of a failure in one actuator.

Gimbals are fitted at the wing box junction and a clevis attaches to the uni-ball at the nacelle truss. This type of mounting will allow axial loading of the actuator under conditions when misalignment is incurred due to structural deflections. The ball-nut is held stationary by the gimbal and the ball-screw is driven. This method was selected because it allows closer spacing of the actuators. The close spacing limits the stiffness change in the event that one actuator becomes decoupled. Each actuator in the nacelle is coupled to a separate hydraulic system. The actuator ball screw barrel can be made hollow to use the ISIS system discussed in Appendix 1 for fail safety. This provides a weight saving as well as increased safety.



ACTUATOR MOMENT ARM AND DISPLACEMENT CURVE.
 ACTUATOR ANGLE RELATIVE TO ROTOR
 105 MAX NACELLE EXCURSION
 HOVER
 CRUISE
 ACTUATOR & NACELLE ANGLE (DEGREES)
 FIGURE V-4 NACELLE ACTUATOR KINEMATICS



DYNAMIC LOAD AT MAX. RATE = ± 65,000 lbs.

MAX STATIC LOAD =

MAX LINEAR RATE = 2.3 ins/sec.

FIGURE V-5 ACTUATOR FOR TWIN INSTALLATION

5.2.2 ACTUATOR DESIGN B

Due to the weight increase over initial estimates, a design review was carried out. This review pin-pointed the actuator area for a large weight saving through a variation in our design approach. Reducing the number of actuators in each nacelle to one as shown in Figure V-6 and redesigning as follows:

- a. Fit a ball nut to each end of the screw
- b. Drive each nut through an epi-cyclic reduction box by a hydraulic motor
- c. Each motor will be capable of driving both nuts by means of a drive/synchronizing shaft
- d. Evaluate the ball screw barrel and install an ISIS crack detector for fail safety

System B weighs 401 pounds less than System A as described in the weight section.

5.3 SPACE FRAME PRIMARY STRUCTURE DESIGN

The space frame is comprised of four main forged trusses joined together in a redundant manner (Figures V-1, V-2 and V-7). Eight pick up points are provided, two for actuators, four points for the transmission and two for the nacelle pivot bearings.

The pivot bearings are uni-ball with dual concentric pins giving a redundant load path. The uni-ball housing is mounted in the truss which has redundancy through a continuous structure backed up by a bolted on secondary structure. The four pick up points to mount

the transmission use concentric dual tension bolts in "bath tubs" which have integral shear bosses. The whole of the primary structure is forged.

6. STRUCTURAL ANALYSIS

6.1 DESIGN LOADS

Table V-2 contains a summary of nacelle hinge moments, actuator and bearing loads for ten basic conditions. Investigations of critical design conditions are based on conditions listed in Table V-1 and the geometry of Figure V-6. Calculations are conservative and include the gyroscopic effects based on a rigid propeller and 55% of the aircraft limited horsepower converted to rotor torque. It is assumed that the rotor control feedback system which is to reduce hub moments (including gyroscopic) is inoperative.

For the helicopter flight mode, the maximum positive and negative hinge moments are produced by condition (3), Maximum Cyclic. Condition (8), Maximum Positive Gust, and condition (10), Yawing, produce the maximum negative and positive hinge moments, respectively, for the aircraft flight mode.

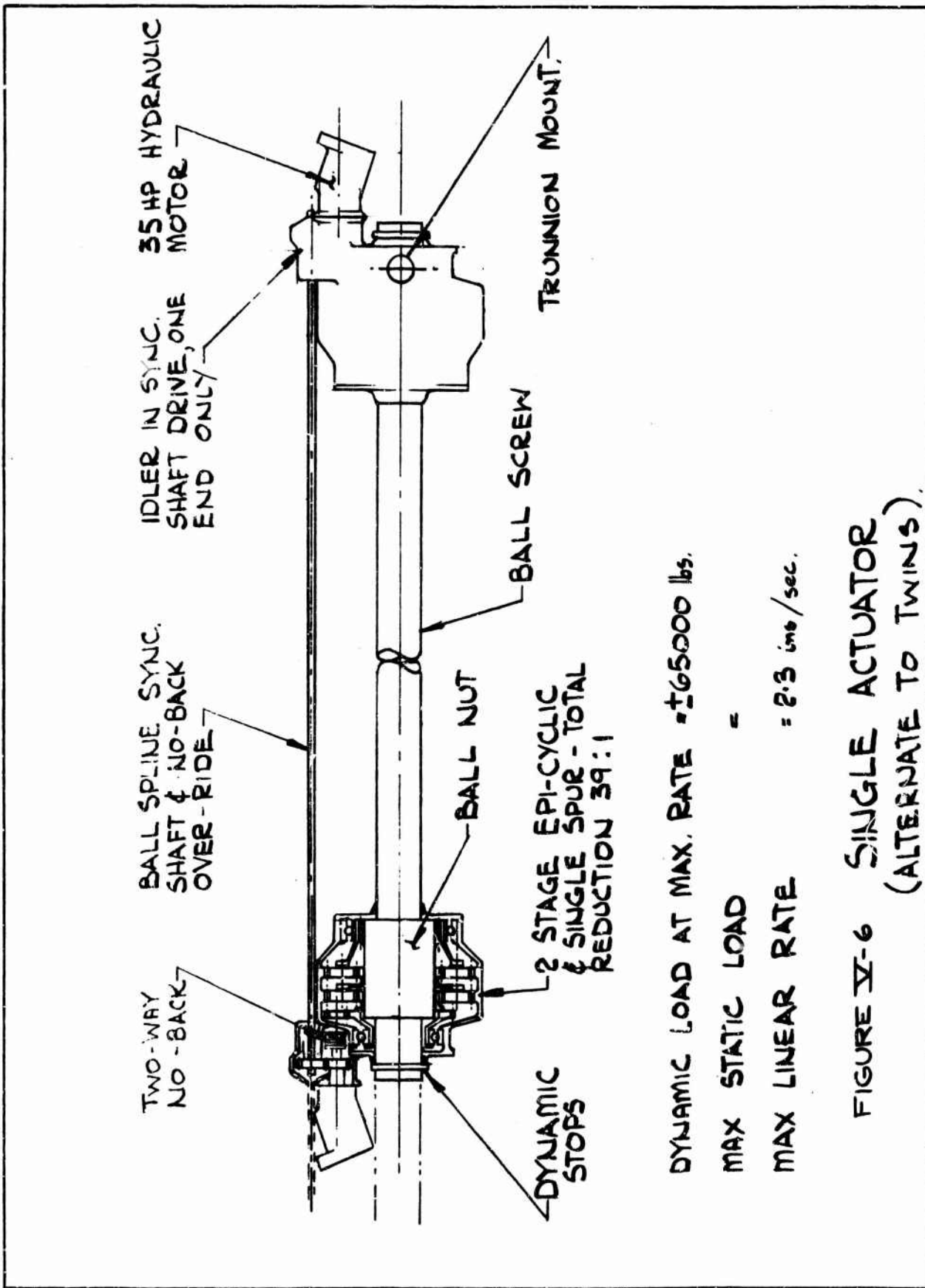
The critical design position of the actuator is in the aircraft flight mode. At this point, the actuator column length is approximately 78 inches versus 29 inches in the helicopter flight mode. Condition (10), Yawing, produces the maximum compression load in the actuator at its maximum length.

TABLE V-2

SUMMARY OF ULTIMATE NACELLE HINGE MOMENTS, ACTUATOR AND BEARING LOADS

CONDITION NUMBER	HINGE MOMENT (IN-LBS)	LOAD PER ACTUATOR (LBS)	RESULTANT BEARING LOAD, DIRECTION AND ANGLE		FLIGHT MODE
			INBOARD (LBS)	OUTBOARD (LBS)	
①	-0.926 x 10 ⁶	+11,900	142,000	127,000	H
②	+0.593 x 10 ⁶	-7,630	103,500	114,000	H
③	+6.6 x 10 ⁶	-85,000	108,000	200,000	H
③ Mod.	+6.6 x 10 ⁶	-85,000	106,500	204,000	H
③ Mod.	-6.6 x 10 ⁶	+85,000	192,500	87,800	H
④	+1.8 x 10 ⁶	-23,100	137,000	158,000	H
⑤	+5.3 x 10 ⁶	+69,300	118,000	250,000	H
⑥	-1.13 x 10 ⁶	+32,000	117,000	181,000	A/C
⑦	+1.13 x 10 ⁶	-32,000	181,000	177,000	A/C
⑧	-4.64 x 10 ⁶	+132,500	199,000	246,000	A/C
⑨	+2.43 x 10 ⁶	-69,400	209,500	182,000	A/C
⑩	+3.24 x 10 ⁶	+92,800	218,000	211,000	A/C

NOTES:
 (+) Hinge Moment Produces Compression in Actuator
 (-) Actuator Load is Compression
 (+) Actuator Load is Tension
 H Helicopter Flight Mode
 A/C Aircraft Flight Mode



DYNAMIC LOAD AT MAX. RATE = ±65000 lbs.
 MAX STATIC LOAD =
 MAX LINEAR RATE = 2.3 ins/sec.

FIGURE V-6 SINGLE ACTUATOR
 (ALTERNATE TO TWINS)

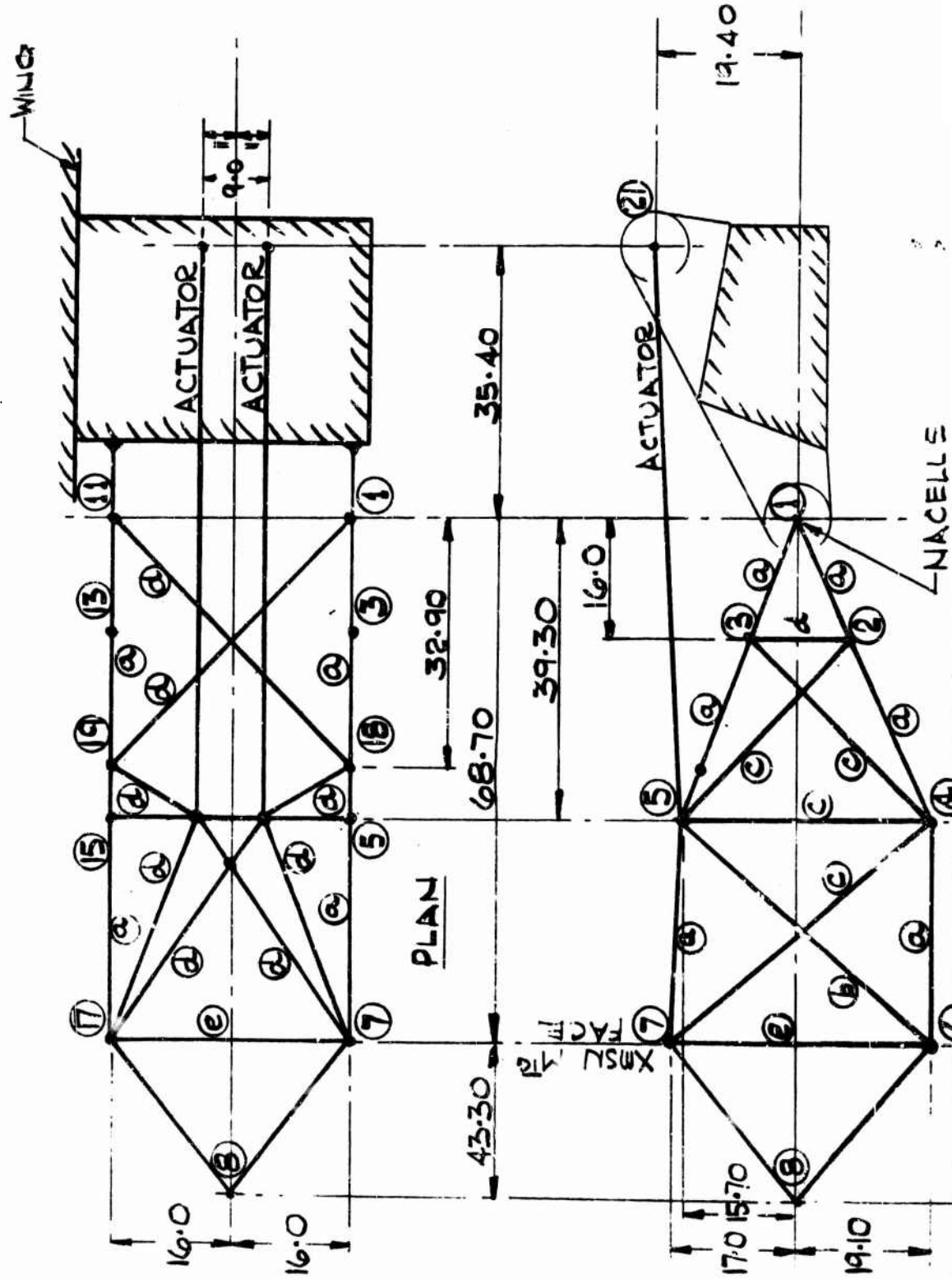
A

THE **BOEING** COMPANY

PREPARED BY:
CHECKED BY:
DATE:

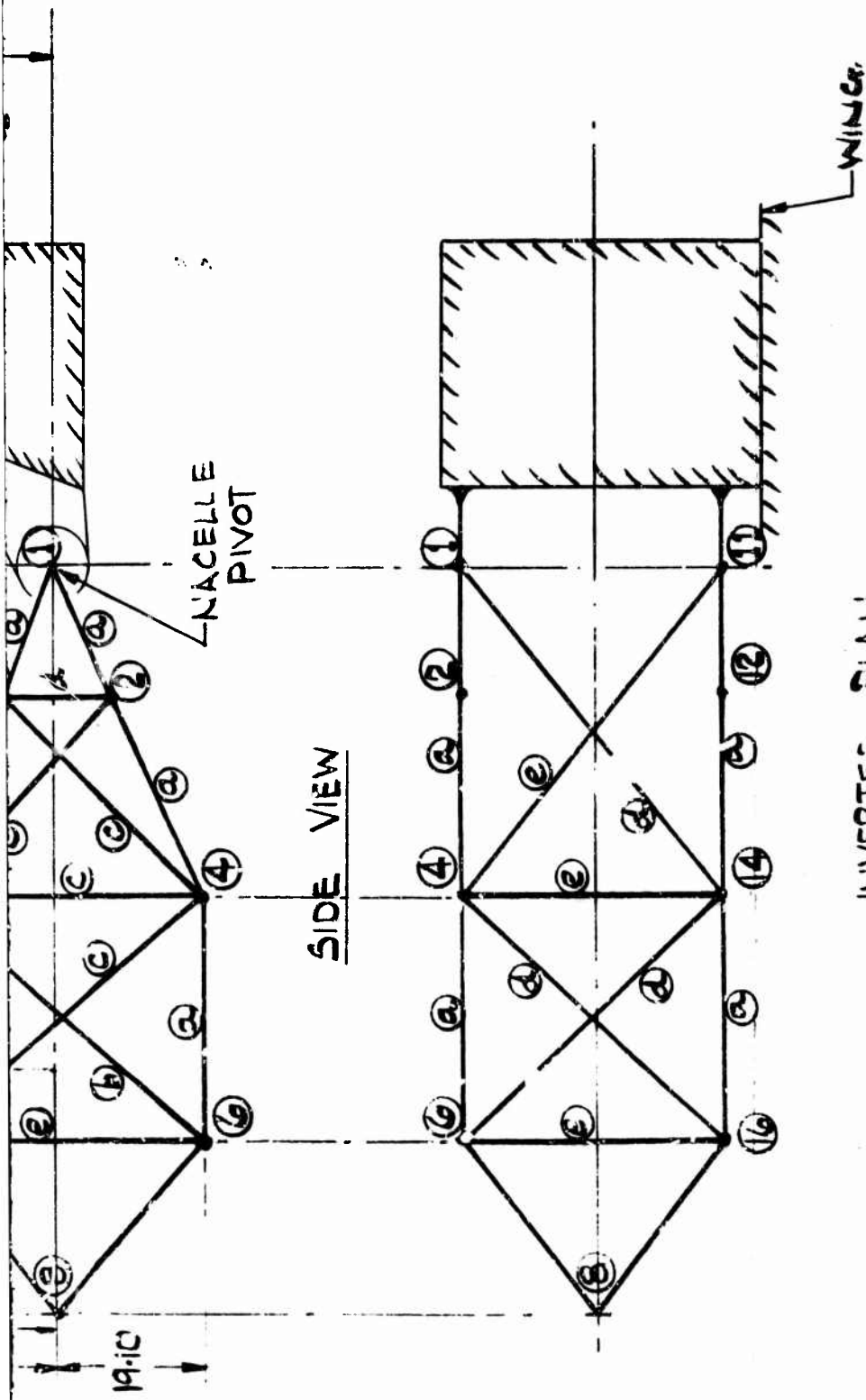
MODEL NO.

FIGURE V-7 IDEALIZED NACELLE STRUCTURE



B

NUMBER
REV LTR

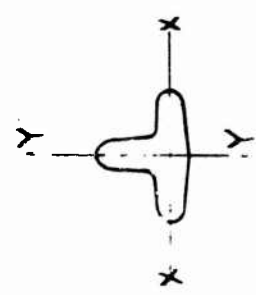


NOTATION REFERS
TO S47 PROGRAM
INPUTS.

INVERTED PLAN

INBOARD & OUTBOARD SIDE VIEW IDENTICAL
PROPERTIES OF MEMBERS.

	(a)	(b)	(c)	(d)	(e)
$I_x \times 10^4$	5.31	2.455	1.46	0.776	0.297
$I_y \times 10^4$	11.122	5.035	2.775	1.661	0.419
AREA m^2	6.6	4.57	3.3	2.75	1.55



Condition (5), Maximum Rolling Plus Trim, generated the maximum outboard bearing load while Condition (3), Modified, produces the maximum inboard bearing load for the helicopter flight mode. Aircraft flight mode condition (8), Maximum Positive Load at Sea Level, produces the maximum outboard bearing load while condition (10), Yawing, is critical for the inboard bearing for the aircraft flight mode.

The critical bending moments, shears and torsions imposed on the wing-nacelle support structure are shown in Figures V-8 through V-10. The reference axis for box torsion is the geometric center of the box and is assumed to be the elastic axis. Bearing loads are applied as concentrated loads at station 410.5 and 378.5. Actuator loads are applied equally to stations 402.5, 395.5, 393.5 and 386.5.

6.2 MATERIAL SELECTION

Material selection for the wing-nacelle support structure box is 2024-T3/T351 for the spar webs and skins, 7075-T73 for forgings and 7075-T73511 for extruded caps sections. This area is exposed to a fatigue loading environment and a stress corrosion environment due to the large number of fittings and local load introduction areas. The materials selected are exceptionally resistant to stress corrosion and have a high fracture toughness and/or high fatigue strength.

The primary nacelle structure shown in Figures V-1 and V-2 is forged

CONDITION ①, REF. TABLE V-1, SECTION V

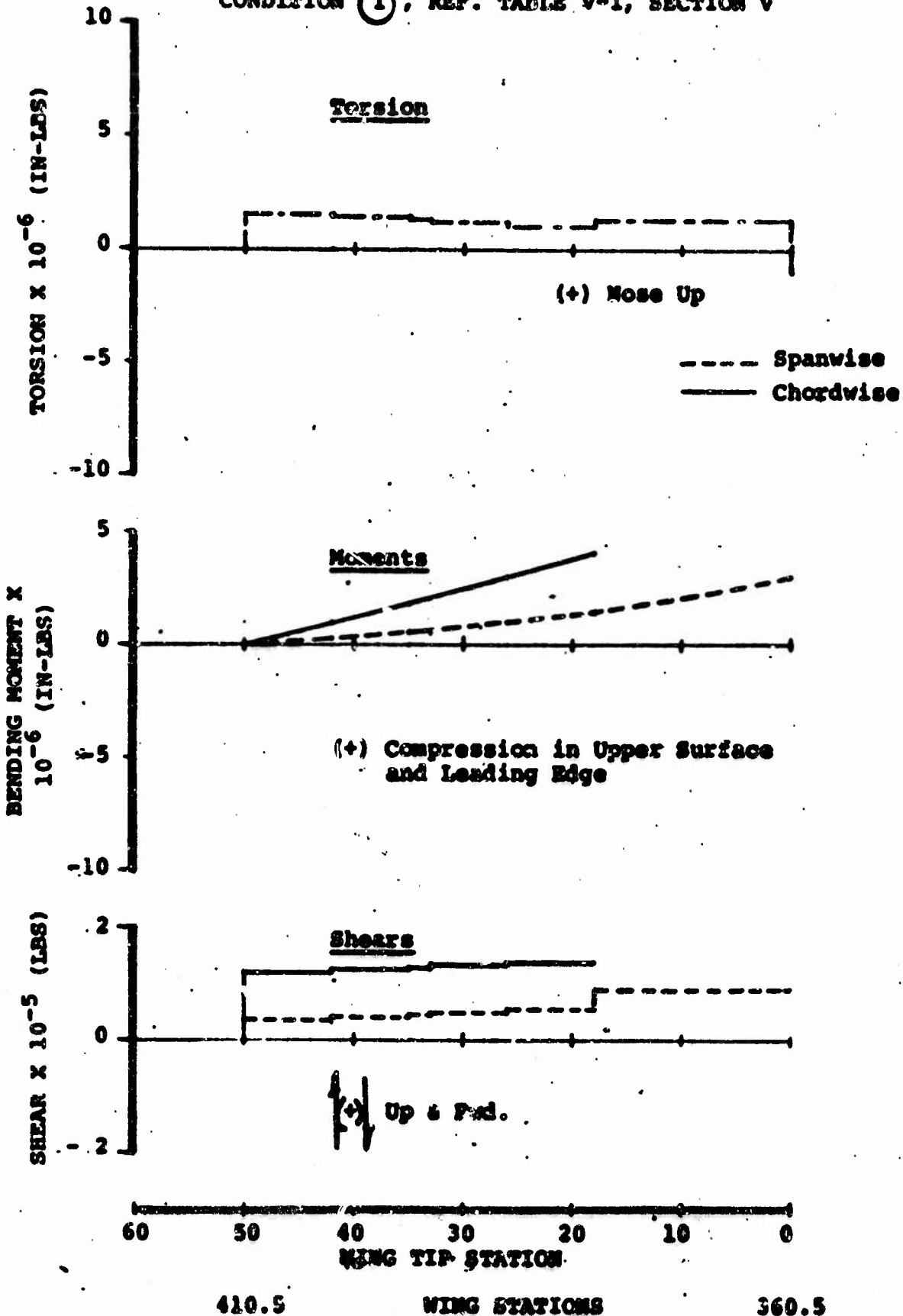


FIGURE V-8 LOADS FOR 2.5g TAKEOFF IN HOVER

CONDITION (3), REF. TABLE V-1, SECTION V

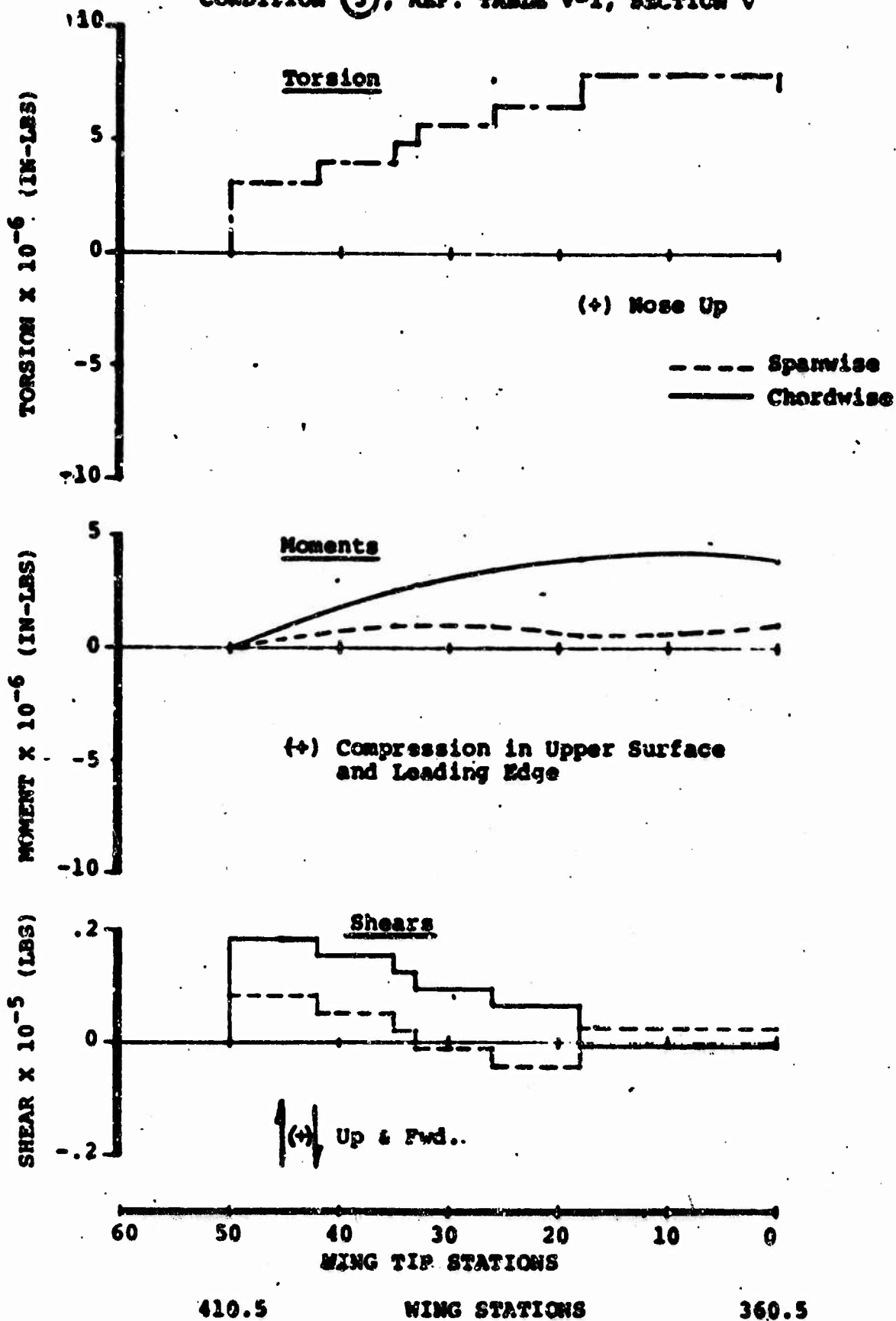


FIGURE V-9 LOADS FOR MAXIMUM CYCLIC CONDITION IN HOVER

CONDITION ⑧, REF. TABLE V-1, SECTION V

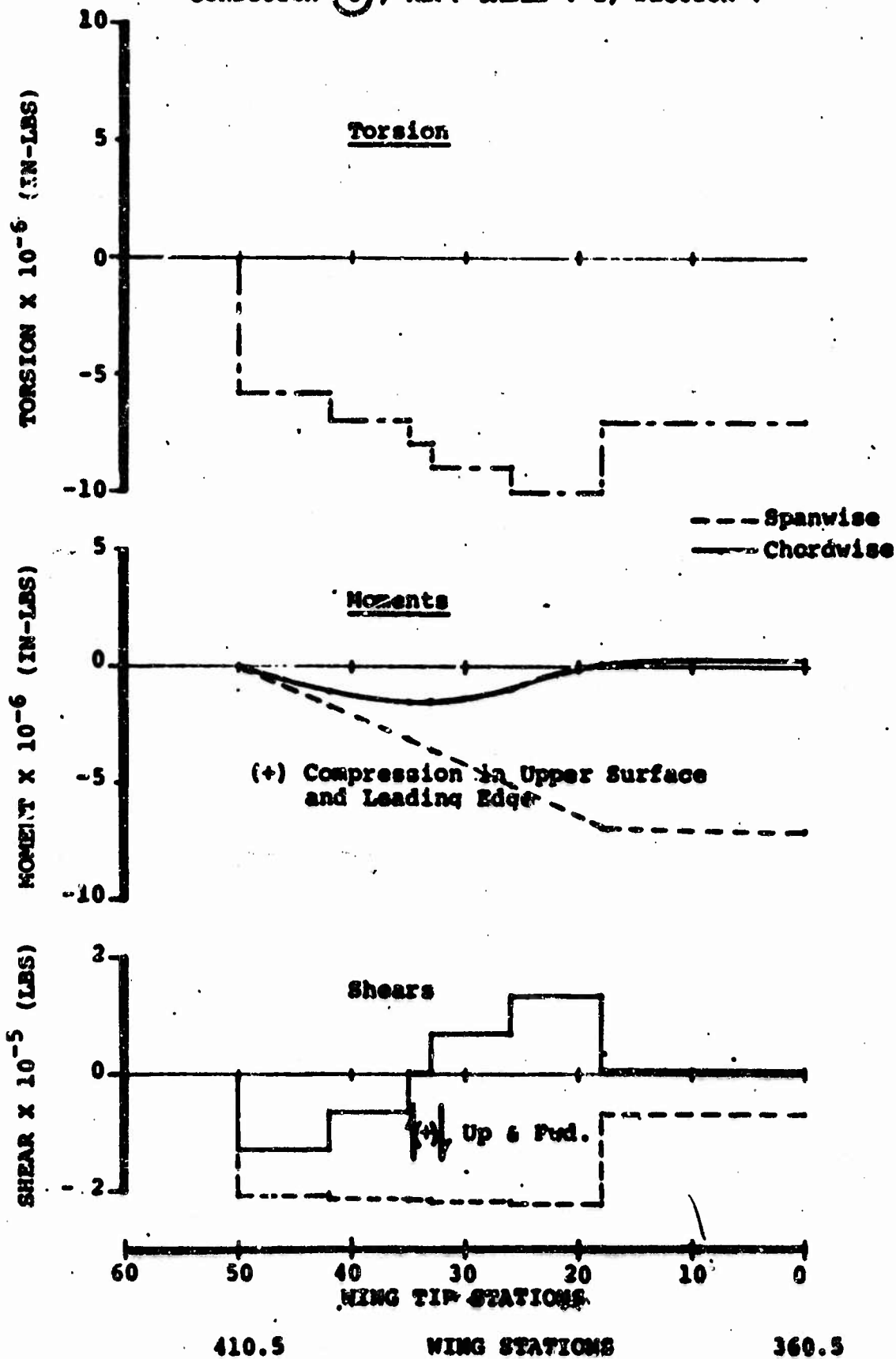


FIGURE V-10 LOADS FOR MAXIMUM POSITIVE GUST CONDITION

from 7075-T73. This alloy condition is virtually immune to stress corrosion cracking. The tilting mechanism ball screw is made from 4340 Modified alloyed steel.

6.3 STRESS ANALYSIS

6.3.1 WING-NACELLE ATTACHMENT

In the area of the wing-nacelle support structure, the section is analyzed as a box beam. The skins and webs are shear resistant to limit load conditions. Table V-3 represents a summary of wing-nacelle support structure skin, webs and caps sizes and material to meet the loading conditions.

6.3.2 TILT ACTUATOR

In the aircraft flight mode, the actuator is in the extended position and critical as a long column. The method of analysis is the standard long column equation for steel alloy. Column and fixity coefficient is 1.0, L/ρ is 125. In the helicopter flight mode, the L/ρ is 46.9 and is in the short column range. Ultimate strength requirements based on equal distribution to each actuator result in a ball screw rod root diameter of 2.48 inches. Maximum stress level is 19,200 pounds per square inch in compression and 28,000 pounds per square inch in tension for the aircraft flight mode. With one of the two actuators failed the stress level is 22,600 pounds per square inch in compression and 32,300 pounds per square inch in tension.

Maximum ultimate static bearing load is 250,000 pounds compared to static capacity of 1.8×10^6 pounds. The size of the bearing is such

TABLE V-3

SUMMARY OF WING-NACELLE SUPPORT STRUCTURE -
WEB, SKINS AND FLANGES

WING TIP STATION	WING STATION	SKIN THICKNESS		SPAR WEB THICKNESS		SPAR CAPS
		UPPER	LOWER	AUX.	REAR	
0	360.5	.235	.228	.282	.231	2 x 2 x .250
18	378.5	.235	.228	.282	.231	↑
		.338	.282	.505	.223	
26	386.5	.338	.282	.505	.223	
		.322	.229	.472	.263	
33	393.5	.322	.229	.472	.263	
		.233	.229	.433	.230	
35	395.5	.233	.229	.433	.230	
		.172	.196	.400	.200	
42	402.5	.172	.196	.400	.200	
		.157	.217	.349	.165	
50	410.5	.157	.217	.349	.165	2 x 2 x .150

- NOTES: 1. Skin and spar web thickness are step-tapered as shown
2. Spar caps are tapered linear
3. Material - 2024-T3/T351 spar webs and skins
7075-T73511 extruded spar caps

that a single fracture of the ball will not prevent reaction of the ultimate load.

6.3.3 NACELLE PRIMARY STRUCTURE

Table V-4 is a summary of the stresses in the truss structure for the following four loading conditions:

- a. Rolling pullout, loading condition (8)
- b. Balanced symmetrical maneuver, loading condition (10)
- c. Hover roll, loading condition (3)
- d. Collective dump in hover, loading condition (5)

The stresses in the members are low compared with the allowable stresses. Further work is needed to define the strength and stiffness criteria required for dynamic stability with failed members.

7. WEIGHT ANALYSIS

The items analyzed in this section are the wing tip nacelle support outboard of wing station 360.5, the tilting mechanism and the primary nacelle truss. For the first two items direct comparisons can be made to weights predicted in Reference I-1 and these are summarized in Table V-5 and V-6.

The target weight in Reference I-1 was based on 1.5% of gross weight (1005 pounds). The baseline design which consists of wing tip nacelle support A and twin solid screw actuators for the tilt mechanism weighs 2157 pounds. This weight is decreased to 1756 pounds by using the single actuator scheme B. By further changing the design to use

A

TABLE V-4

SUMMARY OF NACELLE TRUSS MEMBER STRESSES

MEMBER	L I M I T S T R E S S E S					$\frac{F_c}{1.5}$	$\frac{F_{TU}}{1.5}$
	CONDITION	CONDITION	CONDITION	CONDITION	CONDITION		
	(8)	(10) - MOD.	(3)	(5)	(5)		
11-12	11300	16100	18100	21900	21900	44000	
11-13	-25000	-16000	-11800	-5760	-5760		
12-13	376	-934	-1960	-2840	-2840		
12-14	11500	15800	17400	20800	20800		
13-19	-24800	-16300	-12500	-6760	-6760		
12-15	-530	1130	2350	3460	3460		
13-14	-1020	661	1800	3000	3000		
14-15	3770	-1860	-1380	-5730	-5730		
14-17	-11100	-8630	-4440	-5750	-5750		
15-16	7160	6050	4570	5360	5360		
14-16	2350	6790	11200	14000	14000		
15-17	-19000	-9430	-7930	-3580	-3580		
16-17	334	-1220	-1000	-2540	-2540		
16-8	42	312	647	813	813		
17-8	-93	5	-524	-251	-251		
18-10	6600	7030	4170	3200	3200		
19-9	-6700	-6890	-4030	-3170	-3170		
10-9	2160	-2010	-5600	-4180	-4180		
10-20	11900	11300	5430	3310	3310		
9-20	-1890	-2550	-2290	-1770	-1770		
18-5	-39	+402	230	159	159		
19-15	-16	-7	-7	-2	-2		
9-17	33	11	-10	-5	-5		
20-17	27	26	12	7	7		
10-7	1260	-1310	-2850	-2370	-2370		
20-7	-3660	-5400	-4130	-3090	-3090		
9-14	2490	188	-9530	-7330	-7330		
10-4	2890	951	-15400	-12800	-12800		
11-18	-18800	-18600	-11600	-8900	-8900		
11-4	+17800	+18600	20200	22300	22300		
1-19	15400	17400	10200	8480	8480		
1-14	-22100	-19500	-8820	-10800	-10800		
14-6	15800	15800	13100	14800	14800		
4-16	-17300	-16100	8150	9830	9830		
16-6	1370	211	-4400	-4770	-4770		
17-7	-9440	-3450	5300	3900	3900		

2

9-20	-1890	-2550	-2290	-1770		
18-5	-39	+402	230	159		
19-15	-16	-7	-7	-2		
9-17	33	11	-10	-5		
20-17	27	26	12	7		
10-7	1260	-1310	-2850	-2370		
20-7	-3660	-5400	-4130	-3090		
9-14	2490	188	-9530	-7330		
10-4	2890	951	-15400	-12800		
11-18	-18800	-18600	-11600	-8900		
11-4	+17800	+18600	20200	22300		
1-19	15400	17400	10200	8480		
1-14	-22100	-19500	-8820	-10800		
14-6	15900	15800	13100	14800		
4-16	-17300	-16100	8150	9830		
16-6	1370	211	-4400	-4770		
17-7	-9440	-3450	5300	3900		
14-4	737	120	-457	-1260		
1-2	-19100	-17600	-292	-3350	37200	
1-3	7490	12500	8130	5910		
2-3	2150	1440	-1280	-425		
2-4	-18200	-17100	-779	-352	37000	
3-18	8190	13000	7660	5650		
2-5	-2600	-1790	1410	456		
3-4	-1950	-1130	1320	401		
4-5	5870	3790	1130	1880		
4-	4440	7020	8860	7990		44000
5-6	-3920	-5240	-4960	-4570	30800	
4-6	-8110	-7740	5320	3940		
5-7	378	5350	4550	3390	37000	
6-7	630	1300	-834	-684		
6-8	-370	-362	399	342		
7-8	295	51	-284	-246		

(-) Compression

(+) Tension

TABLE V-5
SUMMARY OF WING TIP
AND NACELLE SUPPORT WEIGHT

	ORIGINAL ESTIMATE (TARGET)	BASIC DESIGN		PROPOSED DESIGN	
		BUILT-UP SKIN AND STRINGERS	MACHINED INTEGRAL SKIN AND STRINGERS	BUILT-UP SKIN AND STRINGERS	MACHINED INTEGRAL SKIN AND STRINGERS
Upper Cover		98	87	69	61
Lower Cover		107	91	70	60
Forward Spar		250	250	356	356
Aft Spar		140	140	216	216
Ribs		148	148	178	178
Rotation Fittings		290	290	300	300
Actuator Fittings		336	336	200	200
Total (1970 Technology)		1369	1342	1389	1369
1972 Technology Reduction (12.5%)		-171	-169	174	-171
Total (1972 Technology)	450	1198	1174	1215	1198

TABLE V-6

SUMMARY OF TILT MECHANISM AND ATTACHMENTS

	ORIGINAL ESTIMATE (TARGET)	D E S I G N		
		<u>A</u> DUAL ACTUATORS	<u>B</u> SINGLE ACTUATOR	<u>C</u> (2) LIGHTEST WEIGHT
Wing Tip and Nacelle Support (Design A)				
Upper Cover		87	87	56
Lower Cover		91	91	62
Forward Spar		127	127	116
Rear Spar		61	61	54
Ribs		98	79	60
Bearing Fittings		374	374	360
Actuator Fittings		292	150	150
Total Wing Tip and Nacelle Support				
1970 Technology		1130	969	858
1972 Technology	450	989	848	751
Mechanism				
Ball Screw		560 (1)	300 (1)	300 (1)
Motors		40	40	40
Gearboxes		408	408	408
Gearbox Mounts		160	160	160
Total Mechanism	555	1168	908	908
Total Tilt Mechanism and Provisions				
1970 Technology		2298	1877	1766
1972 Technology	1005	2157	1756	1659 (1609) (1)

(1) Hollow Shaft for "ISIS" Would Weigh 16.6% Less

(2) Single Actuator, Nacelle Support "B"

the deeper box (nacelle support B) and the single hollow actuator the weight of the wing tip and actuator package is estimated to be 1609 pounds. This is 160% of the target weight.

The primary nacelle truss weight has not been calculated pending the failure mode analysis of the truss.

7.1 WING TIP AND NACELLE SUPPORT WEIGHT

The wing tip and nacelle support is a torque box extending outboard of wing station 360.5 and from a point slightly aft of the wing center spar to the wing rear spar. In construction, it is similar to the wing torque box.

Table V-5 summarizes the weights of designs A and B and shows that design B is 10% lighter than design A. The baseline design uses 1970 Technology. If 1972 Technology was used 12.5% weight reduction could be realized by substituting boron-epoxy components in the design. This design with composites is scheduled for Phase IV of the contract.

7.2 NACELLE TILT ACTUATOR WEIGHT

The baseline design shows two side-by-side actuators for each rotor pod. However, the design can be improved and an 18.6% weight saving realized by installing the double-action single actuator, shown in Figure V-6. This is summarized in Table V-6. The weight can further be reduced by 8.4% by using wing tip box B and a hollow shaft actuator. The most optimistic nacelle tip and actuator design weighs 1609 pounds.

7.3 NACELLE PRIMARY TRUSS STRUCTURE WEIGHT

The rotor nacelle can be divided into five basic sections:

- a. the space truss
- b. transmission mount
- c. engine mount
- d. fire walls
- e. nacelle fairing

Only the space truss, shown in Figure V-7, is considered in this study since it constitutes the largest percentage of the nacelle weight. The weight of the truss will be calculated when failure mode criteria are defined and used to size the truss members.

8. SURVIVABILITY

A survivability analysis was not part of the basic contract but the following aspects of design and material choice contribute to survivability:

- a. dual actuators are used for the nacelle tilt in the baseline design each capable of ultimate load
- b. the dual actuators are fed from independent hydraulic supplies
- c. the actuators can be evacuated and provided with crack detection systems
- d. the actuators are shielded by the rotor hub, transmission and engines
- e. the forgings are made from 7075-T73. This material is exceptionally resistant to stress corrosion and has high fracture toughness

9. CONCLUSIONS AND RECOMMENDATIONS

1. The wing tip nacelle support, the tilting actuator system and the transmission support truss are all heavier than the target weight. The criteria for structural loads, fail safety and survivability need examination in order to ensure that they are realistic.
2. A detailed design review is required to determine if re-design will decrease weight.
3. A criteria must be established for the nacelle truss to account for the effect of failed members on prop/rotor stability and component stresses.

SECTION VI

ROTOR BLADE DESIGN

1. INTRODUCTION

In this section, the detailed design of the rotor blade outboard of 7.5% radius (station 2/75) is discussed. The root end retention is discussed in Section VII with the hub and controls.

The weight allocated to the rotor blade in Reference I-1 was 2,880 pounds. The design discussed here, Boeing Design TR-2B, weighs 2,238 pounds and is therefore 22% lighter than the value in Reference I-1. This difference is discussed in the blade weight analysis section.

The design objectives, structural design criteria, aerodynamic characteristics, structural and weight analyses for blade TR-2B are discussed.

2. OBJECTIVE

Design a rotor blade based on the geometry and criteria determined in Reference I-1 in order to verify the weight prediction and satisfy the structural and dynamic requirements discussed below.

3. DESIGN CRITERIA

3.1 DYNAMICS

The blade dynamic requirements are defined by the blade natural frequencies and are specified as follows:

- a. The first lag bending frequency ratio ω/Ω at normal helicopter RPM shall be .70 to .80.
- b. The first flap bending natural frequency ratio ω/Ω at normal helicopter RPM shall be 1.1 to 1.25.
- c. There shall be no coincident resonance crossings during runup.
- d. The first three flap-lag coupled natural frequencies shall be displaced $\pm 10\%$ of rotor RPM and $\pm 15/\text{rev}$ from any integer harmonic for both helicopter and airplane flights.
- e. The first torsional natural frequency shall be displaced $\pm 10\%$ of rotor RPM and $\pm 25/\text{rev}$ from any integer harmonic for both helicopter and airplane flights.
- f. There shall be no resonance crossings within the normal operating RPM range; i.e., from cruise to hover RPM.
- g. The blade shall be free from conventional and stall flutter in all normal operating conditions.
- h. The dynamic balance axis shall be at or forward of 25% chord.

3.2 DESIGN CONDITIONS

Both ultimate and fatigue design conditions are evaluated for the blade. Fatigue design loads for design TR-2B are those produced by a hover cyclic control fatigue condition. This single fatigue condition produces loads that are higher than all other normal flight conditions including hover with wind, sideslips in high-speed flight in the airplane mode and ground runups and shutdowns through blade resonances points.

Ultimate Loading: Two conditions are considered for ultimate load analysis:

- a. Application of maximum cyclic pitch (limit)
- b. 2.5g (limit) vertical takeoff

The cyclic pitch for both conditions includes that required to trim the aircraft level at the extreme C.G. position.

- a. The ultimate load is 1.5 times the limit load.
- b. A limit load factor of 1.25 is applied to account for transient effects.
- c. The limit rotor speed is 1.25 times the normal operating rotor speed.

The maximum cyclic pitch is limited by a mechanical stop set for the greater of:

- a. Trim Cyclic + Yaw Control Cyclic + .50 Pitch Control Cyclic

OR

- b. Trim Cyclic + .50 Yaw Control Cyclic + Pitch Control Cyclic

Fatigue Loading: The fatigue design loads for preliminary design are based on application of hover cyclic pitch control. Rotor blade alternating stresses shall be less than the fatigue endurance limit for the following cyclic control condition:

- a. Cyclic pitch to trim aircraft level at the extreme critical C.G. position, plus 25% of the maximum yaw control available.

4. ROTOR GEOMETRY

The chord, thickness airfoil section and twist distributions are shown in Figure VI-1.

The following are some primary characteristics:

- a. Rotor diameter = 55.0 feet
- b. Power limit per rotor = 5,860 horsepower in hover
- c. Disc loading = 14.3 PSF at design gross weight
- d. Solidity = .091
- e. Blades per rotor = 3
- f. Average blade chord = 2.65 feet
- g. Hover tip speed = 850 feet per second
- h. Cruise tip speed = 595 feet per second

5. ROTOR BLADE DESIGN DESCRIPTION

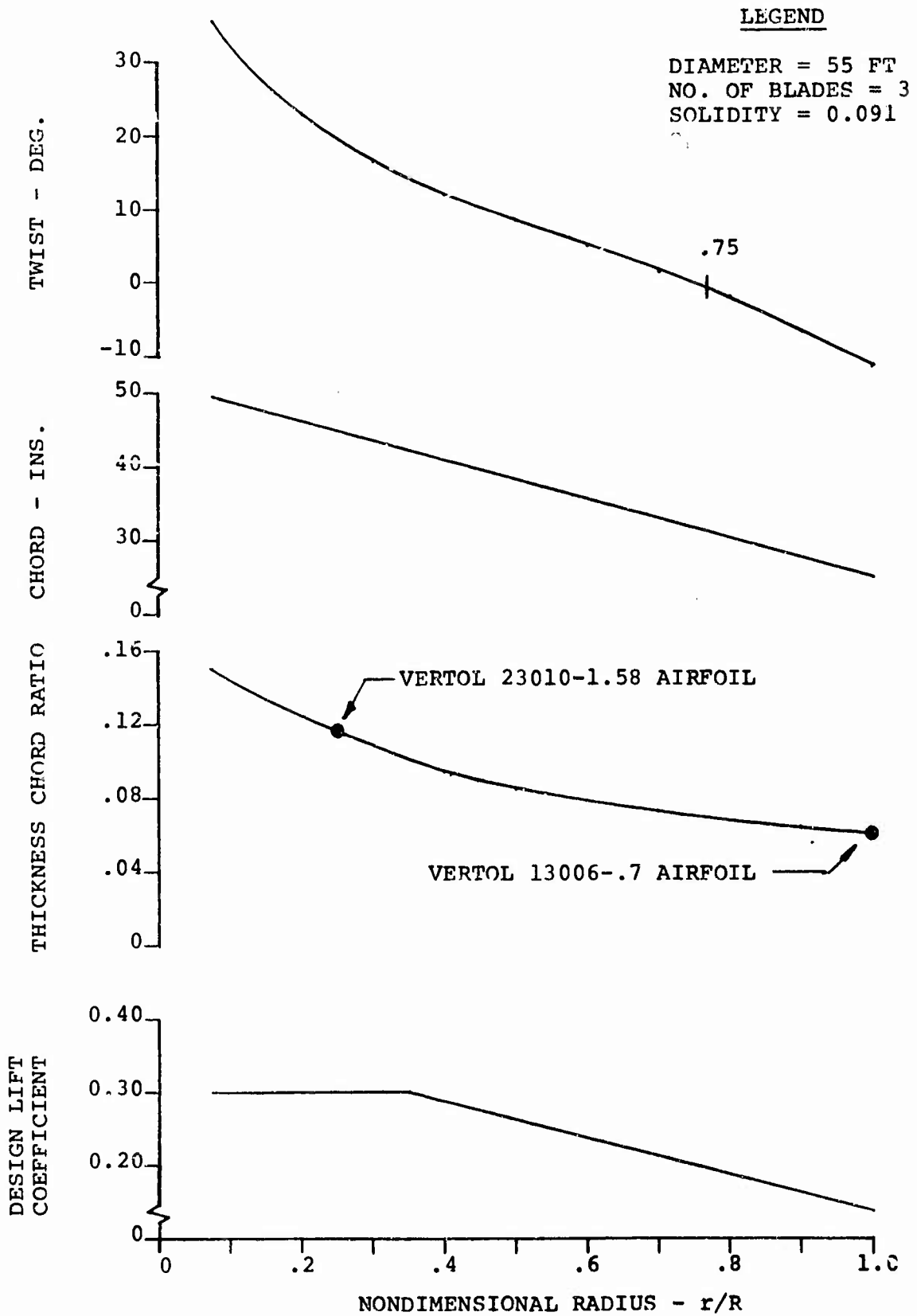
5.1 INTRODUCTION

Model 215 prop/rotor blade design TR-2B is a soft in-plane non-articulated rotor blade with a pitch bearing to provide cyclic and collective control for soft in-plane rotor blades. The first in-plane frequency is placed at less than 1/rev (.75/rev) similar to the BO-105 helicopter rotor blade. This design feature reduces in-plane loads by a factor of four when compared with stiff in-plane blades as described in Reference VI-1, and allows the design to be built within the allocated target weight in Reference I-1.

The blade assembly is a composite structure consisting of a fiberglass spar assembly with titanium root end fittings, aluminum honeycomb core assemblies with fiberglass skins and molded fiber-

FIGURE VI-1

MODEL 215 BLADE CHARACTERISTICS



glass channels and trailing edge wedges, titanium leading edge erosion protection strips, a tip weight assembly and tungsten nose balance weights.

The blade structural configuration is the "C"-spar design which is based on the Boeing-Vertol AGB (Advanced Geometry Blade) concept. The "C"-spar design was chosen because it utilizes Boeing-Vertol past experience in the design and fabrication of the all-fiberglass AGB blades which have been successfully flown on a CH-47. Figures VI-2, 3 and 4 illustrate the design details of the blade assembly.

Figure VI-5 presents an alternate blade assembly design TR-3A. In this design, additional structure has been added to transfer the trailing edge loads from chordwise bending into the spar. The transition from the inboard spar flexure region to the outboard "C"-spar has been lengthened (station 115.50 to station 165.00). Also shown is an ISIS system, described in Appendix 1, to provide crack detection in the root attachment and spar. Blade design TR-3A has not been structurally analyzed and weighed.

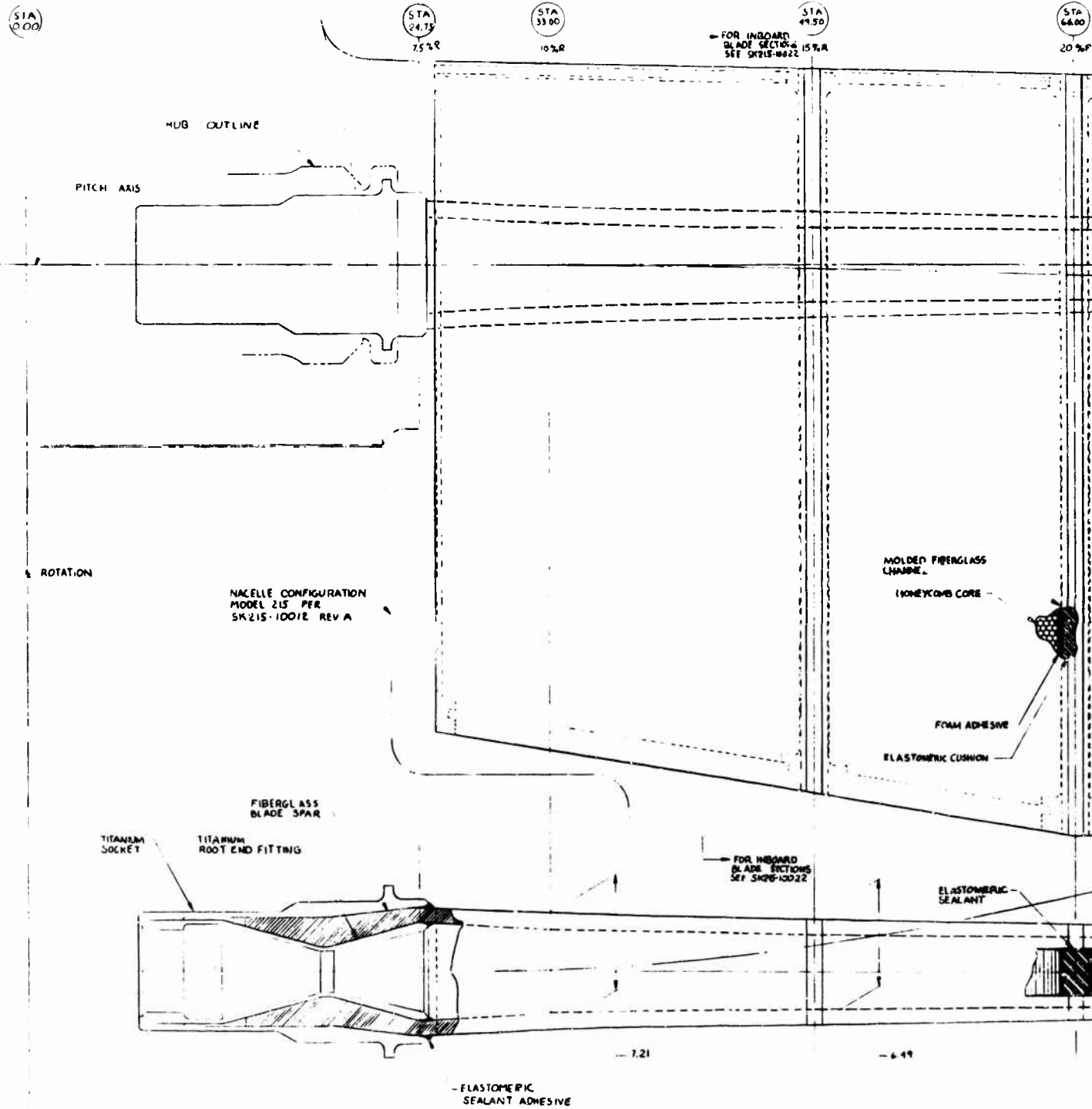
5.2 DESIGN DESCRIPTION OF ROOT RETENTION AND SPAR ASSEMBLY

5.2.1 Root Retention

The root retention fitting inboard of blade station 24.75 and the root socket are integral members of the spar assembly as shown in Figures VI-2 and 6. During manufacture, the spar is "laid up" on the retention fitting, the socket is installed and the spar is cured with these members in place.

The blade centrifugal force loads are transferred from the spar

A



B

STA
88.00
25%R

STA
99.00
30%R

STA
115.50
35%R

STA
132.00
40%R

STA
148.00
45%R

WRAP DIRECTION 45° ± 3°
TORMON LAYERS

- CHORDWISE
DEFLECTION

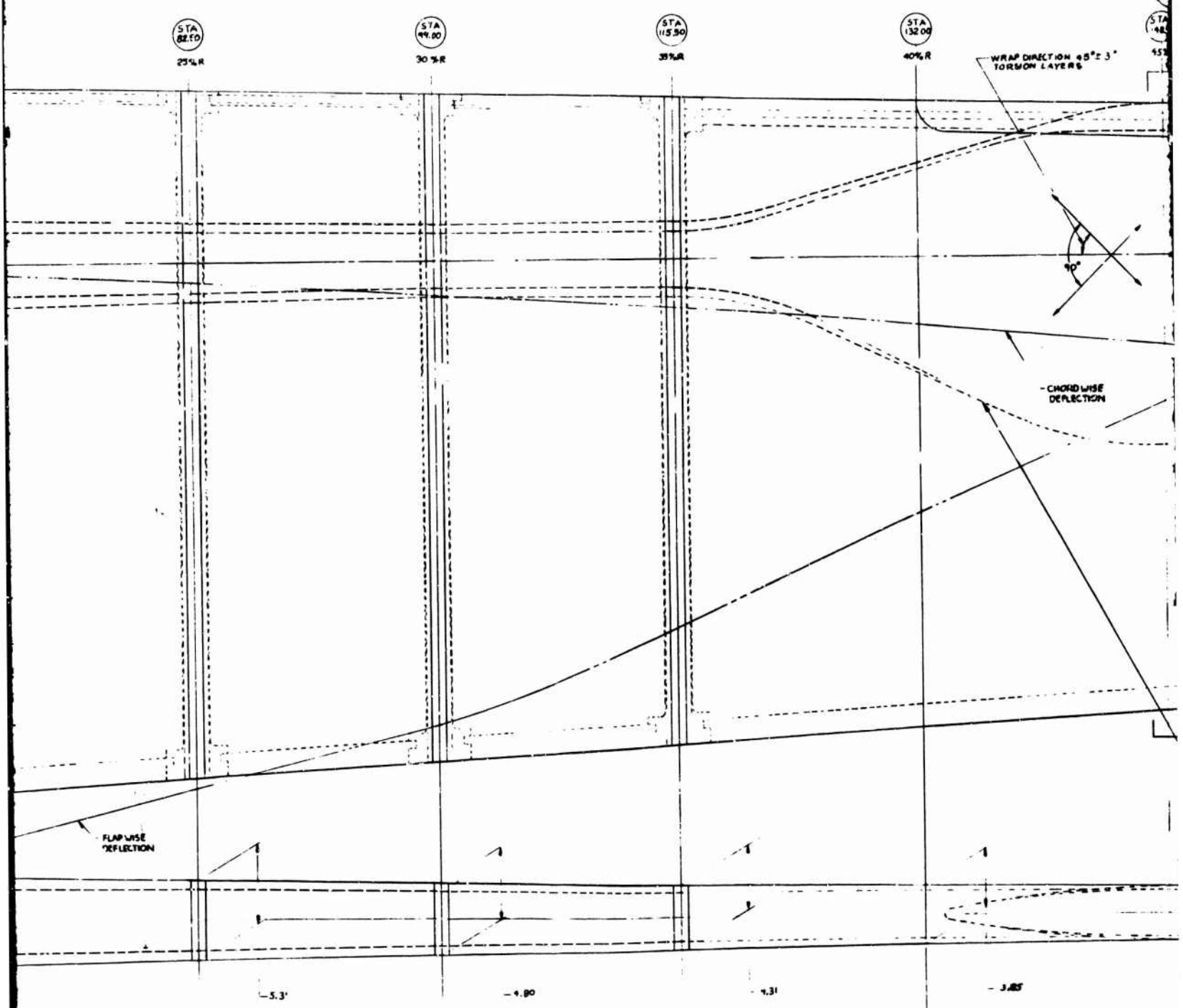
FLAPWISE
DEFLECTION

-5.3'

-4.90

-4.31

-3.85



5

STA 14850

STA 148500

STA 14860

STA 14800

DIRECTION 45° ± 3°
FROM LAYER 6

FOR OUTBOARD
BLADE SECTIONS
SEE SKRM-10023

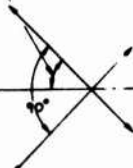
EROSION STRIP

453R

309R

359R

409R



- CHORDWISE
DEFLECTION

FOR OUTBOARD
BLADE SECTIONS
SEE SKRM-10023

1. SPAR

PLAN VIEW
(NO TWIST SHOWN)

3.257

3.033

2.781

D

STA
234.00
10%R

STA
242.50
7%R

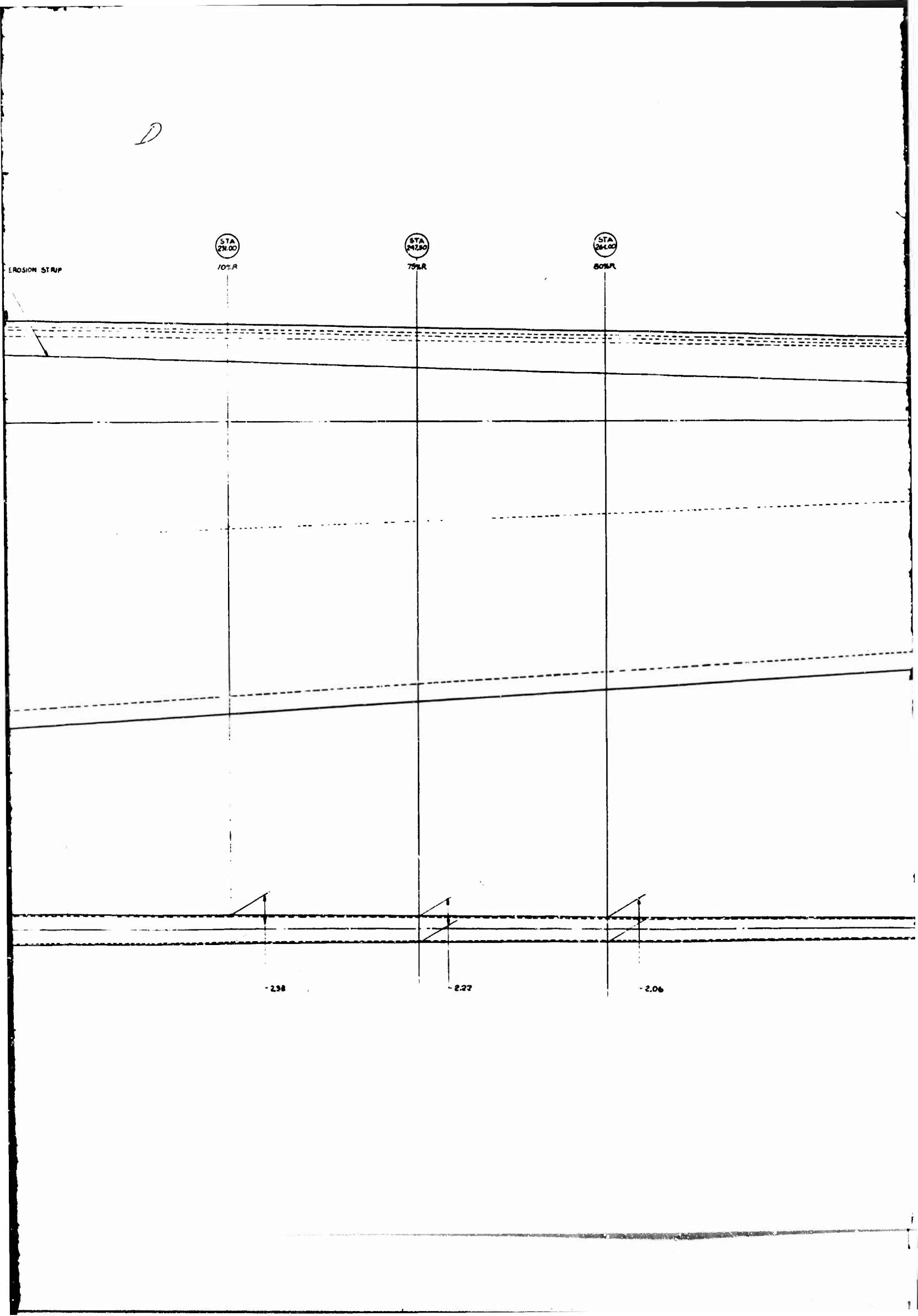
STA
254.00
5%R

EROSION STRAP

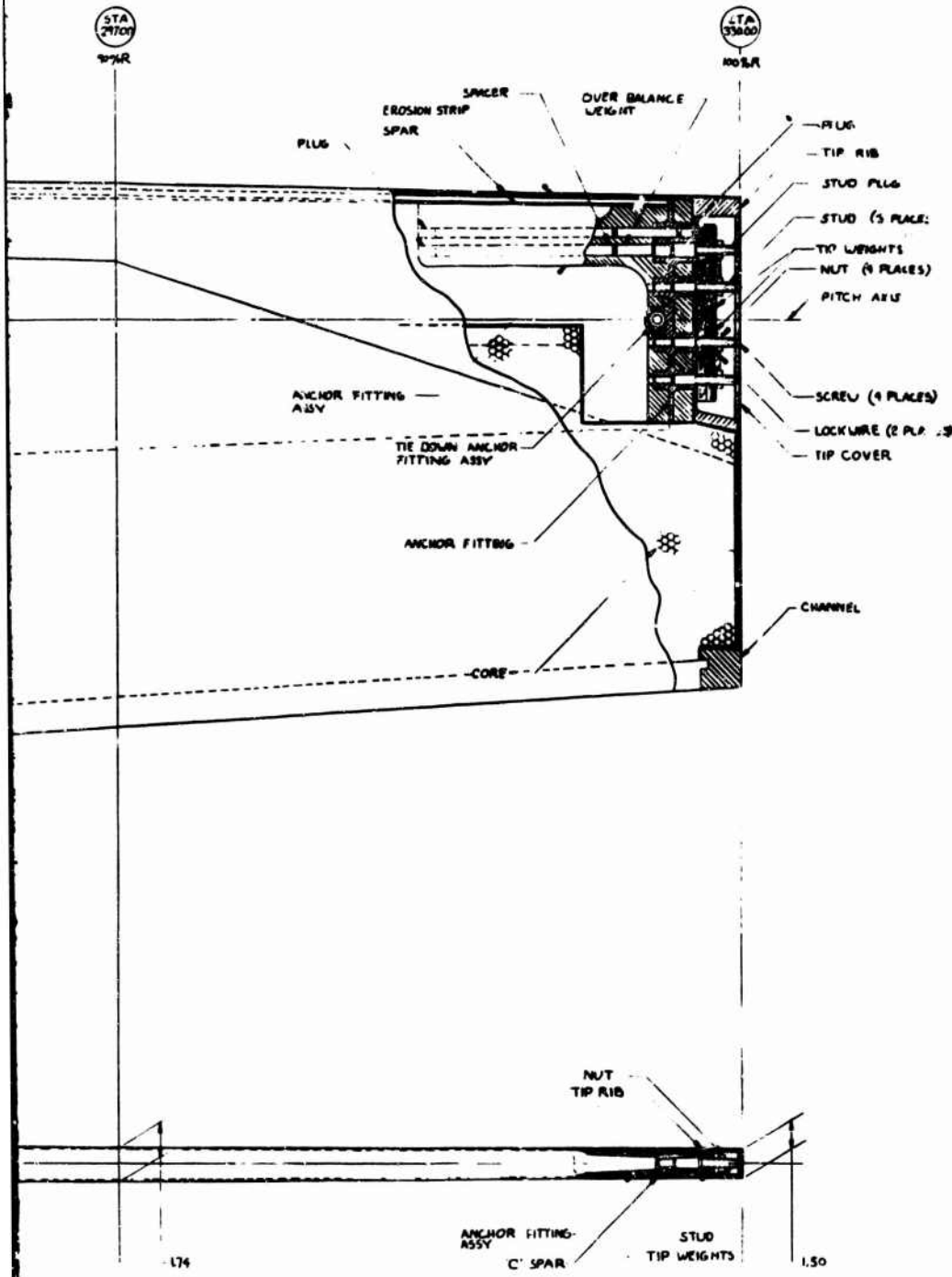
-2.38

-2.27

-2.06



E



BLADE ASSEMBLY
FIGURE VI-2

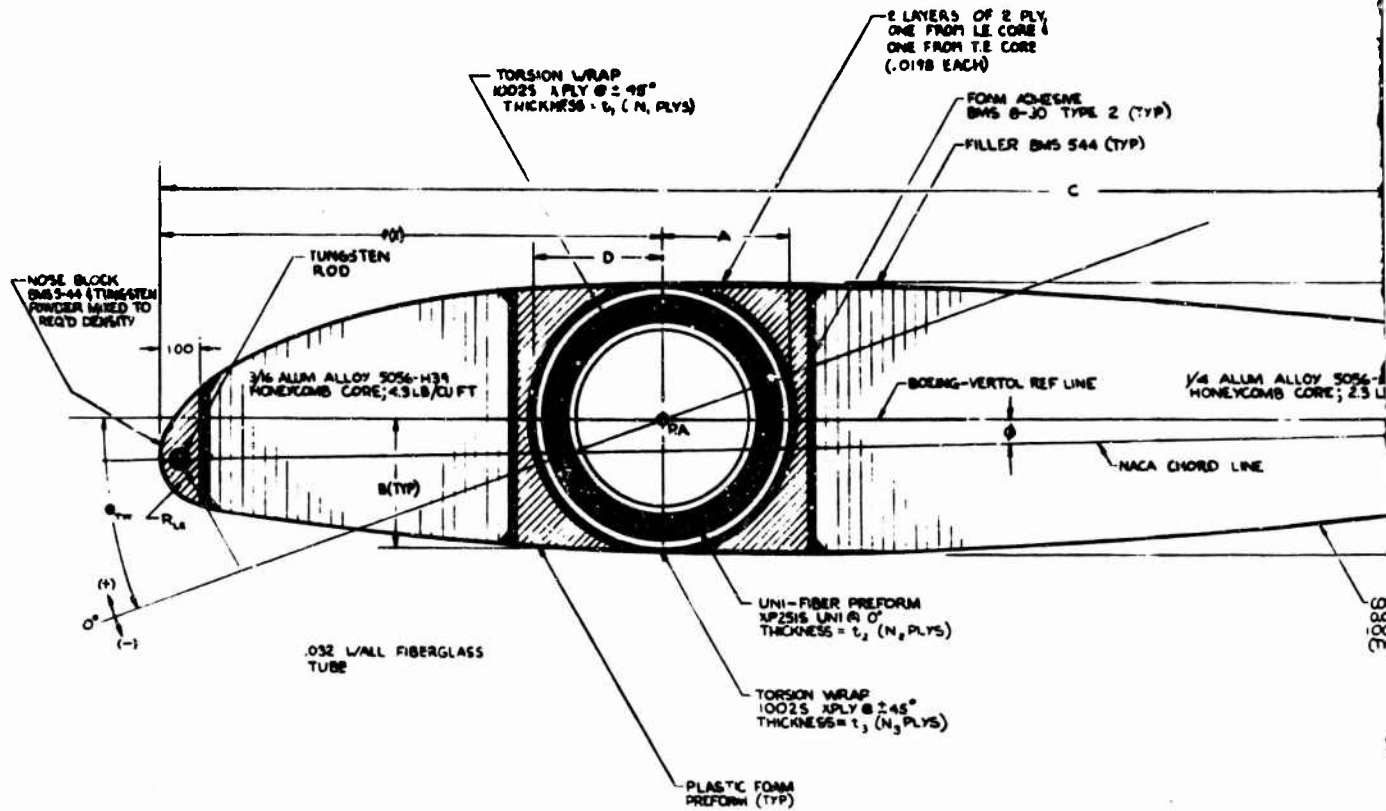
VI-7

REV	DATE	BY	CHKD	APP'D	THE BOEING COMPANY PORTER DIVISION PHILADELPHIA, PA.
					LAYOUT, BLADE ASSEMBLY TRB 215-28, MOD. 815
					7781 SK215-10021
					FORM 101

F

r/r	STA	C	T	f(X)	Θ_{TW}°	Φ°	R _{LE}	A	B	D	N ₁	t ₁	N ₂	t ₂
.075	24.75													
.10	38.00	48.17	22.10	12.242	7.75	1.263	1.157	3.57	3.45	3.57	19.108	.72	21.628	.620
.15	41.50	47.630	6.97	11.904	21.50	1.286	1.009	3.192	3.42	3.192	19.108	.72	21.628	.620
.20	64.00	46.304	7.507	11.576	23.00	1.380	.576							
.25	82.50	44.978	7.507	11.248	19.50	1.243	.810	2.655	2.655	2.655	12.117	.46	26.9	.46
.30	91.00	43.652	4.777	10.920	16.00	1.287	.783	2.357	2.357	2.357	10.077	.50	31.0	.50
.35	116.50	42.326	4.310	10.577	14.00	1.230	.647	2.444	2.444	2.444	10.077	.40	31.0	.40
.40	132.00	40.788	3.852	10.235	12.00	1.190	.610	3.020	3.020	3.020	5.050	.21	14.0	.21

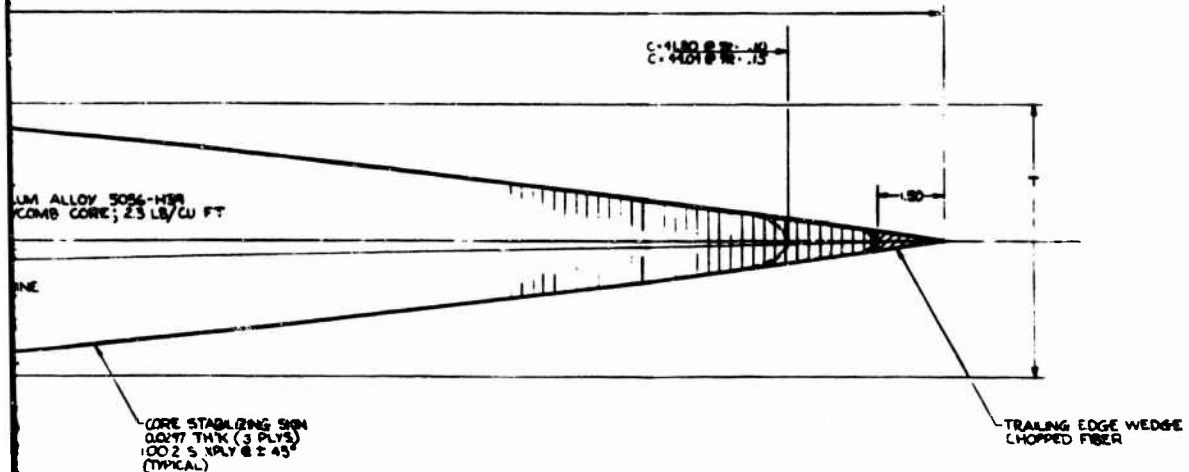
* VIRTUAL DIMS ONLY. ACTUAL DIMS ARE SHOWN ON DETAIL.



13

N ₁	t ₁	N ₂	t ₂	N ₃	t ₃
19	.188	72	.560	19	.188
21	.200	81	.630	21	.200
19	.188	72	.560	19	.188
18	.177	66	.577	13	.187
10	.077	90	.310	11	.107
10	.077	90	.310	11	.107
2	.050	87	.169	6	.067

DETAIL

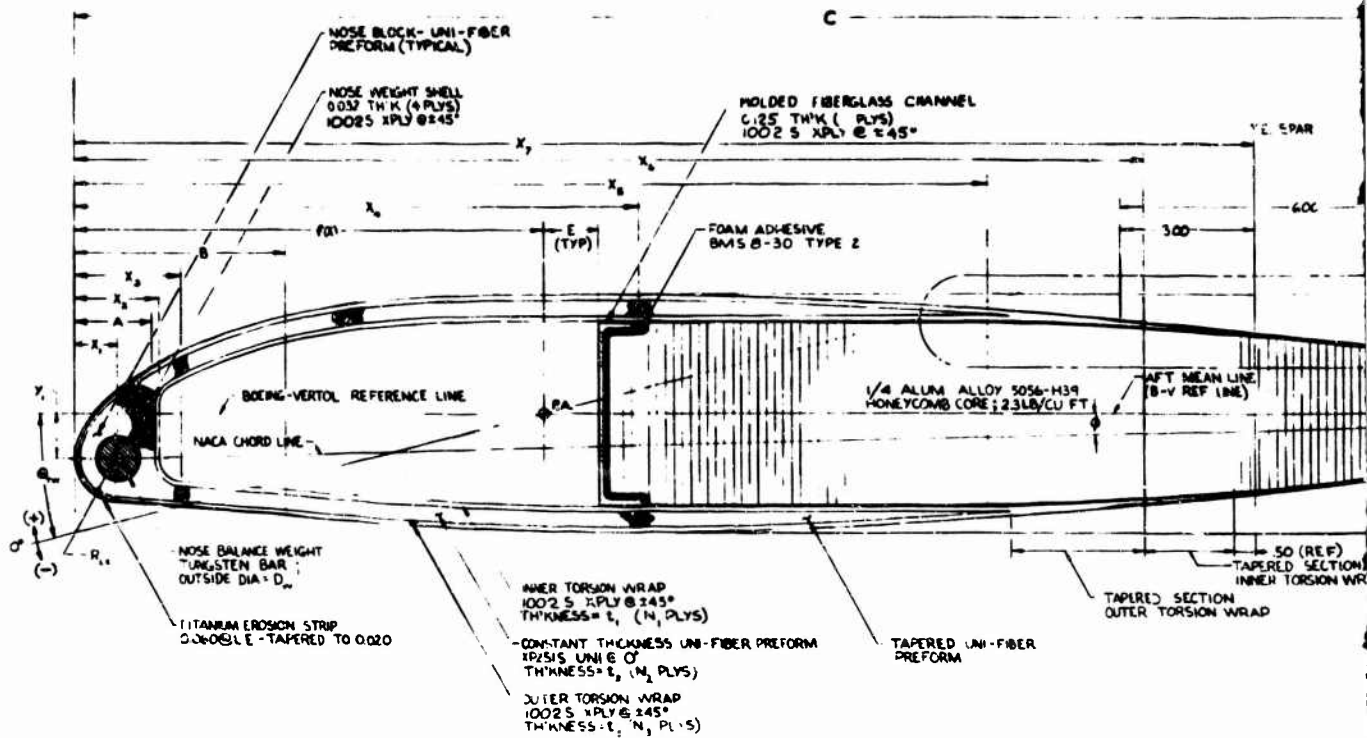


DATE	BY	CHKD	APP'D	THE BEING COMPANY VERTICAL DIVISION PHILADELPHIA PA
DESIGNED BY	DATE	BY	CHKD	BLADE SECTION, INBOARD MODEL 215; DESIGN NO. 28
DESIGNED BY	DATE	BY	CHKD	
DESIGNED BY	DATE	BY	CHKD	SK215-10022
DESIGNED BY	DATE	BY	CHKD	
DESIGNED BY	DATE	BY	CHKD	
DESIGNED BY	DATE	BY	CHKD	
DESIGNED BY	DATE	BY	CHKD	

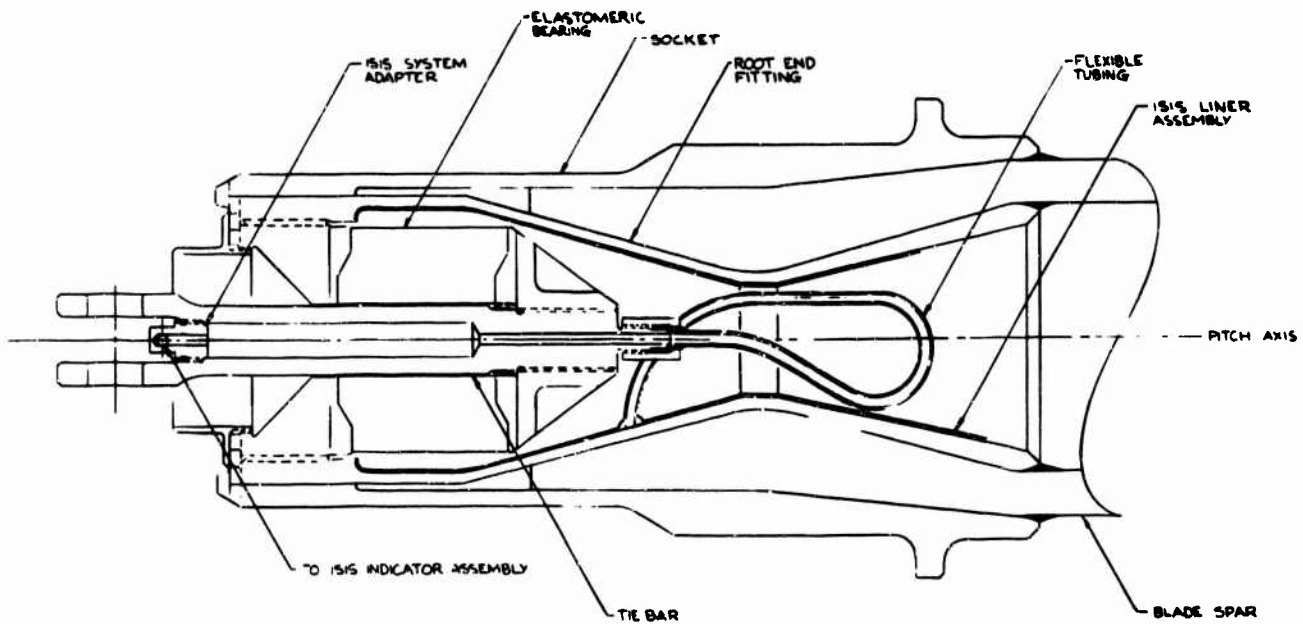
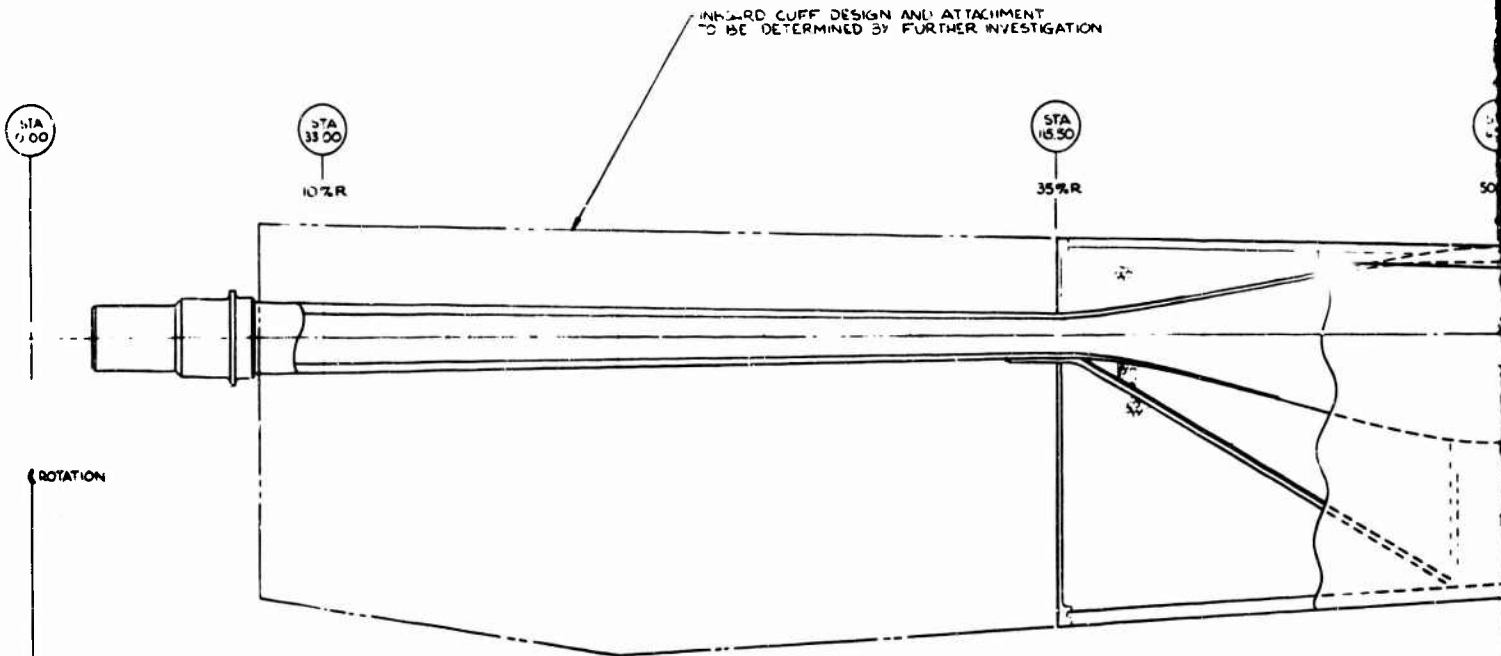
BLADE SECTION - INBOARD
FIGURE VI-3

A

C/R	STA	C	T	F(X)	G _Y	Φ*	X ₁	Y ₁	X ₂	X ₃	X ₄	X ₅	X ₆	X ₇	A	B
.35	115.90	42.304		0.577	14.00	1.23	1.000	.838	1.800						1.75	4.75
.40	132.00	40.978		0.245	12.00	1.19		.791							1.96	5.11
.50	165.00	38.315	3.237	9.579	8.30	1.10	.850	.697		2.194	8.595	15.326	18.327	21.327	2.35	5.81
.55	181.30	36.984	3.033	9.246	6.30	1.06	.825	.630	1.600	2.008					2.54	6.20
.60	198.00	35.652	2.781	8.913	4.75	1.02		.609	1.923	8.485	15.261	16.761	19.261	2.74	6.57	
.70	231.00	31.981	2.875	8.247	1.50	.93		.508	1.692	8.379	13.198	15.193	17.196	3.13	7.30	
.75	247.00	31.687	2.216	7.914	0	.84		.461	1.577					3.34	7.66	
.80	264.00	30.326	2.063	7.582	-1.75	.85		.414	1.462	8.157	12.130	13.630	15.630	3.58	8.00	
.90	297.00	27.648	1.743	6.916	-8.75	.77		.280	1.231	7.894	11.066	12.066	13.566	3.71	8.35	
1.00	330.00	23.088	1.300	6.290	-11.25	.68	.350	.286	.530	7.00	7.500	10.000	11.000	12.000	3.50	9.00



A



PLAN
(NO TWIST)
(SCALE:)

DETAIL-ROOT RETENSION SYSTEM
WITH ISIS SYSTEM PROVISION
(SCALE FULL)

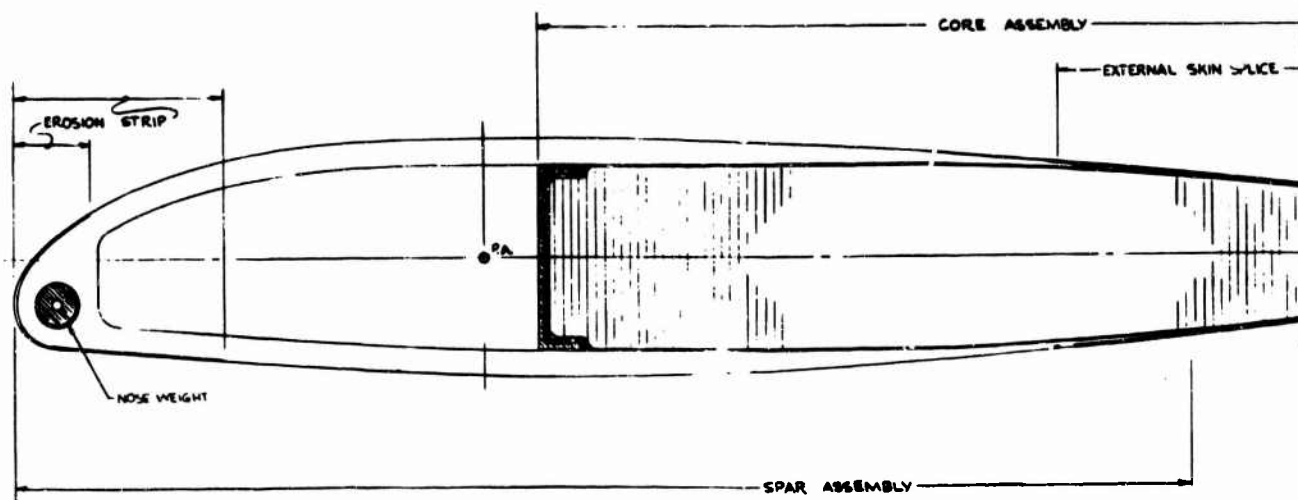
B

STA 33000

100%R

TE SPAR

VIEW SHOWN (5)

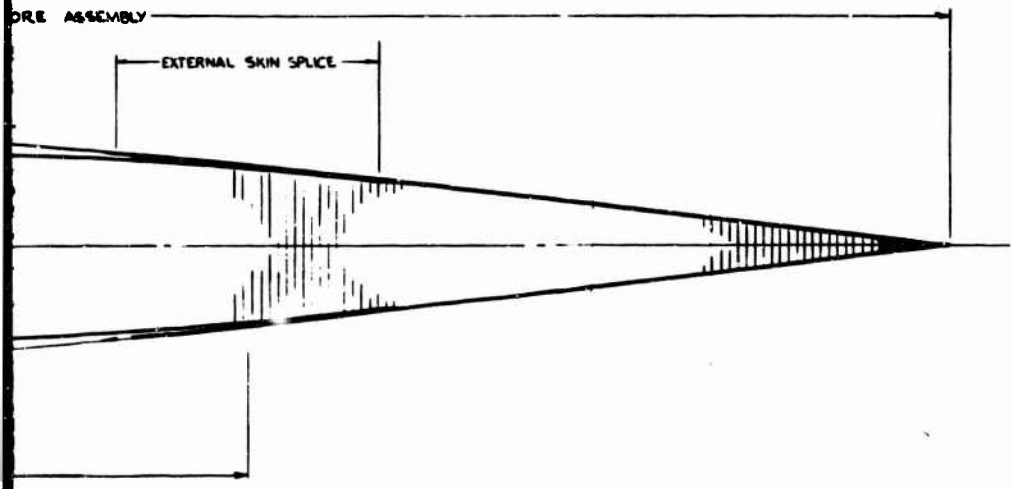


TYPICAL OUTBOARD BLADE SECTION
(SCALE: NONE)

L

STA
33000

100%R



BLADE SECTION

DESIGNER	THE BOYD COMPANY
DATE	RESEARCH DIVISION PHILADELPHIA, PA.
BY	ALTERNATE BLADE DESIGN
NO.	MODEL 215
REV.	7/77 SK215-10027
APP.	

ALTERNATE BLADE DESIGN

FIGURE VI-5

VI-13

to the root retention fitting by the wedge action of the conical shape of the fitting. Blade bending and shear loads are transferred from the spar to the fittings by socket action. Blade pitching moments are transferred from the spar to the fittings through the longitudinal spline projections as shown in Figure VI-6. The stress analysis for the root retention is described in Section VII.

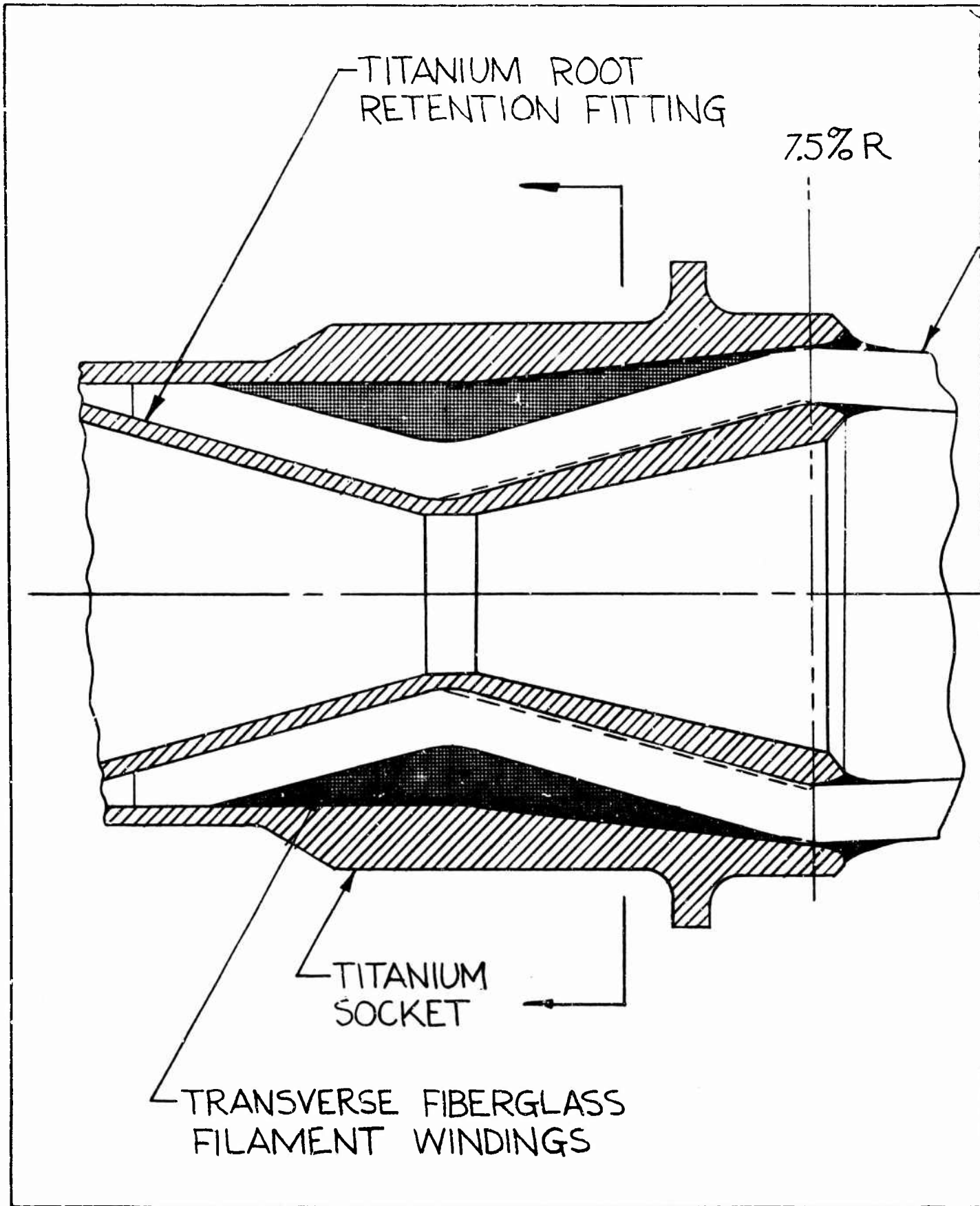
5.2.2 Spar

The spar is the primary structural member of the blade. Between stations 24.75 and 115.5 it is round to provide the flexure required for the soft in-plane and out-of-plane motions. This flexure design has been optimized for constant bending stress and tapers, therefore, in diameter from the root toward station 115.5. The spar inboard of station 115.50 alone provides the required stiffness and strength along this region of the blade span. The skins and core structures of the individual blade segments transfer the aerodynamic and inertial loading contribution of these segments to the spar.

The transition between stations 115.50 and 148.50 forms a "C"-spar at station 148.50 and the spar remains a "C" section outboard to the blade tip. The composite makeup of the spar is XP251S preformed unidirection fiberglass sandwiched between layers of 1002S crossply fiberglass skins in the proportion of 60/40 respectively.

5.2.3 Failure Detection

Figure VI-5 illustrates a preliminary design for the incorporation of the Boeing-Vertol developed ISIS (Integral Spar Inspection System). The interface between the ISIS liner assembly and spar is



1 B

NUMBER
REV LTR

R

FIBERGLASS
BLADE SPAR

SPLINE
PROJECTION
(TYP)

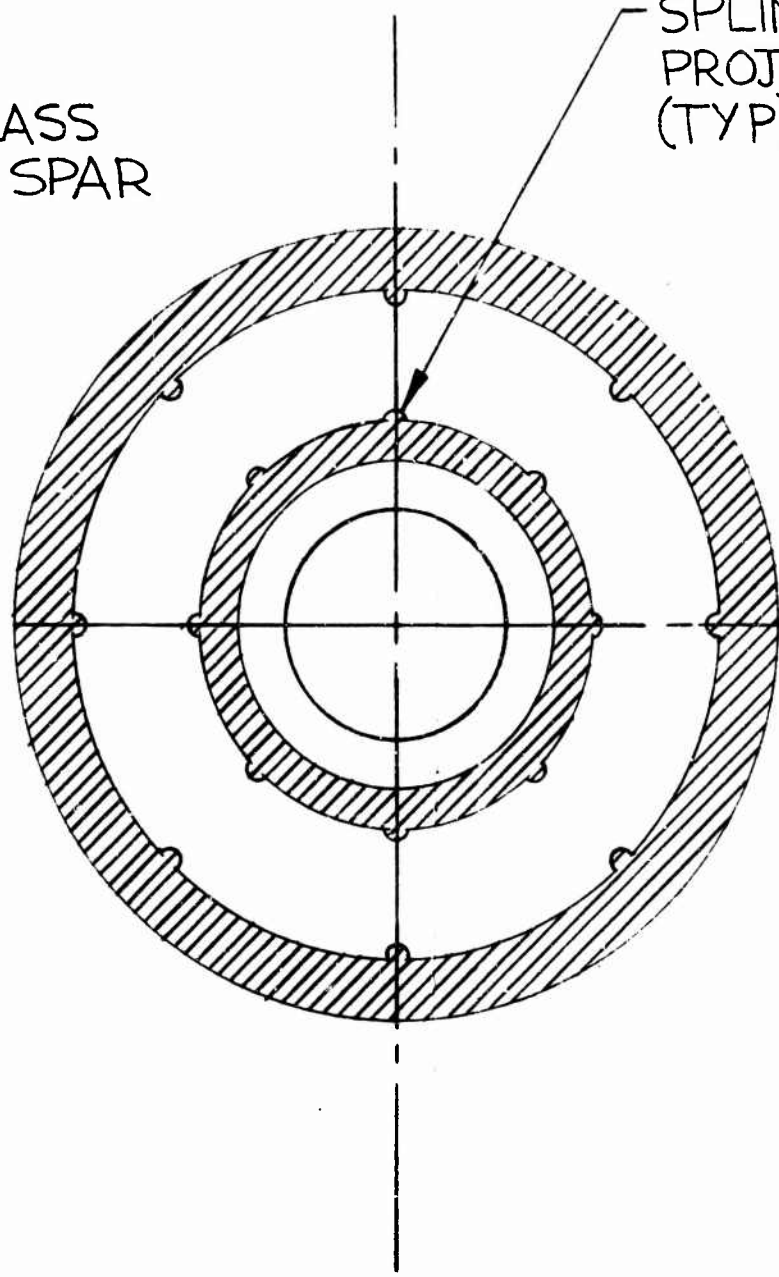


FIGURE VI-6

evacuated. With the occurrence of a crack anywhere in the spar area to be monitored, there is an increase in pressure in the interface which is indicated by the ISIS indicator assembly. A detailed description of this system is included in Appendix 1.

5.3 DESIGN DESCRIPTION OF BLADE FAIRING AND BALANCE PROVISIONS

5.3.1 Blade Sections

The sections of the blade assembly inboard of station 115.50 (35%R) shown in Figure VI-3 are composed of individual blade segments attached to the spar and separated by an elastomeric cushion. These segments have lifting capacity but contribute a negligible amount to blade stiffness.

The sections of the blade assembly outboard of station 115.5 to the tip are shown in Figure VI-4. The aft section of the blade has fiberglass crossply skins which are stabilized by an aluminum honeycomb core.

5.3.2 Core Assemblies

The honeycomb from station 148.50 to the blade tip is bonded to the internal surface of the spar. In the flexure area, the honeycomb is foam bonded along the external spar surface. The density of the honeycomb is 2.3 pounds per cubic foot except in the leading edge area in the flexure region from station 24.5 to 115.5. In this area, the density is 4.4 pounds per cubic foot to provide a better balance for the aerodynamic fairing blade segments.

5.3.3 Nose Balance Weights

The nose balance weights are tungsten rods that are cut into short lengths and drilled to meet the required station by station balance about the pitch axis.

5.3.4 Tip Hardware

The spar unidirectional and crossply laminates are wrapped around the tip anchor fitting shown in Figure VI-2 during the spar molding operation. Four studs are attached to the fitting which retain the tracking and balance weights. The tip rib provides a housing for the weights and is foam bonded to the anchor fitting and honeycomb. It is also bonded to the top and bottom crossply skins. A molded glass fabric tip cover mounts on the open end of the tip rib. The tip cover is retained by four screws.

The overbalance fitting is bonded to the inside contour of the spar and provides a housing for the overbalance weight. The weight can be cut in length to readjust the dynamic and static balance axes of the blade. It is snugly retained, inboard by the fitting, and outboard by the forward tracking weight stud and a spacer.

5.3.5 Leading Edge Erosion Strip

The leading edge erosion protection strip is made of titanium segmented to provide strain compatibility with the low modulus fiberglass blade structure. A similar system has been used on the fiberglass BO-105 blade.

5.3.6 Material Selection

The selection of materials for the rotor blade primary structure was made after an extensive review of both existing and advanced materials. A major requirement in the development of a soft in-plane prop/rotor system is that the material must have high fatigue strength and low modulus of elasticity. An evaluation of a number of materials on the basis of strength-to-stiffness was made with

the results presented in Figure VI-7. This figure shows that fiberglass composites of S-glass with epoxy resin offer the best structural properties for this design application. The composite of 60% XP251S unidirectional fibers and 40% 1002S 45° crossplied fibers was selected as the optimum arrangement for strength and stiffness in bending and torsion.

Manufacturing techniques for fiberglass blades have been developed at Boeing in conjunction with the Advanced Geometry Blade program. These blades were successfully flight tested on the CH-47C.

6. STRUCTURAL ANALYSIS

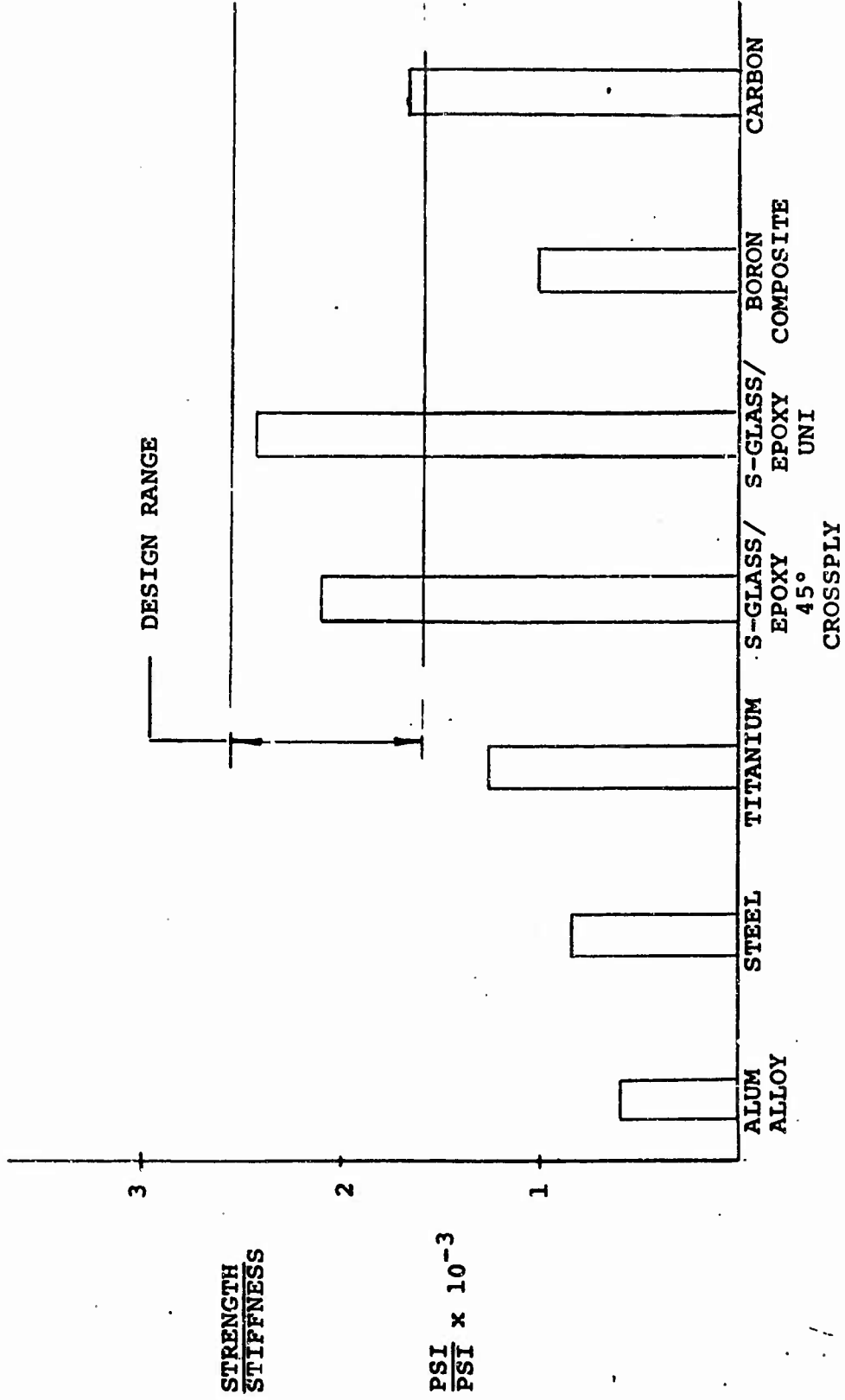
The flow diagram for blade structural analysis is shown in Figure VI-8. Each element of the flow chart will be described in detail in this section.

The margins of safety of the blade TR-2B are summarized in Figure VI-9. The negative margin of 4% at the 7.5% radius station can be eliminated by local strengthening without adverse effects on weight and blade dynamics.

6.1 PRELIMINARY CALCULATION OF ROOT FLEXURE PROPERTIES

Preliminary properties for the critical root flexure region were calculated by using the equations presented in Reference VI-2 modified for preliminary design of soft in-plane rotors (Reference VI-3). Only the weight of the blade, control requirements of the aircraft and fatigue design criterion are required. From this calculation, the root of the blade was chosen to be 7.5% radius and the flexure length to be approximately 25 to 35% radius. Prelim-

FIGURE VI-7 COMPARISON OF MATERIALS ON FATIGUE STRENGTH/STIFFNESS BASIS



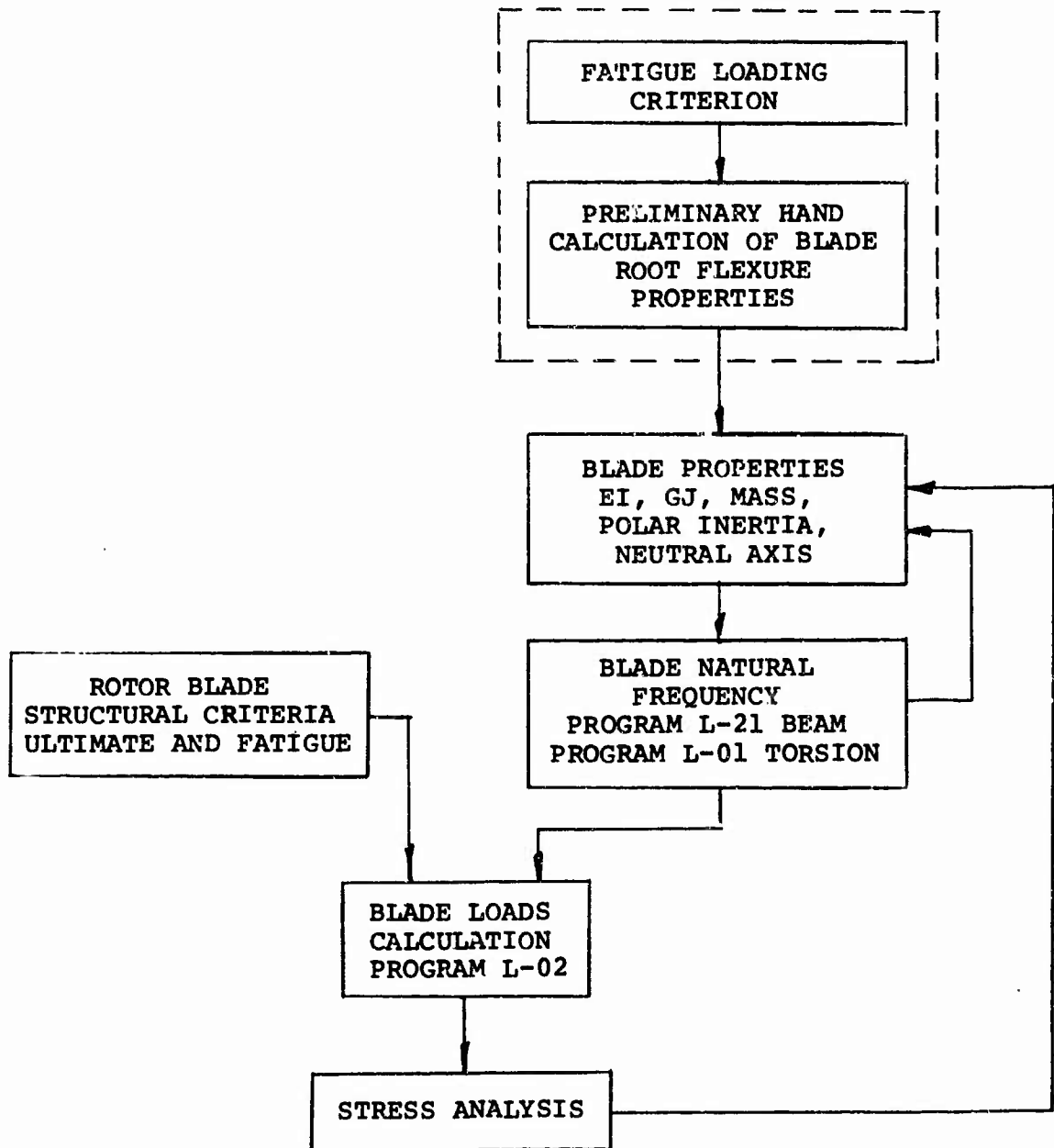
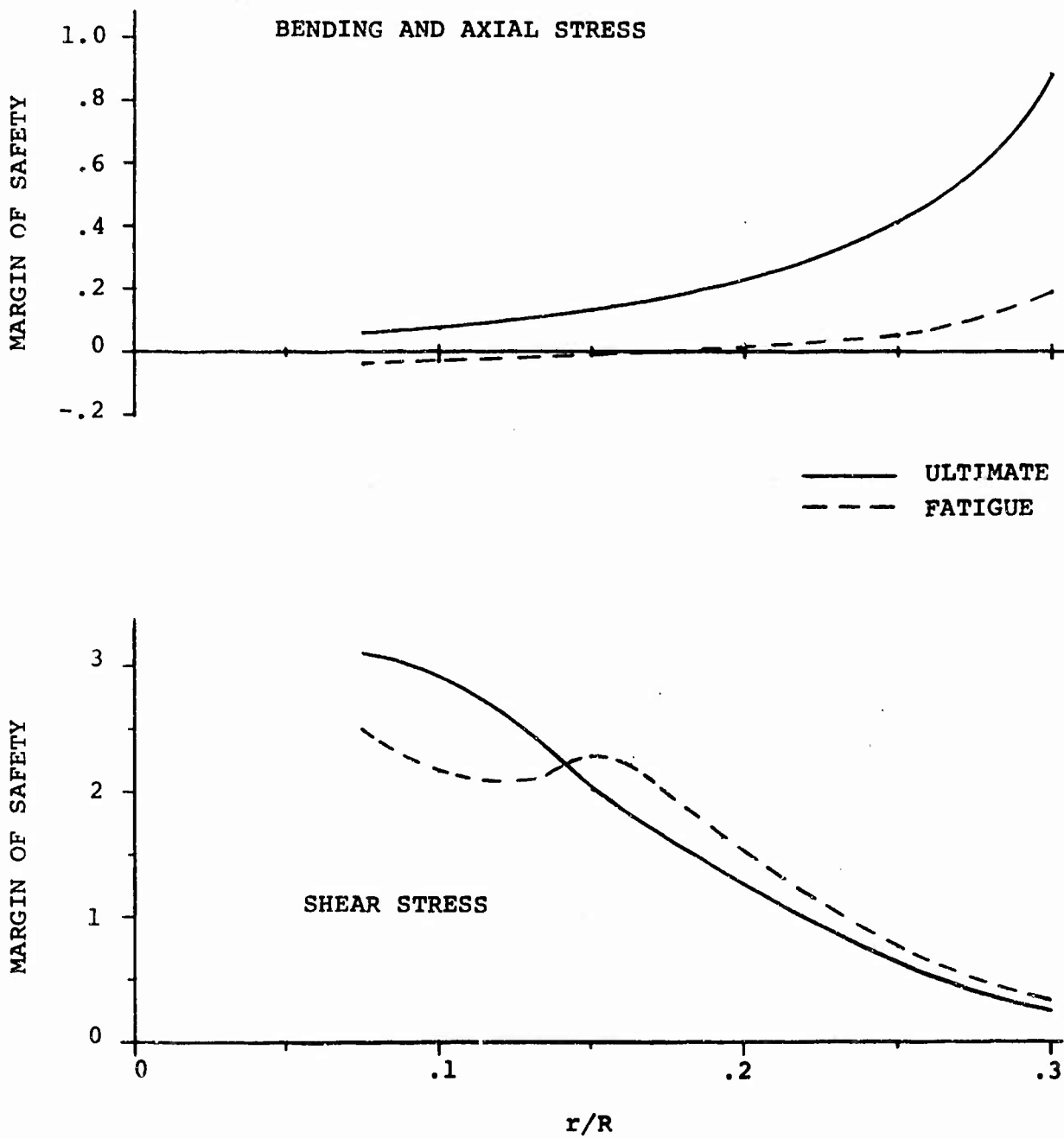


FIGURE VI-8 FLOW CHART OF BLADE STRESS CALCULATION

FIGURE VI-9
MARGIN OF SAFETY VS. BLADE SPAN



inary values of EI in the flapwise and chordwise directions were also chosen. From this, a preliminary blade design was sketched and iterated through the main loop of Figure VI-8 until the criteria were satisfied by design TR-2B.

6.2 ROTOR BLADE PHYSICAL PROPERTIES

The blade physical properties required for input to the L-02 and L-21 computer programs which yield outputs of blade natural frequencies, mode shapes and rotor loads include the following:

- a. Weight distribution
- b. Flapwise bending stiffness distribution
- c. Chordwise bending stiffness distribution
- d. Polar mass moment of inertia distribution
- e. Torsional stiffness distribution
- f. Locus of neutral axes

These are shown in Figures VI-10 through VI-15. The blade is balanced about the 25% chord and a 10-pound tip weight is used for dynamic balance.

6.3 ROTOR BLADE NATURAL FREQUENCY CALCULATION AND FLUTTER EVALUATION

Programs L-01 and L-21 were used to calculate the torsional and in-plane and out-of-plane frequencies for the rotor blade hover and cruise collectives. Summaries of these computer programs are shown in Appendix 2.

The calculated blade bending natural frequency ratios (1st and 2nd modes) at the design hover rotor speed are .76 (lag) and 1.25 (flap). The blade natural frequencies for the normal operating

FIGURE VI-10 MODS - 21'S AIRCRAFT
 TILT ROTOR - PROP/ROTOR AIRCRAFT
 BLADE SPAN vs WEIGHT DISTRIBUTION

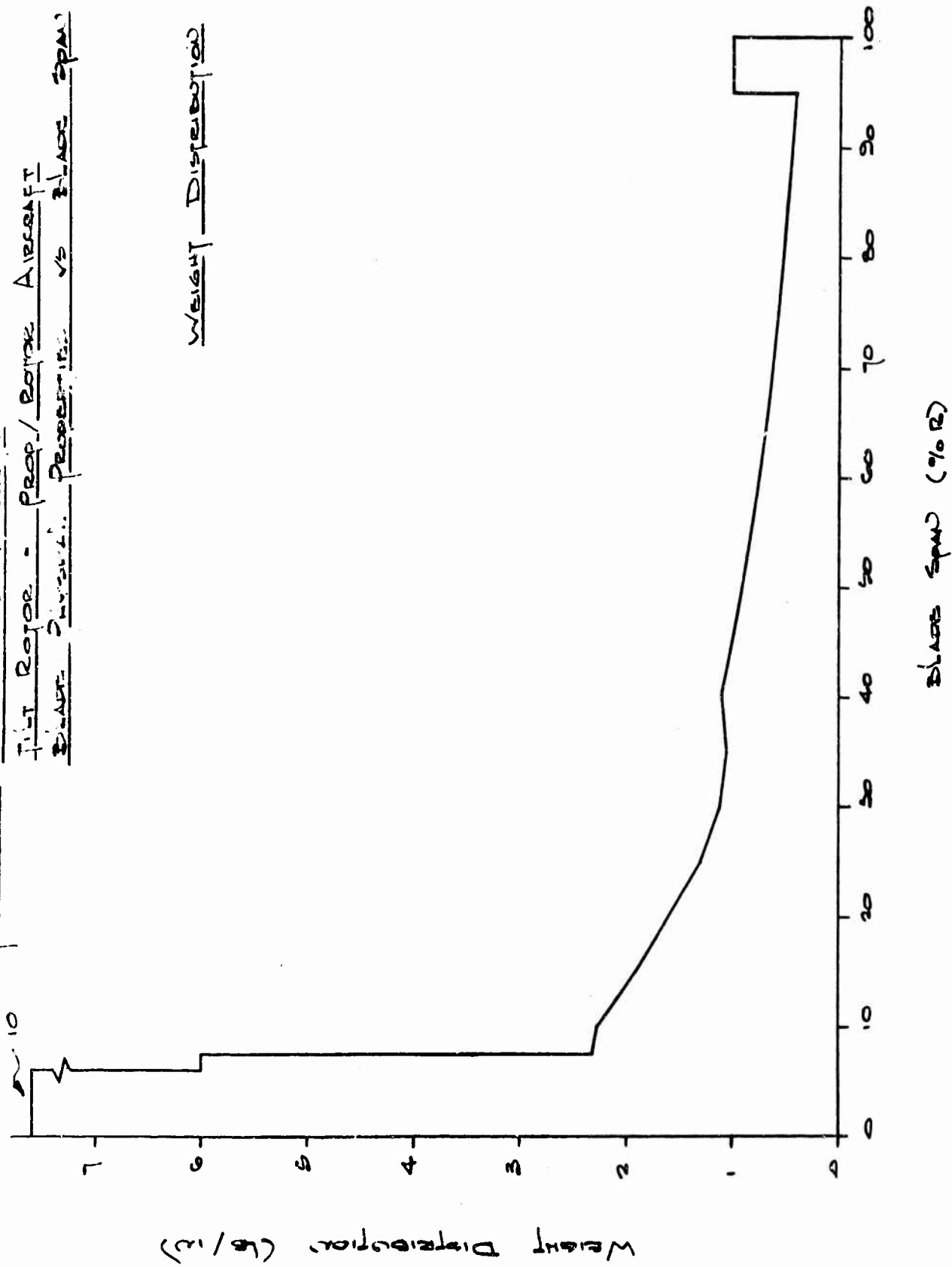


FIGURE VI-11 MODE - 2 1/2 AIRCRAFT

FIT ROTOR - PROP / ROTOR BLADE

BLADE: PHYSICAL PROPERTIES VS BLADE SPAN

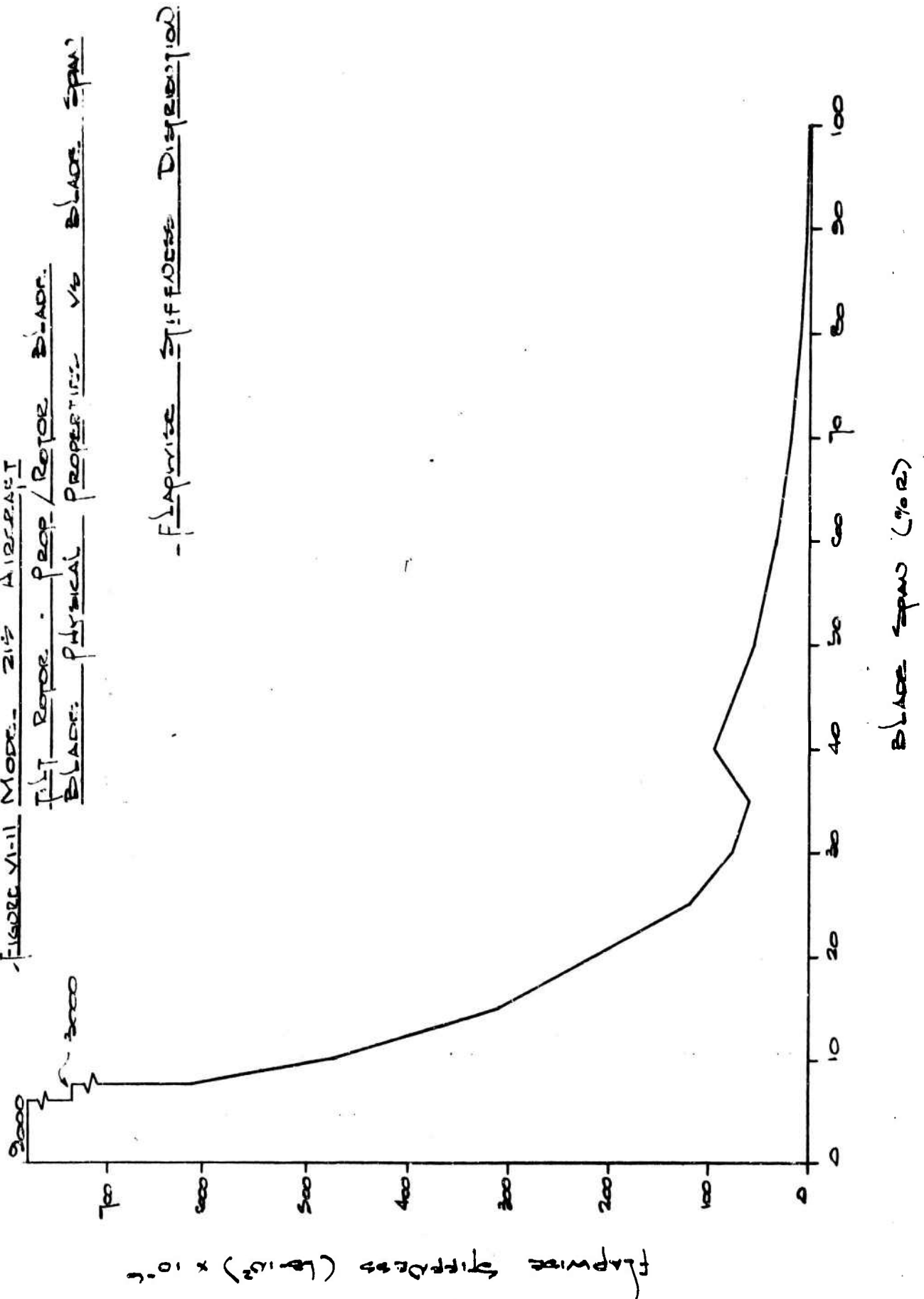
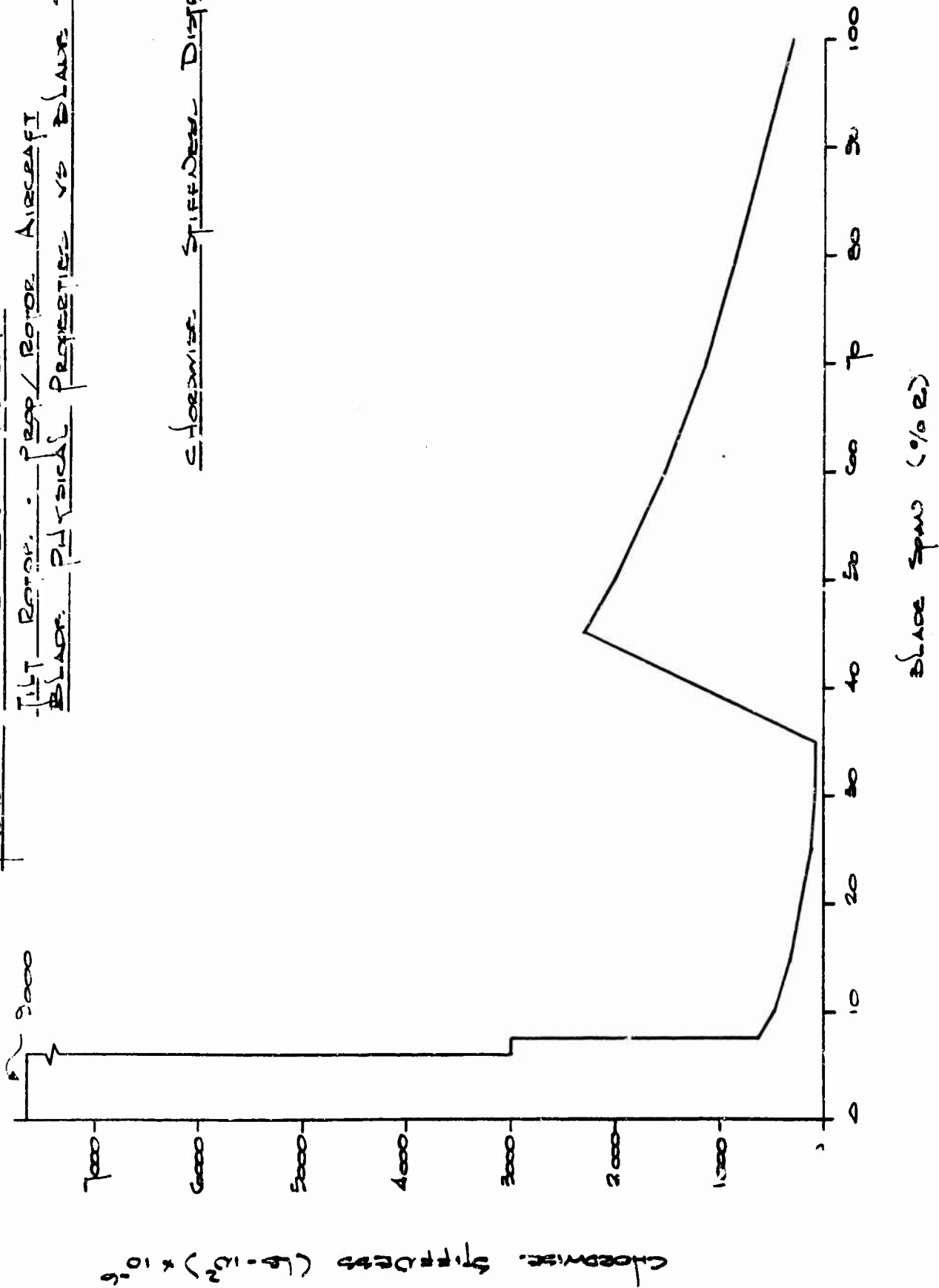


FIGURE VI-12 MODE - 212 AIRCRAFT

TILT ROTOR - PROP/ROTOR AIRCRAFT
BLADE PHYSICAL PROPERTIES VS BLADE SPAN

CHORDWISE STIFFNESS DISTRIBUTION



Chordwise Stiffness (lb-in^2) $\times 10^6$

Blade Span (%)

FIGURE VI-13 MODEL 215 AIRCRAFT TILT ROTOR - PROP/ROTOR BLADE
 BLADE PHYSICAL PROPERTIES VS. BLADE SPAN

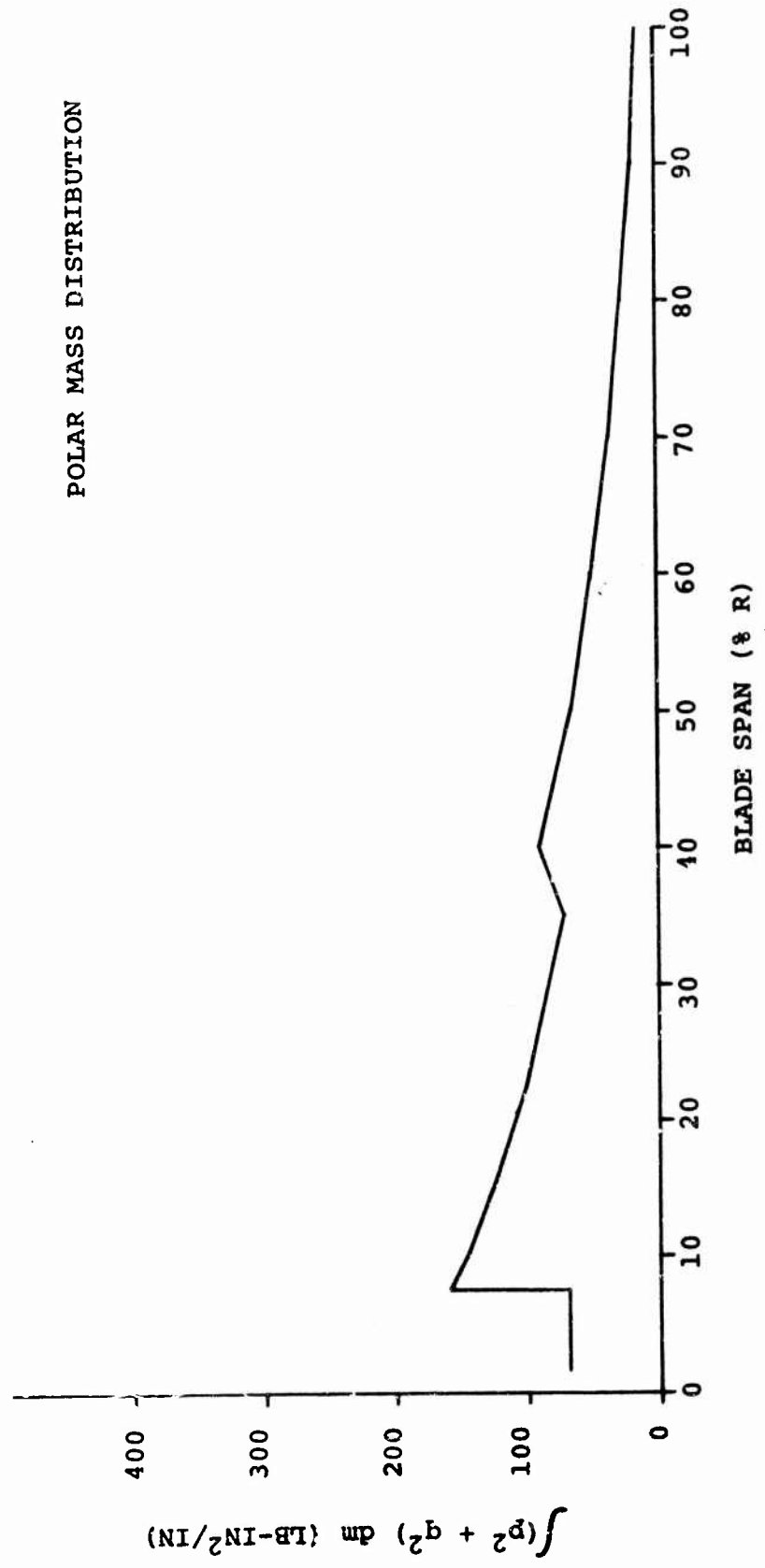


FIGURE VI-14

MODEL 215 AIRCRAFT TILT ROTOR-
PROP/ROTOR BLADE - BLADE PHYSICAL
PROPERTIES VS. BLADE SPAN

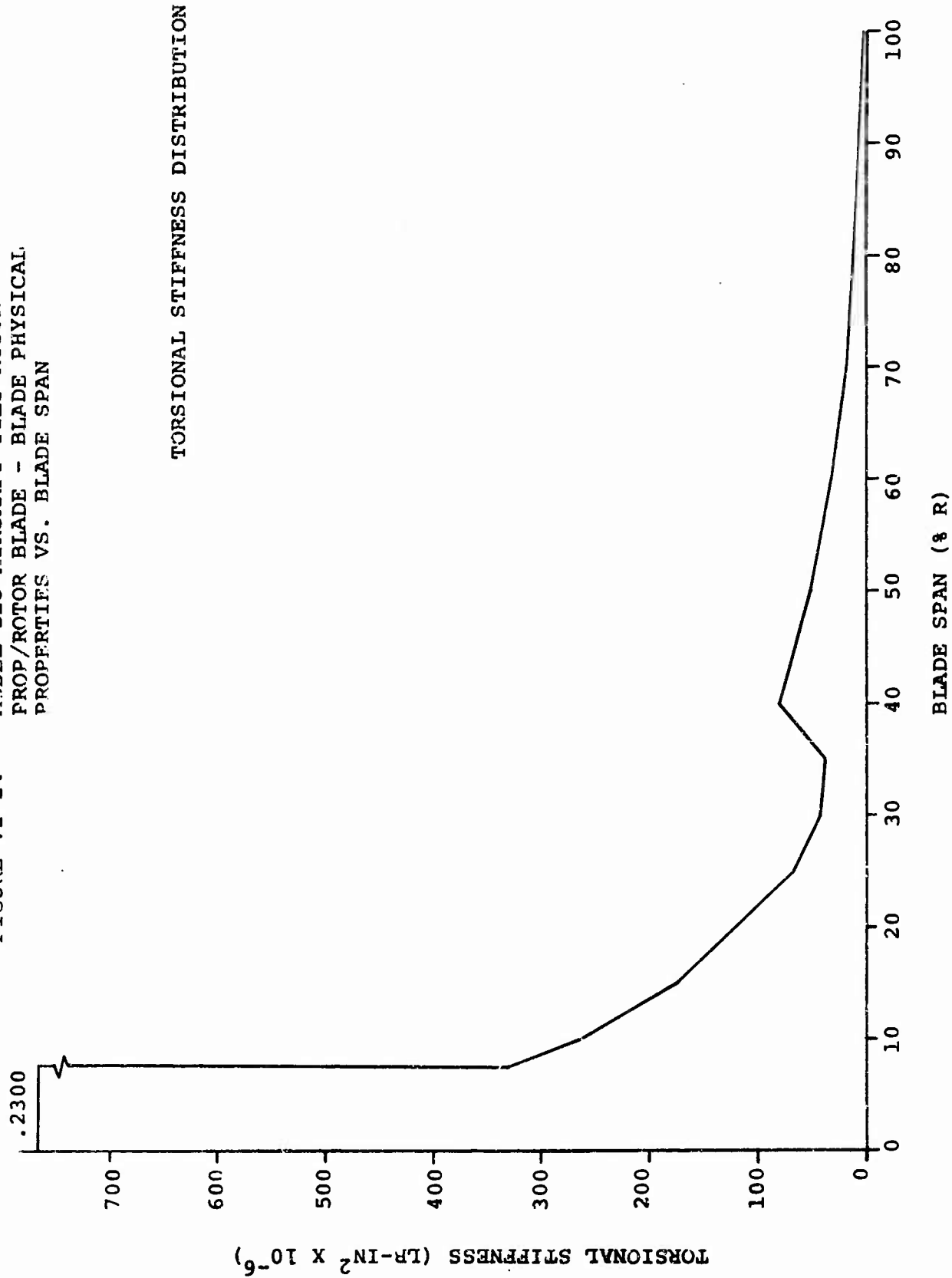
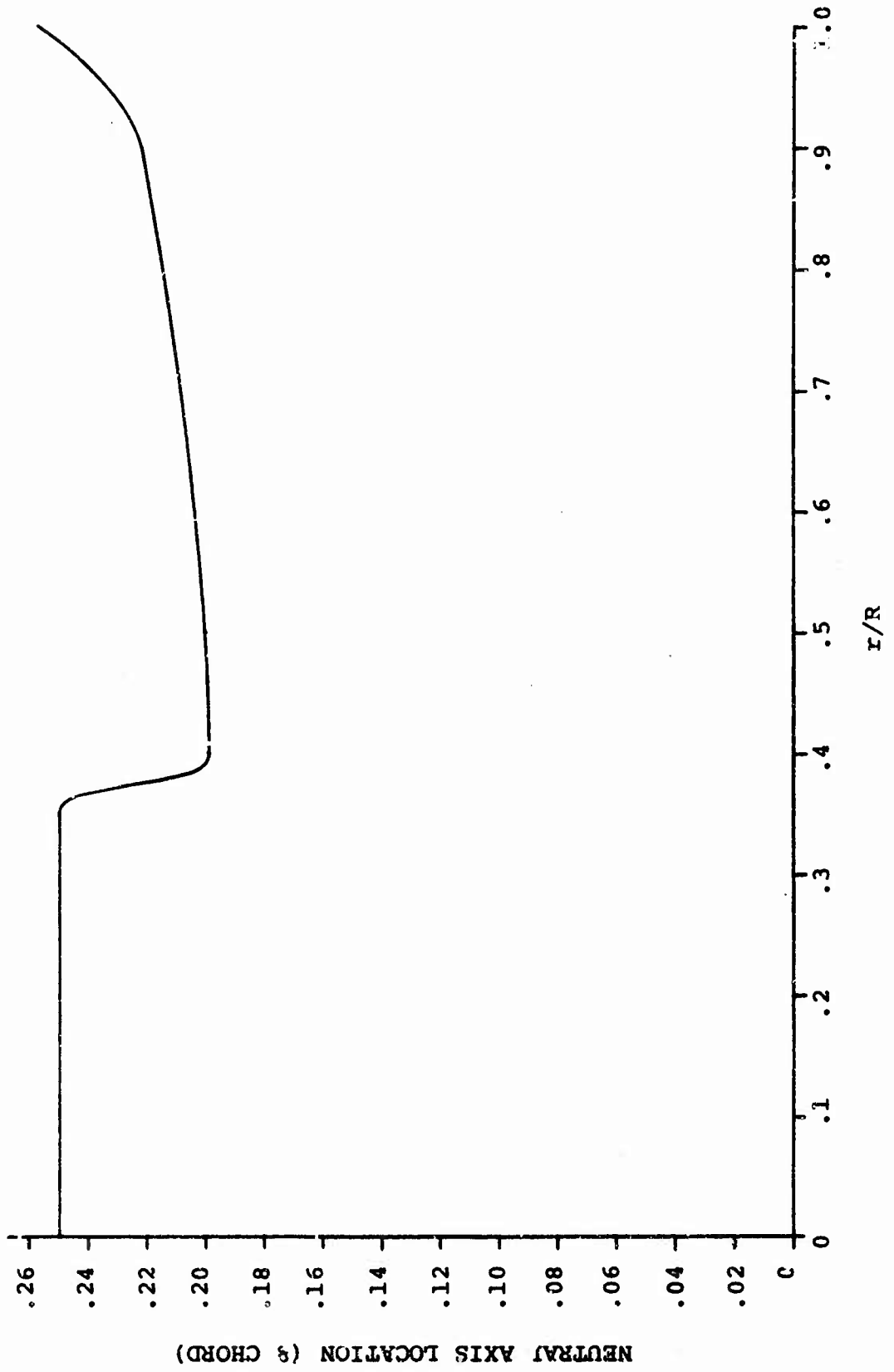


FIGURE VI-15
SPANWISE DISTRIBUTION OF CHORDWISE NEUTRAL AXES



VI-31

rotor speeds in hover and cruise are presented in Table VI-1. A natural frequency spectrum for the rotor speeds in hover and cruise is presented in Figures VI-16 and VI-17. All the frequency criteria and objectives defined in the dynamic criteria have not been met, but can be achieved by fine tuning the design. In particular, the blade third mode bending frequency ratio falls close to an integer harmonic as can be seen in the frequency spectrum plot. The third mode frequency can be lowered by redistributing the weight and stiffness in the 30 to 50% radius location. This change will also eliminate the 3 per rev crossing of the third mode in going from hover to cruise RPM.

6.3.1 Stall Flutter

The stall flutter characteristics of the rotor blade were evaluated for hover at normal design gross weight. Thrust is based on gross weight plus hover download and a 15% thrust control maneuver margin. The results from Figure VI-18 show the blade to be free from stall flutter since the hover condition was chosen to be at the inception of stall flutter to minimize aircraft weight.

6.3.2 Conventional Flutter

The blade is balanced at 25% chord to prevent conventional flutter. This has been verified by program L-01 which calculates the modal damping.

TABLE VI-1

BLADE NATURAL FREQUENCIES FOR BLADE DESIGN TR-2B

CONDITION	RPM	$\theta_{.75R}$	BENDING MODE	ω/Ω	TORSIONAL MODE	ω/Ω	ZERO TUNING WEIGHT
Hover	295	10.87°	1	.759 I	1	4.19	
			2	1.249 O	2	8.33	
			3	2.890 O			
			4	4.560 I			
Cruise	207	55°	1	.864 I			
			2	1.338 O			
			3	3.073 I			
			4	5.701 O			

I - Dominant Deflection In-Plane

O - Dominant Deflection Out-of-Plane

FIGURE VI-16 NATURAL FREQUENCY SPECTRUM

BENDING
HOVER CONDITION

COLLECTIVE ANGLE = 10.87°
L-21 ANALYSIS
DESIGN M215-2B
ZERO TUNING WEIGHT

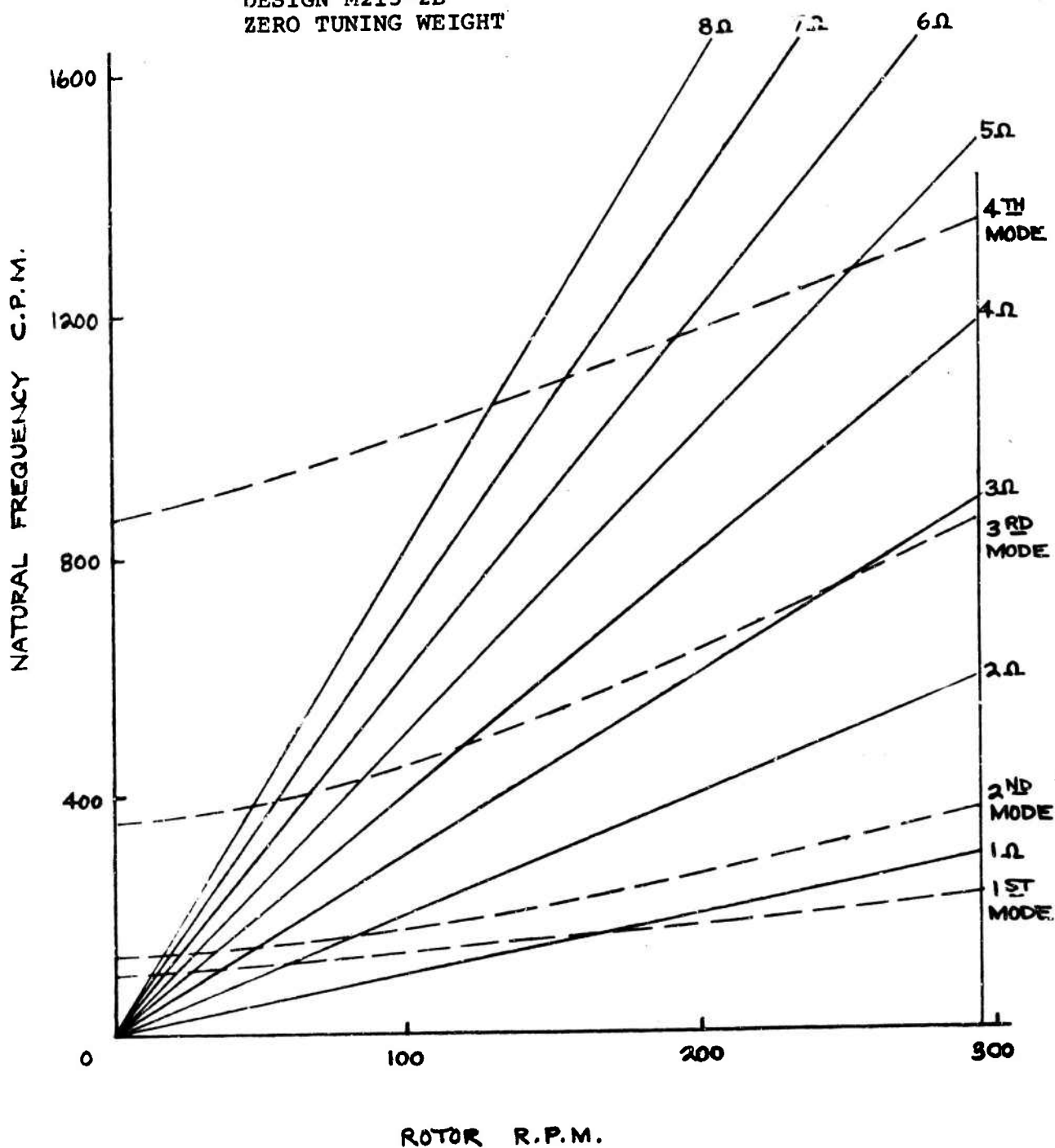


FIGURE VI-17 NATURAL FREQUENCY SPECTRUM

BENDING
CRUISE CONDITION

COLLECTIVE ANGLE = 55°
L-21 ANALYSIS
DESIGN M215-2B
ZERO TUNING WEIGHT

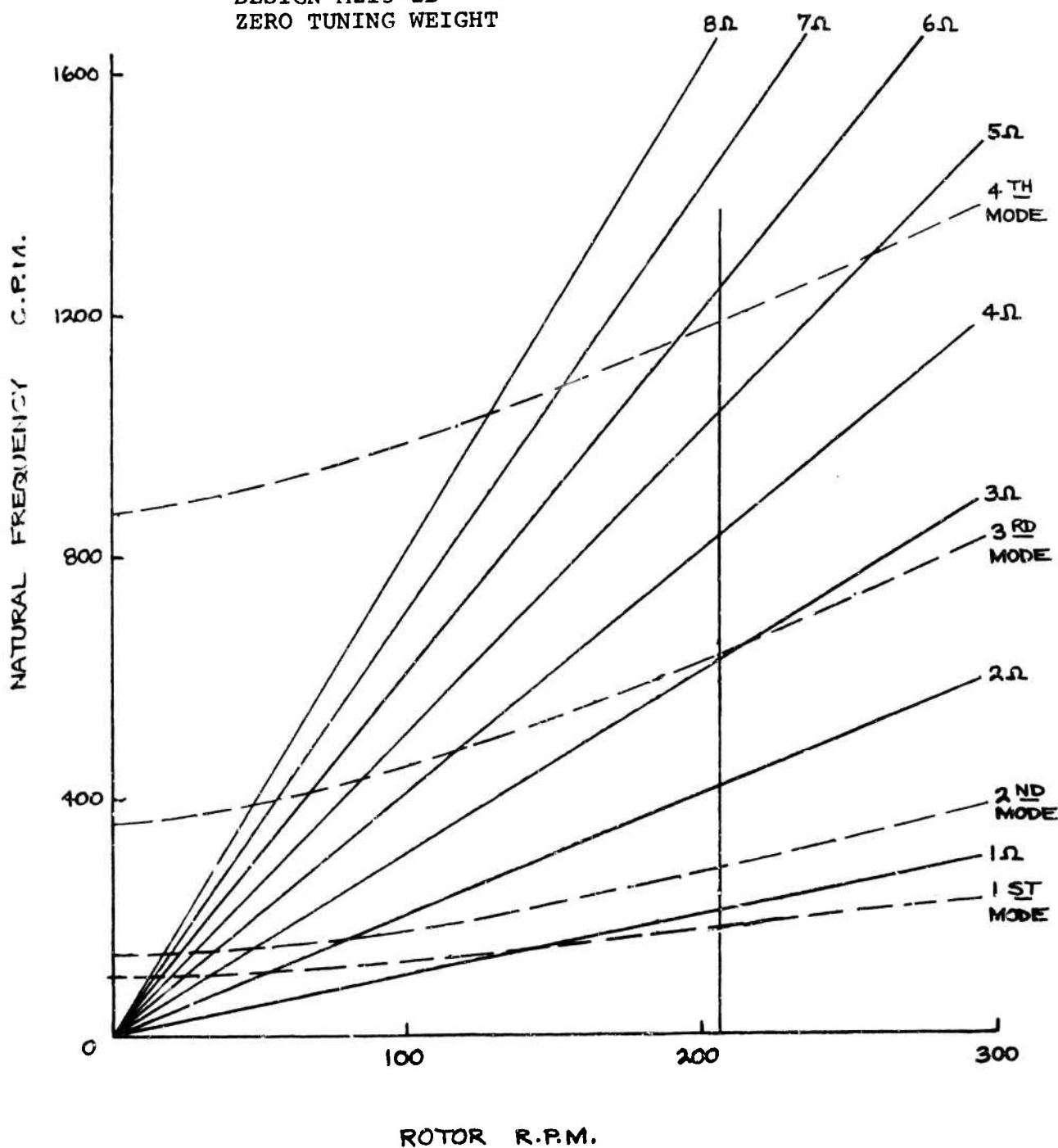
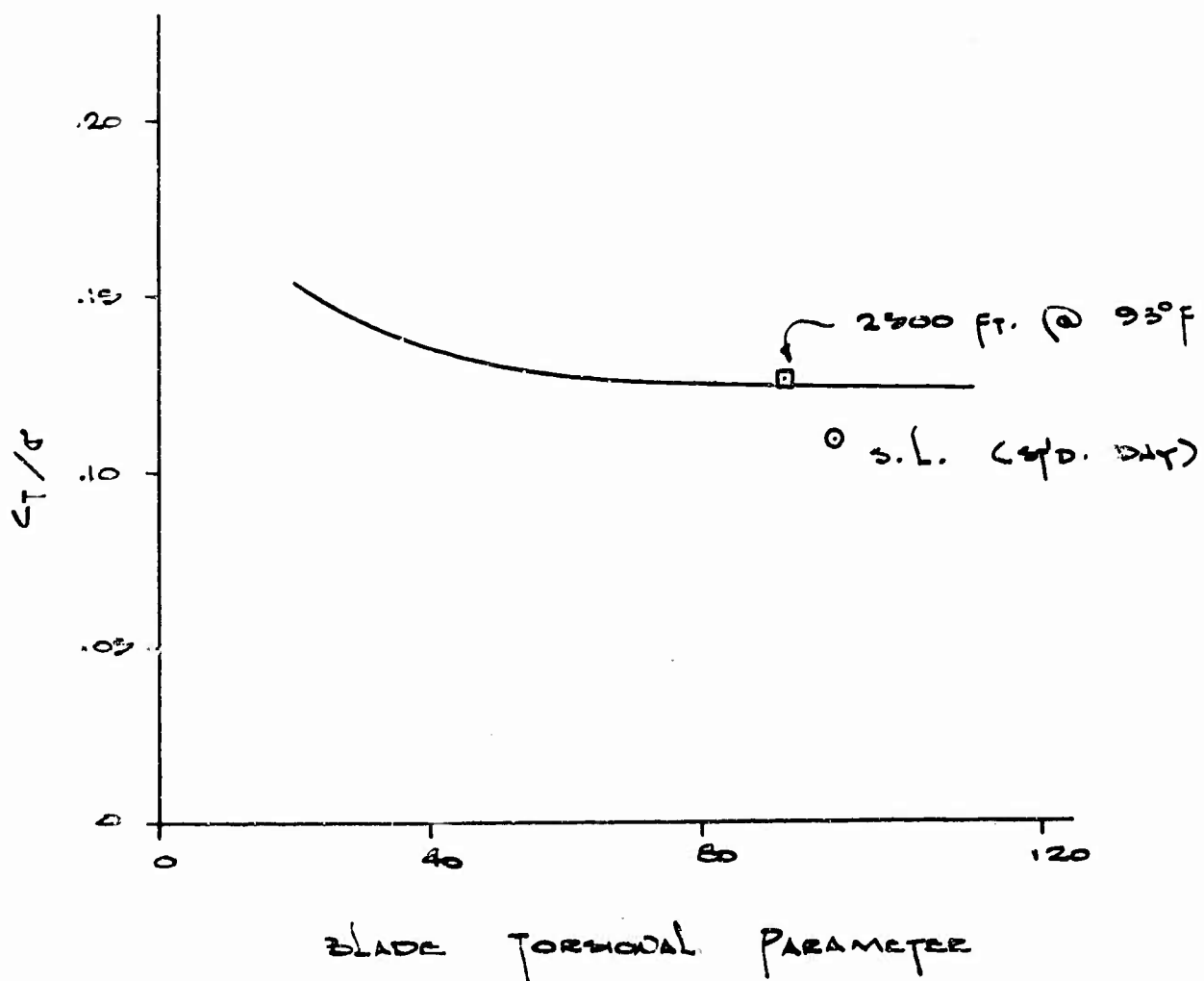


FIGURE VI-18

TILT ROTOR - PROP/ROTOR BLADE
STALL FLUTTER EVALUATION

ROTOR STALL FLUTTER CRITERIA
CURVE GIVES INCEPTION OF
FLUTTER CONDITIONS

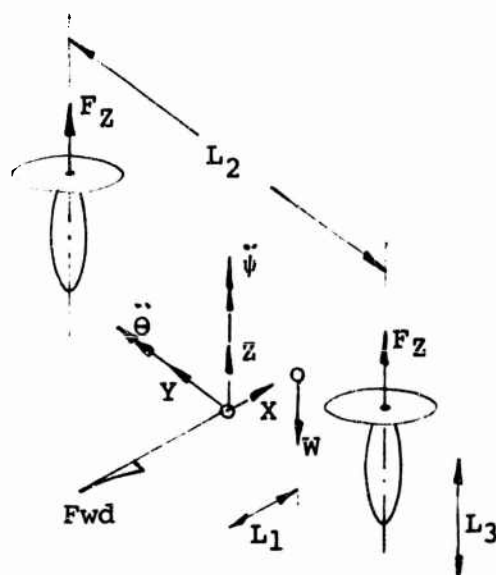


$$\frac{(P/P_0)^{1/2} V_T c \sqrt{R}}{\omega_0 \sqrt{I_0}}$$

6.4 ROTOR BLADE LOADS CALCULATION

The design blade loads were calculated by the L-02 computer program which incorporates the Leone-Myklestad analytical method for computing rotor loads. The outputs yield blade spanwise distributions of steady and alternating flapwise, chordwise and torsional moments and centrifugal force for each of the design conditions considered. The design load condition was hover flight with cyclic control. The flying qualities criteria for aircraft initial accelerations in hover are 0.5 rad/sec^2 for aircraft yaw and 0.6 rad/sec^2 for aircraft pitch. The control moments required to produce these accelerations are calculated below. Also included is the control moment required to trim the aircraft to a level position for the extreme C.G. condition. The calculation of cyclic required to produce control moment includes the effect of wing twist.

6.4.1 Required Aircraft Trim and Inertia Moments



- $W = 67,000 \text{ lbs}$
- $I_Y = 244,124 \text{ slug/ft}^2$
- $I_Z = 1,109,183 \text{ slug/ft}^2$
- $L_1 = 11.6 \text{ in}$
- $L_2 = 789 \text{ in}$
- $L_3 = 112 \text{ in}$
- $\ddot{\theta} = 0.6 \text{ rad/sec}^2$
- $\ddot{\psi} = 0.5 \text{ rad/sec}^2$

Required Trim Moment:

$$M_{\text{TRIM}} = W L_1 = 11.6 (67,000)$$

$$M_{\text{TRIM}} = 777,600 \text{ in-lbs}$$

Required Yaw Moment:

$$M_{\text{YAW}} = I_Z \ddot{\psi} = 1,109,183 (12) (0.5)$$

$$M_{\text{YAW}} = 6,655,100 \text{ in-lbs}$$

Required Pitch Moment:

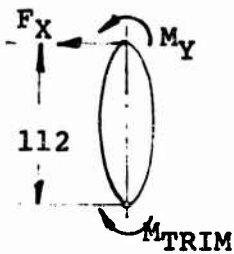
$$M_{\text{PITCH}} = I_Y \ddot{\theta} = 244,124 (12) (0.6)$$

$$M_{\text{PITCH}} = 1,757,700 \text{ in-lbs}$$

6.4.2 Required Rotor Forces and Moments

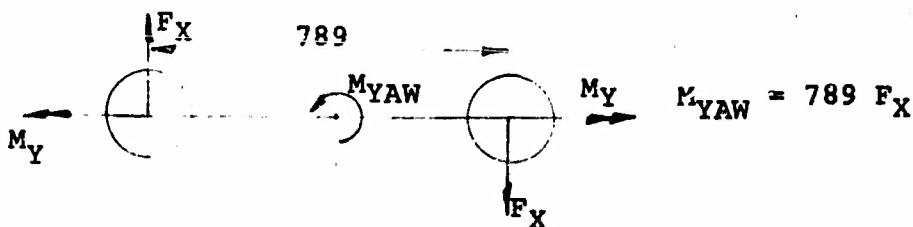
The cyclic inputs required to react the externally applied moments are now considered in this analysis. Hub forces generated by the cyclic inputs react the applied moments as follows:

Trim Control:

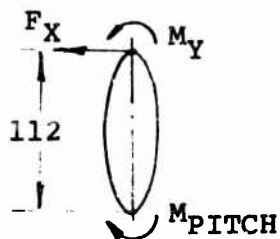


$$M_{\text{TRIM}} = M_Y + 112 F_X$$

Yaw Control:



Pitch Control:



$$M_{\text{PITCH}} = M_Y + 112 F_X$$

6.4.3 Rotor Hub Forces and Moments Produced by Cyclic Pitch

The rotor hub forces calculated by the L-02 computer program for 1° cyclic input are as follows:

$$F_X = 736 \text{ lbs}$$

$$F_Y = 92 \text{ lbs}$$

$$F_Z = 34,180 \text{ lbs}$$

$$M_X = 83,189 \text{ in-lbs}$$

$$M_Y = 224,020 \text{ in-lbs}$$

$$M_Z = 1,136,300 \text{ in-lbs}$$

The amount of cyclic pitch required to produce the aircraft moments specified for the fatigue condition in paragraph 6.4.1 can now be calculated as follows:

$$M_{\text{TRIM}} = \frac{777,600}{2} = 388,600 \text{ in-lbs}$$

$$M_{\text{YAW}} = .25 (6,655,100) = 1,663,775 \text{ in-lbs}$$

$$M_{PITCH} = \frac{.25 (1,757,700)}{2} = 219,713 \text{ in-lbs}$$

For 1° cyclic input, the available control moments are as follows:

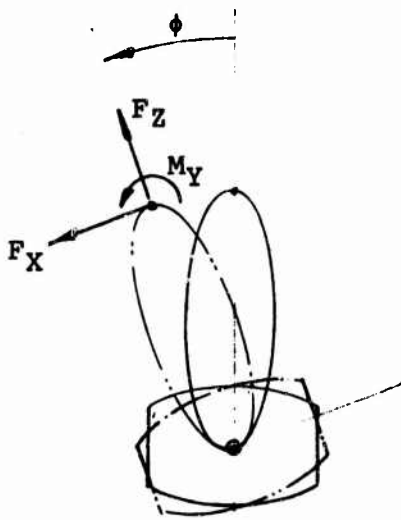
$$M_{TRIM} = M_{PITCH} = M_Y + 112 F_X = 224,020 + 112 (736)$$

$$\therefore M_{TRIM} = M_{PITCH} = 308,000 \text{ in-lbs}$$

$$M_{YAW} = 789 (736 + \Delta F_X)$$

The force ΔF_X is the X-component of thrust brought about by the nacelle tilt resulting from a wing twist.

The incremental force ΔF_X is determined as follows:



$$\phi = \frac{ML}{GJ} = \frac{(M_Y + 112 F_X) L}{GJ}$$

$$L = \frac{789}{2} = 394.5 \text{ in}$$

$$J = 2.23 \times 10^{10} \text{ lb-in}^2$$

$$M = 308,000 \text{ in-lbs (for 1° cyclic input)}$$

$$\phi = \frac{308,000 (394.5)}{2.23 \times 10^{10}}$$

$$= .00545 \text{ rads.}$$

$$\Delta F_X = F_Z \phi = 34,180 (.00545)$$

$$\Delta F_X = 186 \text{ lbs.}$$

$$\therefore M_{YAW} = 789 (736 + 186)$$

$$= 730,000 \text{ in-lbs.}$$

The cyclic inputs required may now be computed as follows:

$$\theta_{\text{TRIM}} = \frac{388,600}{M_y + 112 F_x} = \frac{388,600}{308,000} = 1.26^\circ$$

$$\theta_{\text{YAW}} = \frac{1,663,775}{789 (F_x + \Delta F_x)} = \frac{1,663,775}{730,000} = 2.28^\circ$$

$$\theta_{\text{PITCH}} = \frac{219,713}{M_y + 112 F_x} = \frac{219,713}{308,000} = .71^\circ$$

The cyclic input required for fatigue design is:

$$\begin{aligned}\theta_{\text{CYCLIC}} &= \theta_{\text{TRIM}} + \theta_{\text{YAW}} \\ &= 1.26^\circ + 2.28^\circ\end{aligned}$$

$$\theta_{\text{CYCLIC}} = 3.54^\circ$$

From the L-02 computer program, the radial distribution of steady and alternating blade loads have been computed for the design cyclic input and are presented in Figures VI-19 through VI-25.

6.4.4 Ultimate Loads

The greater of the two following conditions determines the design ultimate loads for the rotor blades. These are namely the maximum cyclic condition and the 2.5g vertical takeoff condition.

FIGURE VI-19 MODEL 215 TILT ROTOR - PROP/ROTOR BLADE
RADIAL DISTRIBUTION OF CENTRIFUGAL FORCE

HOVER CONDITION
 $\Omega = 295 \text{ RPM}$

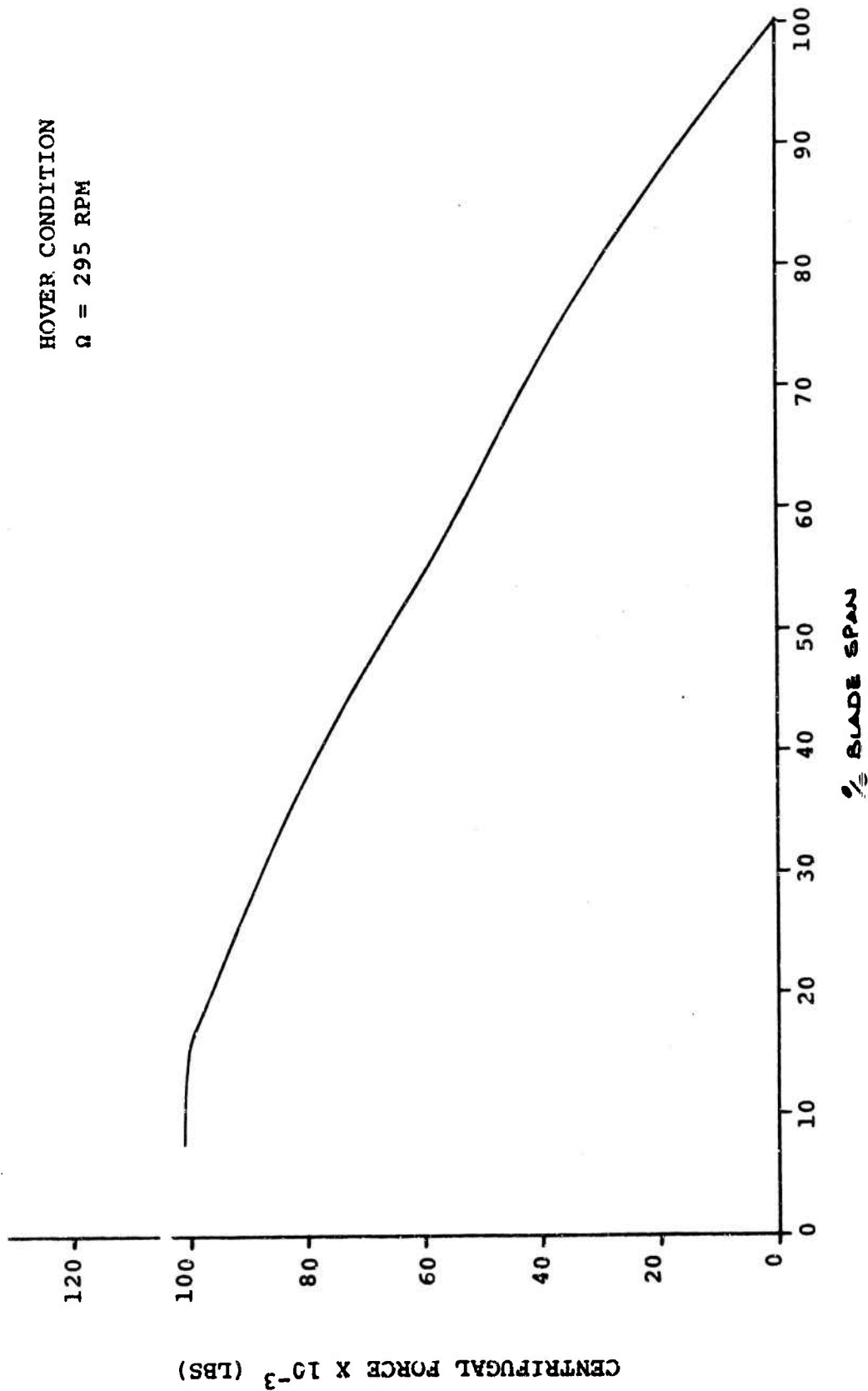


FIGURE VI-20 MODEL 215 TILT ROTOR - PROP/ROTOR BLADE
RADIAL DISTRIBUTION OF VIBRATORY FLAP
BENDING MOMENT

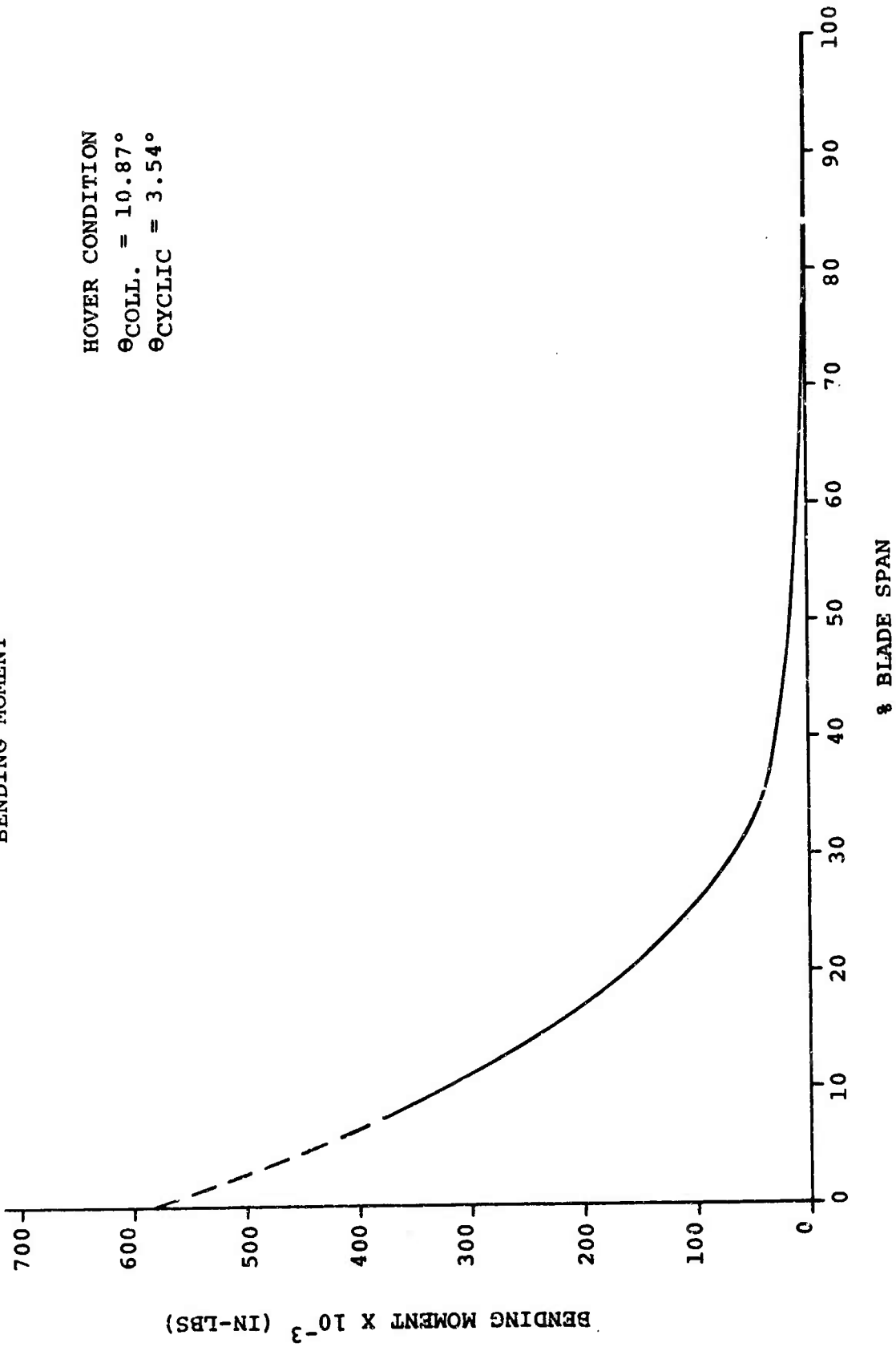


FIGURE VI-21

MODEL 215 TILT ROTOR - PROP/ROTOR BLADE
RADIAL DISTRIBUTION OF VIBRATORY CHORD
BENDING MOMENT

HOVER CONDITION
 $\theta_{COLL.} = 10.87^\circ$
 $\theta_{CYCLIC} = 3.54^\circ$

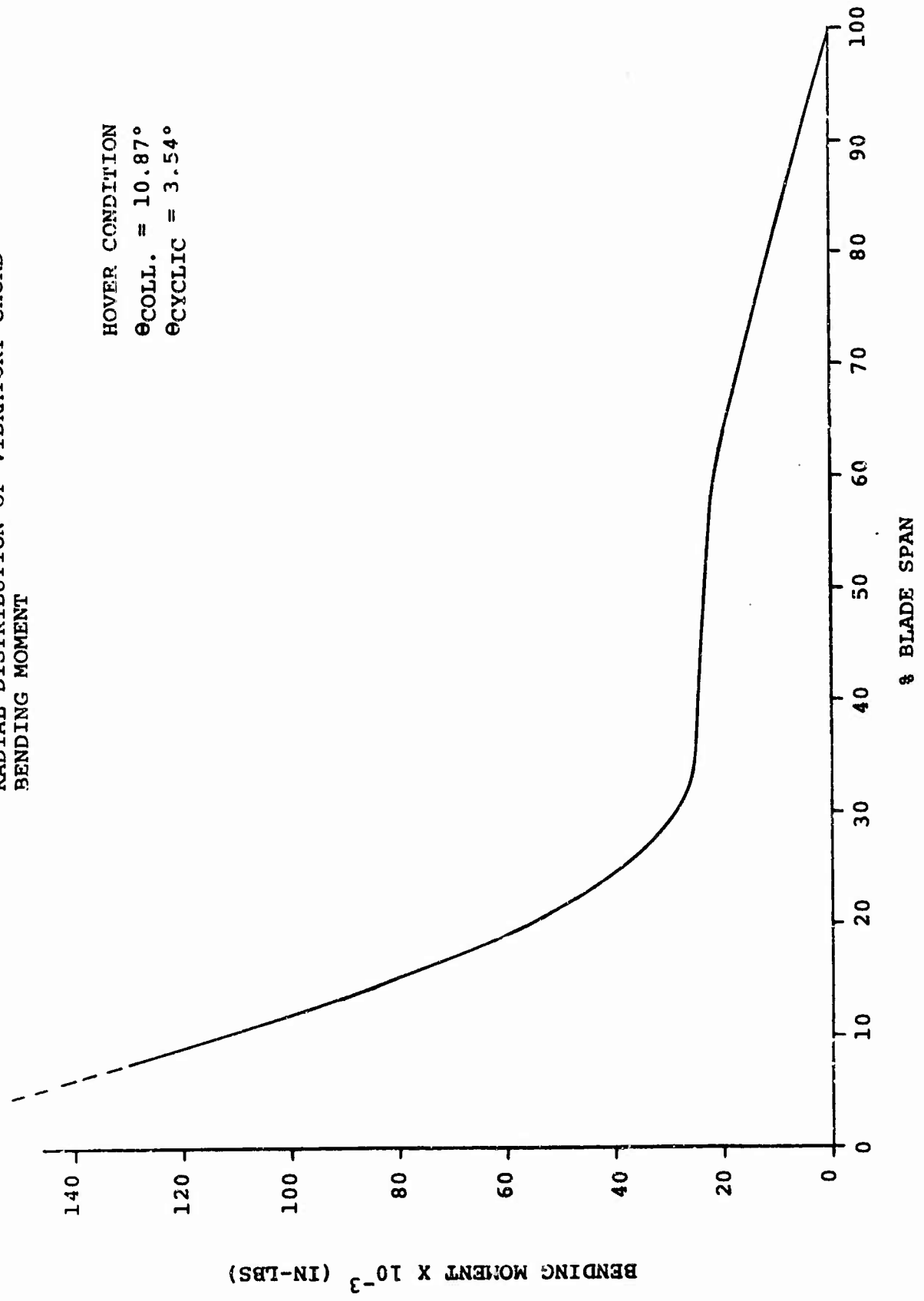


FIGURE VI-22 MODEL 215 TILT ROTOR PROP/ROTOR BLADE
 RADIAL DISTRIBUTION OF CONSTANT FLAP
 BENDING MOMENT, LEONE-MYKLESTAD METHOD

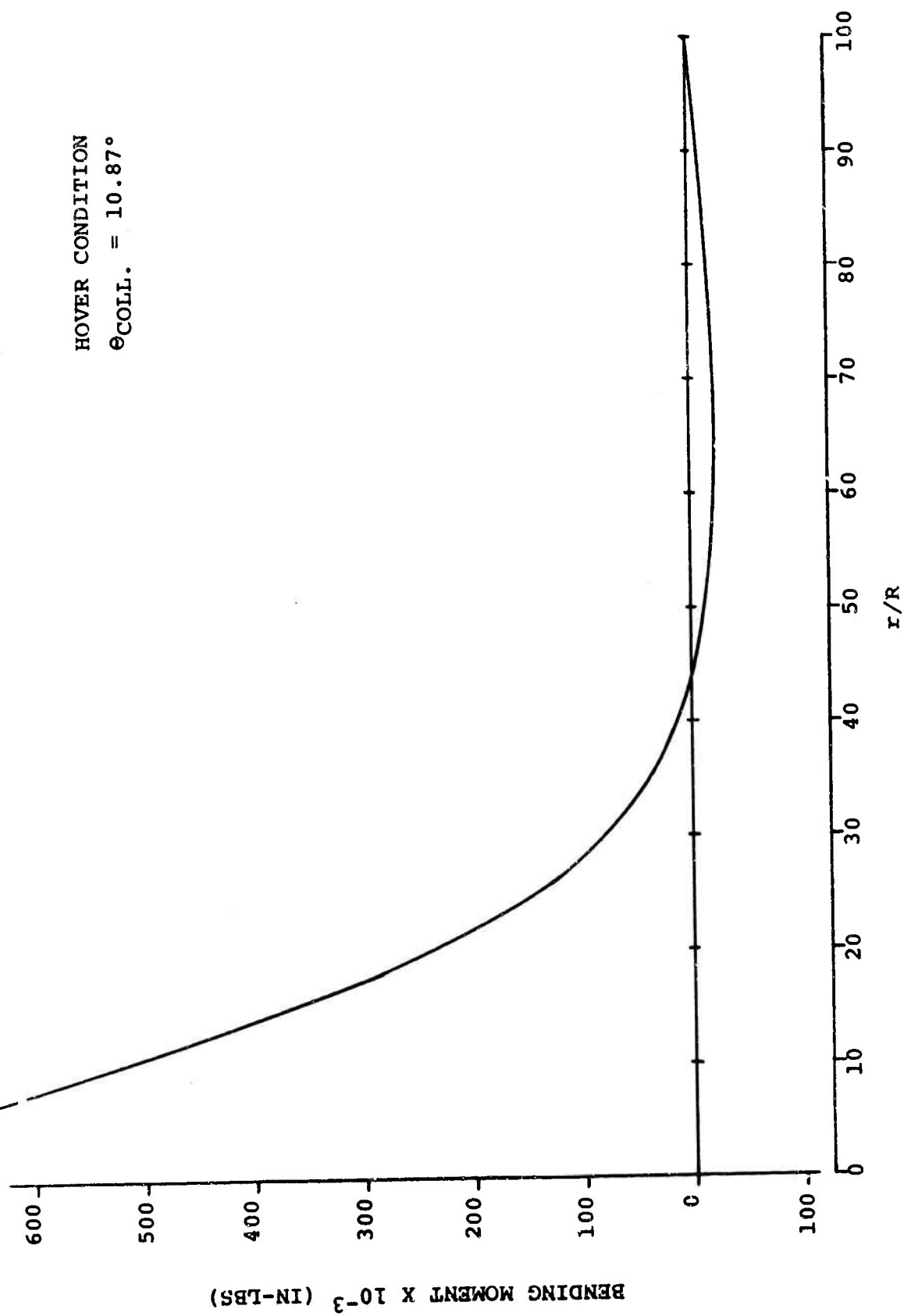


FIGURE VI-23

MODEL 215 TILT ROTOR PROP/ROTOR BLADE
RADIAL DISTRIBUTION OF CONSTANT CHORD
BENDING MOMENT, LEONE-MYKLESTAD METHOD

HOVER CONDITION
 $\theta_{\text{COLL.}} = 10.87^\circ$

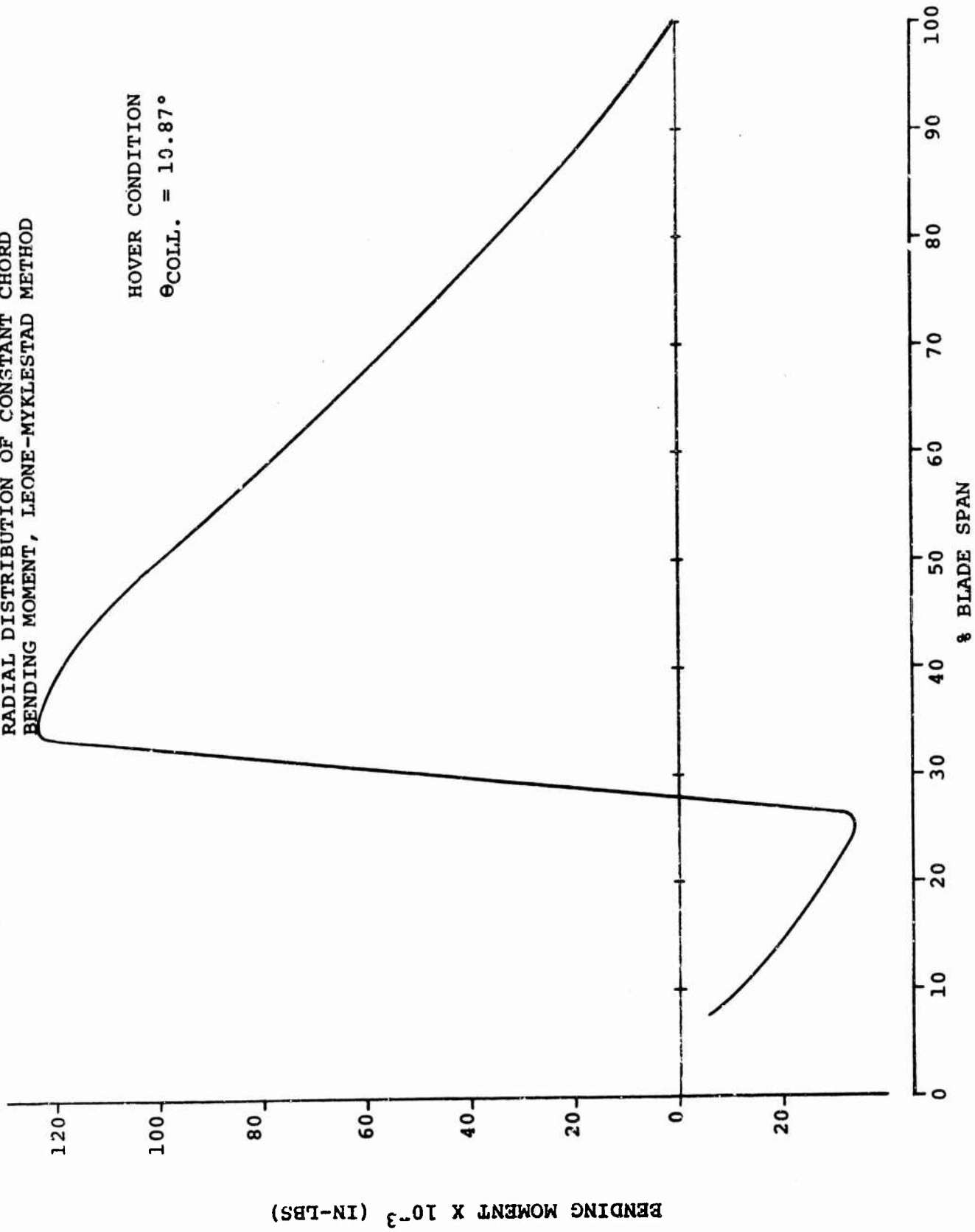


FIGURE VI-24
ALTERNATING TORSIONAL MOMENT VS. BLADE SPAN

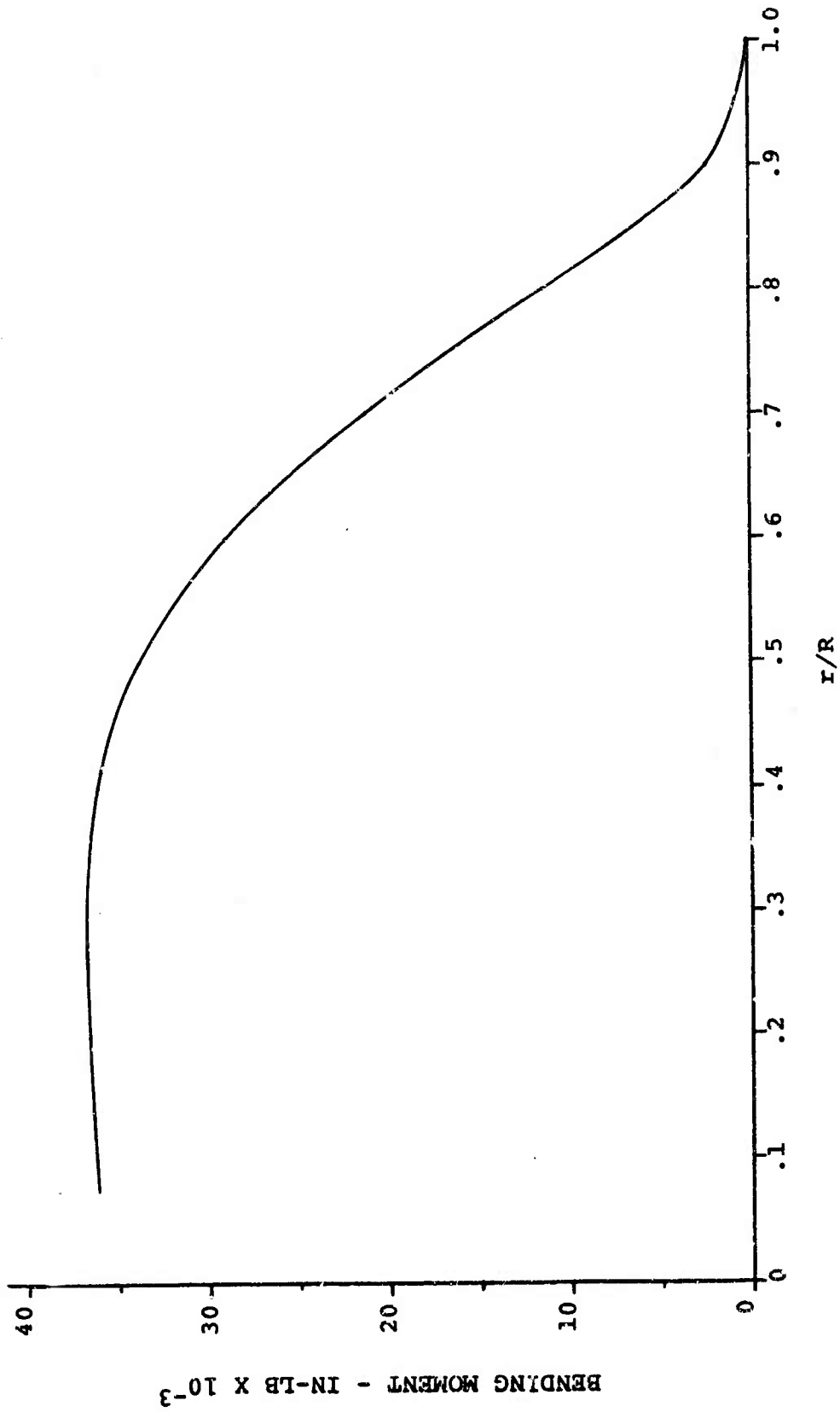
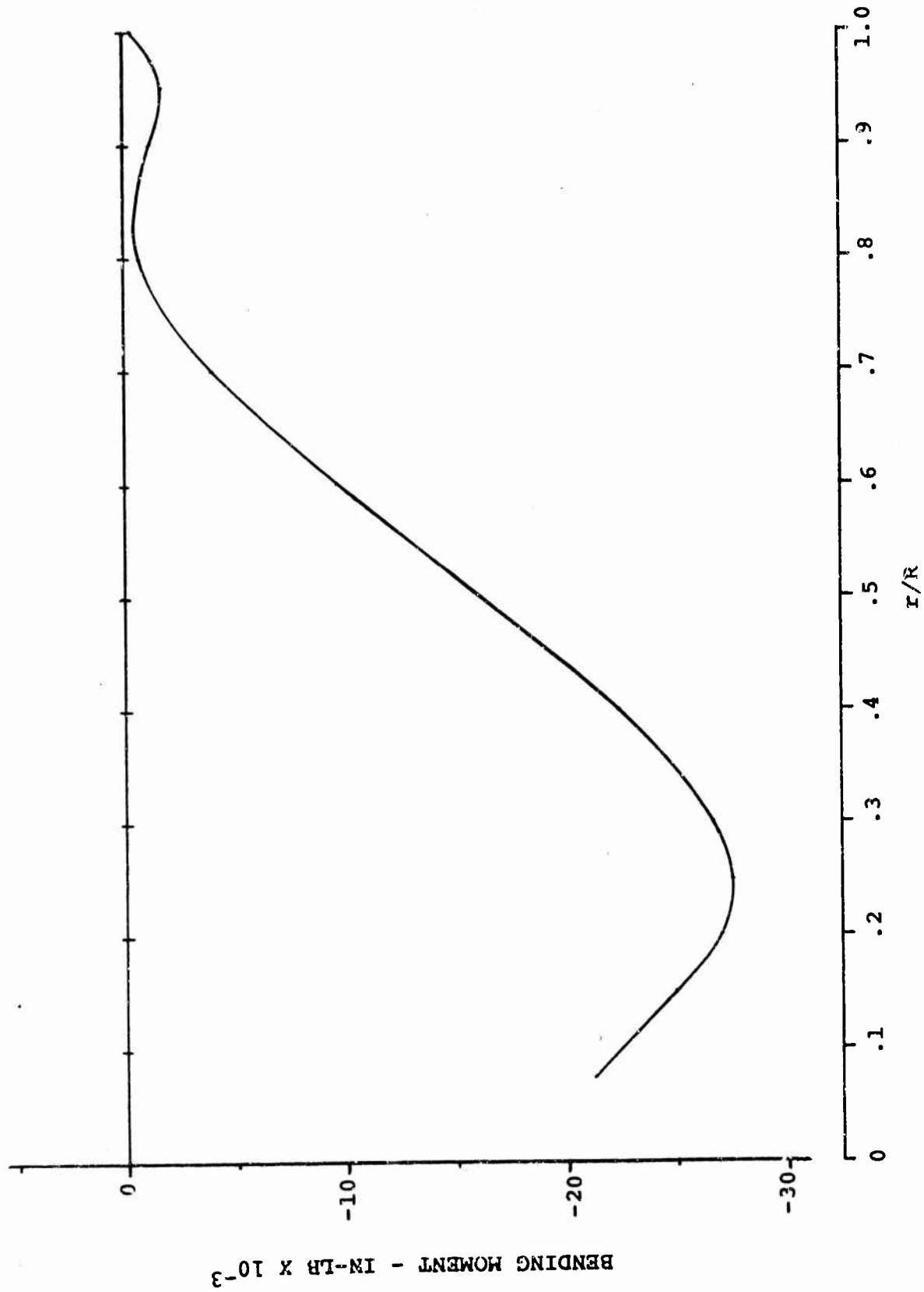


FIGURE VI-25
STEADY TORSIONAL MOMENT VS. BLADE SPAN



VI-41

The maximum cyclic condition is defined as:

a. Trim Cyclic + Yaw Control Cyclic + .50 Pitch Control Cyclic

OR

b. Trim Cyclic + .50 Yaw Control Cyclic + .50 Pitch Cyclic,

whichever is greater. Accordingly,

$$\theta_{\text{TRIM}} = \frac{388,600}{308,000} = 1.26^\circ$$

$$\theta_{\text{YAW}} = \frac{6,655,100}{730,000} = 9.12^\circ$$

$$\theta_{\text{PITCH}} = \frac{878,000}{308,000} = 2.84^\circ$$

$$\theta_{\text{CYCLIC}} = 1.26^\circ + 9.12^\circ + .50 (2.84^\circ)$$

$$\theta_{\text{CYCLIC}} = 11.80^\circ$$

The ultimate blade bending and torsional moments and shears for the maximum cyclic condition are determined by modifying the steady and alternating loads of the fatigue loading condition in the following manner:

$$M = \left[\left(\frac{11.80}{3.54} \right) M_{\text{ALTERNATING}} \leftrightarrow M_{\text{STEADY}} \right] \quad (1.50)$$

$$V = \left[\left(\frac{11.80}{3.54} \right) V_{\text{ALTERNATING}} \leftrightarrow V_{\text{STEADY}} \right] \quad (1.50)$$

The ultimate blade bending and torsional moments and shears for the 2.5g vertical takeoff condition are determined by modifying the steady and alternating loads of the fatigue loading condition in the following manner:

$$M = \left[\begin{array}{ccc} \left(\frac{1.26}{3.54} \right) & M_{\text{ALTERNATING}} & \longleftrightarrow M_{\text{STEADY}} \end{array} \right] (2.50) (1.50)$$

$$V = \left[\begin{array}{ccc} \left(\frac{1.26}{3.54} \right) & V_{\text{ALTERNATING}} & \longleftrightarrow V_{\text{STEADY}} \end{array} \right] (2.50) (1.50)$$

6.5 STRESS ANALYSIS

This stress analysis of the rotor blade is limited to an evaluation of the strength of the primary structure which is composed of a fiberglass composite spar and 45° crossply fiberglass skins.

The critical blade inboard section is investigated in detail for the combined loadings of bending, shear, torsion and centrifugal force determined by the loading conditions of hover flight with cyclic control. It is shown to be structurally adequate within the limits established.

The bending and axial stresses are calculated for the composite of 45° crossply and unidirectional fiberglass using the allowables from Reference III-2 and tabulated in Table VI-14.

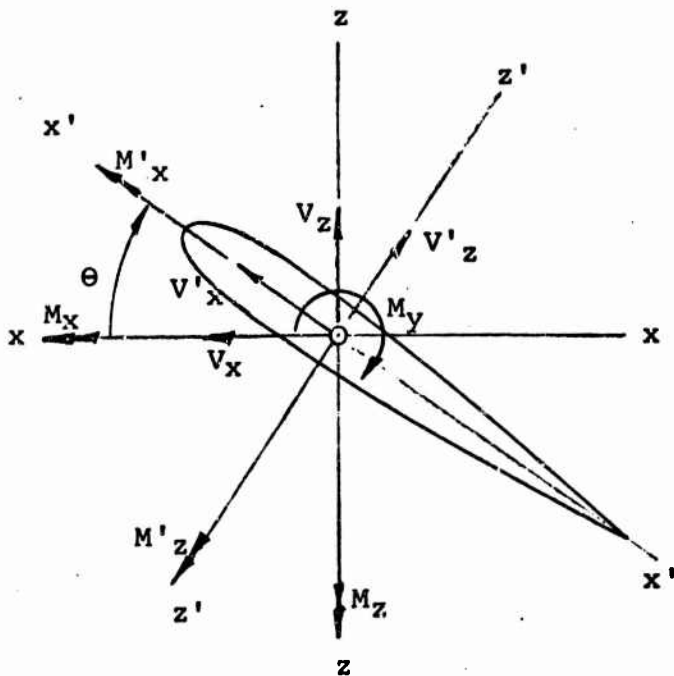
The shear and torsional loads are assumed to be taken by the 45° crossply only. The margins of safety have been computed without considering the effects of stress interaction.

6.5.1 Rotor Blade Loads and Stresses

The rotor blade loads relative to the in-plane and out-of-plane axes at several inboard blade stations for the fatigue, maximum cyclic and 2.5g vertical takeoff conditions are presented in Tables VI-2, VI-3 and VI-4. Positive sign convention for blade loads is shown in Figure VI-26.

These loads have been resolved to yield the resultant steady and alternating loads using the equations on Figure VI-27. These loads are shown in Tables VI-5 through VI-10.

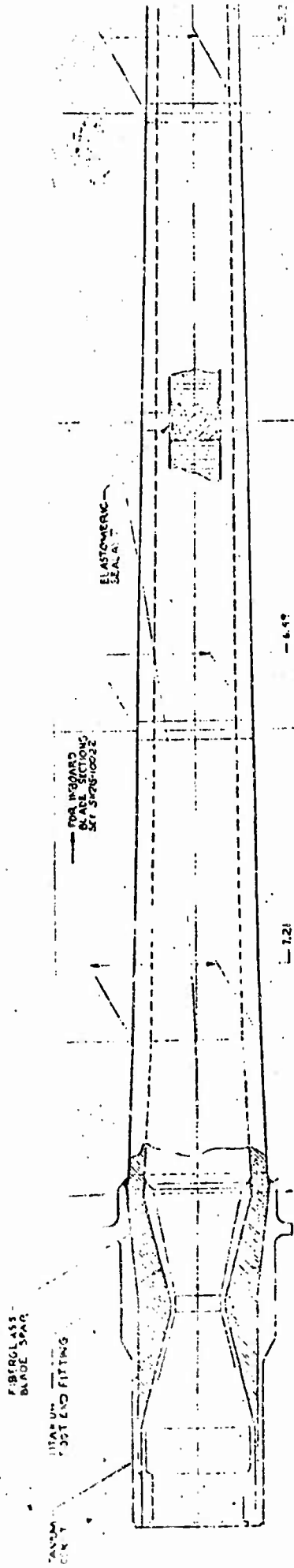
FIGURE VI-26 POSITIVE SIGN CONVENTION FOR BLADE LOADS



- V_x = In Plane Shear
 - V_z = Out of Plane Shear
 - M_x = Out of Plane Moment
 - M_y = Torsional Moment
 - M_z = In Plane Moment
 - V'_x = Chordwise Shear
 - V'_z = Beamwise Shear
 - M'_x = Beamwise Moment
 - M'_z = Chordwise Moment
- Centrifugal Force is Normal to the Z-X Plane

ROTOR BLADE LOADS:

HOVER - 3.54° CYCLIC

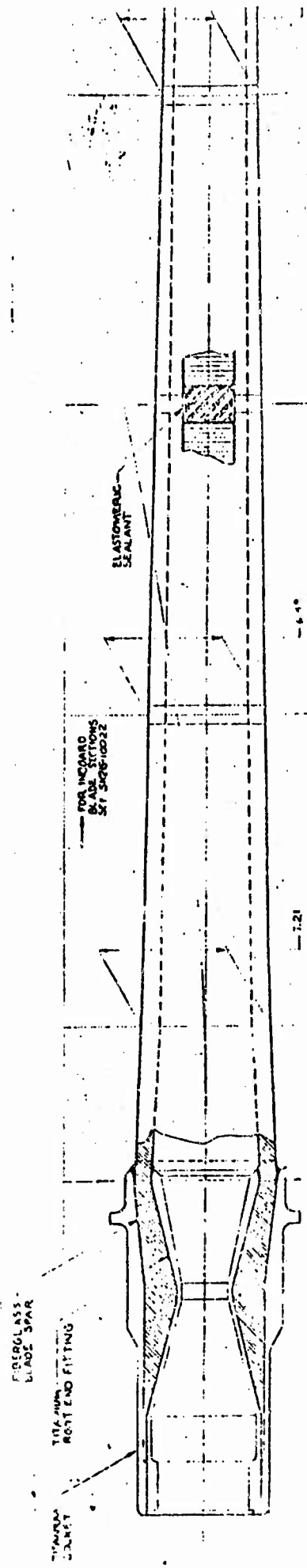


LOAD CONDITION	BLADE STATION (I/R)	MOMENTS						C.F.
		VX	VZ	MX	MY	MZ		
STEADY LOADS	.075	889	11064	617800	-21290	-5630	105200	
	.100	676	10515	524900	-21240	-11960	103800	
	.150	457	8628	366800	-24970	-20780	100500	
	.250	528	4928	144300	-27500	-34480	92070	
	.300	921	3195	78360	-26650	-23770	97610	
ALTERNATING LOADS	.075	2224	6756	387512	42645	135818		
	.100	2091	6394	331698	42763	115902		
	.150	1674	5207	236118	42976	83367		
	.250	835	2929	102606	43306	39459		
	.300	395	1834	52469	43318	22521		

ROTOR BLADE LOADS:

TABLE VI-3

HOVER - MAXIMUM CYCLIC CONDITION (11.80° CYCLIC)

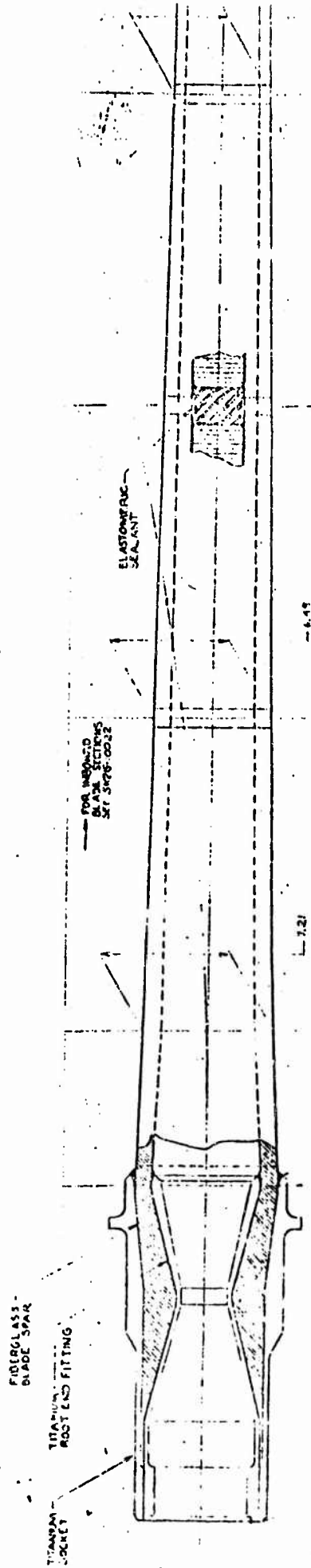


LOAD CONDITION	BLADE STATION (r/R)	V			M			C.F.
		VX	VZ	VY	MX	MY	MZ	
STEADY LOADS	.075	889	11054	-21290	617800	-21290	-5630	105200
	.100	676	10515	-21240	524900	-21240	-11960	103800
	.150	457	8628	-24970	366800	-24970	-20780	100500
	.250	528	4928	-27500	144300	-27500	-34480	92070
	.300	921	3195	-26650	78360	-26650	-33770	87610
ALTERNATING LOADS	.075	741	22518	142151	1291707	142151	452727	X
	.100	6970	21315	142544	1105660	142544	386607	
	.150	5581	17358	143252	787060	143252	277890	
	.250	2785	9763	144353	342121	144353	131531	
	.300	1318	6112	144393	211495	144393	95069	

ROTOR BLADE LOADS:

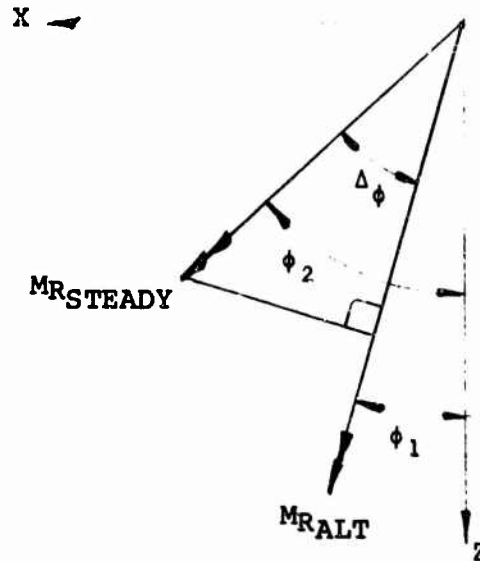
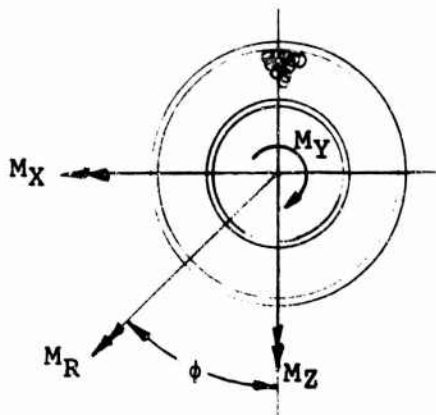
TABLE VI-4

2.5g VERTICAL TAKEOFF CONDITION



LOAD CONDITION	BLADE STATION (r/R)	MOMENTS					C.F.
		VX	VZ	MX	MY	MZ	
STEADY LOADS	.075	2223	27660	1544500	-53225	-14075	105200
	.100	1690	26288	1312250	-53100	-29900	103800
	.150	1143	21570	917000	-62425	-51950	100500
	.250	1320	12320	360750	-68750	-86200	92070
	.300	2303	7988	195900	-66625	-84425	87610
ALTERNATING LOADS	.075	1979	6012	344885	37954	120878	
	.100	1861	5696	295211	38059	103224	
	.150	1489	4634	210145	38248	74196	
	.250	743	2607	91346	38542	35119	
	.300	352	1832	56489	38553	25284	

FIGURE VI-27 RESOLUTION OF BLADE MOMENTS AND SHEARS



$$\phi_1 = \tan^{-1} (M_X/M_Z)_{ALT}$$

$$\phi_2 = \tan^{-1} (M_X/M_Z)_{STEADY}$$

$$\Delta\phi = |\phi_2 - \phi_1|$$

For fatigue analyses:

$$M_{FATIGUE} = M_{RALT} + M_{RSTEADY} \cos$$

$$T_{FATIGUE} = M_{YALT} + M_{YSTEADY}$$

$$C.F. = C.F. \text{ at hover rotor speed}$$

for ultimate analyses:

$$M_{ULTIMATE} = 1.5 \sqrt{(M_{RALT})^2 + (M_{RSTEADY})^2 + 2 M_{RALT} M_{RSTEADY} \cos\Delta\phi}$$

$$T_{ULTIMATE} = 1.5 (M_{YALT} + M_{YSTEADY})$$

$$C.F. = (C.F. \text{ at hover rotor speed}) (1.25) (1.25) (1.5)$$

(for max. tension stress)

$$= (C.F. \text{ at hover rotor speed}) (1.5)$$

(for max. compressive stress)

The same method is used for the shear loadings.

TABLE VI-5

FATIGUE ANALYSIS (3.54° CYCLIC) (MOMENT)

BLADE STATION (r/R)	(1) M _{XALT}	(2) M _{ZALT}	(3) φ ₁	(4) M _{XSTEADY}	(5) M _{ZSTEADY}	(6) φ ₂	(7) Δφ	(8) COS Δφ
.075	387512	135818	70.69	617800	-5630	90.52	15.83	.941
.100	331698	115982	70.73	524900	-11960	91.31	20.58	.936
.150	236118	83367	70.55	366800	-20780	93.24	22.69	.923
.250	102636	39459	68.97	144300	-34480	103.44	34.47	.824
.300	63449	28521	65.80	78360	-33770	113.31	47.51	.675

BLADE STATION (r/R)	(9) M _{RALT}	(10) M _{RSTEADY}	(11) (10) x (8)
.075	410624	617826	581191
.100	351391	525036	491529
.150	250403	367388	38954
.250	109960	148362	122313
.300	69564	85327	57635

TABLE VI-6

ULTIMATE ANALYSIS (MAX. CYCLIC COND.) (MOMENT)

BLADE STATION (r/R)	(1) M_{X_ALT}	(2) M_{Z_ALT}	(3) ϕ_1	(4) M_{X_STEADY}	(5) M_{Z_STEADY}	(6) ϕ_2	(7) $\Delta\phi$	(8) $\cos \Delta\phi$
.075	1291707	452727	70.69	617800	-5630	90.52	19.83	.941
.100	1105660	386607	70.73	524900	-11960	91.31	20.58	.936
.150	787060	277890	70.55	366800	-20780	93.24	22.69	.923
.250	342121	131531	68.97	144300	-34480	103.44	34.47	.824
.300	211495	95069	65.80	78360	-33770	113.31	47.51	.675

BLADE STATION (r/R)	(9) M_{R_ALT}	(10) M_{R_STEADY}	(11) ϕ_2	(12) 10^2	(13) $2.9 \times 10^0 \cos \Delta\phi$	(14) $(11) + (12) + (13)$	(15) $1.5 \sqrt{14}$
.075	1368747	617826	1.873×10^{12}	3.817×10^{11}	1.591×10^{12}	3.846×10^{12}	2941754
.100	1171302	525036	1.372×10^{12}	2.767×10^{11}	1.151×10^{12}	2.799×10^{12}	2509563
.150	834677	367388	6.967×10^{11}	1.350×10^{11}	5.658×10^{11}	1.397×10^{12}	1773235
.250	366534	148362	1.343×10^{11}	2.201×10^{10}	8.966×10^{10}	2.460×10^{11}	744009
.300	231880	85327	5.377×10^{10}	7.281×10^9	2.673×10^{10}	8.778×10^{10}	444410

TABLE VI-7

ULTIMATE ANALYSIS (2.5g VERTICAL TAKEOFF) (MOMENT)

BLADE STATION (r/R)	(1) M_{XALT}	(2) M_{ZALT}	(3) ϕ_1	(4) $M_{XSTEADY}$	(5) $M_{ZSTEADY}$	(6) ϕ_2	(7) $\Delta\phi$	(8) $\cos \Delta\phi$
.075	344885	120878	70.69	1544500	-14075	90.52	19.83	.941
.100	295211	103224	70.73	1312250	-29900	91.31	20.58	.936
.150	210145	74196	70.55	917000	-51950	93.24	22.69	.923
.250	91346	35119	68.97	360750	-86200	103.44	34.47	.824
.300	56469	25384	65.80	195900	-84425	113.31	47.51	.675

BLADE STATION (r/R)	(9) M_{RALT}	(10) $M_{RSTEADY}$	(11) ϕ_2	(12) 10^2	(13) $2 \times 10^2 \cos \Delta\phi$	(14) $(11) + (12) + (13)$	(15) $1.5 \sqrt{14}$
.075	365455	1544564	1.335×10^{11}	2.386×10^{12}	1.062×10^{12}	3.581×10^{12}	2838621
.100	312737	1312590	9.780×10^{10}	1.723×10^{12}	7.686×10^{11}	2.589×10^{12}	2413693
.150	222859	918470	4.967×10^{10}	8.436×10^{11}	3.777×10^{11}	1.271×10^{12}	1591045
.250	97864	370905	9.577×10^9	1.376×10^{11}	5.985×10^{10}	2.070×10^{11}	682456
.300	61912	213318	3.833×10^9	4.550×10^{10}	1.784×10^{10}	6.718×10^{10}	388784

TABLE VI-8

FATIGUE ANALYSIS (3.54° CYCLIC) (SHEARS)

BLADE STATION (r/R)	1		2		3		4		5		6		7	
	V _{XALT}	V _{ZALT}	V _{XALT}	V _{ZALT}	φ ₁	V _{XSTEADY}	V _{ZSTEADY}	V _{XSTEADY}	V _{ZSTEADY}	φ ₂	Δφ	COS Δφ		
.075	2224	6756	18.22	889	11064	4.59	13.63	.972						
.100	2091	6394	18.11	676	10513	3.68	14.43	.968						
.150	1674	5207	17.82	457	8628	3.03	14.79	.967						
.250	835	2929	15.91	528	4928	6.12	9.80	.985						
.300	395	1834	12.15	921	3195	16.08	3.93	.998						

BLADE STATION (r/R)	9		10		11	
	V _{RALT}	V _{RSTEADY}	V _{RALT}	V _{RSTEADY}	10 x 8	11
.075	7112	11100	10787	10787		
.100	6727	10537	10204	10204		
.150	5470	8640	8354	8354		
.250	3046	4956	4834	4834		
.300	1876	3325	3317	3317		

TABLE VI-9

ULTIMATE ANALYSIS (MAX. CYCLIC COND.) (SHEARS)

BLADE STATION (r/R)	1		2		3		4		5		6		7		8	
	V _{XALT}	V _{ZALT}	φ ₁	V _{XSTEADY}	V _{ZSTEADY}	φ ₂	V _{XSTEADY}	V _{ZSTEADY}	φ ₂	Δφ	COS Δφ					
.075	7414	22518	18.22	889	11064	4.59	11064	11064	4.59	13.63	.972					
.100	6970	21315	18.11	676	10515	3.68	10515	10515	3.68	14.43	.968					
.150	5581	17358	17.82	457	8628	3.03	8628	8628	3.03	14.79	.967					
.250	2785	9763	15.92	528	4928	6.12	4928	4928	6.12	9.81	.985					
.300	1318	6112	12.17	921	3195	16.08	3195	3195	16.08	3.91	.998					

BLADE STATION (r/R)	9		10		11		12		13		14		15	
	V _{RALT}	V _{RSTEADY}	9 ²	10 ²	11 ²	12 ²	13 ²	14 ²	15 ²	16 ²	17 ²	18 ²	19 ²	20 ²
.075	23708	11100	5.620 x 10 ⁸	1.232 x 10 ⁸	5.620 x 10 ⁸	1.232 x 10 ⁸	5.115 x 10 ⁸	1.197 x 10 ⁹	5.115 x 10 ⁸	1.197 x 10 ⁹	51890			
.100	22425	10537	5.029 x 10 ⁸	1.110 x 10 ⁸	5.029 x 10 ⁸	1.110 x 10 ⁸	4.577 x 10 ⁸	1.012 x 10 ⁹	4.577 x 10 ⁸	1.012 x 10 ⁹	49103			
.150	18233	8640	3.324 x 10 ⁸	7.465 x 10 ⁷	3.324 x 10 ⁸	7.465 x 10 ⁷	3.046 x 10 ⁸	7.117 x 10 ⁸	3.046 x 10 ⁸	7.117 x 10 ⁸	40017			
.250	10152	4956	1.031 x 10 ⁸	2.456 x 10 ⁷	1.031 x 10 ⁸	2.456 x 10 ⁷	9.917 x 10 ⁷	2.268 x 10 ⁸	9.917 x 10 ⁷	2.268 x 10 ⁸	22590			
.300	6253	3325	3.909 x 10 ⁷	1.106 x 10 ⁷	3.909 x 10 ⁷	1.106 x 10 ⁷	4.418 x 10 ⁷	9.163 x 10 ⁷	4.418 x 10 ⁷	9.163 x 10 ⁷	14359			

TABLE VI-10

ULTIMATE ANALYSIS (2.5g VERTICAL TAKEOFF) (SHEARS)

BLADE STATION (I/R)	1		2		3		4		5		6		7		8	
	V _{XALT}	V _{ZALT}	V _{ZALT}	V _{ZALT}	φ ₁	V _{XSTEADY}	V _{XSTEADY}	V _{ZSTEADY}	V _{ZSTEADY}	φ ₂	Δφ	Δφ	COS Δφ			
.075	1979	6012	6012	18.22	2223	27660	27660	4.59	13.63	.972						
.100	1861	5696	5696	18.09	1690	26288	26288	3.68	14.41	.969						
.150	1489	4634	4634	17.81	1143	21570	21570	3.03	14.78	.967						
.250	743	2607	2607	15.91	1320	12320	12320	6.12	9.79	.985						
.300	332	1632	1632	12.17	2303	7988	7988	16.00	3.91	.998						

BLADE STATION (I/R)	9		10		11		12		13		14		15	
	V _{RALT}	V _{RALT}	V _{RSTEADY}	V _{RSTEADY}	9 ²	10 ²	10 ²	29.10 COS Δφ	11 + 12 + 13	1.5	14	1.5	14	
.075	6329	27749	27749	4.006 x 10 ⁷	7.700 x 10 ⁸	7.700 x 10 ⁸	3.414 x 10 ⁸	1.151 x 10 ⁹	50900					
.100	5992	26342	26342	3.591 x 10 ⁷	6.939 x 10 ⁸	6.939 x 10 ⁸	3.058 x 10 ⁸	1.036 x 10 ⁹	48271					
.150	4867	21600	21600	2.369 x 10 ⁷	4.666 x 10 ⁸	4.666 x 10 ⁸	2.033 x 10 ⁸	6.930 x 10 ⁸	39504					
.250	2711	12391	12391	7.348 x 10 ⁶	1.535 x 10 ⁸	1.535 x 10 ⁸	6.620 x 10 ⁷	2.271 x 10 ⁸	22603					
.300	1670	8313	8313	2.787 x 10 ⁶	6.911 x 10 ⁷	6.911 x 10 ⁷	2.769 x 10 ⁷	9.959 x 10 ⁷	14969					

A summary of the section properties is presented in Table VI-11. The fatigue analysis stresses are summarized in Table VI-12 and the margins of safety and the allowable material endurance limit in Table VI-14.

The two ultimate conditions were examined for maximum loads and the maximum cyclic in hover was found to be critical. These loads are summarized in Table VI-13 and the resulting margins of safety and material allowables in Table VI-14.

The largest negative margin of safety of 4% occurs for the hover fatigue condition. This is within the tolerance of the study and can be corrected by locally strengthening the beam at the inboard end.

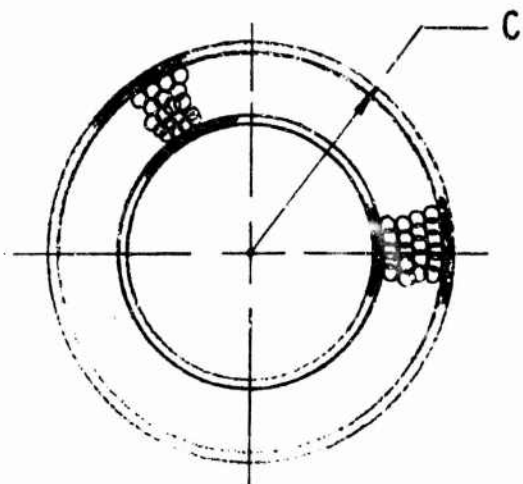
7. WEIGHT ANALYSIS

The target total rotor weight was determined in Reference I-1 as 2628 pounds per rotor based on a sea level, standard day horsepower requirement. The actual design condition is for a 2,500-foot altitude hot day and a re-evaluation of the blade weight has been made. The new prediction of 2,220 pounds agrees very well with the current design weight of 2,238 pounds. The weight accounting based on the 67,000-pound aircraft of Phase I, however, shows a net weight saving of 22%. These data are summarized in Table VI-15.

Blade root retention weights are based on the stress analysis in Section VII.

TABLE VI-11

BLADE SECTION PROPERTIES:



(r/R)	① C	② E x 10 ⁻⁶	③ G x 10 ⁻⁶	④ EI x 10 ⁻⁶	⑤ GJ x 10 ⁻⁶	⑥ EA x 10 ⁻⁶
.075	3.900	5.106	1.85	596.24	331.88	101.96
.100	3.560	↑	↑	474.41	264.06	101.85
.150	3.192	↑	↑	309.50	172.82	182.20
.250	2.609	↓	↓	118.76	67.24	44.39
.300	2.357	5.106	1.85	76.87	42.98	34.75

(r/R)	⑦ GA x 10 ⁶	⑧ CE/EI	⑨ E/AE	⑩ CG/GJ	⑪ G/GA
.075	27.95	.0333	.0500	.0217	.0662
.100	27.92	.0383	.0501	.0249	.0663
.150	22.53	.0526	.0621	.0342	.0821
.250	12.17	.1120	.1150	.0720	.1520
.300	9.52	.1565	.1469	.1010	.1943

SUMMATION OF

TABLE VI-12

FATIGUE CONDITION:

BLADE STATION (r/R)	(12) M_{RALT}	(13) $M_{RSTEADY}$	(14) σ_{BALT} (12) x (8)	(15) $\sigma_{BSTEADY}$ (13) x (8)	(16) CF	(17) σ_{CF} (16) x (9)
.075	410624	581191	13674	19354	105200	5260
.100	351391	491529	13458	18826	103800	5200
.150	250403	338954	13171	17829	100500	6241
.250	109960	122313	12338	13724	92070	10588
.300	69564	57835	10887	9020	87610	12870

BLADE STATION (r/R)	(18) $\Sigma \sigma_{STEADY}$ (15) + (17)	(19) M_{YALT}	(20) $M_{YSTEADY}$	(21) τ_{ALT} (9) x (10)	(22) τ_{STEADY} (20) x (10)	(23) V_{RALT}
.075	24614	42645	21290	925	462	7112
.100	24026	42763	21240	1065	529	6727
.150	24069	42976	24970	1470	854	5470
.250	24312	43306	27500	3118	1980	3046
.300	21890	43318	26650	4375	2692	1876

BLADE STATION (r/R)	(24) $V_{RSTEADY}$	(25) τ_{ALT} (23) x (11)	(26) $\Sigma \tau_{STEADY}$ (24) x (11)	(27) $\Sigma \tau_{ALT}$ (21) + (25)
.075	10787	471	714	1396
.100	10204	446	677	1511
.150	8354	449	686	1919
.250	4884	463	742	3581
.300	3317	365	644	4740

TABLE VI-13

SUMMARY OF
ULTIMATE CONDITION:

BLADE STATION (r/R)	(28) M_{RULT}	(29) σ_{BULT} (28) x (8)	(30) CF	(31) σ_{CF} (30) x (9)	(32) CF'
.075	2941754	97960	246563	12328	157800
.100	2509563	96116	243281	12188	155700
.150	1773235	93272	235547	14627	150750
.250	744009	83329	215789	24816	138105
.300	444410	69550	205336	30164	131415

BLADE STATION (r/R)	(33) σ'_{CF} (32) x (9)	(34) σ_{ULT} (29) + (31)	(35) σ_{ULT}' (39) - (33)	(36) M_{YULT}	(37) τ_{ULT} (36) x (10)
.075	7890	110288	90070	245161	5320
.100	7801	108304	88315	245676	6117
.150	9362	107899	83910	252333	8630
.250	15882	108145	67447	257779	18560
.300	19305	99714	50245	256565	25913

BLADE STATION (r/R)	(38) V_{ULT}	(39) τ_{ULT} (38) x (11)	(40) $\Sigma \tau_{ULT}$ (37) + (39)
.075	51890	3435	8755
.100	49103	3256	9373
.150	40017	3285	11915
.250	22590	3434	21994
.300	14359	2790	28703

TABLE VI-14

SUMMARY OF
MARGINS OF SAFETY:

ULTIMATE ANALYSIS:

r/R	(41) σ_{ULT}	(42) MS	(43) σ_{ULT}	(44) MS	(45) τ_{ULT}	(46) MS
.075	110288	.30	90070	.06	8755	3.10
.100	108304	.32	88315	.07	9373	2.92
.150	107899	.32	83910	.13	11915	2.01
.250	108145	.32	67447	.41	21994	.64
.300	99714	.44	52045	.88	28703	.25

FATIGUE ANALYSIS:

r/R	(47) σ_{BALT}	(48) MS	(49) τ_{ALT}	(50) MS
.075	13674	-.04	1396	3.50
.100	13458	-.03	1511	3.16
.150	13171	-.01	1919	2.28
.250	12338	.05	13581	.76
.300	10887	.19	4740	.33

ALLOWABLE STRESSES:

- = 13000 PSI
- = 63000
- = 36000 PSI
- = 143000 PSI
- = 94500 PSI

TABLE VI-15
ROTOR BLADE WEIGHT

	ORIGINAL WEIGHT (TARGET)	REVISED TARGET WEIGHT	CURRENT DESIGN WEIGHT
Spar			134
Skin			55
Honeycomb Core			29
Leading Edge Balance Weight			63
Erosion Strip			7
Tip Fitting			10
Root Retention Fitting			70
Trailing Edge Wedge			1
Pressure Shell			4
Total Blade	480	370	373
Total Rotor	1440	1110	1119
Total Aircraft	2880	2220	2238

8. SURVIVABILITY

A survivability analysis was not a part of the basic contract but the following aspects of design and material choice contribute to survivability:

- a. Fiberglass is not subject to corrosion.
- b. Fiberglass is less notch sensitive than metal.
- c. Failures in fiberglass are less abrupt than in metal.
- d. Elimination of flap and lead-lag hinges reduces the number of critically stressed moving parts.
- e. The high stress area in the rotor blade is limited to the flexure. The flexure area is only 5% of the total blade area.
- f. ISIS gives indication of cracking or punctures.
- g. Rotor rotation is chosen to throw pieces of rotor blade away from the fuselage in an emergency landing with the rotor in the cruise mode.

9. CONCLUSIONS AND RECOMMENDATIONS

- a. The basic rotor design proposed for the Model 215 Prop/Rotor Aircraft is structurally sound and within the weight target. The following details will require additional work later:
 1. Detail study of the third mode frequency reduction by stiffness changes at 30% radius
 2. Increase of the fatigue margin of safety at 7.5% radius
 3. Detail fatigue life analysis including fatigue damage caused by other than normal flight conditions

4. Effects of load interactions on allowable blade stresses

- b. Criteria for damage tolerance to gunfire, bird and tree strikes and loss of blade sections need to be established.
- c. De-icing requirements and methods need to be established.
- d. The design details required for lightning protection of the blade must be established and included.
- e. Redundant solution of air/ground resonance dynamic problems would require that provisions for adding viscous dampers for chordwise blade bending be included in the design. Design of such provisions and the required dampers is recommended.
- f. It is recommended that a full-scale blade root component be fabricated and fatigue tested to work out the details of the inboard blade section interfaces. This section is the critical component of the blade design. The inboard blade sections introduce unique requirements that have not been included in previous Boeing-Vertol fiberglass rotor blades.

SECTION VII

ROTOR^RHUB AND CONTROLS DESIGN

1. INTRODUCTION

In this section, the design of the rotor hub and rotor controls is described. Included in the design effort are the hub assembly, rotor blade retention, pitch change bearings and housings, rotor collective and cyclic pitch control mechanism, spinner and a description of the rotor lubrication system. The rotor system is hingeless; i.e., the hub does not contain flap or lag hinges. The upper rotor controls which provide collective and cyclic pitch are mounted above the hub assembly and are contained within the spinner. The weight of the rotor hub assembly per aircraft is 1,632 pounds versus a target weight of 2,576 pounds. The weight of the upper rotor controls is 2,442 pounds versus a target weight of 2,367 pounds.

2. OBJECTIVE

Design the rotor hub and rotor control systems in sufficient detail to establish the hub and control assembly geometry and envelope and to verify weight predictions.

3. DESIGN CRITERIA

The rotor hub is an integral part of the rotor system and the design load criteria for the rotor blade in Section VI shall be applicable.

Collective and bi-cyclic pitch control together with full feather-

ing shall be provided.

All rolling element bearings shall have an analytical determination of a B_{10} life of 3,000 hours.

4. DESCRIPTION OF ROTOR HUB ASSEMBLY

4.1 INTRODUCTION

The rotor hub retains three equally spaced rotor blades and is mounted to the rotor thrust bearing. The hub configuration is hingeless and incorporates the blade pitch bearings. The rotor hub is subjected to loads resulting from rotor blade centrifugal force, bending moments and shear forces.

The rotor controls consisting of the blade control swashplate assembly, cyclic and collective actuators and mechanism linkages are mounted above the hub assembly and are connected to the blade pitch change arm by pitch links.

A common oil lubrication system is provided for the complete pitch change mechanism and swashplate assembly.

The rotor control system provides primary flight control of the aircraft in the hover and transition modes. Longitudinal cyclic pitch change provides aircraft pitching control in hover. Differential rotor collective provides roll control in hover. Differential longitudinal cyclic pitch provides yaw control in hover. Collective pitch provides thrust control in the hover and airplane modes. Lateral cyclic pitch provides control for gust and maneuver rotor load alleviation in hover and airplane modes.

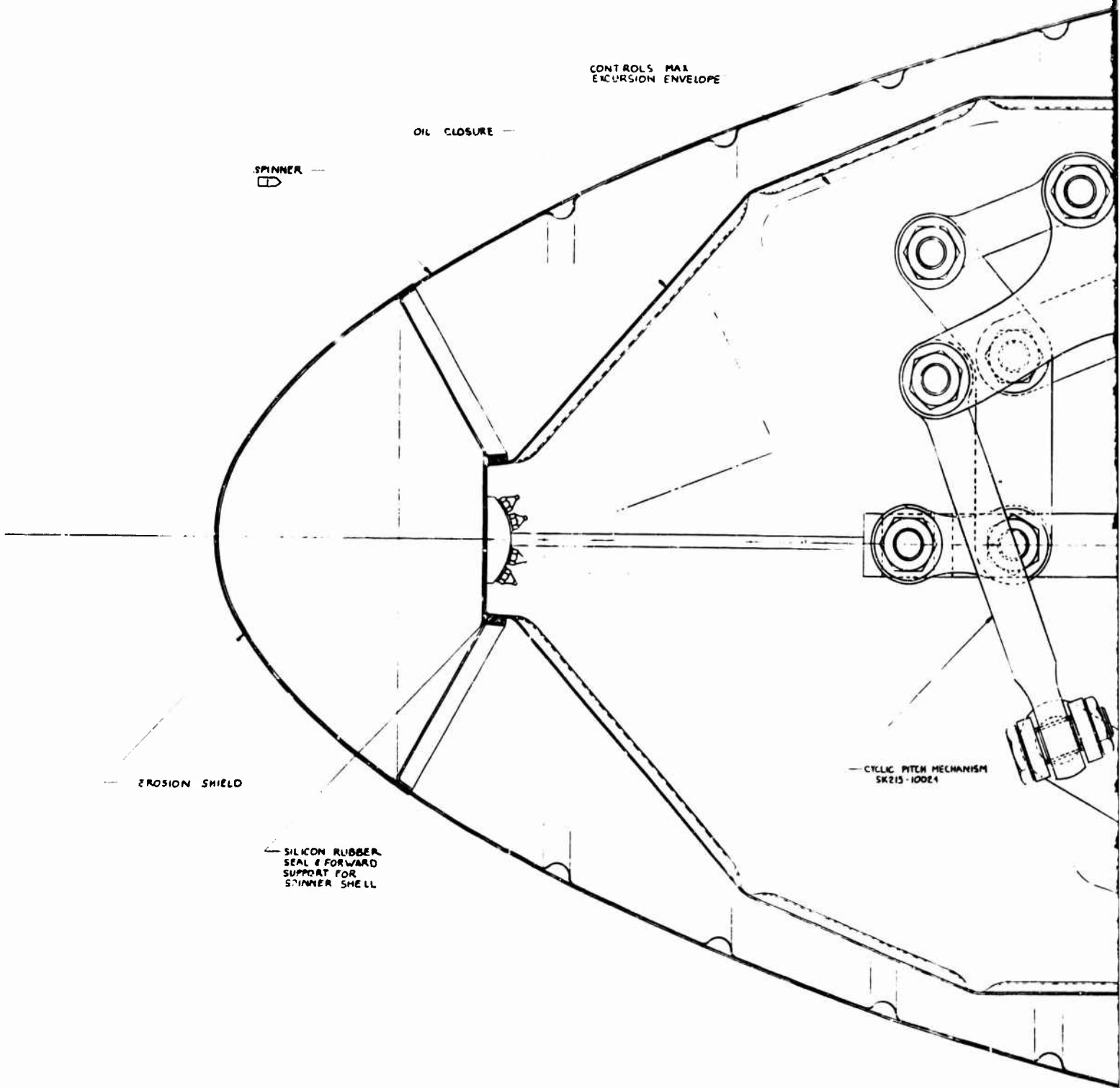
The complete rotor assembly consisting of hub and blade retention rotor controls and spinner is illustrated in Figure VII-1.

4.2 HUB ASSEMBLY

The hub assembly is illustrated in Figure VII-2 and consists of two primary structural components, an outer shell (hub barrel) and an inner hub fitting (hub spider). The aft or lower face of the hub barrel is flange mounted to a nose mount bearing (tapered roller thrust bearing) carried in the transmission mounting ring. This arrangement permits rotor thrust, moment and control loads to be carried directly to the nacelle structure, leaving only torque loads to be transmitted through the transmission case and drive shaft.

The hub barrel incorporates three (needle roller bearing - supported) blade pitch shaft housings which form receptacles for the field removable rotor blade assemblies. Each blade assembly is retained in the hub assembly by a retention pin. The retention pin transfers the rotor blade centrifugal force from the tie bar of the elastomeric thrust bearing cartridge assembly to the hub spider fitting. The pitch shaft housings react blade shear and moment loads. Blade pitch moment is transmitted to the pitch link through the face spline arrangement on the inboard end of the blade assembly. The blade root face spline is seated into the blade assembly spline by tightening the blade pitch shaft housing nut. This arrangement provides a fail-safe feature in that with failure of any centrifugal force reacting member except the blade retention fitting, the pitch arm flange will react the centrifugal force through the pitch

A



B

TYP SPINNER
STIFFENER

BLADE DEICE
BRUSH BLOCK
ASSEMBLY

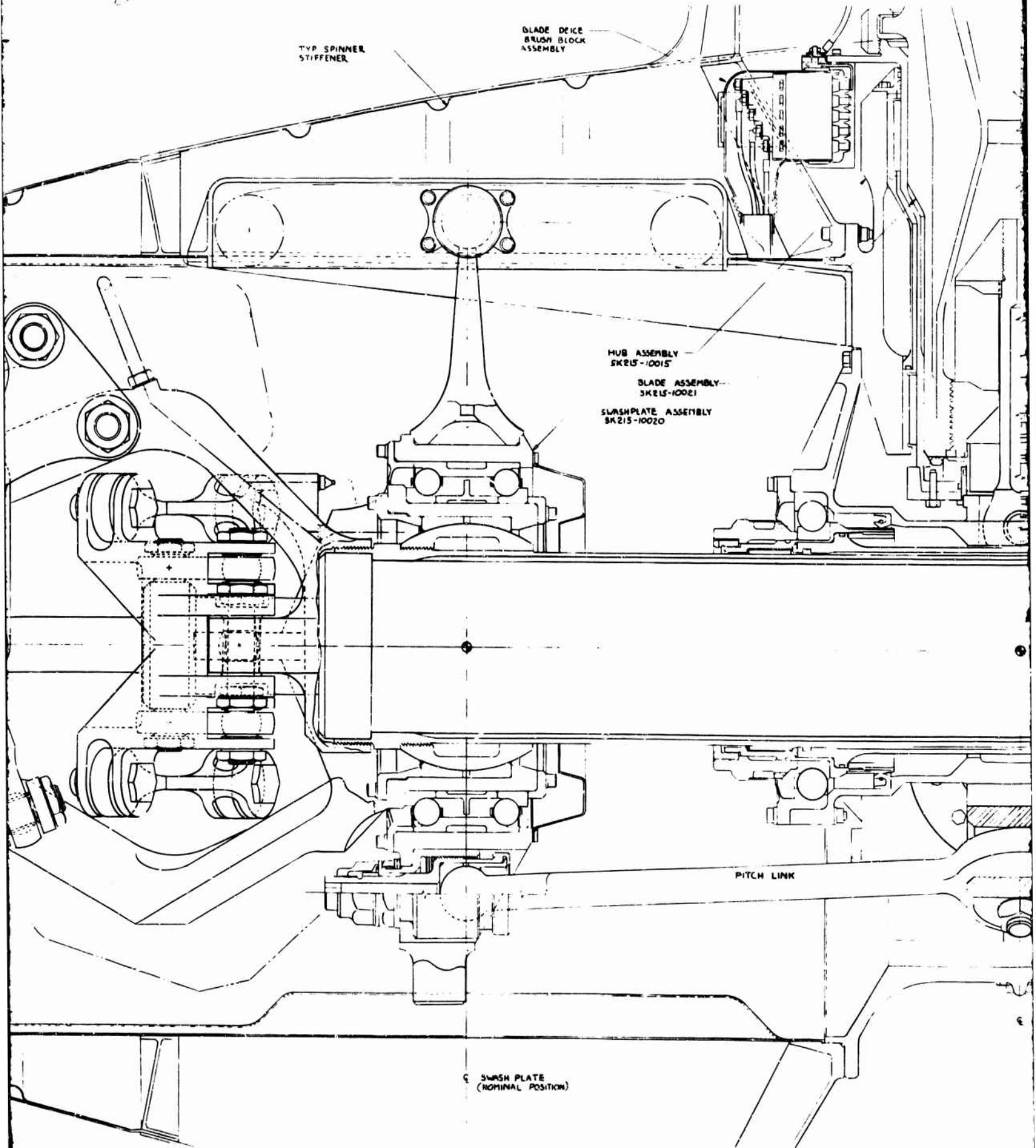
HUB ASSEMBLY
SK215-10015

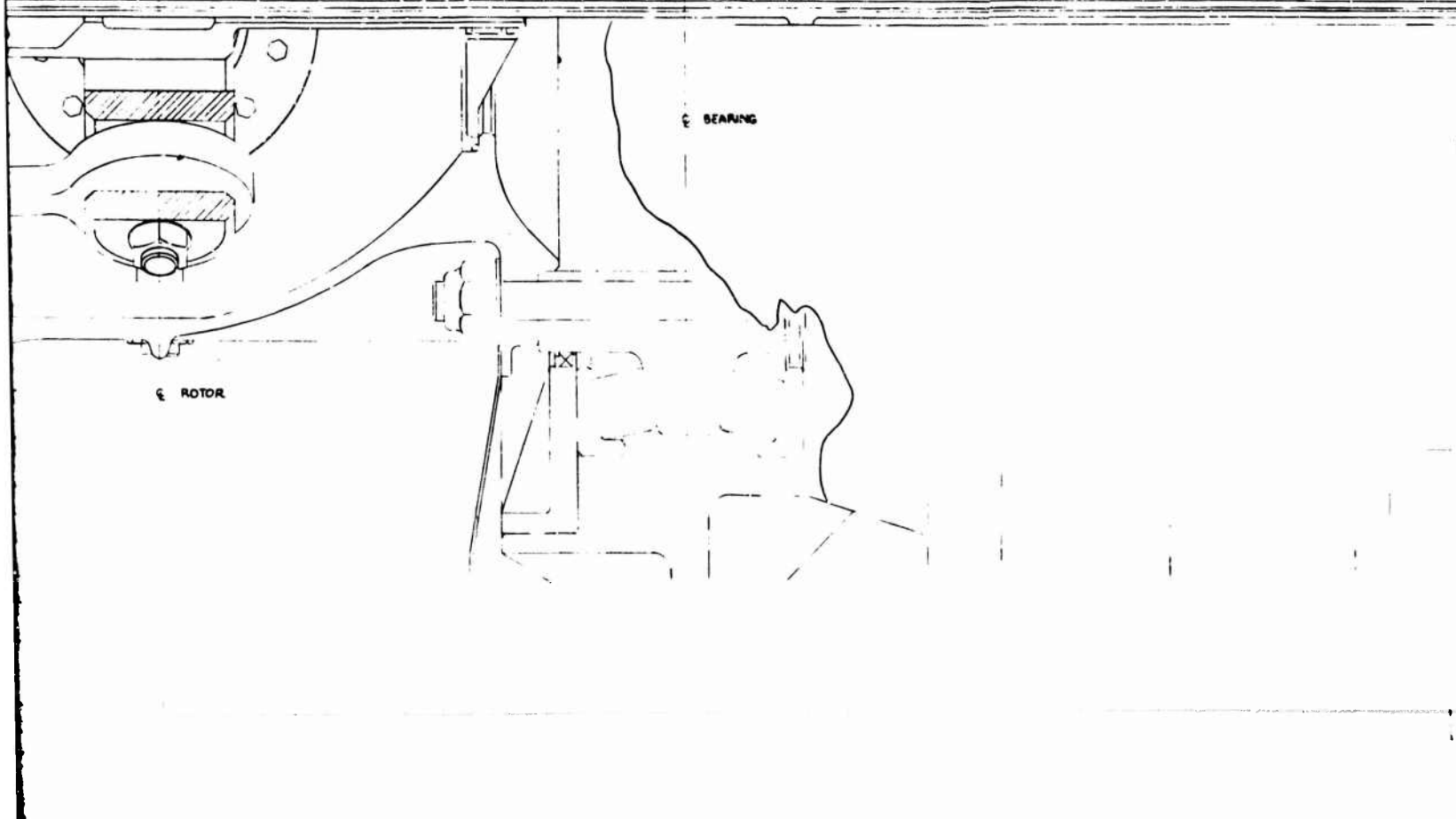
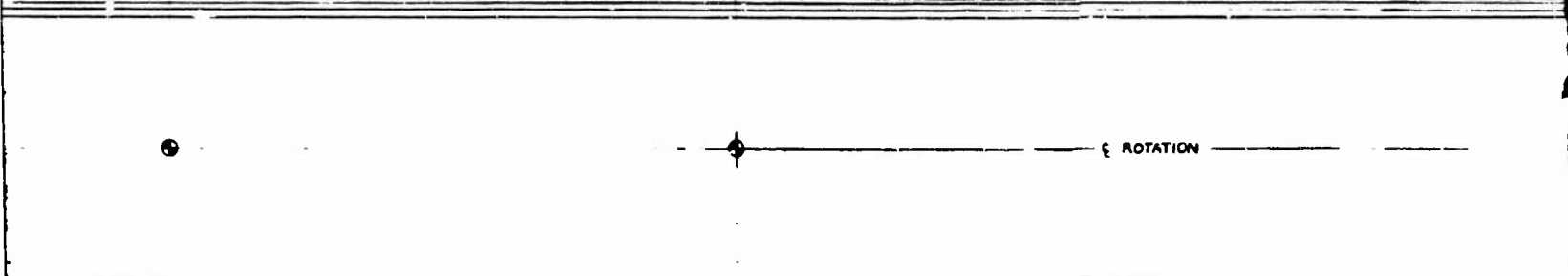
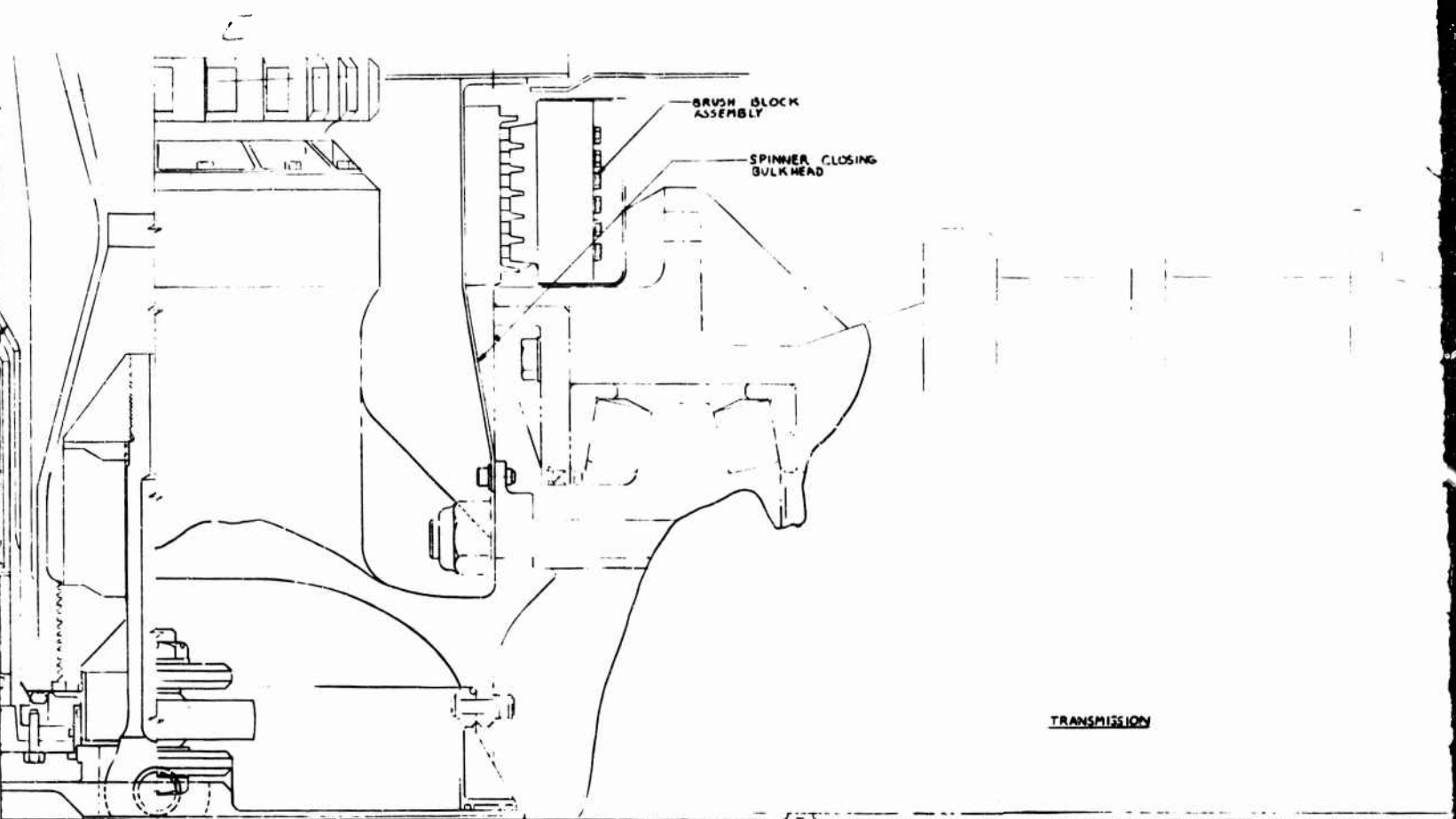
BLADE ASSEMBLY
SK215-10021

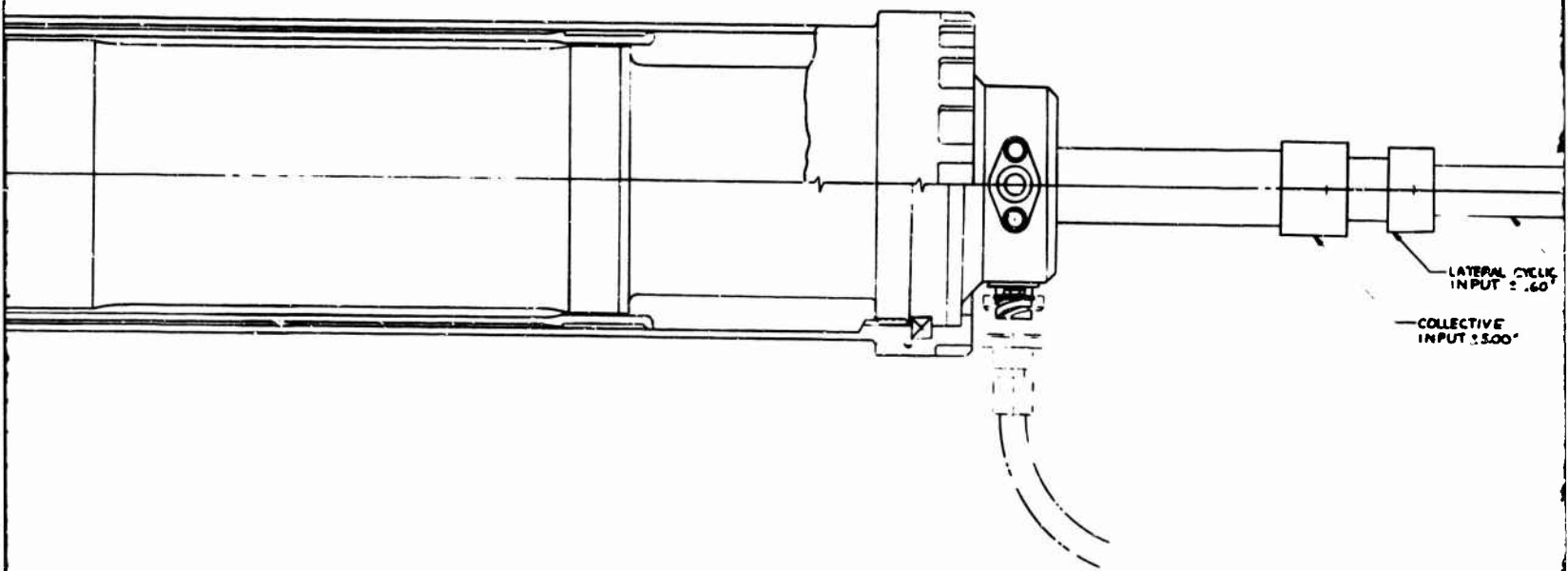
SWASHPLATE ASSEMBLY
SK215-10020

PITCH LINK

SWASH PLATE
(NOMINAL POSITION)



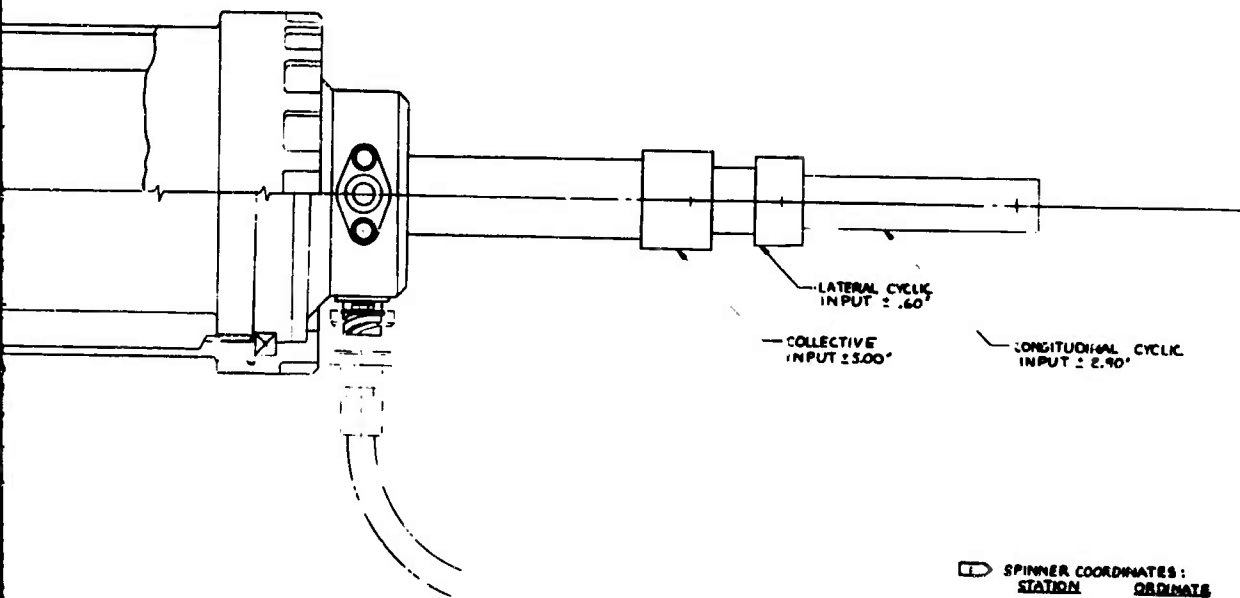




ROTOR ASSEMBLY

FIGURE VII-1

VII-5



SPINNER COORDINATES:

STATION	ORDINATE
0.00°	0.00°
1.00°	3.08°
3.00°	5.03°
5.00°	7.07°
10.00°	10.09°
15.00°	13.18°
20.00°	15.26°
30.00°	17.23°
40.00°	19.45°
50.00°	21.10°
60.00°	22.84°
70.00°	22.86°
76.50°	23.00°

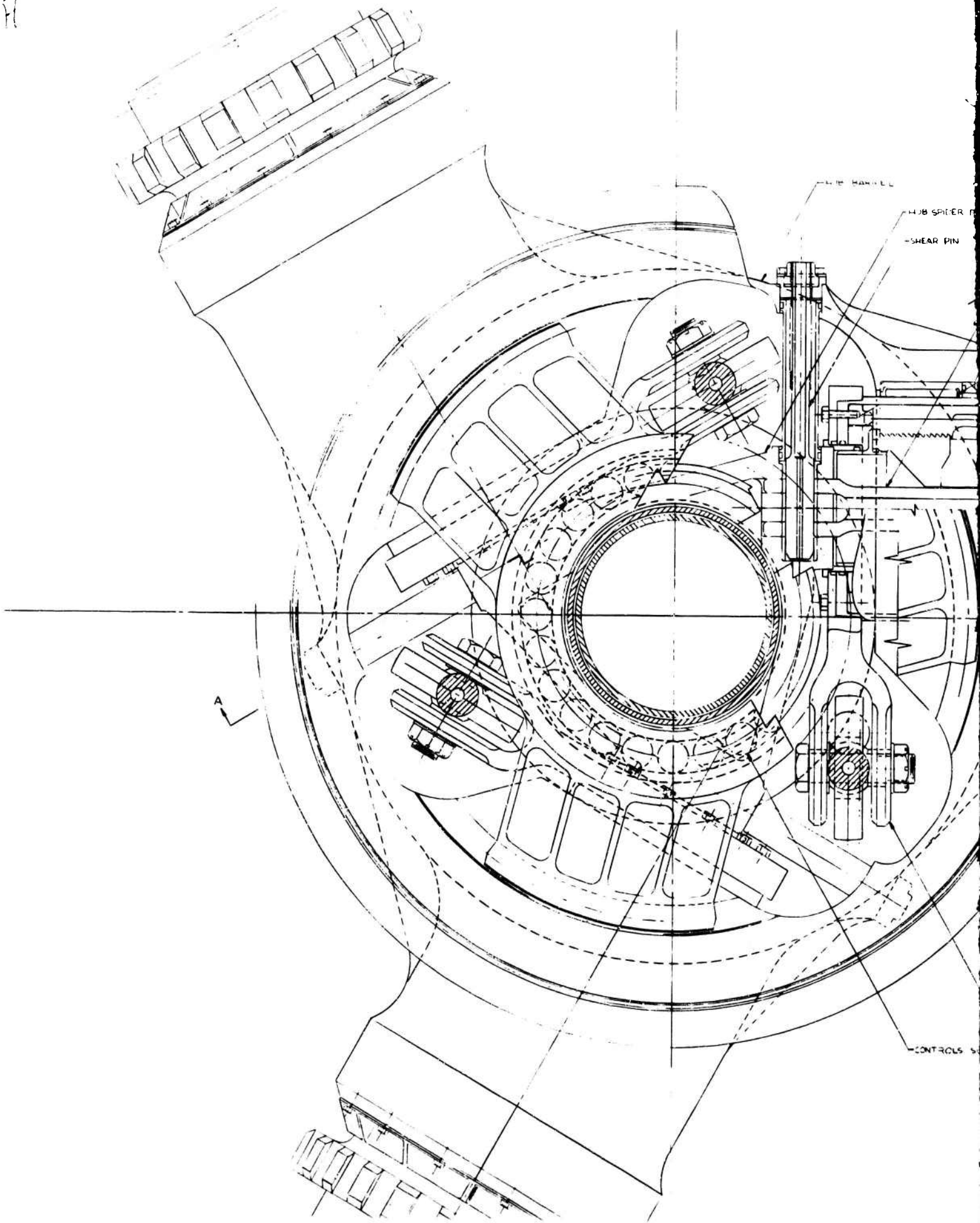
ROTOR ASSEMBLY

FIGURE VII-1

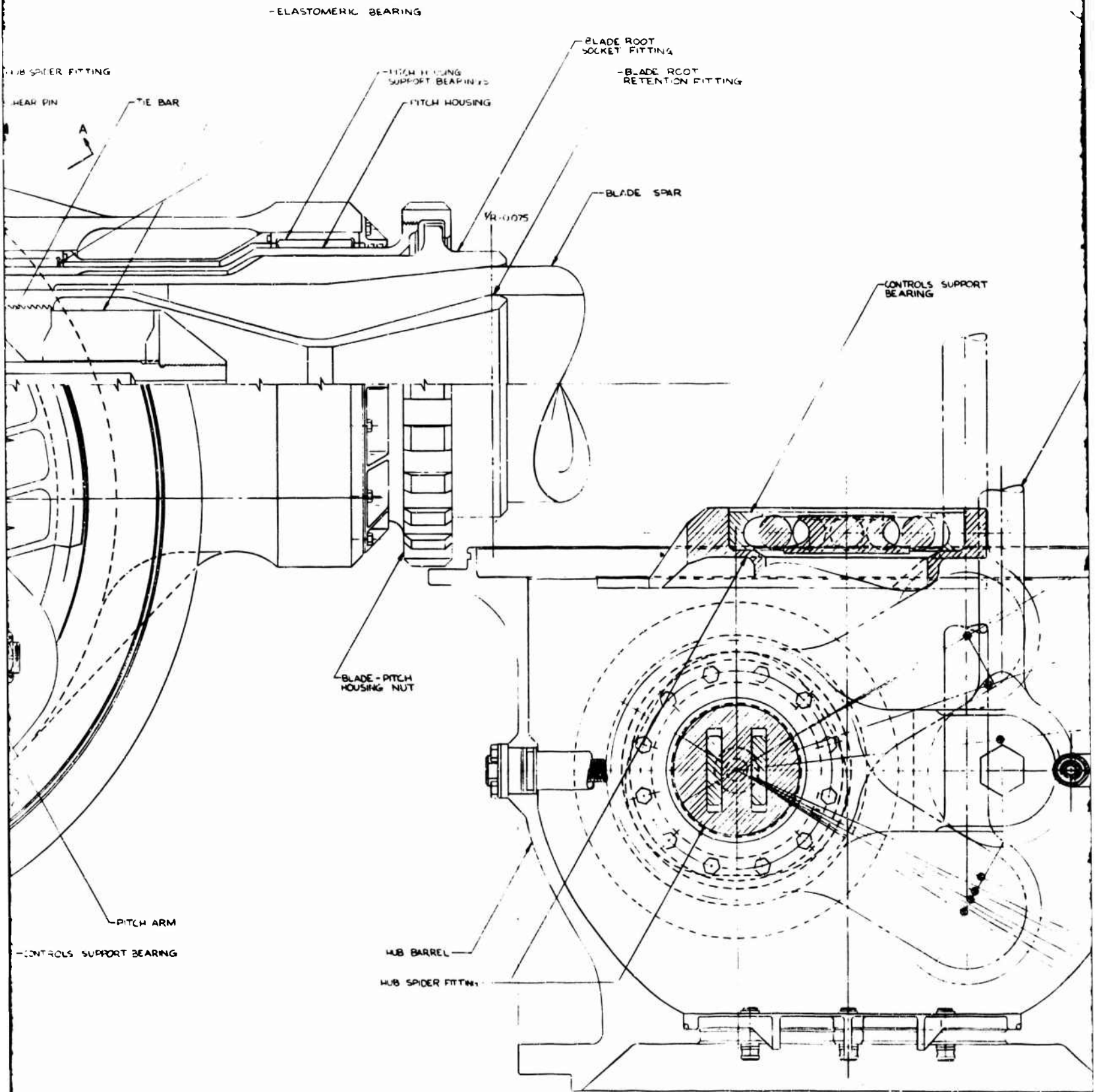
VII-5

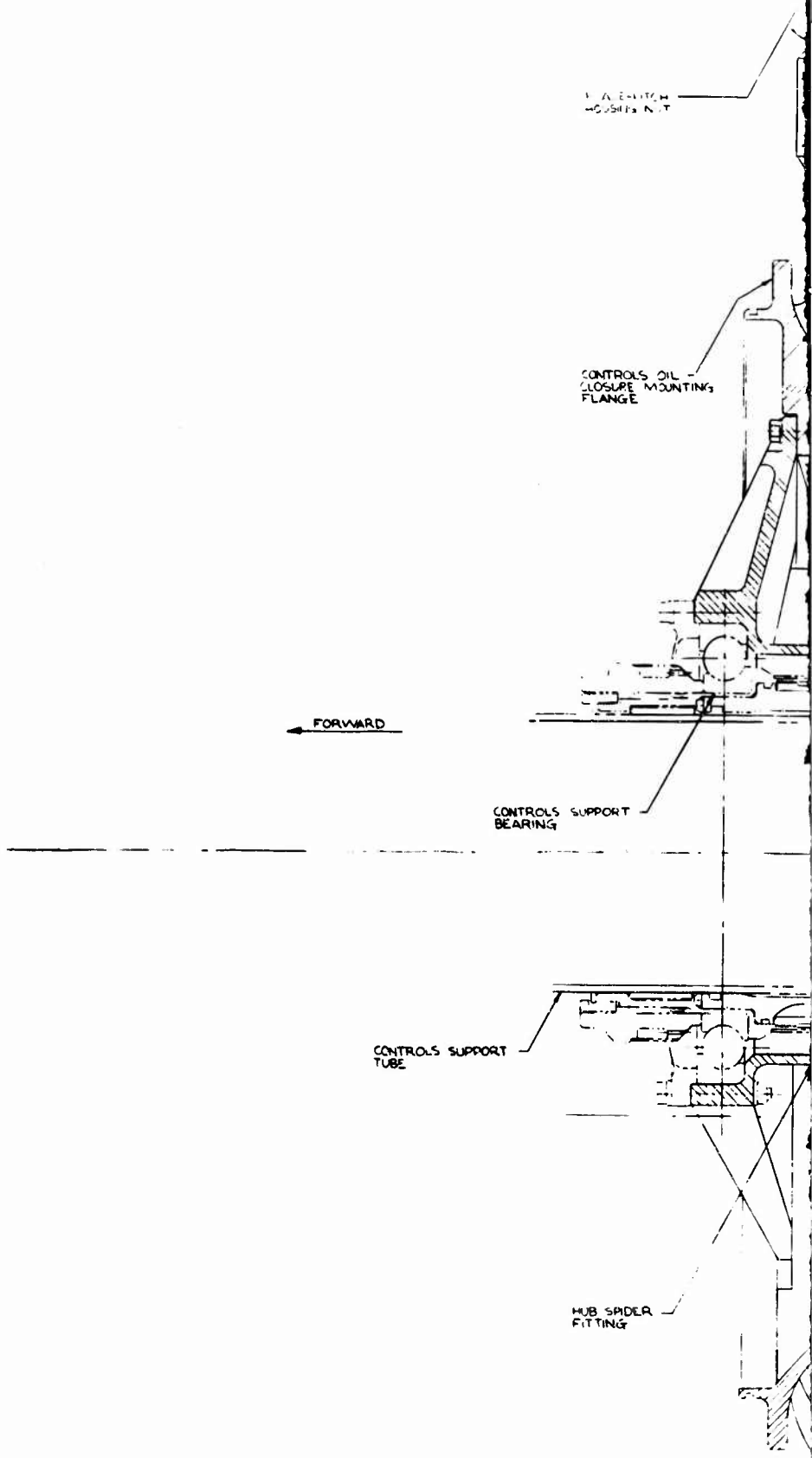
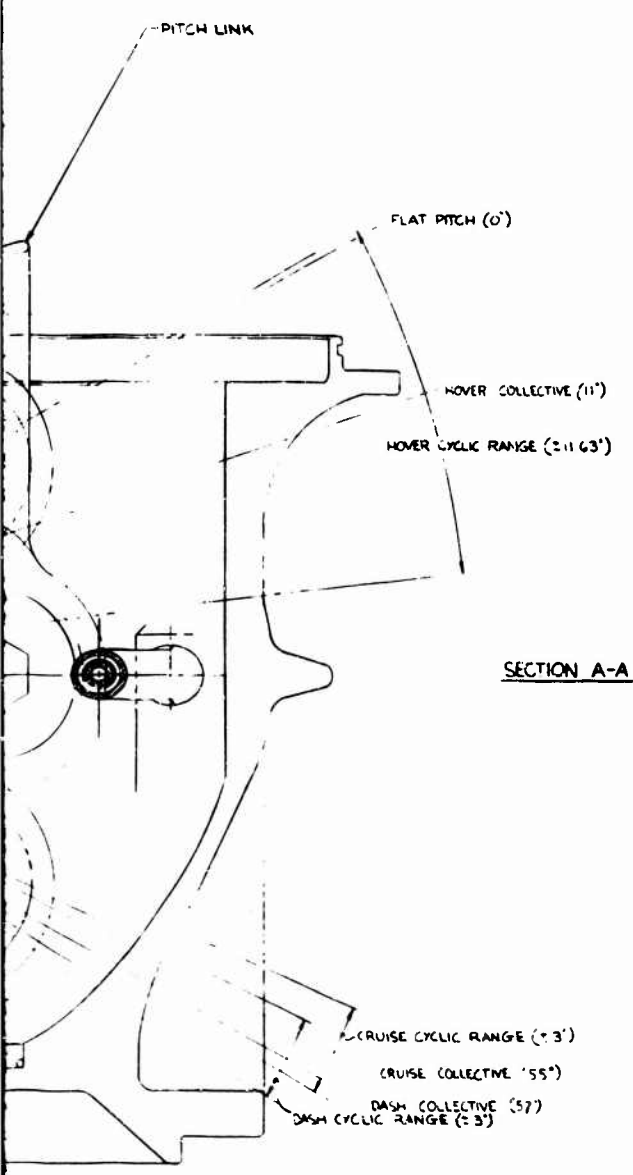
REV.	DATE	BY	CHK.	THE SPRINT COMPANY VERTICAL DIVISION PHILADELPHIA, PA.
				MODEL 215 ROTOR ASSEMBLY
				1777 SK215-10026

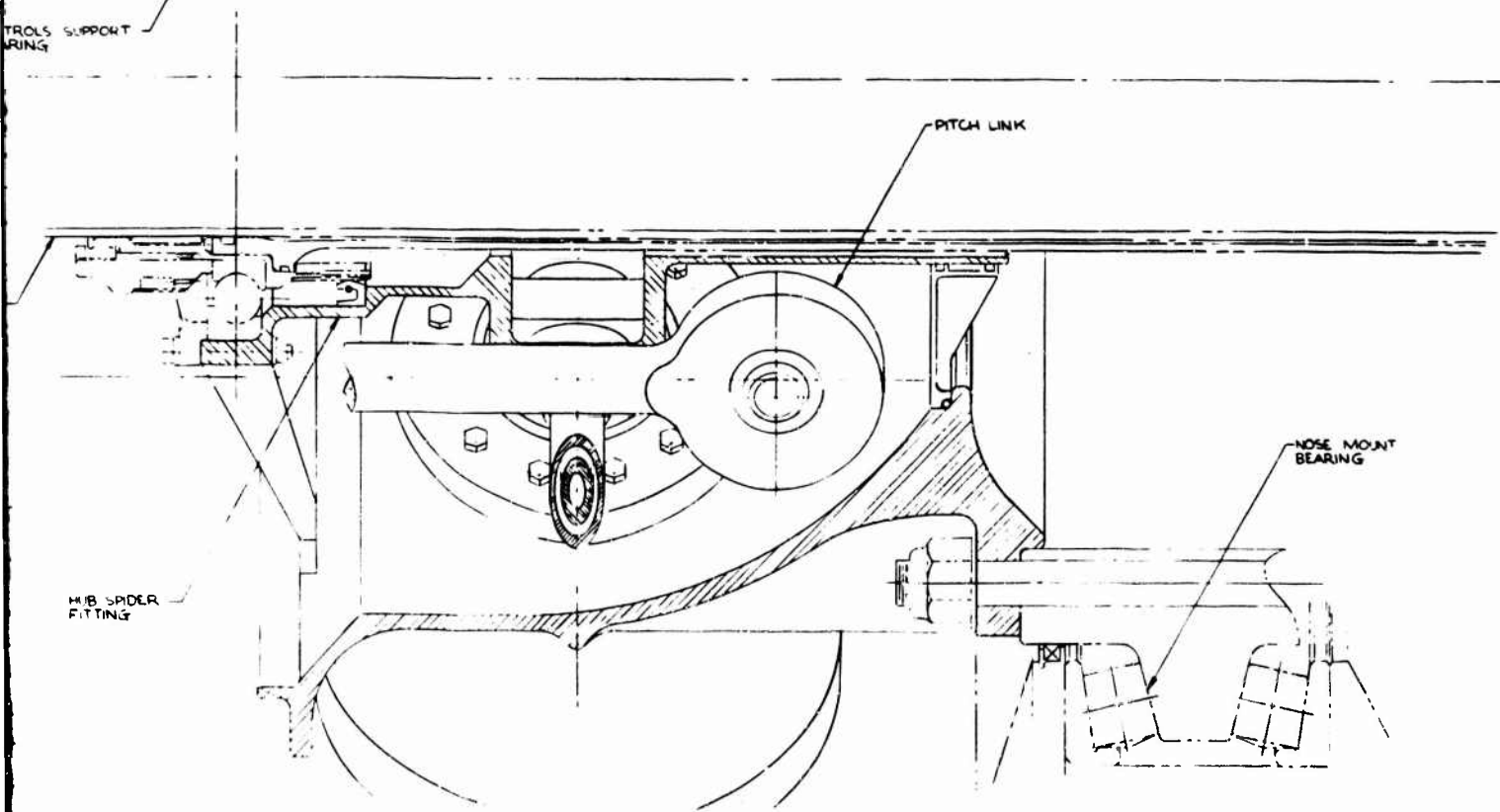
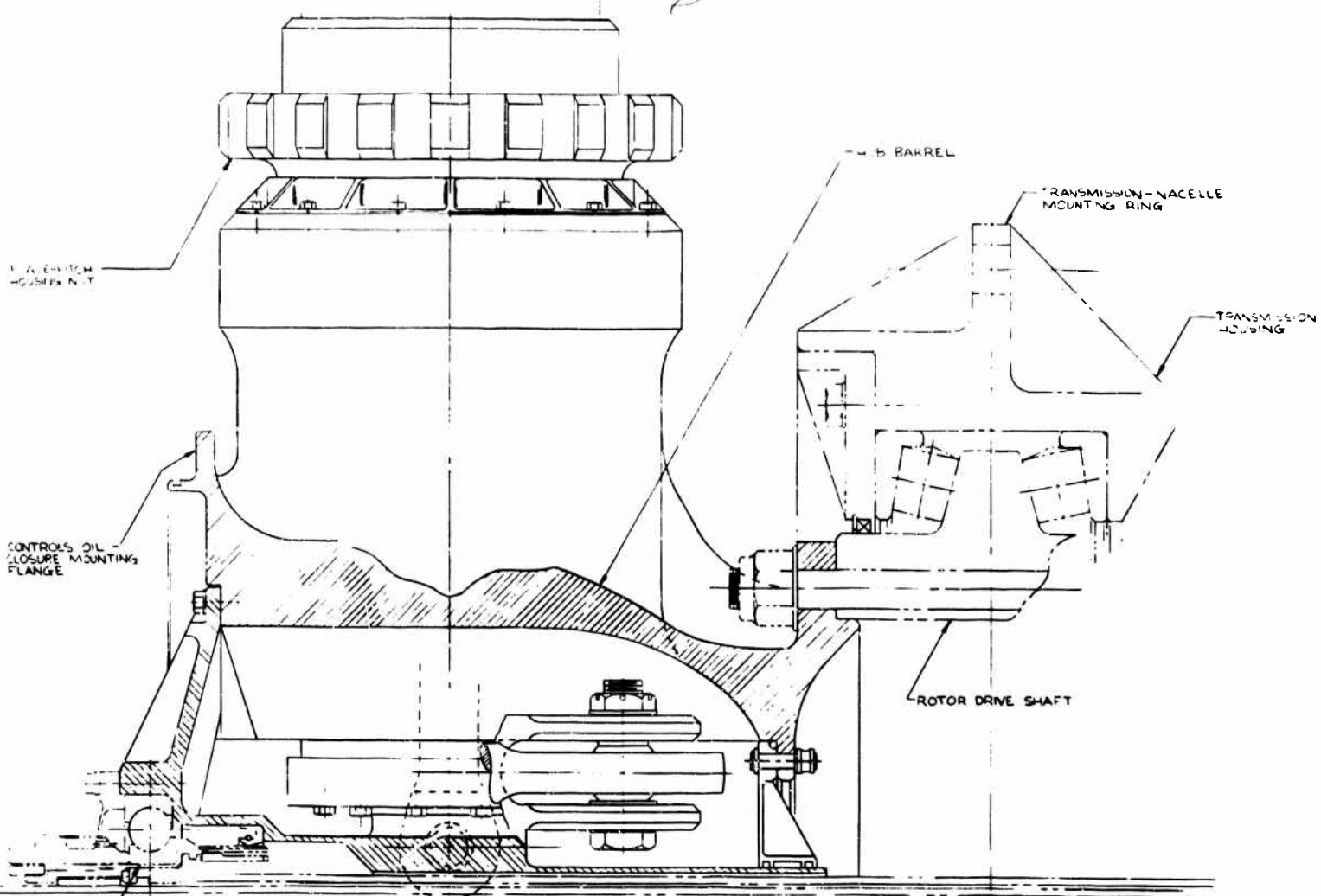
81

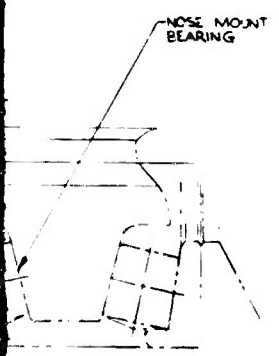
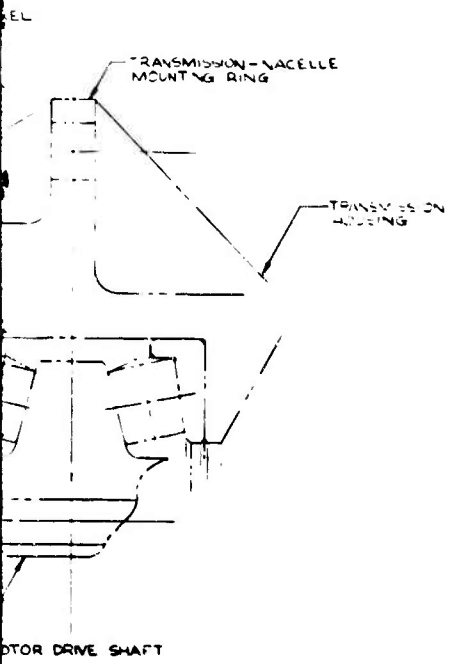


1 B









HUB ASSEMBLY

FIGURE VII-2

VII-7

THE BEING COMPANY	
SERIAL DIVISION PHILADELPHIA, PA.	
LAYOUT, HUB ASSEMBLY	
MODEL 216; DESIGN NO. 4	
DATE	7/27/53
BY	SK215-10015
CHKD	
APP'D	

shaft housing. ISIS will be incorporated to provide crack detection for the blade retention fitting.

The hub spider fitting incorporates a bearing which provides the primary support and location point for the nonrotating controls support tube.

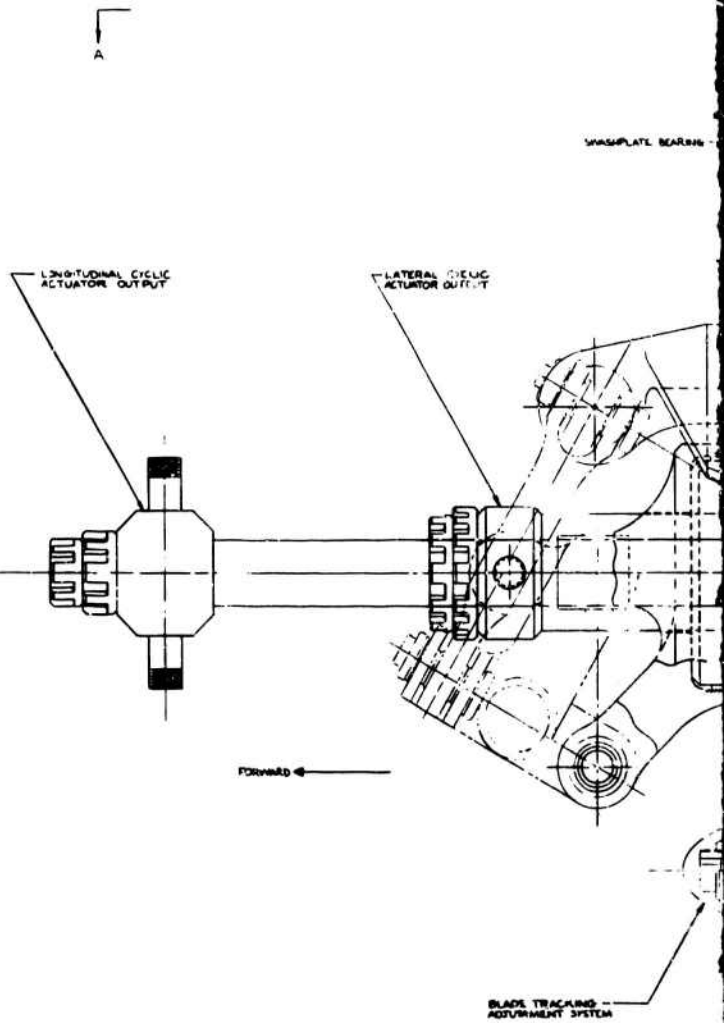
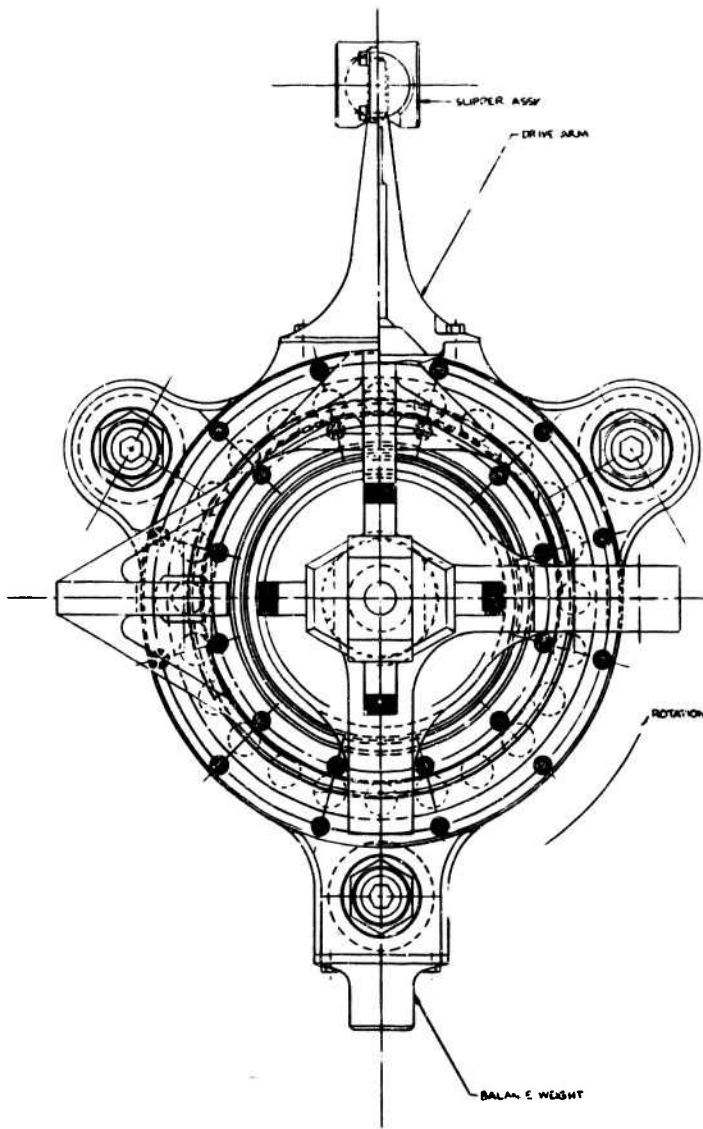
4.3 ROTOR CONTROLS

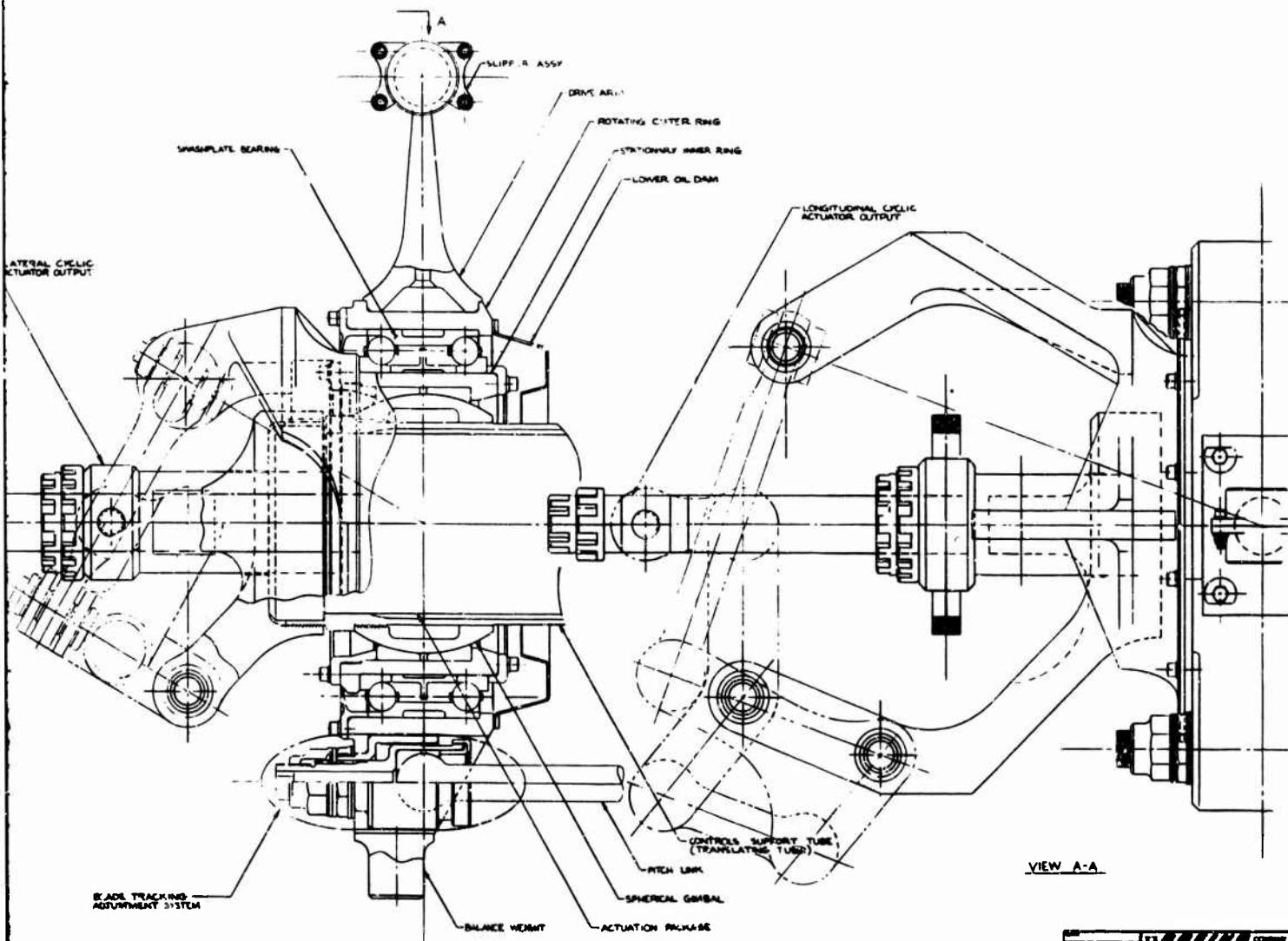
The prop/rotor control system (upper controls) consists of a swashplate assembly, lateral and longitudinal cyclic control mechanisms, and actuator system. Figures VII-3, VII-4 and VII-5 illustrate the design details respectively.

4.3.1 Swashplate Assembly

Blade pitch change is accomplished through a hydraulically actuated helicopter-type control swashplate assembly which transmits the blade pitch change through pitch links to the blade pitch shaft. Bi-cyclic pitch link motion requirements are accommodated by the use of a pitch link with an integral spherical end bearing at the swashplate end and a conventional rod end bearing at the pitch arm end. Blade tracking adjustment is accomplished through the pitch link spherical end bearing.

The swashplate assembly is gimbal (spherical bearing) supported on a translating controls support tube. This tube forms the primary structural component of the actuation package which, in addition to supporting the swashplate, houses the hydraulic cyclic and collective actuators and supports the linkage mechanisms which control swashplate tilt (cyclic pitch change). The swashplate rotating



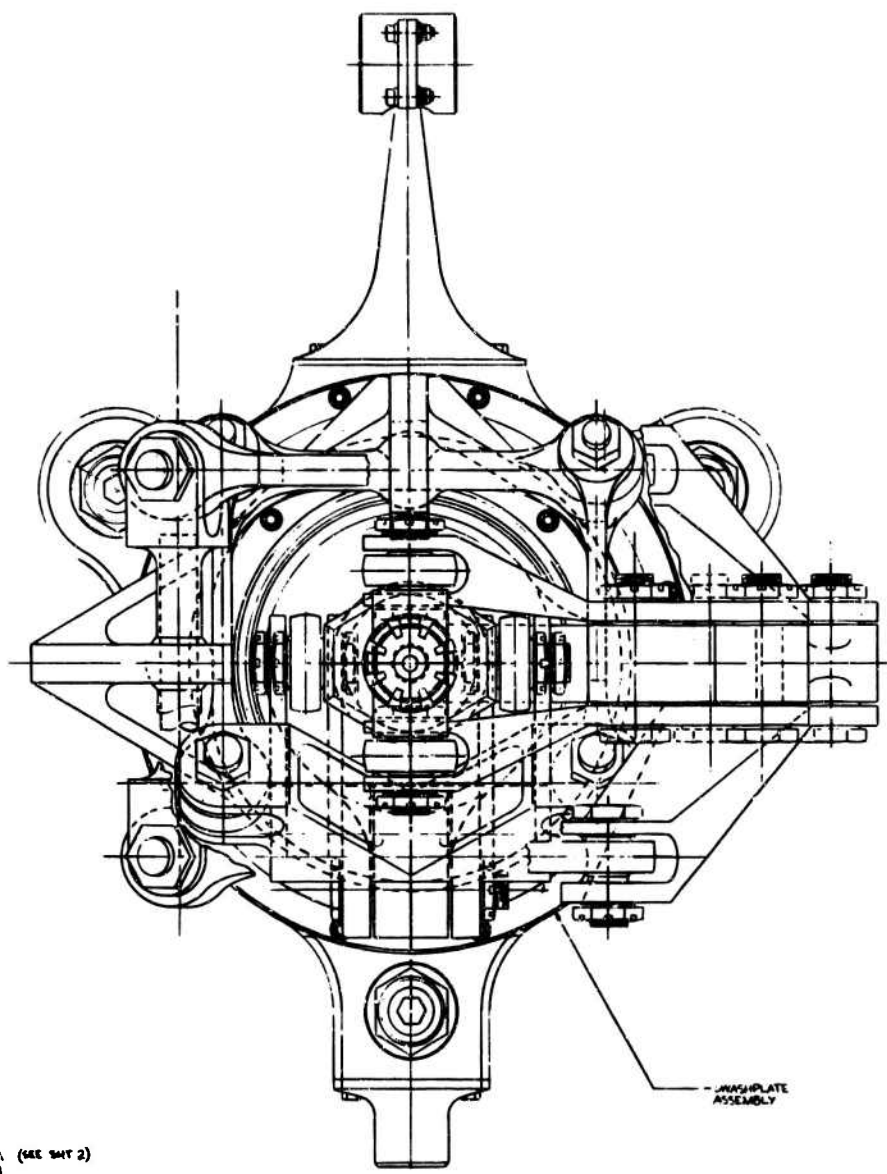


SWASHPLATE ASSEMBLY
FIGURE VII-3

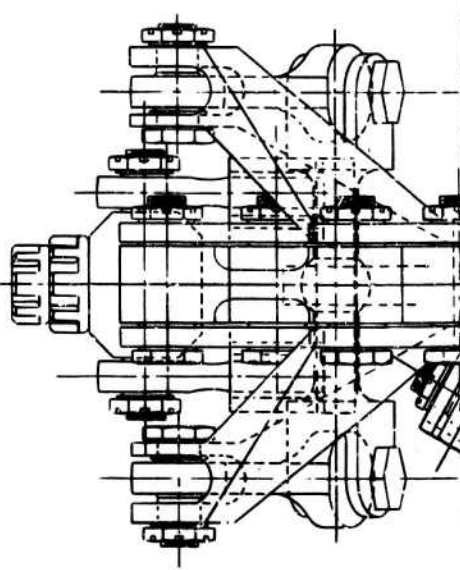
VII-11

REV	BY	DATE	DESCRIPTION
1	LAYOUT SWASHPLATE ASSEMBLY MODEL 28
REV. A			10020

19



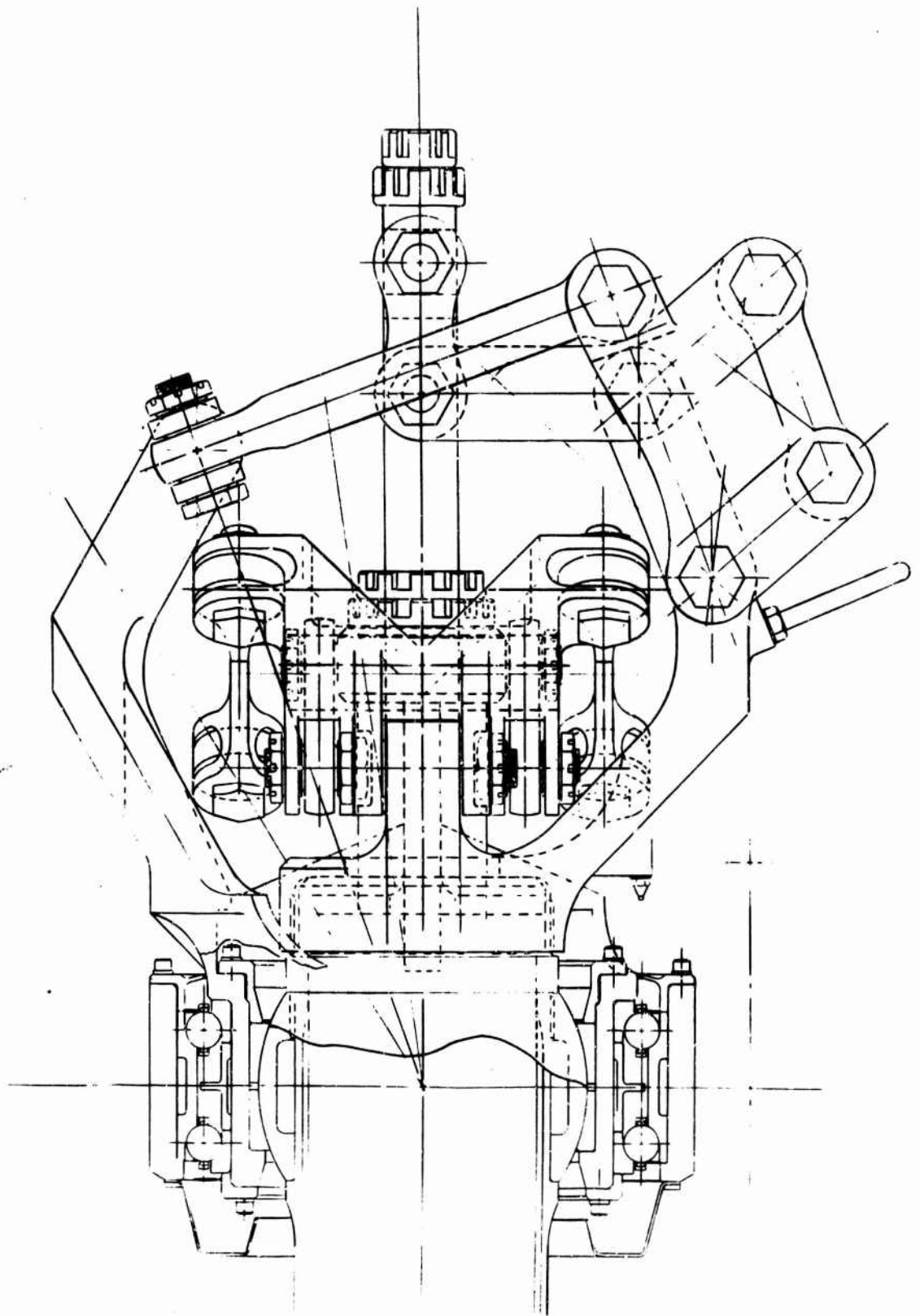
LONGITUDINAL CYCLE CONTROL MECHANISM



A (SEE SHY 2)

A (SEE SHY 2)

A



VIEW A-A

VIEW A-A

DATE		THE BRIND COMPANY
BY	KE-2111	VENTROL DIVISION PHILADELPHIA, PA.
CHKD		LAYOUT CYCLIC PITCH
APP'D		MECHANISM;
		MODEL 215
		DATE 1/17/54
		SK215-10024
		IN 2 V A

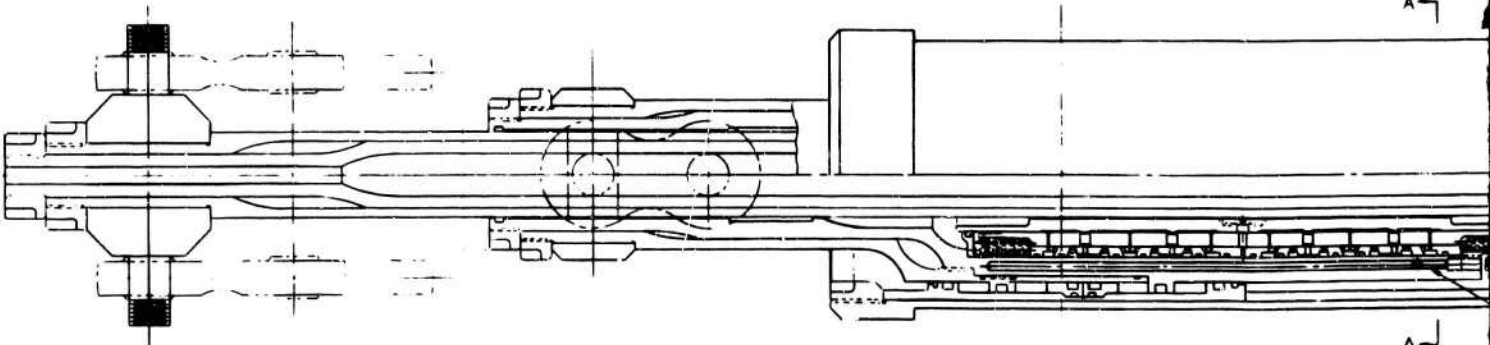
CYCLIC PITCH MECHANISM
FIGURE VII-4, SHEET 2

VII-13a

A



SECTION A-A



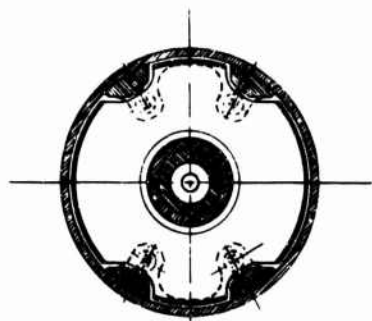
A 7

A 1

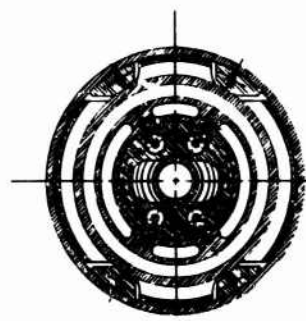
B



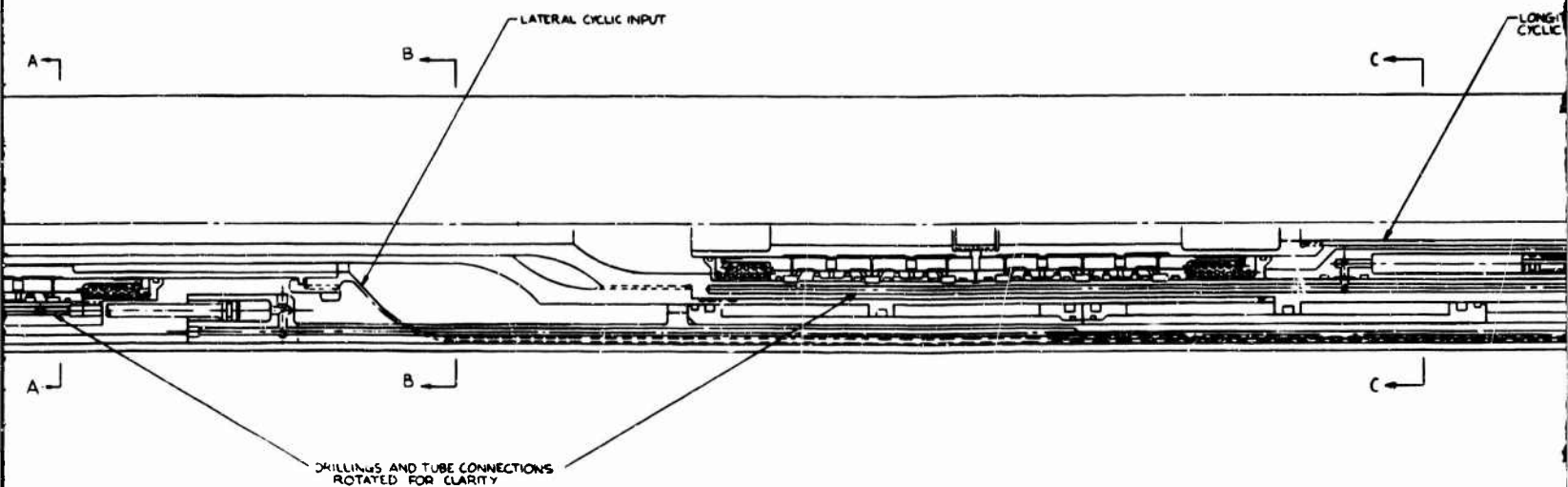
SECTION A-A



SECTION B-B



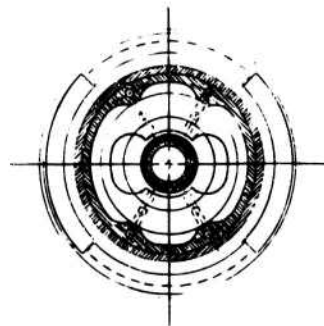
SECTION C-C



LATERAL CYCLIC INPUT

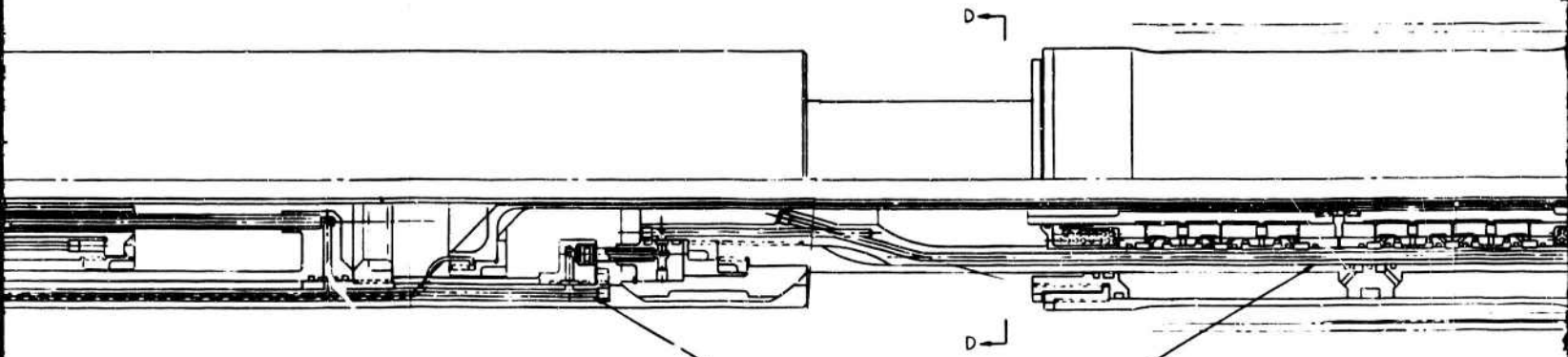
LONGITUDINAL CYCLIC

SKILLINGS AND TUBE CONNECTIONS ROTATED FOR CLARITY



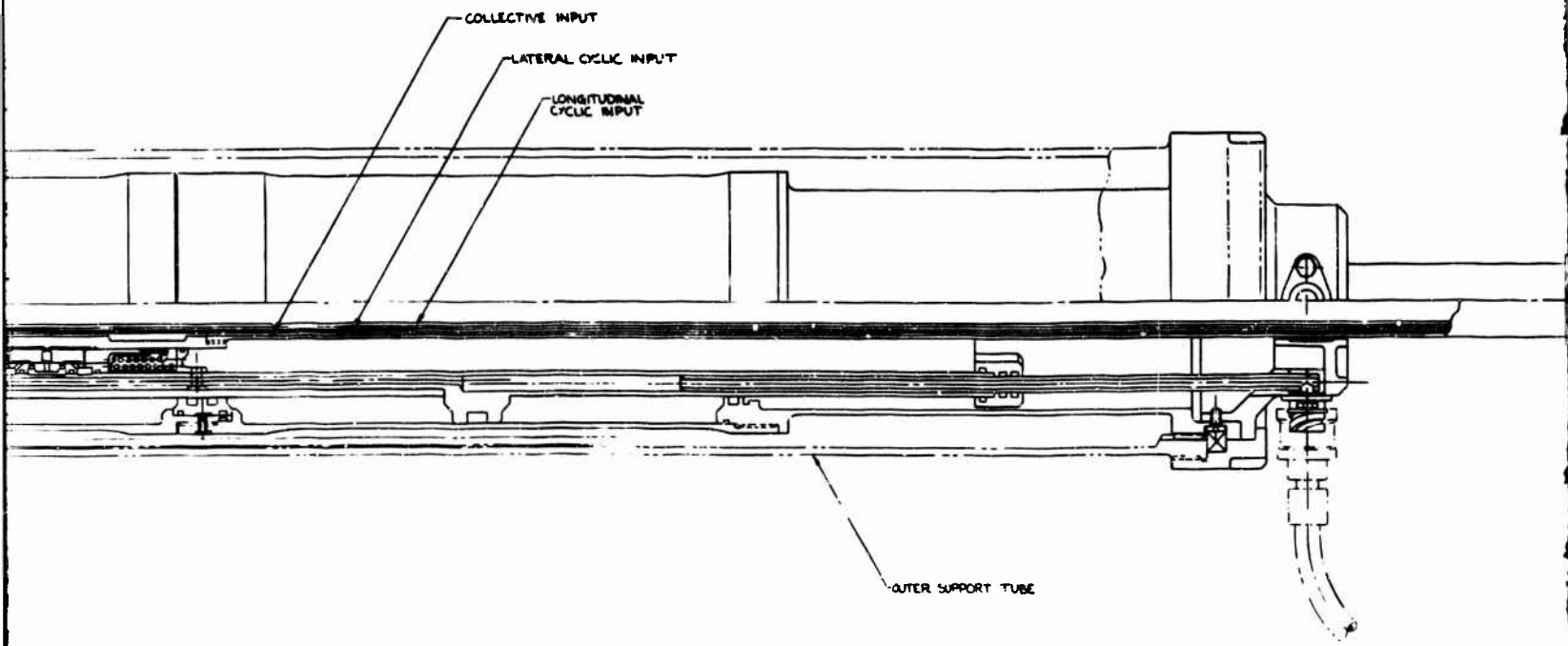
SECTION D-D

TUTORIAL
INPUT

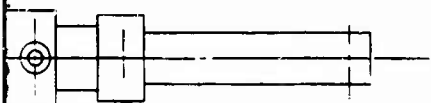


DRILLINGS AND TUBE CONNECTIONS
ROTATED FOR CLARITY

0



15



DESIGNED BY	K. E. SMITH	THE SPIN COMPANY
DRAWN BY		VERTICAL DIVISION PHILADELPHIA, PA.
CHECKED BY		ACTUATOR ASSEMBLY,
DATE		ROTOR CONTROL,
		MODEL 215
		7/27/51 SK215-0025

ACTUATOR ASSEMBLY ROTOR CONTROL

FIGURE VII-5

VII-15

outer ring is driven by the rotating hub through a drive plate and a follower unit (slipper assembly).

4.3.2 Rotor Control Actuators

The actuator system is contained inside the hub and the transmission. Control moment forces are reacted by the forward support bearing and a steady mount at the aft face of the transmission. The control support thrust bearing transfers only shear and torque reaction forces to the transmission end cover through a spline.

The hydraulic dual tandem collective and cyclic actuators are of a design having a fixed housing and a moving piston assembly. The actuators are powered by two independent 3,000 PSI hydraulic systems. Dual mechanical load paths are provided for each actuator.

The aft end piece threaded to the collective actuator housing comprises a tubular extension which serves as an attachment of the actuator to the outer support tube. This is also one of the interface elements between the actuator and the fluid supply assembly.

The pressure and return lines of each hydraulic system leading to the servo valves are formed by the drillings in the walls of the piston rods of each actuator. The servo valves of each actuator are of tandem jam-proof design and are located inside each respective piston rod and concentric with the actuator centerline. The primary spool of the collective actuator servo valve is of a tubular form to provide a passage inside the collective actuator for the cyclic actuator control input tubes. Control passages from the valves to the cylinders are also drilled in the piston rods.

Fluid connections from both hydraulic systems are extended to the cyclic actuator fluid passages in the piston rods through telescopic connections.

The forward end of the collective actuator piston rod is attached to a self-alignment piece having spherical surfaces held by the corresponding surfaces formed in a special cylinder aft end. The forward end of the cylinder is fixed to the swashplate guide cube. The cylinder also contains the two-part cyclic actuator housings.

The forward ends of the cyclic actuator piston rods are connected to collars with trunnions holding the swashplate tilting links.

4.4 LUBRICATION

Lubrication of the pitch shaft bearings is accomplished through centrifugal action on the oil accumulation in the hub barrel. The entire hub barrel is filled with oil to provide lubrication for the upper controls.

All metal bearings are oil lubricated and the complete pitch change mechanism, swashplate assembly and blade retention system are totally enclosed by an oil closure which also serves as a rotating oil sump. While rotating, oil is continually supplied to the upper controls through a ram tube which extends from the stationary longitudinal cyclic control mechanism support member to the annular oil sump of the rotating system. A centrifugal pressure head is generated and the oil is ported into a central oil gallery which distributes the oil to the bearing reservoirs. These reservoirs or dams are provided at all rolling element bearings in order to

provide a "safe" oil supply for startup and loss of sump oil through seal failure or gunfire damage. The reservoirs are designed to hold, in either the cruise or hover mode, that amount of oil required to sustain the respective bearing in the case of an oil system failure during a mission.

Lubrication of the cyclic pitch change mechanism is accomplished through a rotating spray head. Oil is supplied to this spray head from an oil line coming from the oil lubrication pump, through the center of the actuation package.

4.5 SPINNER ASSEMBLY

The aerodynamic spinner is designed in three sections. The forward sections are readily removable to provide access to the rotor system. The aft section of the spinner is removable for maintenance and inspection of the hub assembly. The spinner shells are of aluminum construction. Details of the spinner design are shown in Figure VII-1.

Electrical power is carried forward by a pancake-type slipring and brush block assembly for blade de-icing. Blade de-icing electrical power is carried through a multibrush drum type slipring mounted on the movable pitch shaft housing. The two brush block assemblies are fixed to the hub barrel against rotation but are free to translate axially with elastomeric bearing deflection of the blade assembly and slipring translation.

5. STRUCTURAL ANALYSIS

5.1 INTRODUCTION

Ultimate and fatigue stress analyses of primary load carrying sections of the rotor hub assembly are performed to establish materials and sizes for a detailed weight analysis. The components include the hub barrel, hub spider, tie bar, blade retention and socket fittings and the pitch change bearings. Calculated minimum margins of safety are shown in Table VII-1. These values show the design to be adequate.

5.2 DESIGN LOADS

The hub design loads are calculated for the criteria used for the blade analysis in Section VI. Hub forces are contained in Table VII-2. Blade loads at blade station 7.5% are contained in Table VII-3.

5.3 STRESS ANALYSIS OF BLADE RETENTION

5.3.1 Blade Retention Components

The primary members of the blade retention system are the retention fitting and socket which are an integral part of the blade spar root, the elastomeric bearing and the tie bar. The design loads for the blade retention system are contained in Table VII-4.

5.3.2 Blade Root Assembly C.F. Stress

The distribution of pressure in the spar and retention fitting and the stress due to centrifugal force are presented in Figures VII-6, VII-7 and VII-8.

TABLE VII-1

ROTOR HUB ASSEMBLY MINIMUM MARGINS OF SAFETY

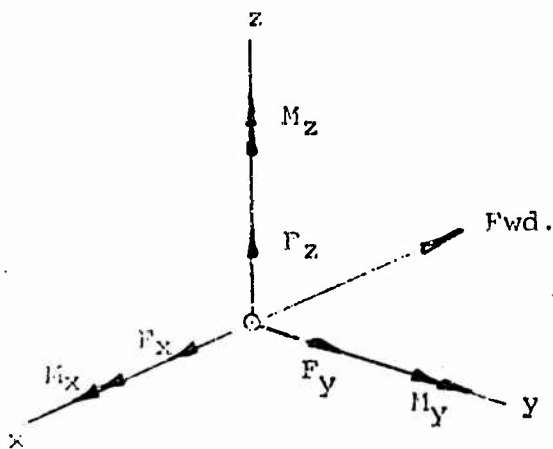
<u>COMPONENT</u>	<u>M.S.</u>
Spar	.54
Root Retention	1.10
Elastomeric Bearing	.13
Tie Bar	.06
Hub Mounting - Bolts	.04
Hub Mounting - Flange	.07
Spider Fitting	.56
Blade Retention Lug	.10
Blade Retention Pin	.18

TABLE VII-2

HUB FORCES

	FATIGUE CONDITION	MAXIMUM CYCLIC CONDITION	2.5g VERTICAL TAKEOFF
F_x	2605 lb	8685 lb	2318 lb
F_y	326 lb	1086 lb	290 lb
F_z	34,180 lb	34,180 lb	85,450 lb
M_x	294,489 in-lb	981,630 in-lb	262,045 in-lb
M_y	793,031 in-lb	2,643,436 in-lb	705,663 in-lb
M_z	1,136,300 in-lb	1,136,300 in-lb	1,136,300 in-lb

Positive Sign Convention - Hub Loads:



- F_x = Hub Force along x Axis
- F_y = Hub Force along y Axis
- F_z = Hub Force along z Axis
- M_x = Moment about x axis (roll)
- M_y = Moment about y axis (pitch)
- M_z = Moment about z axis (yaw)

TABLE VII-3

BLADE LOADS AT 7.5% RADIUS

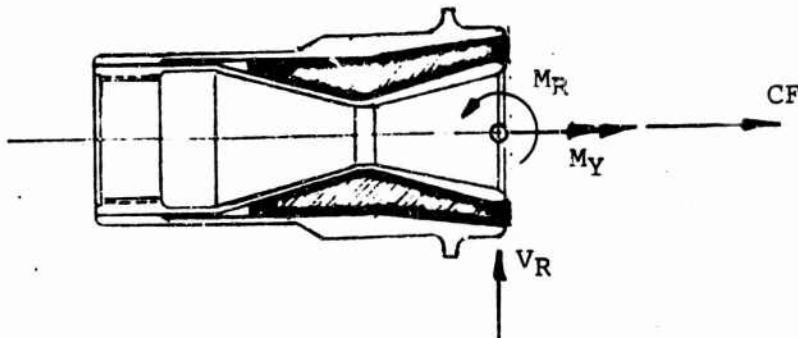
		FATIGUE CONDITION	MAXIMUM CYCLIC CONDITION	2.5g VERTICAL TAKEOFF
STEADY LOADS	V _X	889	889	2223
	V _Z	11064	11064	27660
	M _X	617800	617800	1544500
	M _Y	-21290	-21290	-53225
	M _Z	-5630	-5630	-14075
	CF	105200*	164375**	164375**
ALTERNATING LOADS	V _X	2224	7414	1979
	V _Z	6756	22518	6012
	M _X	387512	1291707	344885
	M _Y	42645	142151	37954
	M _Z	135818	452727	120878

* Normal Rotor Speed

** Limit Rotor Speed

TABLE VII-4

DESIGN LOADS FOR BLADE RETENTION



Fatigue Condition:

$$M_R = 581,191 + 410,624 \text{ in-lbs}$$

$$V_R = 10,787 + 7,112 \text{ lbs}$$

$$M_Y = 21,290 + 42,645 \text{ in-lbs}$$

$$CF = 105,200 \text{ lbs}$$

Ultimate Condition:

$$M_R = 2,941,754 \text{ in-lbs}$$

$$V_R = 51,890 \text{ lbs}$$

$$M_Y = 245,161 \text{ in-lbs}$$

$$CF = 246,563 \text{ lbs}$$

FIGURE VII-6 STRESS ANALYSIS OF BLADE RETENTION SPANWISE HOOP PRESSURE DISTRIBUTION DUE TO CENTRIFUGAL FORCE

— ULTIMATE
 - - - FATIGUE

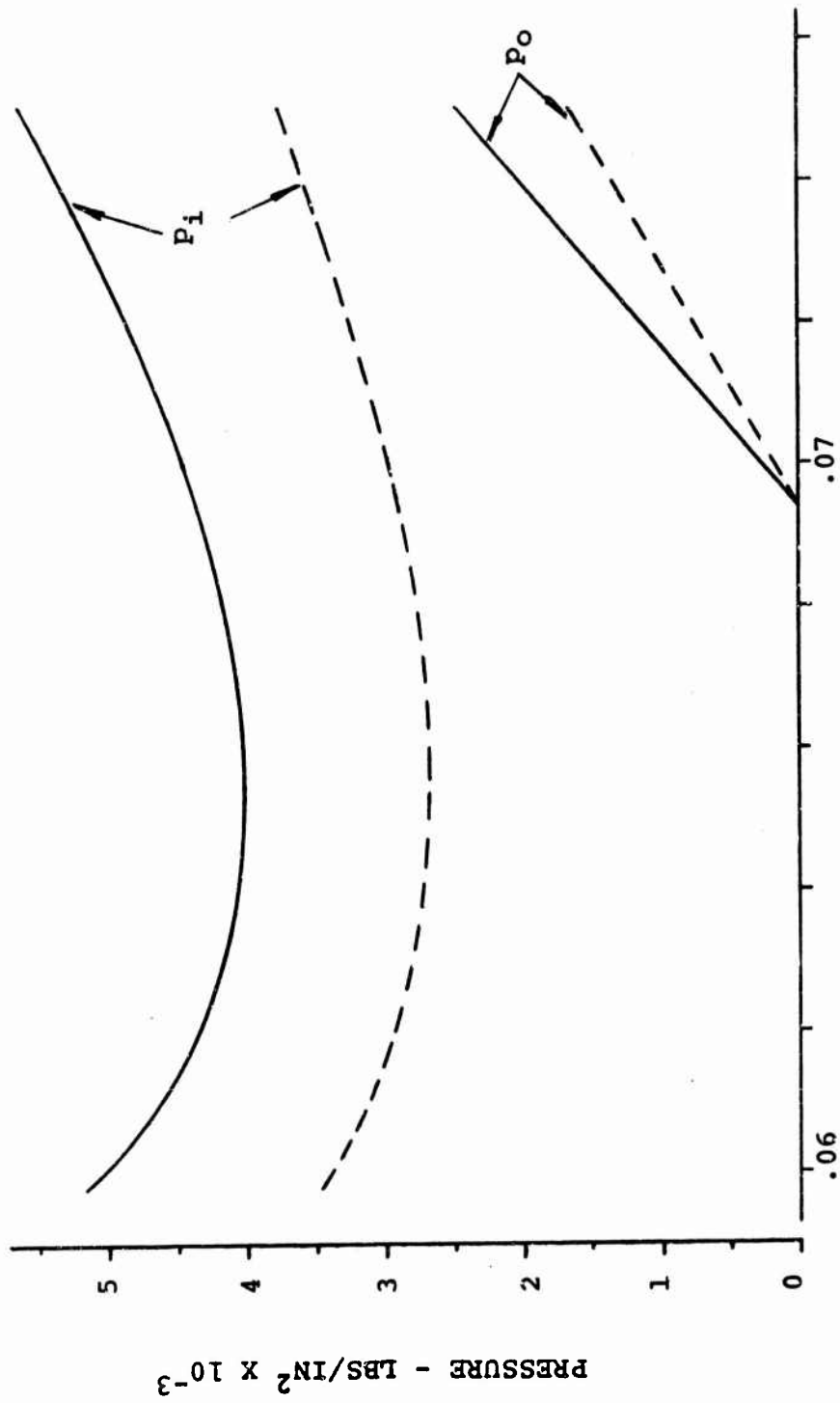


FIGURE VII-7 STRESS ANALYSIS OF BLADE RETENTION SPANWISE HOOPSTRESS DISTRIBUTION IN THE SPAR DUE TO CENTRIFUGAL FORCE

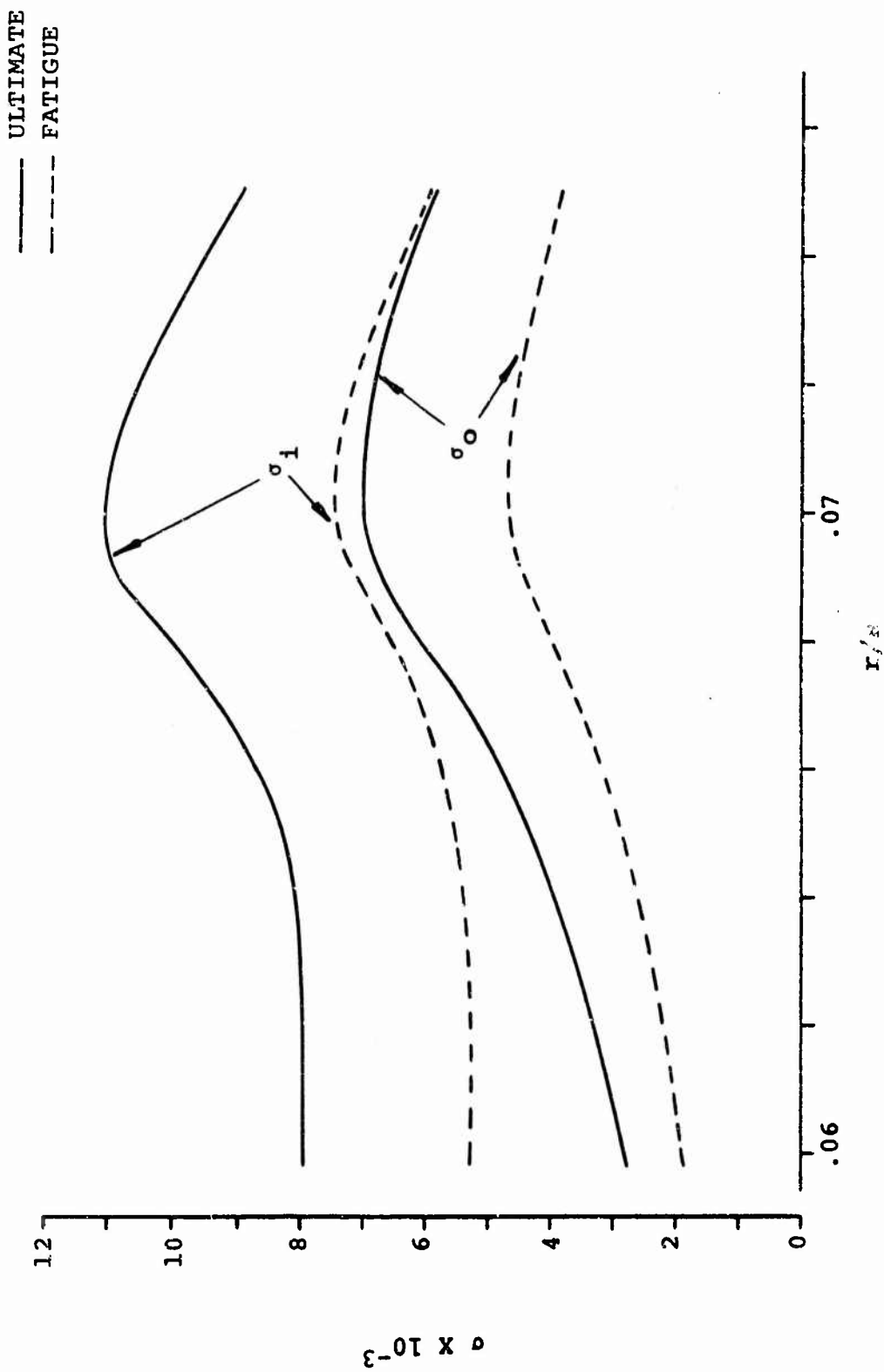
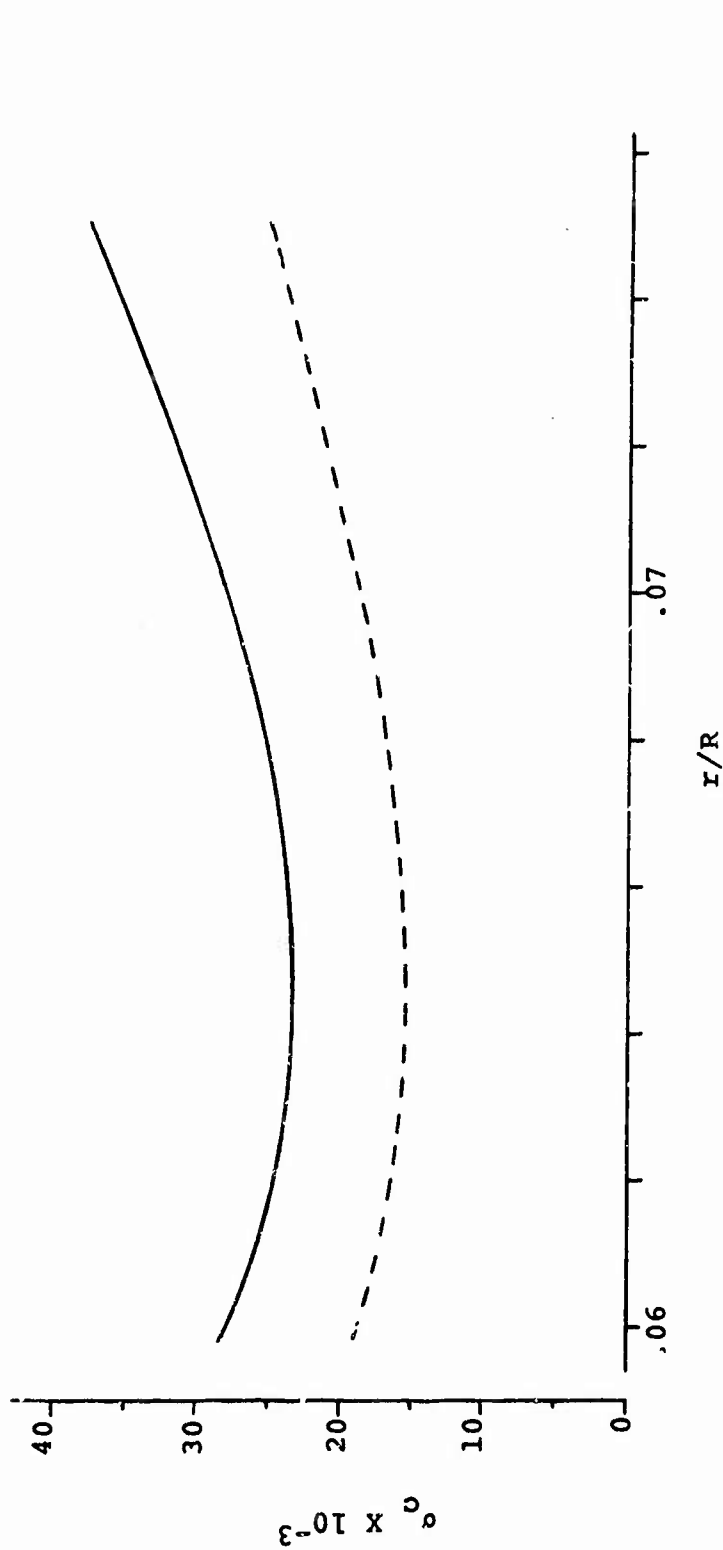
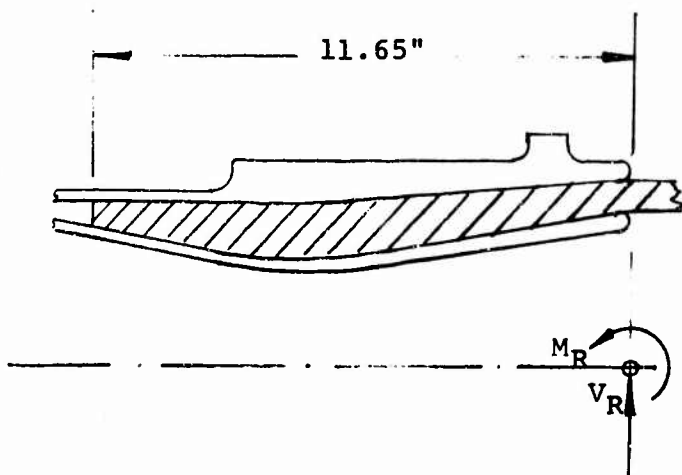


FIGURE VII-8 STRESS ANALYSIS OF BLADE RETENTION SPANWISE HOOPSTRESS
 DISTRIBUTION IN THE RETENTION FITTING DUE TO CENTRIFUGAL FORCE



5.3.3 Blade Root Assembly Socket Analysis

The internal reacting load distribution to the blade root retention fitting and socket is analyzed by the "socket analyses" approach described in Lockheed Stress Memo number 41a.



$$W_1 = \frac{K_1 M}{L^2} \quad \& \quad W_2 = \frac{K_2 M}{L^2}$$

$$V_{MAX} = \frac{K_S M}{L}$$

$$M_{MAX} = K_M M$$

FATIGUE ANALYSIS

$$V_R = 10787 + 7112 \text{ lbs}$$

$$M_R = 581191 + 410624 \text{ in-lbs}$$

$$\frac{V_L}{M} = \frac{7112 (11.65)}{410624} = .202$$

$$K_1 = 6.80$$

$$K_2 = 6.40$$

$$K_a = .48$$

$$K_S = 1.55$$

$$K_M = 1.00$$

ULTIMATE ANALYSIS

$$V_R = 51890 \text{ lbs}$$

$$M_R = 2941754 \text{ in-lbs}$$

$$\frac{V_L}{M} = \frac{51890 (11.65)}{1795000} = .204$$

$$K_1 = 6.80$$

$$K_2 = 6.40$$

$$K_a = .48$$

$$K_S = 1.55$$

$$K_M = 1.00$$

Fatigue Analysis:

$$W_1 = \frac{K_1 M}{L^2} = 6.80 \frac{(581191 + 410624)}{(11.65)^2}$$

$$W_1 = 29000 \pm 20500 \text{ lbs/in}$$

$$W_2 = (6.40/6.80) (29000 \pm 20500)$$

$$W_2 = 27300 \pm 19250 \text{ lbs/in}$$

$$V_{MAX} = 1.55 \frac{(581191 + 410624)}{11.65}$$

$$V_{MAX} = 77500 \pm 54700 \text{ PSI}$$

$$M_{MAX} = 1.00 (581191 + 410624)$$

$$M_{MAX} = 581191 \pm 410624 \text{ in-lbs}$$

Ultimate Analysis:

$$W_1 = \frac{6.80 (2941754)}{(11.65)^2}$$

$$W_1 = 146500 \text{ lbs/in}$$

$$W_2 = (6.40/6.80) (146500)$$

$$W_2 = 137500 \text{ lbs/in}$$

$$V_{MAX} = 1.55 \frac{(2941754)}{11.65}$$

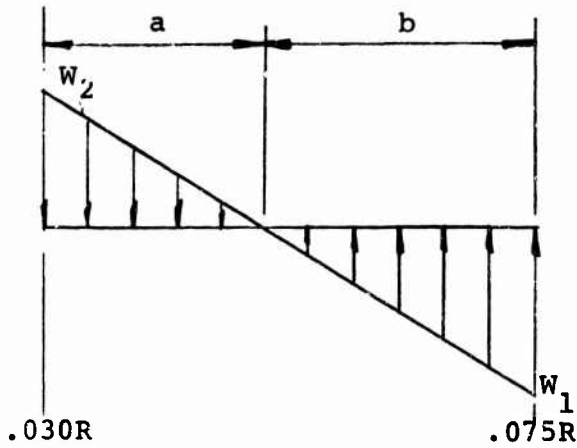
$$V_{MAX} = 380000 \text{ lbs}$$

$$M_{MAX} = 1.00 (2941754)$$

$$M_{MAX} = 2941754 \text{ lbs}$$

5.3.4 Spar Root Stresses

Ultimate Spar Stresses Due to W_1 and W_2 :



$$W_1 = 146500 \text{ lbs/in}$$

$$W_2 = 137500 \text{ lbs/in}$$

$$a = 5.55''$$

$$b = 6.10''$$

Block Compression Stresses:

$$\sigma_c = \frac{W}{2R} \quad (\text{block compression})$$

at .075R:

$$\sigma_c = \frac{146500}{2(3.90)} = 18900 \text{ PSI}$$

at .030R:

$$\sigma_c = \frac{137500}{2(3.30)} = 20300 \text{ PSI}$$

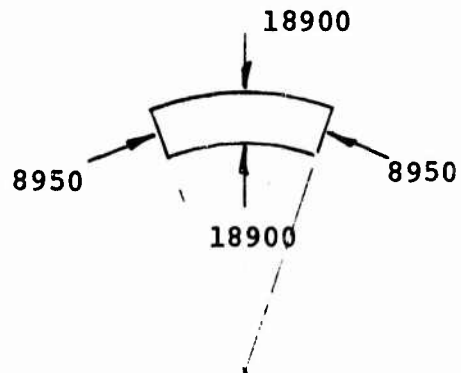
Hoop Stress Due to CF:

$$\sigma_c = 8950 \text{ PSI at } .075R$$

$$\sigma_c = 0 \text{ at } .030R \text{ (contact separation)}$$

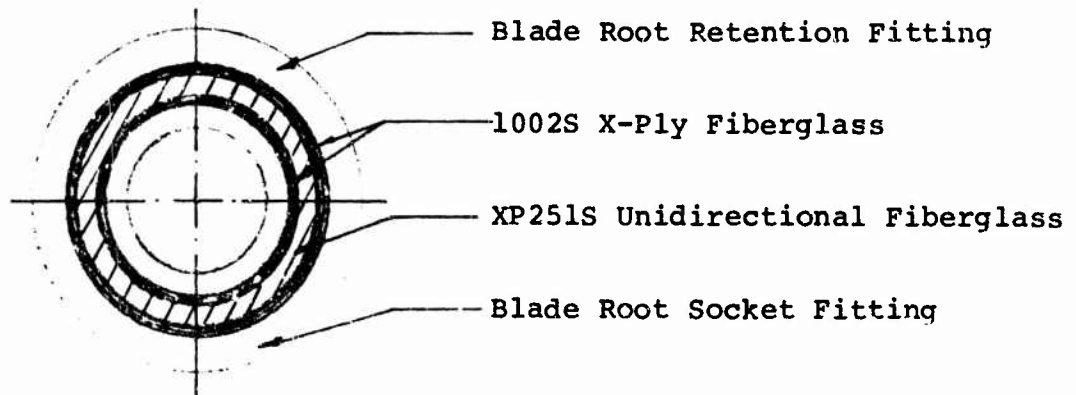
$$\sigma_{\text{TOTAL}} = 18900 + 8950 = 27850 \text{ PSI at } .075R \text{ (conservative)}$$

$$F_{cu} = 43000 \text{ PSI (XP251S @ } 90^\circ)$$



$$MS = \frac{43000}{27850} - 1 = .54$$

Spar Root Shear Stresses:



Shear Stress: Due to Vertical Shear:

$$q = \frac{VE}{\Sigma EI} \int ydA$$

for circular sections:

$$Q = \int ydA = \int_0^{\phi} R^2 t \cos \phi d\phi = [R^2 t \sin \phi]_0^{\pi/2}$$

$$Q = R^2 t$$

Max. Shear Stress

$$\tau = \frac{VEQ}{t \Sigma EI} = \frac{VER^2}{\Sigma EI}$$

Fatigue Stresses

Spar:

$$\tau = \frac{(77500 \pm 54700) (1.59) (3.70)^2}{2903}$$

$$= 577 \pm 410 \text{ PSI}$$

$$F_{SEL} = 6300 \text{ PSI}$$

$$MS = \frac{6300}{410} - 1 = \text{Ample}$$

Root Retention:

$$\tau = \frac{(77500 \pm 54700) (16.0) (4.25)^2}{2903}$$

$$= 7700 \pm 5400 \text{ PSI}$$

$$F_{SEL} = \frac{20000}{\sqrt{3}} = 11500 \text{ PSI (Titanium)}$$

$$MS = \frac{11500}{5400} - 1 = 1.12$$

Ultimate Stresses

Spar:

$$\tau = \frac{380000 (1.59) (3.70)^2}{2903}$$

$$= 2820 \text{ PSI}$$

$$F_{SU} = 36000 \text{ PSI}$$

$$MS = \frac{36000}{2820} - 1 = \text{Ample}$$

Root Retention:

$$\tau = \frac{(380000) (16) (4.25)^2}{2903}$$

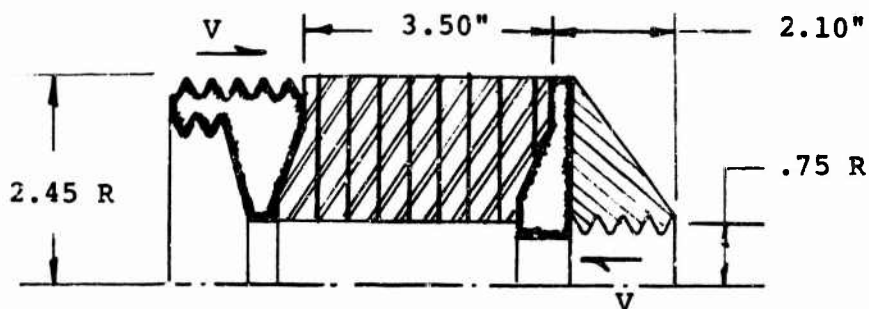
$$= 37800 \text{ PSI}$$

$$F_{SU} = 80000 \text{ PSI}$$

$$MS = \frac{80000}{37800} - 1 = 1.10$$

5.3.5 Elastomeric Bearing Analysis

The elastomeric bearing is sized by an approach developed by the Marlin Rockwell Division of TRW, Inc. The calculation steps are presented below. A stress analysis of the bearing threaded end fittings is also included.



a. Area of Annulus:

$$\begin{aligned} A &= .7854 (D_o^2 - D_e^2) \\ &= .7854 (4.90^2 - 1.50^2) \end{aligned}$$

$$A = 17.09 \text{ in}^2$$

b. Limit Load Capacity:

$$\begin{aligned} C_1 &= 10000 A \\ &= 10000 (17.09) \end{aligned}$$

$$C_1 = 170900 \text{ lbs}$$

c. Ultimate Load:

$$\begin{aligned} C_1 &= 15000 \text{ A} \\ &= 15000 (17.09) \end{aligned}$$

$$C_1 = 256350 \text{ lbs}$$

d. Elasto Length:

$$\begin{aligned} (1) \quad L_{EL} &= \frac{(\text{Cruise Coll. Angle}) (D_o \text{ Circum.})}{(\text{Shear Strain}) (360^\circ)} \\ &= \frac{(57^\circ - 12^\circ) (\pi) (4.90)}{(1.25) (360)} = 1.54'' \end{aligned}$$

$$\begin{aligned} (2) \quad L_{EL} &= \frac{(\text{Hover Coll.} + \text{Cyclic Angle}) (D_o \text{ Circum.})}{(\text{Shear Strain Fatigue}) (360)} \\ &= \frac{(12 + 3.54) (\pi) (4.90)}{(.50) (360)} = 1.34'' \end{aligned}$$

$$e. \quad \frac{L_{EL}}{t_{ELASTO \ ELEM}} = \frac{1.54}{.002} = 769 \text{ (No. of Elasto Elements)}$$

$$f. \quad \text{No. Metal Lamina} = 769 - 1 = 768$$

$$\begin{aligned} g. \quad L_{MET} &= t_{MET \ ELEM} \times \text{No. Metal Lam} \\ &= .002 (768) = 1.54'' \end{aligned}$$

$$h. \quad L_{BRG} = L_{EL} + L_{MET} = 1.54 + 1.54 = 3.08''$$

i. Design Length = 3.50"

$$MS = \frac{3.50}{3.08} - 1 = .13$$

Thread Analysis:

$$CF = 246563 \text{ lbs (1t.)}$$

$$\tau = \frac{246563}{2(3.14)(.65)\left(\frac{2.10}{2}\right)}$$

$$\tau = 57500 \text{ PSI}$$

$$F_{SU} = 80000 \text{ PSI (6 AL-4V)}$$

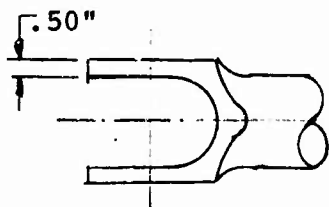
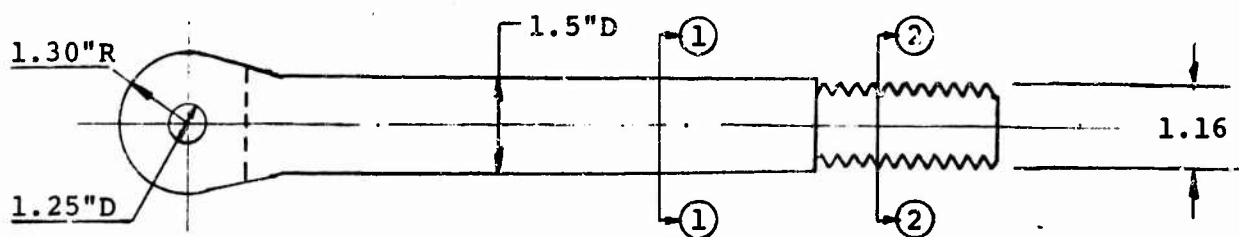
$$MS = \frac{80000}{57500} - 1 = .39$$

5.3.6 Tie Bar Analysis (Material - Stainless Steel, Carpenter Custom 455)

The tie bar is analyzed for C.F. loading.

$$F_{tu} = 240000 \text{ PSI}$$

$$F_{su} = 128000 \text{ PSI}$$



Lug Analysis

$$D = 1.25"$$

$$W = 2.60"$$

$$t = .50"$$

$$P = 2.34 (104919) = 246000 \text{ lbs}$$

$$W/D = 2.60/1.25 = 2.08$$

$$a/D = 1.30/1.25 = 1.04$$

$$D/t = 1.25/.50 = 2.50$$

$$A_{BR} = Dt = 1.25 (.50)$$

$$A_{BR} = .625 \text{ in}^2$$

$$A_t = (W-D)t = (2.60 - 1.25) (.50)$$

$$A_t = .675 \text{ in}^2$$

Tension Across Net Section

$$P_{tu} = K_1 F_{tu} A_t \quad (K_1 = .96)$$

$$= [.96 (240000) (.675)] (2)$$

$$P_{tu} = 310000 \text{ lbs}$$

$$MS = \frac{310000}{246563} - 1 = .26$$

$$P_{BRU} = K_{BR} A_{BR} F_{tux} \quad (K_{BR} = .90)$$

$$= [(.90)(.625)(240000)]2$$

$$P_{BRU} = 261000 \text{ lbs}$$

$$MS = \frac{261000}{246563} - 1 = .06$$

Tension in Sect. ① - ①:

$$A = \frac{3.14}{4} (1.50^2) = 1.77 \text{ in.}^2$$

$$P = 246563 \text{ lbs}$$

$$f_t = \frac{246563}{1.77} = 139500 \text{ PSI}$$

$$MS = \frac{240000}{139500} - 1 = .72$$

Tension in Sect. ② - ②:

$$A = \frac{3.14}{4} (1.16^2) = 1.06 \text{ in.}^2$$

$$f_t = \frac{246563}{1.06} = 232000 \text{ PSI}$$

$$MS = \frac{240000}{232000} - 1 = +.08$$

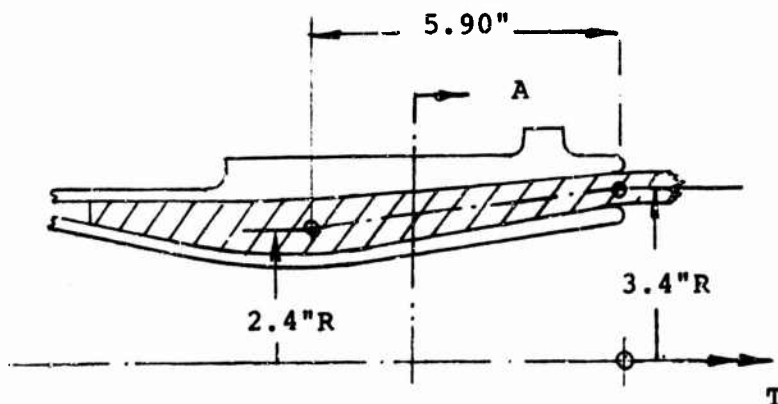
5.3.7 Blade Root Torsion Reaction

The torque resisting capability of the blade retention fitting can be accomplished by the combined or separate actions of the following restraining elements:

- a. Spline embedded in the spar (primary source)
- b. Bond
- c. Friction due to radial pressure

Each of the above have been analyzed separately for the fatigue and ultimate loading arising from hover flight with cyclic control.

Torque Resisting Capability:



Loads - Hover Condition:

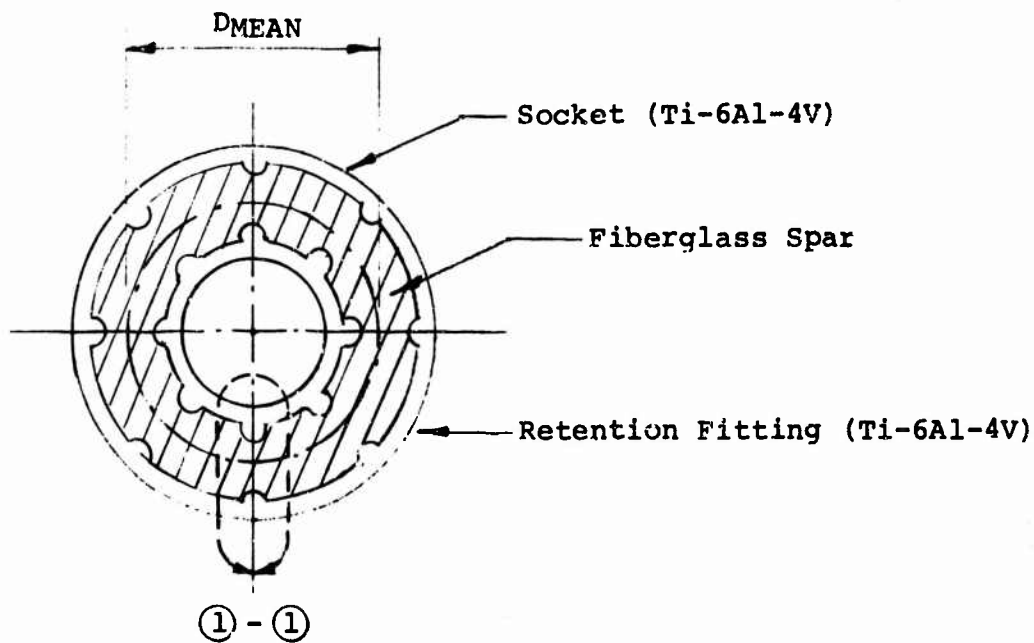
Fatigue Loads (3.54° Cyclic Input)

$$M_y = 21290 \pm 42645 \text{ in-lbs}$$

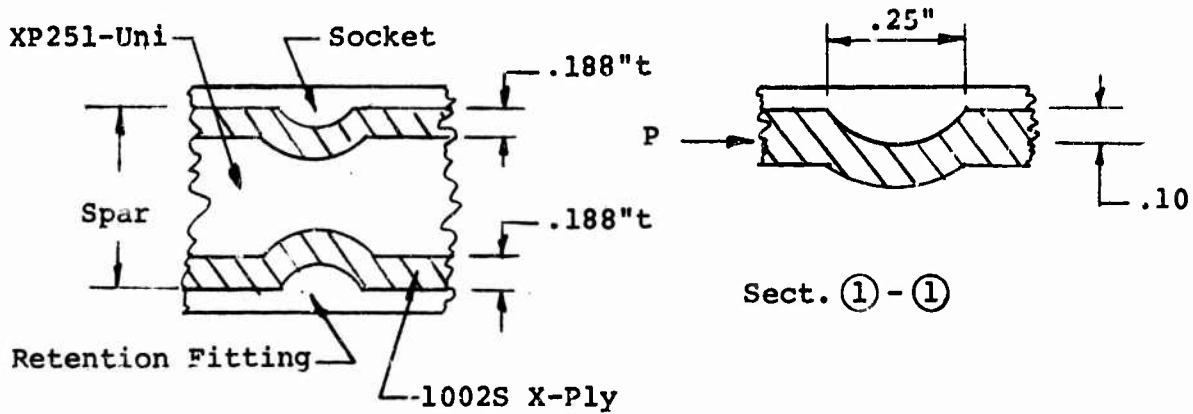
Ultimate Loads (Max. Cyclic Cond.)

$$M_y = 245161 \text{ in-lbs}$$

Torque Reactions - Spline Action:



Section A - A



$$P = \frac{T}{16 D_{MEAN}} = \frac{T}{16(2)(2.9)}$$

$$P = .0108 T$$

$$f_c = \frac{P}{A} = \frac{.0108T}{.10(5.90)}$$

$$f_c = .0183 T$$

Fatigue Analysis:

$$M_Y = 21290 \pm 42645 \text{ in-lbs}$$

$$f_c = .0183 (21290 \pm 42645) = 390 \pm 780 \text{ PSI}$$

$$R = .10; F_{EL} = 1750 \text{ PSI}$$

$$MS = \frac{1750}{780} - 1 = 1.25$$

Ultimate Analysis:

$$T = 245161 \text{ in-lbs}$$

$$f_c = .0108 (245161) = 2650 \text{ PSI}$$

$$F_{cu} = 3500 \text{ PSI}$$

MS = Ample

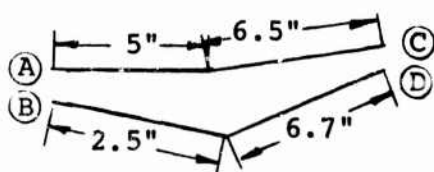
NOTE: Shear in titanium spline is adequate by inspection

Torque Resisted by Bond and Frictional Force:

The above analysis considers torque restraint by mechanical action without the contributions due to bond and frictional force. These will now be considered separately:

Bond Capability:

Bond Area:



$$A = 2\pi [5R_A + 2.5R_B + 6.5R_C + 6.7R_D]$$

$$= 6.28 [5(3.2) + 5.2(2.1) + 6.5(3.6) + 6.7(2.3)]$$

Bond Strength:

$$A = 4.5 \text{ in}^2$$

$$F_{SU} = 2920 \text{ PSI (ult.)}$$

$$R_{MEAN} = 1/4 [3.2 + 2.1 + 3.6 + 2.3]$$

$$F_{SEL} = .10 (2920) = 292 \text{ PSI}$$

$$R_{MEAN} = 2.8"$$

$$q = \frac{T}{2A} = \frac{T}{2(\pi)(R_{\text{MEAN}})^2} = \frac{T}{6.28(2.8)^2}$$

$$q = .0203 T$$

$$\tau = \frac{q}{\text{Leq}} \text{ where } \text{Leq} = \frac{A_{\text{BOND}}}{2\pi R_{\text{MEAN}}} = \frac{415}{6.28(2.8)}$$

$$\text{Leq} = 23.6''$$

$$\tau = \frac{.0203T}{23.6}$$

$$\tau = .00086T$$

Fatigue Analysis:

$$\tau = .00086 (21290 \pm 42645)$$

$$= 18 \pm 36 \text{ PSI}$$

$$\text{MS} = \frac{292}{36} - 1 = \text{Ample}$$

Ultimate Analysis:

$$\tau = .00086 (245161)$$

$$= 210 \text{ PSI}$$

$$\text{MS} = \frac{2920}{210} - 1 = \text{Ample}$$

Torque Capability - Spline Action:

Fatigue Loading:

$$F_{EL} = \pm 1750 \text{ PSI}$$

$$T = \frac{F_c}{.0183} = \frac{\pm 1750}{.0183}$$

$$T = \pm 95500 \text{ in-lbs}$$

Ultimate Loading:

$$F_{cu} = 35000 \text{ PSI}$$

$$T = \frac{35000 (95500)}{1750}$$

$$T = 1910000 \text{ in-lbs}$$

Bond Action:

Fatigue Loading:

$$F_{SEL} = \pm 292 \text{ PSI}$$

$$T = \frac{292}{.00086} = \pm 340000 \text{ in-lbs}$$

Ultimate Loading:

$$T = \frac{2920 (340000)}{.292}$$

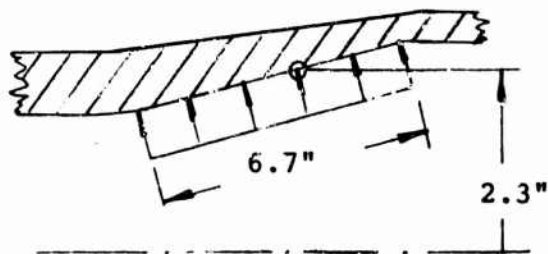
$$T = 3400000 \text{ in-lbs}$$

Friction Capability:

Hoop Pressure:

$$P_i = 2070 \text{ PSI} \\ \text{(Fatigue)}$$

$$P_i = 4820 \text{ PSI} \\ \text{(Ultimate)}$$



Allowable Torque T_o :

$$T_o = 2A q L \quad \text{where } q = \mu P \quad (\mu = .20)$$

$$= 2(\pi)(2.3)^2 (6.7)(.20)P_i$$

$$T_o = 45 P_i$$

Fatigue Analysis:

$$T_o = 45 (2070) = 93000 \text{ in-lbs (allowable)}$$

$$T = 21290 + 42645 \text{ in-lbs}$$

$$MS = 1.19$$

Ultimate Analysis:

$$T_o = 45 (4820) = 216000 \text{ in-lbs}$$

$$T = 245161 \text{ in-lbs}$$

$$MS = \frac{216}{245} - 1 = -.12$$

5.4 STRESS ANALYSIS OF THE HUB ASSEMBLY

5.4.1 Introduction

These structural analyses have been performed to determine the size of the pitch change bearings, hub mounting bolts and flange, hub spider fitting and the blade retention pin and lugs.

5.4.2 Pitch Change Bearing Analysis

The fatigue and ultimate analyses of the pitch change bearing are performed by the Bearing Manufacturer Association methods.

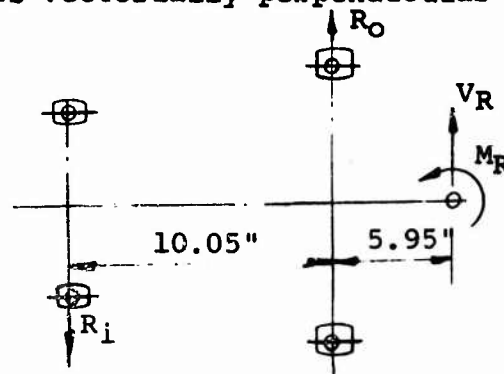
Bearing Reactions

It is conservatively assumed that V_R is vectorially perpendicular to M_R .

$$R_O = \frac{16 V_R + M_R}{10.05}$$

$$R_O = 1.59 V_R + .0995 M_R$$

$$R_i = R_O - V_R$$



Fatigue Loading for Hover Condition (3,54° Cyclic)

$$V_R = 10787 \pm 7112 \text{ Lbs.}$$

$$M_R = 581191 \pm 410624 \text{ In.-Lbs.}$$

$$R_O = 1.59 (10787 \pm 7112) + .0995 (581191 \pm 410624)$$

$$R_O = 74900 \pm 52100 \text{ Lbs.}$$

$$R_i = (74900 \pm 52100) - (10787 \pm 7112)$$

$$R_i = 64113 \pm 44988 \text{ Lbs.}$$

Fatigue Loading for Cruise Condition

$$V_R = 6250 \text{ Lbs.}$$

$$M_R = 487500 \text{ In.-Lbs.}$$

$$R_O = 1.59 (6250) + .0995 (487500)$$

$$R_O = 58440 \text{ Lbs.}$$

$$R_i = 58440 - 6250$$

$$R_i = 52190 \text{ Lbs.}$$

Ultimate Loading

$$V_R = 51890 \text{ Lbs.}$$

$$M_R = 2941754 \text{ In.-Lbs.}$$

$$R_O = 1.59 (51890) + .0995 (2941754)$$

$$R_O = 375700 \text{ Lbs.}$$

$$R_i = 375700 - 51890$$

$$R_i = 323810 \text{ Lbs.}$$

Equivalent Dynamic Loads

$$F_m = (F_{m1n1}^3 + F_{m2n2}^3 + F_{m3n3}^3)^{1/3}$$

F_1 = constant load in radial direction

F_2 = rotating load

F_3 = radial load varying sinusoidally

Outboard Bearing Analysis for Hover Condition

$$F_1 = 74900 \text{ Lbs.}$$

$$R_O = 74900 \pm 52100 \text{ Lbs.}$$

$$F_2 = 0$$

$$F_3 = 52100 \text{ Lbs.}$$

$$\frac{F_2}{F_2 + F_3} = 0 \text{ and } \frac{F_1}{F_1 + F_2 + F_3} = \frac{74900}{74900 + 52100} = .59$$

$$f_m = .70 \quad F_m = .70 (74900 + 52100)$$

$$F_m = 89750 \text{ Lbs.}$$

Inboard Bearing Analysis for Hover Condition:

$$F_1 = 64113 \text{ Lbs.}$$

$$R_i = 64113 + 44988 \text{ Lbs.}$$

$$F_2 = 0$$

$$F_3 = 44988 \text{ Lbs.}$$

$$\frac{F_2}{F_2 + F_3} = 0 \text{ and } \frac{F_1}{F_1 + F_2 + F_3} = \frac{64113}{64113 + 44988} = .60 \therefore f_m = .71$$

$$F_m = .71 (64113 + 44988) = 77000 \text{ Lbs.}$$

Mean Cubic Load for Outboard Bearings:

$$P_1 = \underline{89750 \text{ Lbs.}} \text{ and } N_1 = \underline{295 \text{ rpm}} \text{ and } t_1 = \underline{.20}$$

$$P_2 = \underline{58440 \text{ Lbs.}} \text{ and } N_2 = \underline{207 \text{ rpm}} \text{ and } t_2 = \underline{.80}$$

$$P_m = \left[\frac{(89750)^3 (.20) (295) + (58440)^3 (.80) (207)}{.20 (295) + .80 (207)} \right]^{1/3}$$

$$P_m = \underline{69600 \text{ Lbs.}}$$

Mean Cubic Load for Inboard Bearings:

$$P_1 = \underline{77000 \text{ Lbs.}} \text{ and } N_1 = \underline{295 \text{ rpm}} \text{ and } t_1 = \underline{.20}$$

$$P_2 = \underline{52190 \text{ Lbs.}} \text{ and } N_2 = \underline{207 \text{ rpm}} \text{ and } t_2 = \underline{.80}$$

$$P_m = \left[\frac{(77000)^3 (.20) (295) + (52190)^3 (.80) (207)}{.20 (295) + .80 (207)} \right]^{1/3}$$

$$P_m = \underline{60800 \text{ Lbs.}}$$

$$D_m = \frac{D_o + D_i}{2}$$

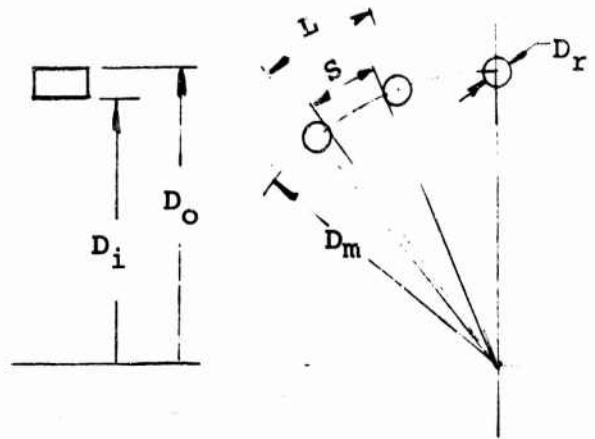
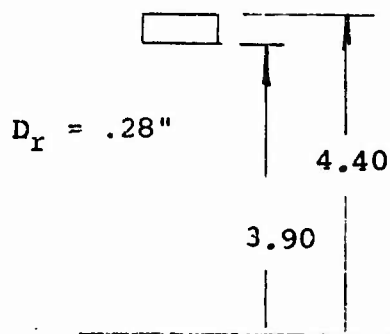
$$C_m = D_m$$

$$S = \frac{.20 C_m}{N} \quad (\text{for preliminary design})$$

$$L = \frac{C_m}{N}$$

$$D_n = L - S = .80 \frac{C_m}{N}$$

Inboard Bearing



N = Number of Rollers.

$$D_m = \frac{7.80 + 8.80}{2}$$

$$D_m = 8.30"$$

$$C_m = \pi D_m = 3.14 (8.3)$$

$$C_m = 26.10"$$

$$N = \frac{.80 C_m}{D_n} = \frac{.80 (26.10)}{.28} = 75$$

$$1 \quad C_{\text{Static}} = 12000 I_p (N-3) = 12000 (2.5) (.28) (75-3) = 605000$$

$$2 \quad C_{\text{osc}} = .354 \text{ Static} = .354 (605000) = 214000$$

$$3 \quad a = 1.00 \quad (60 \text{ Rockwell "c" scale})$$

$$4 \quad b = 1.00 \quad (\text{Race Rotation Factor})$$

$$5 \quad c = 1.50 \quad (\text{Variable with Light Shock})$$

$$6 \quad d = 1.00 \quad (\text{Established Design Practice})$$

$$7 \quad \frac{c^1}{p^1} = \frac{c (a) (b)}{p (c) (d)} = \frac{609000 (1.00) (1.00)}{p (1.5) (1.00)} = \frac{402500}{p} \quad (\text{Static})$$

$$8 \quad \frac{c^1}{p^1} = \frac{214000}{605000} (402500) = \frac{143000}{p} \quad (\text{osc})$$

$$9 \varphi_{cr} = B (1 + D_L/D_O)$$

$$B = \frac{i_i}{D_m} (360) = \frac{(26.10/75) (360)}{3.14 (8.30) (57.3)} = .084 \text{ rad}$$

$$\varphi_{ca} = .084 (1 + \frac{7.80}{8.80}) = .158 \text{ rad}$$

$$10 \text{ OAR} = \varphi_{\text{actual}} / \varphi_{ca}$$

$$\varphi_{\text{actual}} = 3.48/57.3 = .0607$$

$$\text{OAR} = .0607 / .158$$

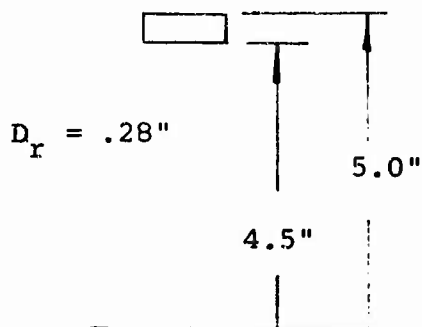
$$\text{OAR} = .384$$

$$11 \text{ Equivalent speed} = \text{operating rpm}$$

$$\Omega = 295 \text{ rpm}$$

$$12 \text{ } 10 = \frac{(214000 / 60800)^{10/3}}{295 (60)} \times 10^6 = 3750 \text{ hours}$$

Outboard Bearing



$$D_m = \frac{9.0 + 10.0}{2}$$

$$D_m = 9.50 \text{ in.}$$

$$C_m = \pi D_m = 3.14 (9.50)$$

$$C_m = 29.80$$

$$N = \frac{.80 C_m}{D_n} = \frac{.80 (29.80)}{.28}$$

$$N = 85$$

$$1 \text{ } C_{\text{static}} = 12000 (2.5) (.28) (85-3)$$

$$C_{\text{static}} = 687000$$

$$2 \text{ } C_{\text{osc}} = .354 (687000)$$

$$C_{\text{osc}} = 243000$$

3 $a = 1.00$ (60 Rockwell "c" scale)

4 $b = 1.00$ (Race Rotation Factor)

5 $c = 1.50$ (Variable with Light Shock)

6 $d = 1.00$ (Established Design Practice)

7 $\frac{c^1}{p^1} = \frac{687000}{605000} = (402500)$

$$\frac{c^1}{p^1} = \frac{457000}{p}$$

8 $\frac{c^1}{p^1} (\text{Cos } c) = \frac{243000}{687000} = \frac{162000}{p}$

9 $B = \frac{(29.80/85) (360)}{3.14 (9.50) (57.3)} = .0738 \text{ rad}$

$$\varphi_{cr} = .0738 (1 + 9/10) = .14 \text{ rad}$$

10 $\text{OAR} = .0607/.14$

$$\text{OAR} = .433$$

11 $\Omega = 295 \text{ rpm}$

12 $L_{10} = \frac{(243000/69600)^{10/3} \times 10^6}{295 (60)}$

$$L_{10} = 3650 \text{ hours}$$

5.4.3 Hub Mounting to Transmission Ring Analysis

The hub is mounted to the transmission ring by a multibolted connection. Stress analyses have been performed to determine bolt requirement and mounting flange thickness. The critical design loads are for the ultimate maximum cyclic condition.

The analysis determined the following bolt requirement:

Number of bolts = 24

Diameter = 1.0 inch

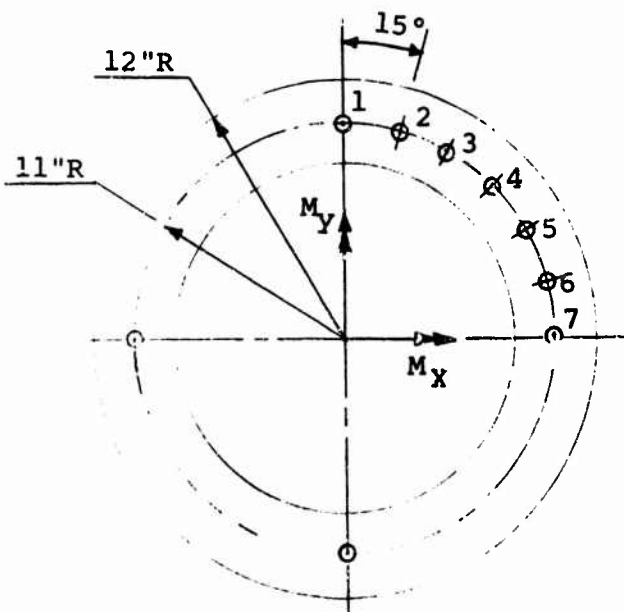
Material = steel, 125000 psi HT

Margin of Safety = .11

The required hub mounting flange thickness is calculated to be 1.0 inches. The analyses are contained in the following pages.

Hub-Transmission Interface

Bolted Joint :



Ultimate Design Loads

Max Cyclic Condition (Cyclic 11.80°)

$$F_x = 8685 (1.5) = 13077 \text{ Lbs.}$$

$$F_y = 1086 (1.5) = 1629 \text{ Lbs.}$$

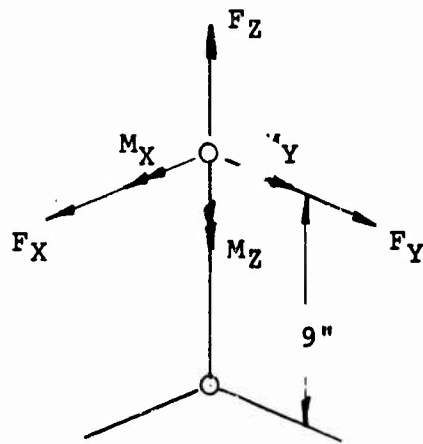
$$F_z = 34180 (1.5) = 51300 \text{ Lbs.}$$

$$M_x = 981630 (1.3) = 1472445 \text{ In.-Lbs.}$$

$$M_y = 2643436 = 3965154 \text{ In.-Lbs.}$$

$$M_z = 1136300 (1.5) = 1704450 \text{ In.-Lbs.}$$

Loads at Hub Base



Loads at Hub-Transmission Interface

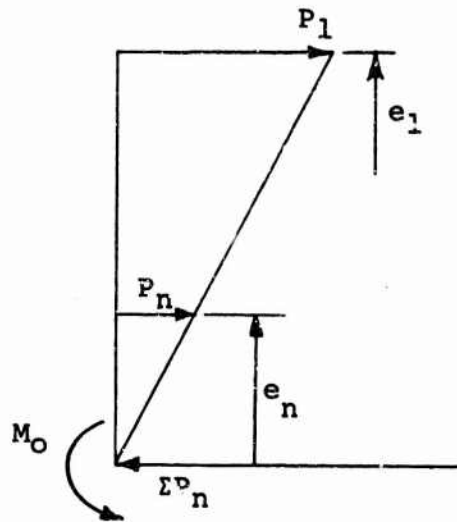
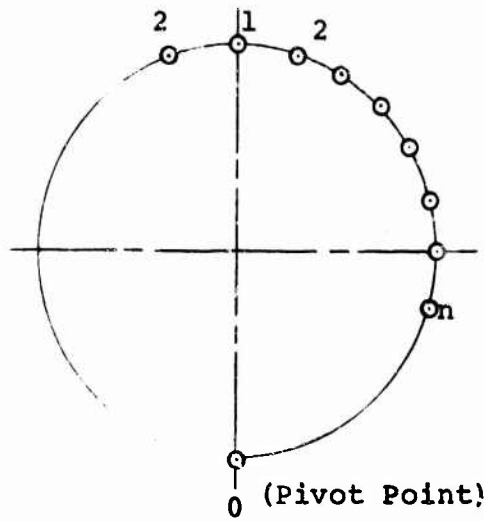
$$M'_x = M_x - 9 F_y = 1472445 - 9 (1629)$$

$$M_x = 1457784 \text{ In.-Lbs.}$$

$$M'_y = M_y + 9 F_x = 3963154 + 9 (13077)$$

$$M_y = 4082847 \text{ In.-Lbs.}$$

Bolt Loads:



$$M_o = P_1 e_1 + 2P_2 e_2 + 2P_3 e_3 + \dots + 2P_n e_n$$

where $\frac{P_1}{e_1} = \frac{P_2}{e_2} = \frac{P_3}{e_3} = \frac{P_n}{e_n}$

$$P_2 = \frac{P_1 e_2}{e_1}$$

$$P_3 = \frac{P_1 e_3}{e_1}$$

$$P_n = \frac{P_1 e_n}{e_1}$$

$$M_o = P_1 e_1 + \frac{2P_1 e_2^2}{e_1} + \frac{2P_1 e_3^2}{e_1} + \dots + \frac{2P_1 e_n^2}{e_1}$$

$$M_o = \frac{P_1}{e_1} \left[e_1^2 + 2e_2^2 + 2e_3^2 + \dots + 2e_n^2 \right]$$

	φ	$\cos \varphi$	$r \cos \varphi$	$r+r\cos \varphi$	e^2
(1)	0	1.00	11.00	22.00	484
(2)	15	.9659	10.61	21.61	466
(3)	30	.8660	9.51	20.51	421
(4)	45	.7071	7.78	18.78	351
(5)	60	.5000	5.50	16.50	272
(6)	75	.2588	2.85	13.85	192
(7)	90	0	0	11.00	121
(8)	105	-.2588	-2.85	8.15	56
(9)	120	-.5000	-5.50	5.50	30
(10)	135	-.7071	-7.78	3.22	10.3
(11)	150	-.8660	-9.51	1.49	2.2
(12)	165	-.9659	-10.61	.39	.15
(13)	180	-1.000	-11.00	0	0

Σ 2406

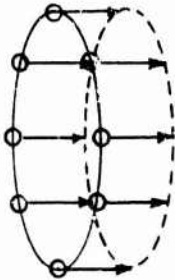
$$r = r + r \cos \varphi$$

$$r = 11 \text{ inches}$$

$$M_o = \frac{P_1}{22} [484 + 2 (2406 - 484)]$$

$$M_o = 65 P_1$$

Due to Axial Load F_3 :

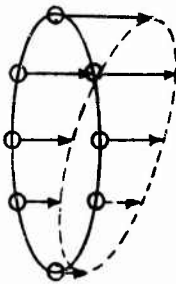


$$P_1 = P_2 = P_n$$

$$F_z = \underline{51300\#}$$

$$P_1 = P_n = \frac{51300}{24} = \underline{2140\#}$$

Due to M'_x :

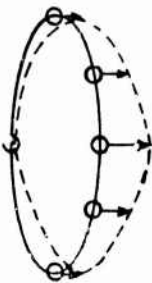


$$P_1 = \frac{M'_x}{65} = \frac{1457784}{65}$$

$$P_1 = \underline{22200\#}$$

$$P_7 = \frac{P_1}{1} \quad 7 = \frac{22200}{22} (11) = \underline{11100\#}$$

Due to M'_y :



$$P_7 = \frac{M'_y}{65} = \frac{4082847}{65}$$

$$P_7 = \underline{62800\#}$$

$$P_1 = \frac{62800(11)}{22} = \underline{31400\#}$$

Max Bolt Axial Load:

$$P_1 = 2140 + 22200 + 31400$$

$$P_1 = \underline{55740\#}$$

$$P_7 = 2140 + 62800 + 11100$$

$$P_7 = \underline{76040\#}$$

Bolt Dia = 1" (HT 125000 psi)

$$P_{ALL} = \underline{79100 \text{ lb}} \text{ (MIL-H'NDBK-5)}$$

Bolt Shears:

Due to F_x :

$$P = \frac{13077}{24} = \underline{545 \text{ lb}}$$

Due to F_y :

$$P = \frac{1629}{24} = \underline{65 \text{ lb}}$$

Due to M_z :

$$P = \frac{1704450}{(22)(12)} = \underline{6440 \text{ lb}}$$

Bolt Loading - Interface:

$$P_{\text{SHEAR}} = 545 + 65 + 6440 = \underline{7050 \text{ lb}} \text{ (conservative)}$$

Combined Loading Evaluation:

$$r_s = \frac{P_s}{P_{\text{ALL}}} = \frac{7050}{98200} = \underline{.0725}$$

$$r_t = \frac{P_t}{P_{\text{ALL}}} = \frac{76040}{79100} = \underline{.960}$$

$$MS = \frac{1}{\sqrt{r_t^2 + r_s^2}} - 1$$

$$= \frac{1}{\sqrt{(.0725)^2 + (.960)^2}} - 1$$

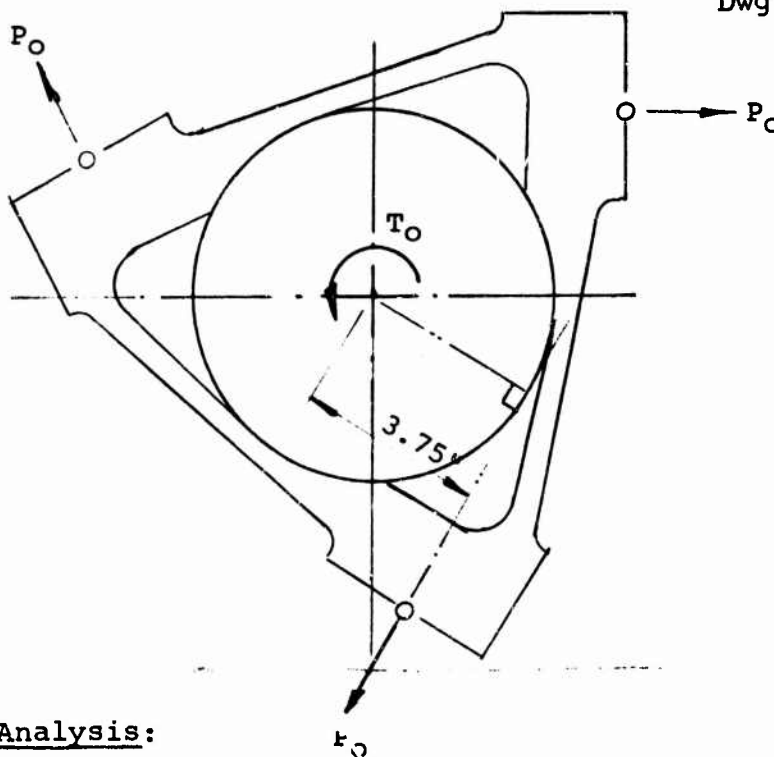
$$MS = .04$$

5.4.4 Spider Fitting Analysis

The primary structural function of the hub spider fitting is to react the blade centrifugal force and to transfer the hub offset to the hub barrel. The spider fitting material is titanium. Stress analyses are performed to determine (a) the size and number of bolts required to attach the spider to the hub barrel, (b) the spider wall thicknesses, (c) the size of the spider blade retention lugs and retention pin. The analyses are contained in the following pages.

SPIDER FITTING

Dwg. No. SK 215-10015



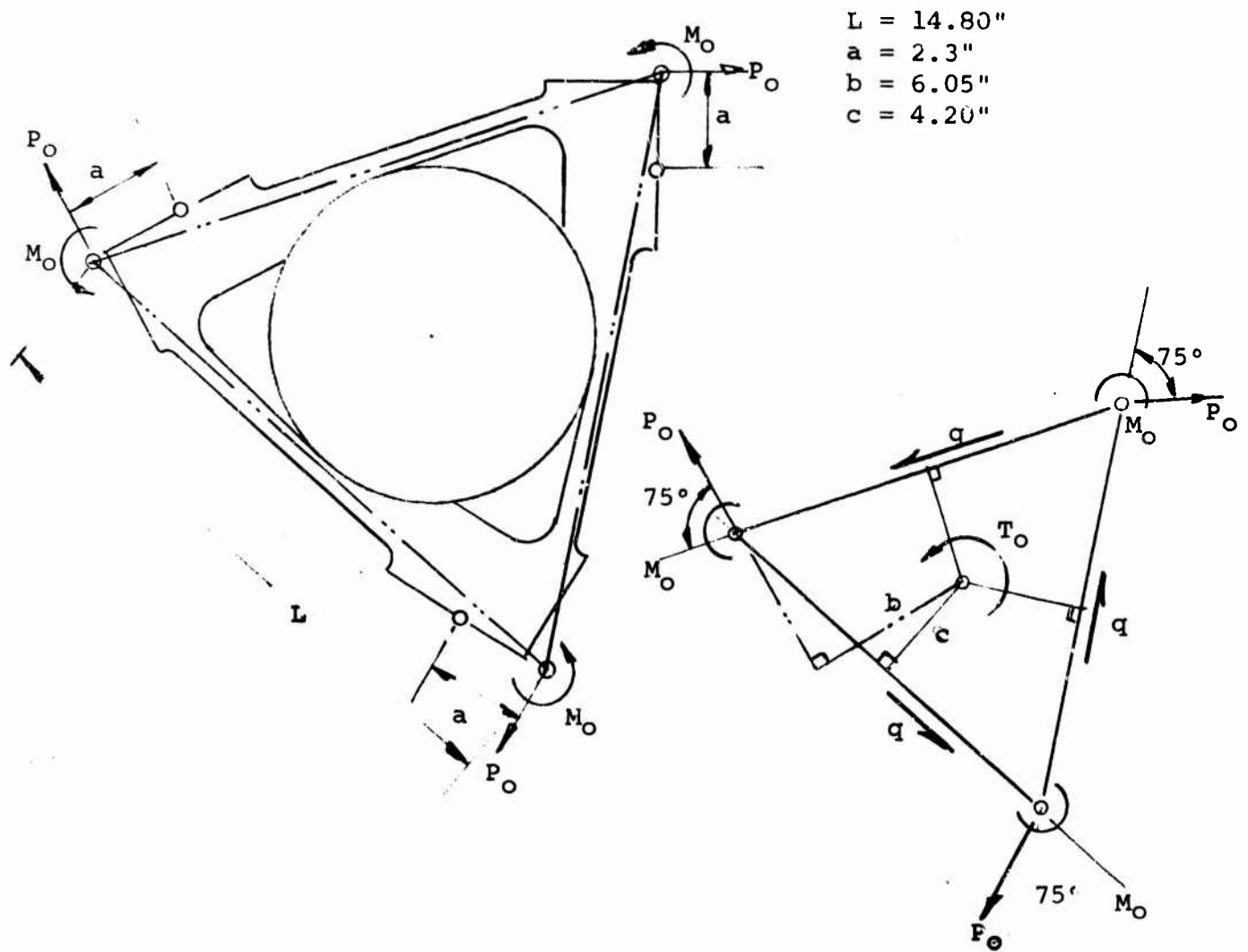
Load Analysis:

Hover Cond. (295 rpm)

$$P_0 = \underline{105200 \text{ lb}} \text{ (limit)}$$

$$P_{ult} = 105200 (1.25)^2 (1.50) = \underline{246563 \text{ lb}} \text{ (ult.)}$$

$$T_0 = 3(3.75) (246000) = \underline{2760000 \text{ in. - lb}} \text{ (ult.)}$$



$$M_o = 2.30 P_o$$

$$T_o = 3 (6.05) P_o - 3 M_o = 3 (6.05 - 2.30) P_o$$

$$T_o = 11.25 P_o$$

$$q = \frac{T_o}{3L} = \frac{11.25 P_o}{3 (14.80) (4.20)}$$

$$q = .0605 P_o$$

Shear Strength:

$$P_o = \underline{246535 \text{ lb}}$$

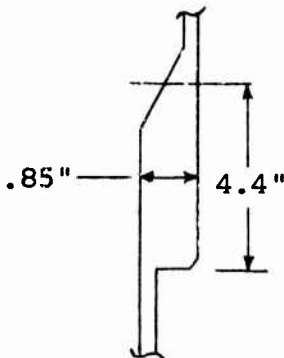
$$T_o = 11.25 (246535) = \underline{2760000 \text{ in.-lb}}$$

$$q = .0605 (246535) = \underline{14900 \text{ lb/in.}}$$

$$L = \frac{q}{t} = \underline{80000 \text{ psi}} \text{ (for Zero Margin)}$$

$$t_{\text{req'd}} = \frac{14900}{80000} = \underline{.186 \text{ in.}}$$

Axial Strength:



$$A = 4.4 (.85) = \underline{3.74 \text{ in.}^2}$$

$$P = P_o \sin 15^\circ - \frac{14.80}{2} q$$

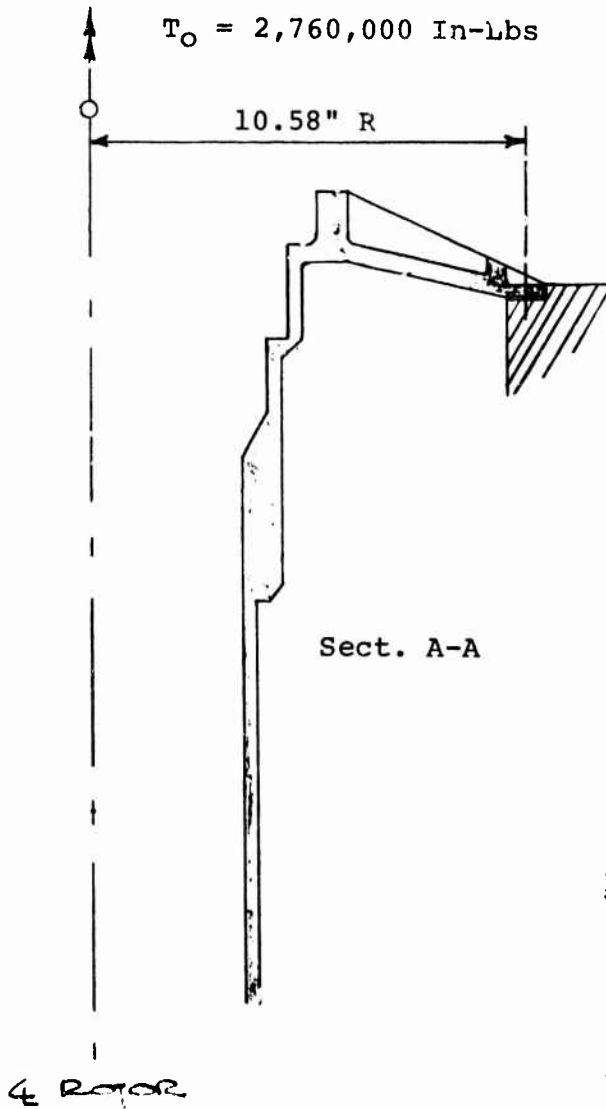
$$= 246000 (.9659) - 7.40 (14900)$$

$$P = \underline{126500 \text{ lb}}$$

$$\sigma_t = \frac{126500}{3.74} = \underline{33800 \text{ psi}}$$

Bolts in Torque Retention Plate:

$$T_o = 2,760,000 \text{ in. lb (ult.)}$$



Bolts in Shear:

$$C = 2 \quad R = 6.28 \text{ (10.58)}$$

$$C = \underline{66.5"}$$

Use 2" Bolt Spacing:

$$N = \frac{606.5}{2} = 33.25 \text{ (say 33)}$$

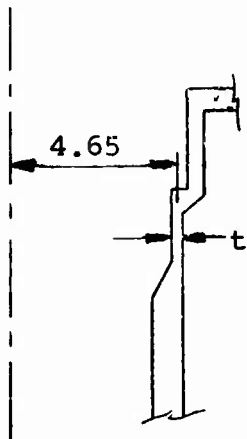
$$P_{\text{BOLT}} = \frac{2760000}{2(33)(10.58)}$$

$$P_{\text{BOLT}} = \underline{3950 \text{ lb}}$$

$$P_{\text{allow}} = \underline{6140 \text{ lb (MIL-H-5)}}$$

$$MS = \frac{6140}{3950} - 1 = \underline{.56}$$

Torsion Analysis:



$$T_o = \frac{2760000 \text{ in.lb}}{}$$

$$\tau = \frac{T_o R}{J}$$

$$J = 2 R^3 t$$

$$= \frac{T_o R}{2 R^3 t} = \frac{T_o}{2 R^2 t}$$

$$\tau = \frac{2760000}{2(3.14)(4.65)^2 t}$$

$$F_{su} = 80000 \text{ psi}$$

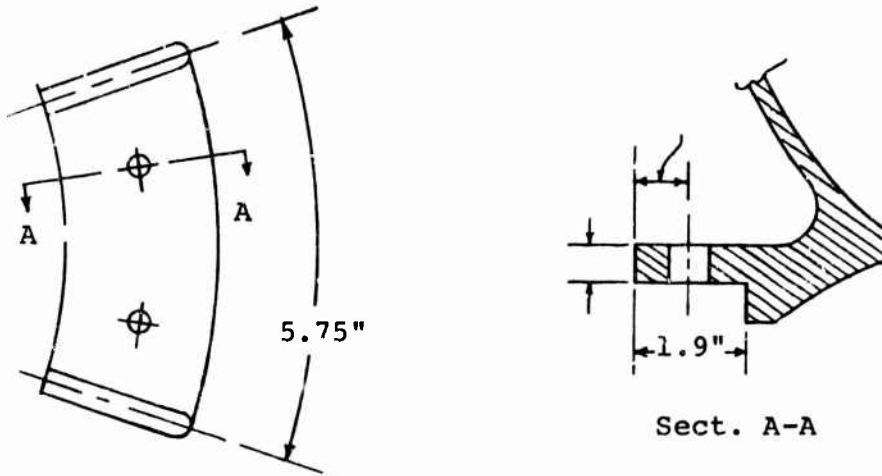
$$\tau = F_{su} = 80000 \text{ psi (for Zero Margin)}$$

Solve for t:

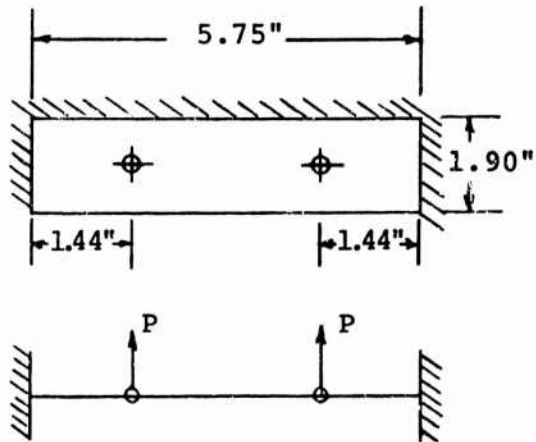
$$t = \frac{2760000}{2(3.14)(4.65)^2(80000)}$$

$$t = \underline{.253 \text{ in.}}$$

Interface - Bolted Flange:



Idealized Configuration:



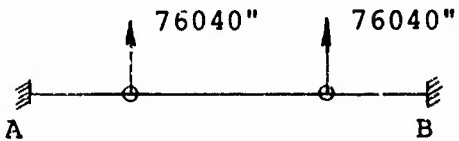
It will be conservatively assumed that the flange plate is clamped at the stiffeners only.

Interface - Bolted Flange:

$$a = \underline{1.44"}$$

$$b = \underline{2.88"}$$

$$L = \underline{5.75"}$$



$$\begin{aligned} M_A = M_B &= \frac{W}{L^2} (a^2b + ab^2) \\ &= \frac{76040}{(5.75)^2} (1.44)^2 (2.88) + (2.88)^2 (1.44) \end{aligned}$$

$$M = \underline{41000 \text{ in. lb}}$$

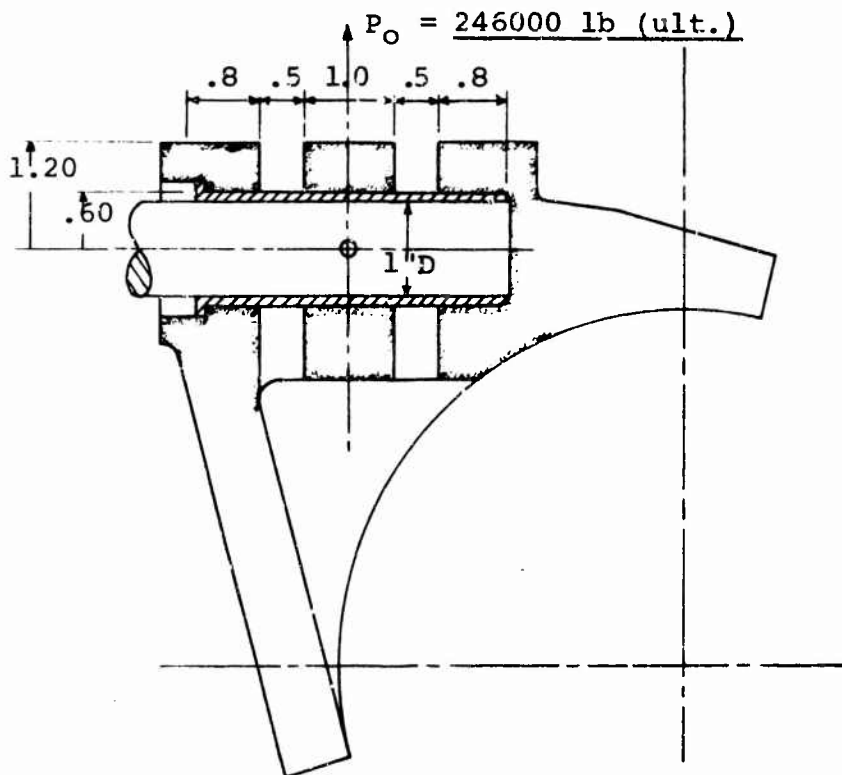
$$T_B = \frac{-6M}{bt^2} = \frac{6 (41000)}{1.9 (1.0)^2}$$

$$T_B = \underline{139000 \text{ psi}}$$

$$F_{to} = \underline{150000 \text{ psi}} \text{ (MIL - H'NBK-5) (T}_1 \text{ 6Ab - 4v)}$$

$$MS = \frac{150000}{139000} - 1 = .07$$

Blade Retention Lug: Ref. III-1 (2.3.7.6)



5 Lugs (Multi-lug Analysis)

$t' = .80$ and $t'' = .50$

= .35

Pin Shear Load = $.50P'$

$$b = \frac{.28 (t' + t'')}{2}$$

$$P'' = \frac{P}{2} \text{ and } P = .35 P' + .35 P' + P'$$

$$P' = \frac{P}{1.7}$$

$$b = .14 (.80 + .50) = \underline{.182''}$$

Evaluating:

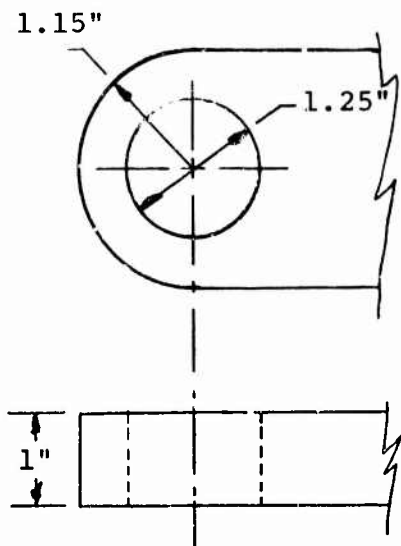
$$P = \underline{246535 \text{ lb}}$$

$$P'' = \frac{246535}{2} = \underline{123268 \text{ lb}}$$

$$P' = \frac{246535}{1.70} = \underline{145000 \text{ lb}}$$

$$\text{and } \beta P' = .35 (145000) = \underline{50500 \text{ lb}}$$

Blade Retention Lug:



Lug Analysis:

$$D = \underline{1.25} \text{ \& } a = 1.15$$

$$W = \underline{2.30}$$

$$t = \underline{1.00}$$

$$P = \underline{145000 \text{ lb}}$$

$$W, D = 2.30/1.25 = \underline{1.84}$$

$$a/D = 1.15/1.25 = \underline{.92}$$

$$D/t = 1.25/1.00 = \underline{1.25}$$

$$A_{br} = Dt = 1.25 (1.00) = \underline{1.25 \text{ in.}^2}$$

$$A_t = (W-D) t = (2.30 - 1.25) (1.00) = \underline{1.05 \text{ in.}^2}$$

Tension Across Net Section:

$$P'_{tu} = K_1 F_{tu} A_t = .97 (160000) (1.05) = \underline{163000 \text{ lb}}$$

Bearing:

$$P'_{bru} = K_{Br} A_{br} F_{tux} = .80 (160000) (1.25) = \underline{160000 \text{ lb}}$$

$$MS = (160/145) - 1 = \underline{.10}$$

Shear in Pin:

$$D = 1''$$

$$P_{\text{shear}} = .50 P' = .50 (145000) = \underline{.72500 \text{ lb}}$$

$$A = .7854 (D)^2 = .7854$$
$$= \frac{72500}{.7854} = \underline{92500 \text{ psi}}$$

for Steel $H_T = 18000_{\text{pt}}$

$$F_{\text{su}} = \underline{109000 \text{ psi}}$$

$$M_s = \frac{109000}{92500} - 1 = \underline{.18}$$

Bending in the Pin:

$$M = \frac{P'b}{2} = \frac{145000 (.182)}{2} = 1300 \text{ in. lb}$$

$$B = \frac{M_C}{I} = \frac{13000 (.50)}{.0491} = \underline{132500 \text{ psi}}$$

$$F_{\text{tu}} = 1.5 (180000) = \underline{270000 \text{ psi}}$$

(Bending Modulus of Rupture)

$$M_s = \frac{270000}{132500} - 1 = \underline{1.04}$$

5.5 ROTOR CONTROL SYSTEM STRESS ANALYSIS

The structural design of helicopter upper rotor control systems is generally controlled by fatigue loads in high speed forward flight. The present tilt rotor control system is based on this experience. It is predicted, however, that the critical fatigue design loads will be those caused by stall flutter in the hover mode. A detailed load and stress analysis of the upper rotor control system will be performed based on loads for this condition to be measured during the Phase III wind tunnel tests of the dynamic model rotor.

5.6 MATERIAL SELECTION

5.6.1 Hub Assembly

The major components of the hub assembly which include the hub barrel, spider fitting, pitch arm, blade socket and retention fitting are designed of titanium alloy 6AL-4V. The pitch housing which seats the pitch change bearings is designed of steel alloy 4340. Where high strength is required and component size is limiting, such as for the tie bar and retention pin, high strength steel is specified.

5.6.2 Rotor Controls

The control system design uses titanium alloy 6AL-4V for the stationary and rotating swashplate rings. Where high stiffness is required in the cyclic control mechanism steel alloy 4340 is used.

6. WEIGHT ANALYSIS

6.1 HUB ASSEMBLY

Similarly, to the blade, the hub target weight was high due to the procedure used in VASCOMP. Table VII-5 is a summary of the hub weight breakdown and shows the original and revised target weights.

The weights were calculated in detail from the data presented in Paragraphs 4 and 5 of this section. The basic material is titanium with steel as required. The spinner weight is for that part which is removable from the controls cover.

6.2 ROTOR CONTROLS

The weights of the upper rotor controls were calculated in detail from the data as presented in Parts 4 and 5 of this section. Table VII-6 is a summary of these weights. Rotating controls are those which rotate with the hub and include the rotating outer ring of the swashplate, blade tracking adjustment mechanism bearings, arms and balance weight. The fixed controls are those which do not rotate with the hub and include the swashplate, gimbals, links, fittings, etc. The support weight consists of the actuator support tube and its support. Three actuators, collective, pitch cyclic and lateral cyclic, are designed into one long unit which is housed inside the control actuator tube mentioned above. Lubrication includes the oil sumps, casing and oil.

TABLE VII-5
WEIGHT SUMMARY
ROTOR HUB

	ORIGINAL WEIGHT (TARGET)	REVISED TARGET WEIGHT	CURRENT DESIGN WEIGHT
Hub Housing			337
Elastomeric Bearings			63
Pitch Housing			179
Pitch Arm & Hardware			32
Hub Spider Fitting			64
Miscellaneous			45
Total Weight	1188	900	720
Spinner	100	100	96
Total Hub and Spinner/Rotor	1288	1000	816
Total Hub and Spinner/ Aircraft	2576	2000	1632

TABLE VII-6
WEIGHT SUMMARY
UPPER ROTOR CONTROLS

	TARGET	CURRENT
Rotating Controls		(185)
Outer Swashplate Ring		39
Blade Tracking Adjusting Mechanism		64
Balance Weight		5
Bearings, Etc.		77
Fixed Controls		(210)
Gimbals		33
Swashplate		40
Links, Fittings, Etc.		137
Supports		(225)
Support Tube		155
Supports		70
Actuators		536
Lubrication		65
Total Upper Controls/Rotor	1183	1221
Total Upper Controls/Aircraft	2367	2442

7. SURVIVABILITY

A survivability analysis was not a part of the basic contract but the following design features contribute to survivability:

- a. Elimination of flap and lag hinges reduces the number of critically stressed parts
- b. Hub is mounted to the transmission lug by a multi bolt connection
- c. The blade retention elastomeric bearing is loaded in compression thus failure will not result in loss of blade retention
- d. Upper control system is protected by the spinner, hub barrel and the transmission support. The spinner will tumble small calibre bullets.
- e. Secondary lubrication of pitch change bearings is adequate for return home if loss of oil due to hub barrel damage occurs
- f. Dual rotor control actuators with dual hydraulic supply are provided
- g. Backup lubrication of the swashplate is provided

8. CONCLUSIONS AND RECOMMENDATIONS

1. The basic rotor assembly design proposed for the model 215 prop/rotor aircraft is within the target weight.
2. The upper rotor control system fatigue strength must be analysed for blade stall flutter loads to be measured during the Phase III wind tunnel test of the dynamic rotor model.
3. Additional work is needed to incorporate fail safe designs and to evaluate effect on component and system weight.

SECTION VIII

SUPPORTING TECHNOLOGY

1. SUMMARY

The design study report in the prior sections of this report has included consideration of flight controls, aeroelastic stability and vibration suppression requirements. Control power requirements have a large influence on the baseline aircraft since this is an airframe design based on static strength. In this section, this design is shown to also satisfy the requirements of the other technologies.

Flight control requirements require minimal stability augmentation which can be included in the prop/rotor control feedback systems being provided for rotor loads alleviation. Considerably more effort is required to define the details of this control system but the impact of further definition on the aircraft weight and complexity will be small. Present definition of the rotor feedback control system to maintain zero rotor hub moment results in considerable rotor lift loads due to vertical gusts. This could require a stronger wing and needs further study.

Aeroelastic stability analyses show that the baseline 215 aircraft dynamic modes will be adequately damped and require no compromises from the strength design. Analysis of damaged structural configurations shows this design to be tolerant of significant damage even with the rotor control feedback system inoperative.

Requirements for vibration suppression have been evaluated for the

most critical transition flight condition. This analysis shows that the large nacelle mass acts on the wing vertical bending spring to isolate the fuselage from the rotor vibratory forces. Vibration which reaches the fuselage apparently will be small so the weight penalty associated with fuselage vibration tuning will not be required.

2. FLIGHT CONTROL REQUIREMENTS

A preliminary stability analysis and control system evaluation was performed of the Model 215 in the hover and low-speed flight regimes (helicopter mode) for the purposes of weight verification, control system definition and definition of areas requiring further analysis. Although the stability analysis shows a need for a stability augmentation system, there are no unusual flying qualities problems.

A preliminary investigation into the use of rotor controls in cruise as well as hover was favorable and needs to be continued. Savings in control system weight can result.

Further work is required to continue the control system optimization (phasing and mixing), rotor SAS system development and optimization and turbulence and gust alleviation system development.

2.1 CRITERIA

The flying qualities criteria to be applied are given in the Proposed Flying Qualities Specification (Reference VIII-1) for hovering and low-speed flight, and MIL-8785 (Reference VIII-2) for airplane mode flight. The aircraft is a Class II heavy, utility/

search and rescue or assault transport and was evaluated for category B flight phases. Considerations are given to achieve Level 1 flying qualities during normal operation and at least Level 3 for all failure modes. Additional flight control criteria based on the data of Reference VIII-3 will be used where applicable.

2.2 CONTROL SYSTEM

2.2.1 Description

Control in the helicopter mode is conventional; i.e., pitch is controlled by longitudinal cyclic, roll is obtained from differential collective and yaw control is through differential longitudinal cyclic.

In these studies, the feasibility of utilizing rotor controls throughout transition and in the cruise mode was investigated. Rotor pitch authority will be reduced as the horizontal tail effectiveness is increased with increasing speeds. In transition, differential collective rotor control must be mixed with the longitudinal cyclic pitch and yaw control to minimize coupling. In the cruise mode, differential collective is used for yaw control, longitudinal cyclic for pitch control and differential longitudinal cyclic for roll control.

The present baseline aircraft design includes conventional airplane control surfaces but it appears that these controls are not required.

2.2.2 Control Response and Power

The cockpit travels in accordance with the requirements of Reference VIII-6 for the Model 215 are as follows:

- a. Climb - +5.0 inches (collective pitch)
- b. Pitch - +7.0 inches (longitudinal cyclic pitch)
- c. Yaw - +2.5 inches (differential longitudinal cyclic)
- d. Roll - +3.2 inches (differential collective pitch)

Control sensitivity for the 215 compared with the proposed specifications (Reference VIII-1) is shown in the following table.

RESPONSE TO CONTROL INPUT IN ONE SECOND

(Degrees/Inch)

	<u>Level 1 Required</u>		Model 215
	Min.	Max.	
Pitch	3	20	3.15
Roll	4	20	4.10
Yaw	6	23	6.45

It can be seen that all of the Level 1 requirements for control sensitivity are met. Control power criteria from References VIII-1 and VIII-4 are compared with the Model 215 data on Figures VIII-1 through VIII-3. Adequate pitch and roll control power and damping are provided with the basic Model 215. Yaw damping needs to be provided by the rotor feedback system.

Response to collective pitch control is given in terms of rate of climb per inch of control deflection. Level 1 flying qualities specifies 100 ft/min. minimum and 750 ft/min. maximum for the first

DR. BY J. BENDO
(7/23/70)

EUGENE DIETZGEN CO.
MADE IN U. S. A.

NO. 340R-MP DIETZGEN GRAPH PAPER
MILLIMETER

HOVER CONTROL POWER IN PITCH

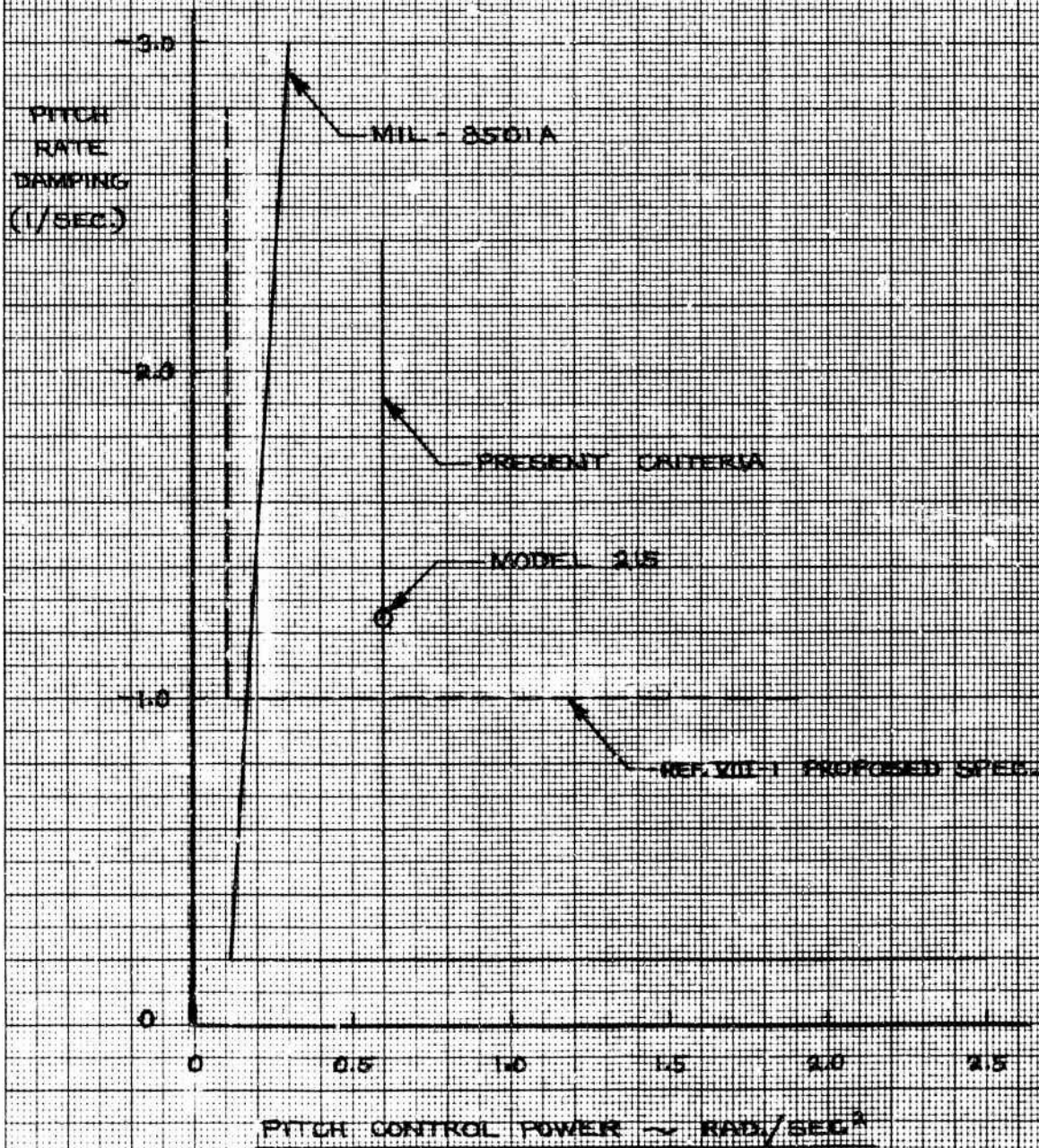


FIGURE VII-1

DR. BY J. BENDO
(7/23/70)

HOVER CONTROL POWER IN ROLL

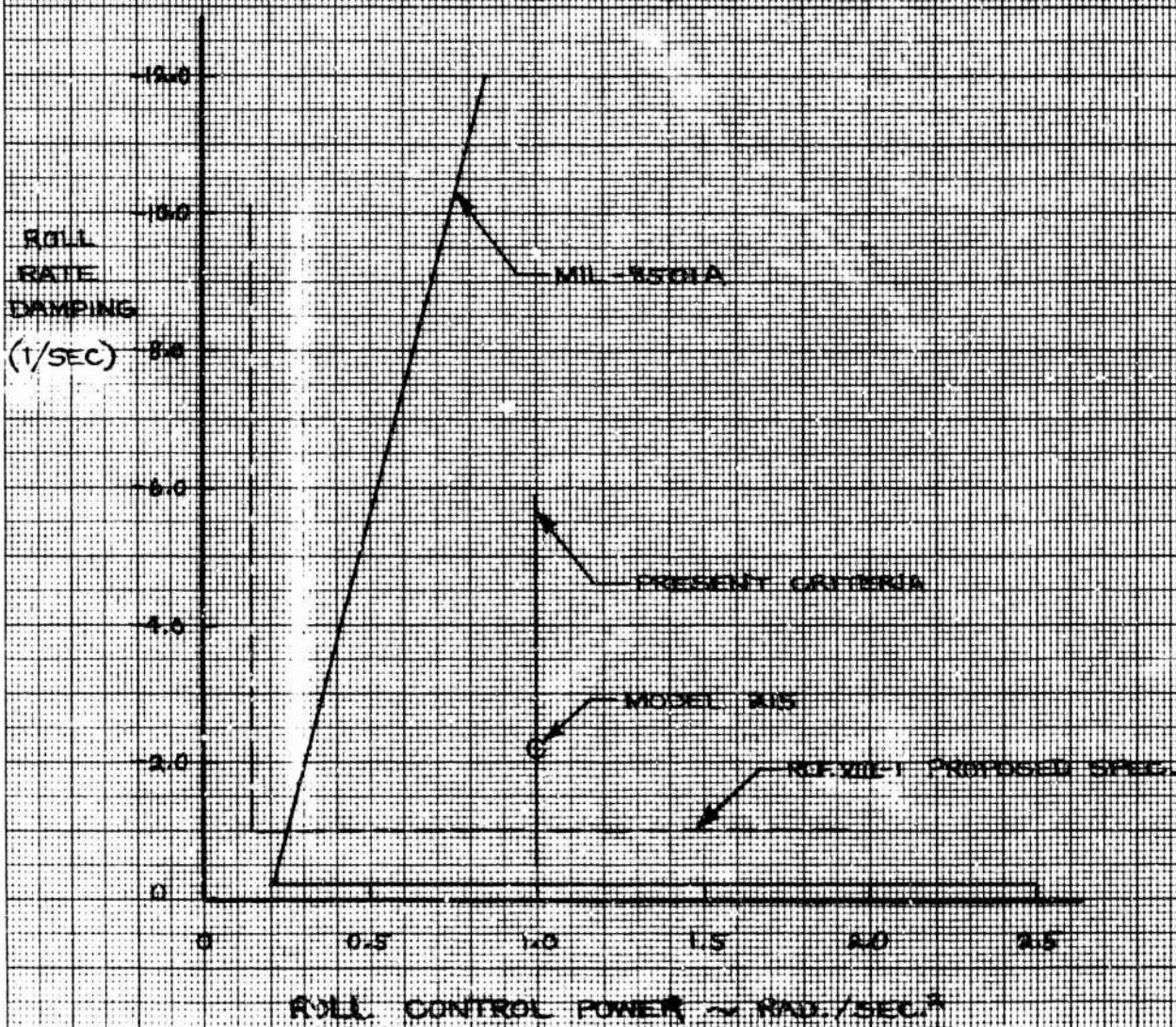


FIGURE VIII-2

DR. BY J. BENDO
(7/23/70)

EUGENE DIETZGEN CO.
MADE IN U. S. A.

ND. 340R-MP DIETZGEN GRAPH PAPER
MILLIMETER

HOVER CONTROL POWER IN YAW

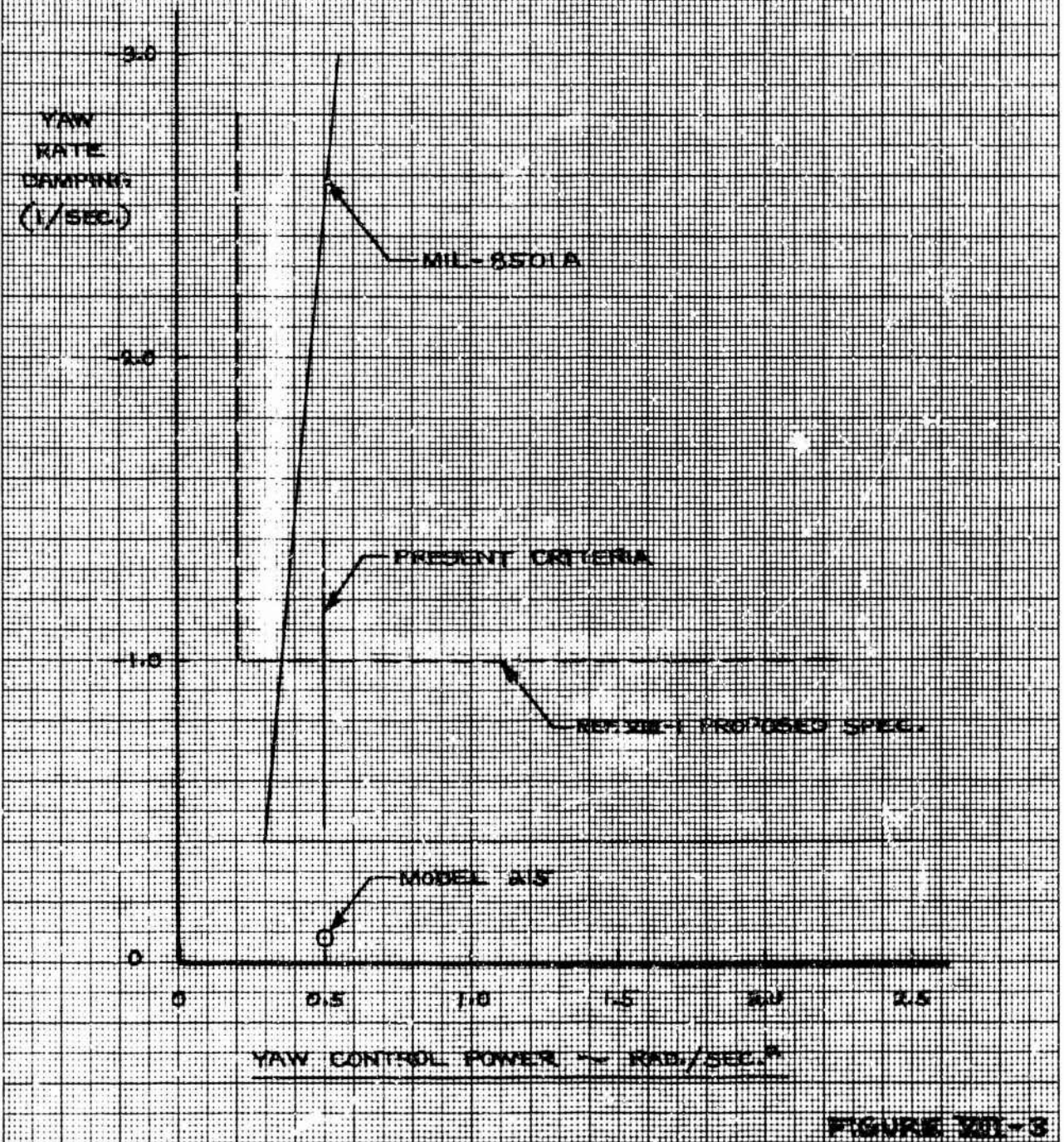


FIGURE VII-3

second. Figure VIII-4 shows response to a one-inch collective pitch input. At one second, the rate of climb is 140 ft/min. which meets the above requirements. A similar requirement from Reference VIII-3, shown in Figure VIII-5, presents collective control sensitivity in terms of pilot rating. The sensitivity of Model 215 is .075 g's/in. This gives a pilot rating of 2.0 which is close to the optimum rating.

2.3 DYNAMIC STABILITY

2.3.1 Introduction

Dynamic stability was analyzed for hovering and low-speed flight in the helicopter mode. Studies included the use of the stability and control computer program, Reference VIII-5, and an analog simulation of the rotor control system. Calculations are for sea level conditions for the unaugmented aircraft.

2.3.2 Stability Derivatives

The static and dynamic stability derivatives used in the dynamic stability analysis for low-speed flight are summarized in Table VIII-1. These derivatives are calculated using the methods in Reference VIII-5 about the trim point. The derivatives are calculated for incremental trim changes after the rotor is allowed to re-establish flapping equilibrium.

2.3.3 Results of the Stability Analysis in Hover

The longitudinal dynamic stability criteria obtained from Reference VIII-1 are shown on Figure VIII-6 in terms of the allowable motions. The roots of the Model 215 characteristic equation for

DR. BY J. BENEDIC
(7/27/70)

EUGENE DIETZGEN CO.
MADE IN U. S. A.

NO. 340R-MP DIETZGEN GRAPH PAPER
MILLIMETER

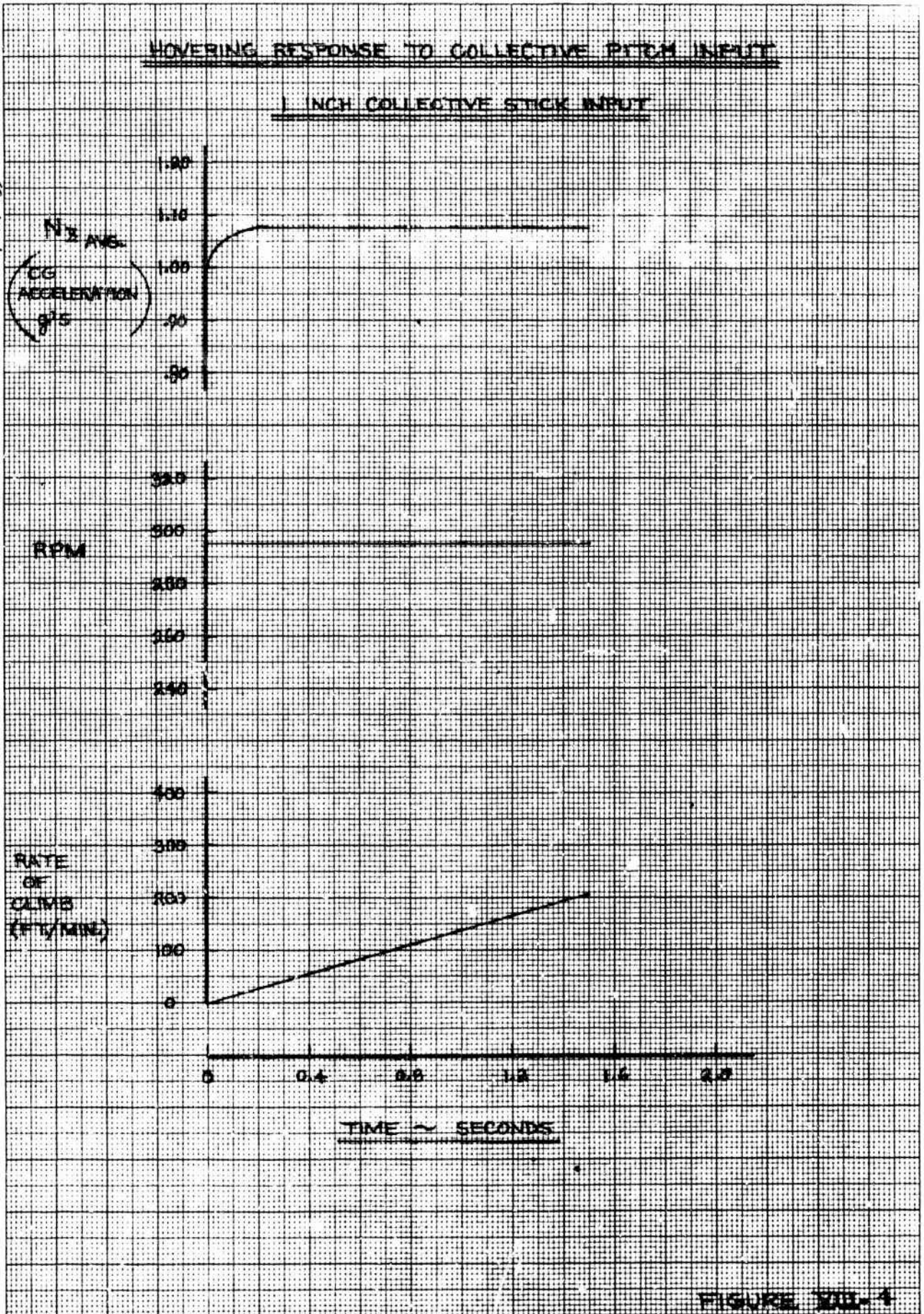


FIGURE VIII-4

DR. BY J. LENDO
(7/24/70)

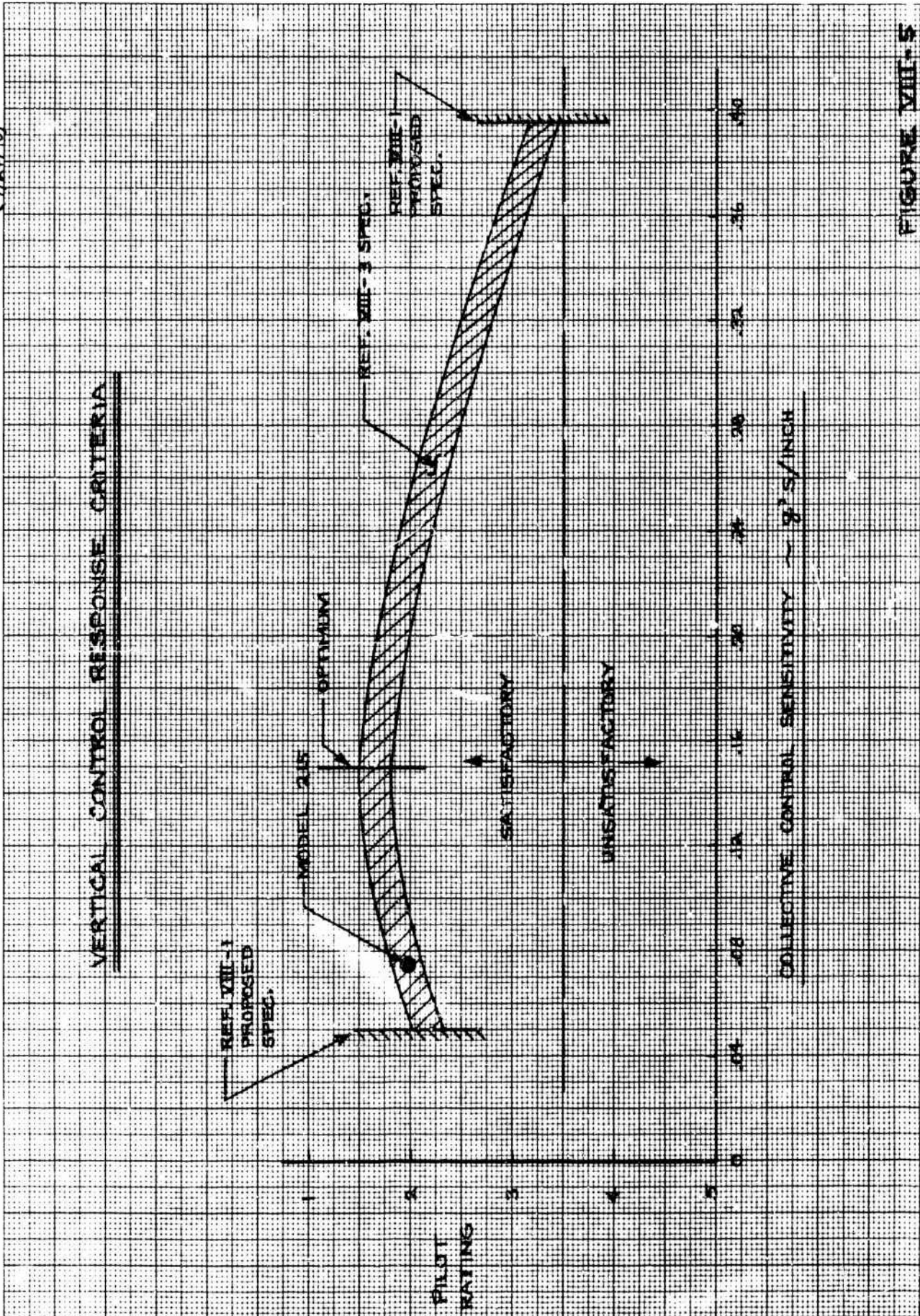


FIGURE VIII-5

DR. BY J. BENDO
(7/22/70)

HOVERING PITCH DYNAMIC STABILITY REQUIREMENTS

REF. VII-1 PROPOSED SPEC.

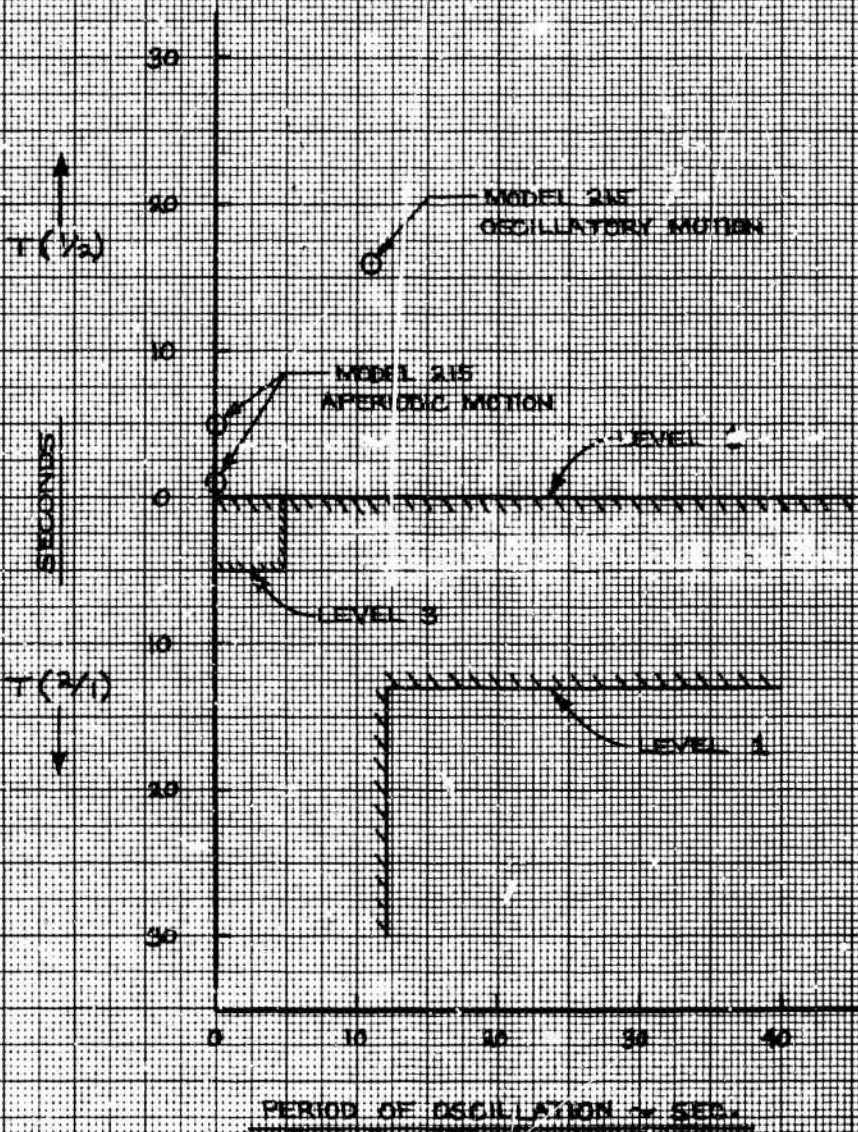


FIGURE VIII-6

EUGENE DIETZGEN CO.
MADE IN U. S. A.

NO. 340R-MP DIETZGEN GRAPH PAPER
MILLIMETER

TABLE VIII-1

STABILITY DERIVATIVES FOR MODEL 215 AIRCRAFT (1)

CG = 410.46 In., W = 67,000 Lb.
Sea Level, Low-Speed Flight

	ΔU	ΔV	ΔW	ΔP	ΔQ	ΔR
ΔX -Force/m	-.0626	.0017	-.0217	-.2263	1.091	-0.2669
ΔY -Force/m	~ 0	-.1916	~ 0	-.8048	-.0009	.7002
ΔZ -Force/m	-.0154	-.0002	-.1197	-1.3187	-2.0366	-.6849
Δ Pitch-Moment/ I_{YY}	0.0079	.0001	-.0063	-.0678	-.7489	.0029
Δ Roll-Moment/ I_{XX}	~ 0	-.0004	~ 0	-2.324	-.0001	.0896
Δ Yaw-Moment/ I_{ZZ}	~ 0	-.0003	~ 0	-.0300	~ 0	-.1039

(1) $V = 35$ kts $\alpha_N = 90^\circ$ (Nacelle Tilt) $\Omega = 295$ RPM $I_{XX} = 1.02 \times 10^6$ Slugs-Ft² (Roll Inertia) $I_{YY} = .244 \times 10^6$ Slugs-Ft² (Pitch Inertia) $I_{ZZ} = 1.1 \times 10^6$ Slugs-Ft² (Yaw Inertia)

Geometrical Data From Figure I-1

the pitch-heave motion show two aperiodic roots (heavily damped) and one oscillatory root with a period of 11 seconds. Level 1 flying qualities criteria are met.

The lateral dynamic stability criteria in hovering is shown in Figure VIII-7. The Model 215 again exhibits two heavily damped aperiodic roots and one mildly divergent mode with a period of 34 seconds. Level 1 flying qualities are also met in roll.

2.3.4 Results of Stability Analysis for Low-Speed Flight

The response requirements of Reference VIII-1 to angle of attack and pitch attitude following an abrupt pitch control input are shown in Figure VIII-8. This figure shows that the unaugmented aircraft in the helicopter mode at 50 kts has flying qualities approaching Level 1. Level 1 flying qualities is achieved by providing 8% damping by means of the rotor SAS.

The requirements for frequency, W_n , and damping ratio of the lateral-directional oscillations following a disturbance input are shown in Figure VIII-9 from Reference VIII-1. The unaugmented Model 215 meets Level 1 flying qualities.

2.4 GUST AND TURBULENCE RESPONSE

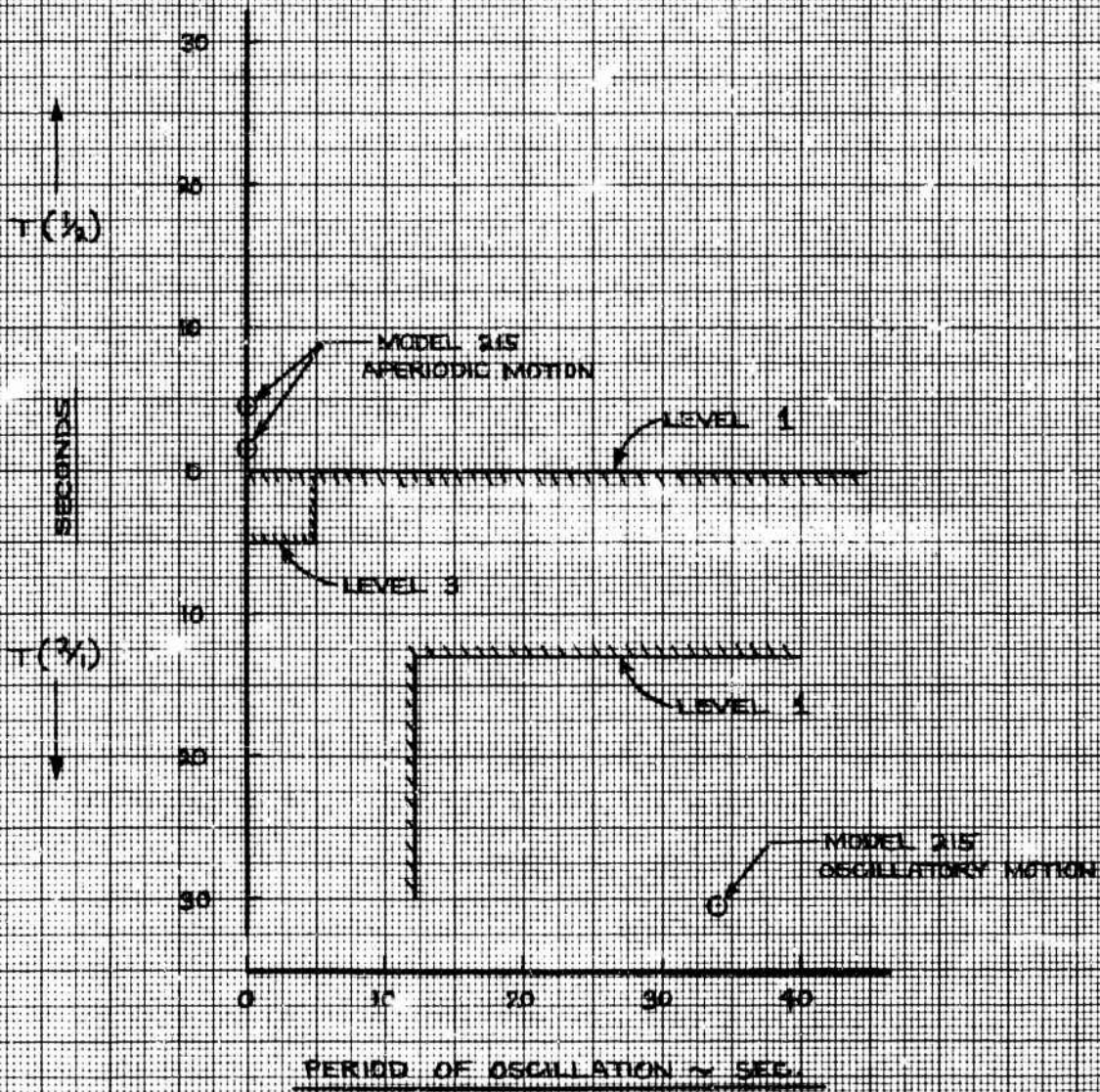
The peak angular and vertical accelerations created by sine-squared gusts at low flight speed are shown in Figure VIII-10 and VIII-11. Figure 10 shows that the level of vertical acceleration is well below the required value of 0.15.

The criteria of Reference VIII-1 state that the pilot rating shall be 3.5 for $\sigma_g = 5$ ft/sec. for a PSD gust representation. A 5 ft/sec.

DR. BY J. BENDO
(7/22/70)

HOVERING ROLL DYNAMIC STABILITY REQUIREMENTS

REF. VII-1 PROPOSED SPEC.

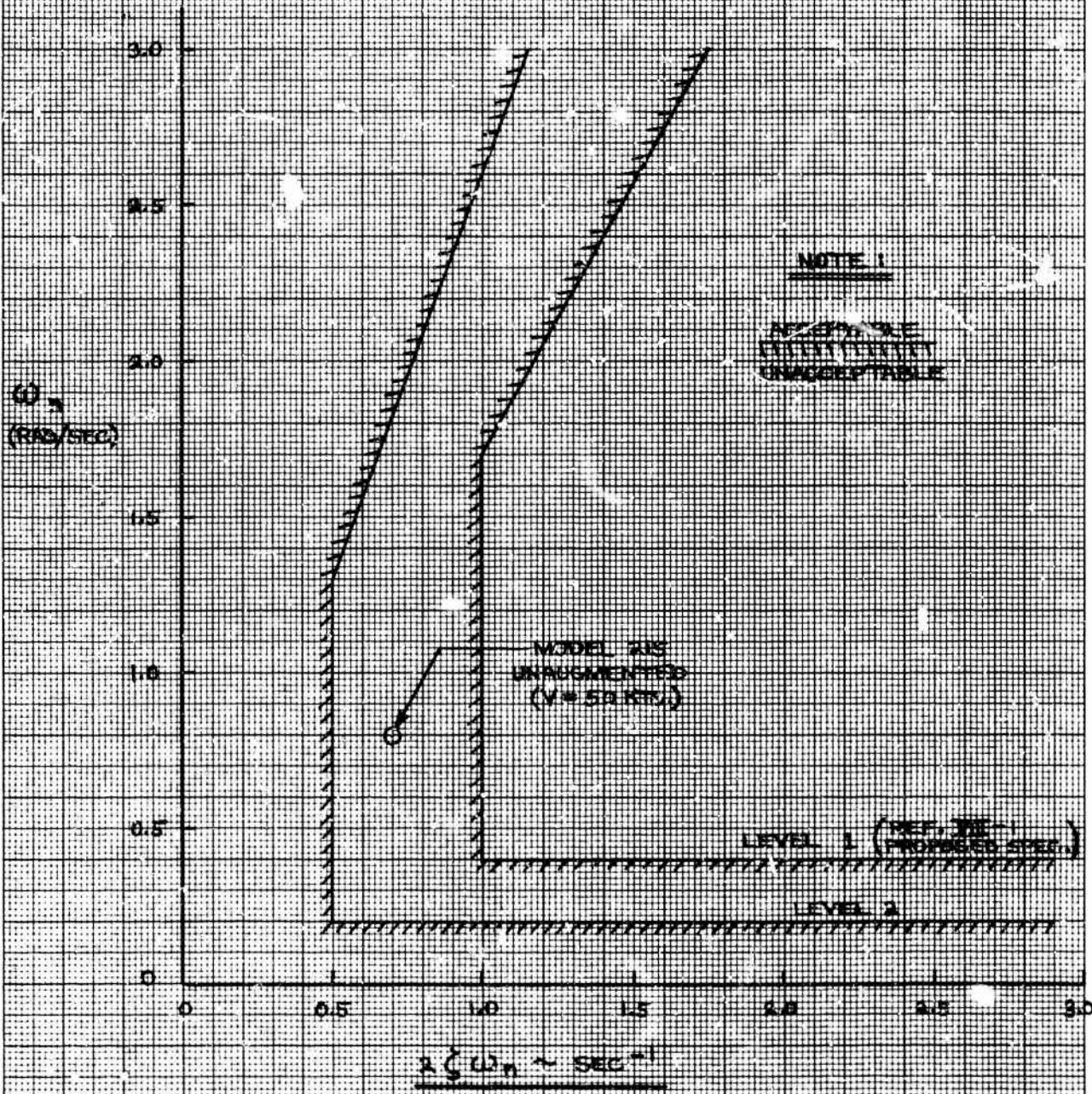


MILLIMETER

FIGURE VIII-7

DR. BY J. BENJDO
(7/22/70)

LOW SPEED FLIGHT
SHORT TERM PITCH RESPONSE REQUIREMENTS
HELICOPTER MODE



EUGENE DIETZGEN CO.
MADE IN U. S. A.

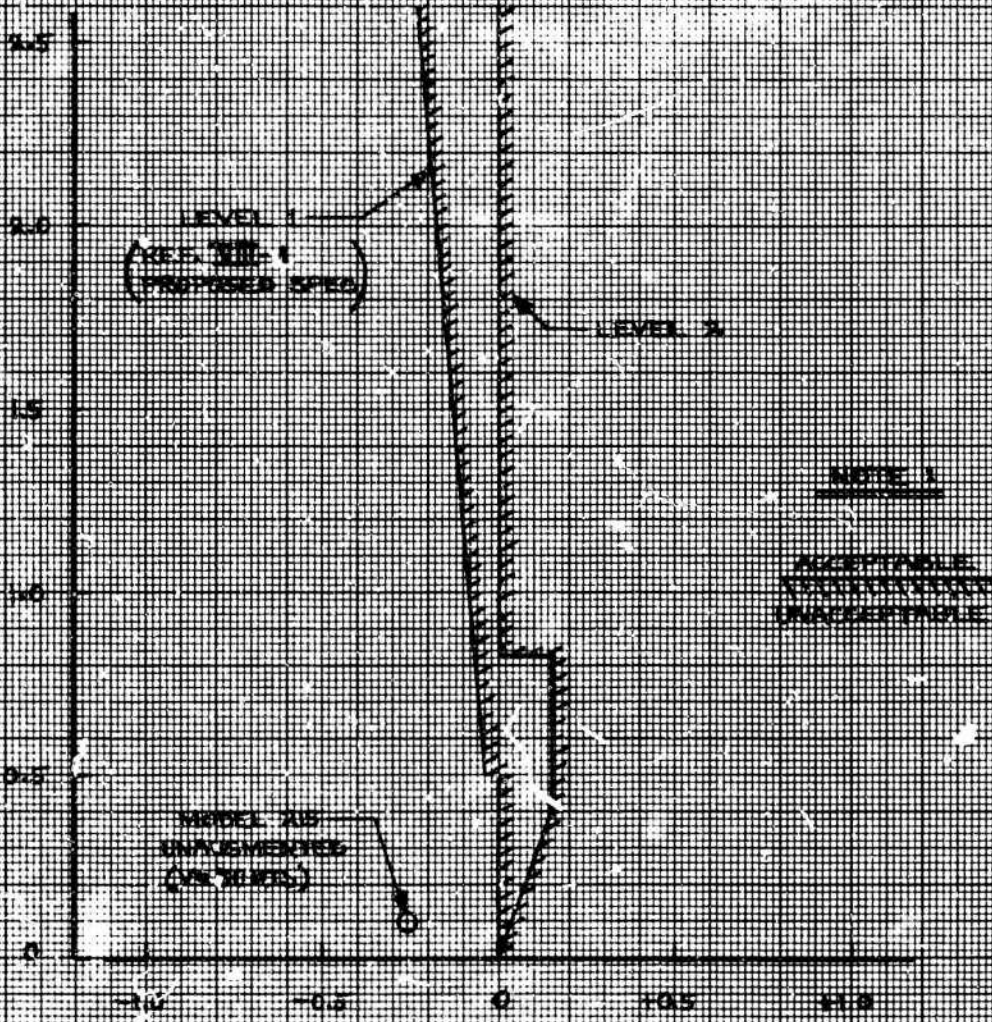
NO. 340R-MP DIETZGEN GRAPH PAPER
MILLIMETER

FIGURE XII-8

DR. BY J. BENDO
(1/22/70)

LOW SPEED FLIGHT
SHORT TERM LATERAL-DIRECTIONAL RESPONSE REQUIREMENTS
HELICOPTER MODE

$\omega_{n\psi}$



MILLIMETER

MADE IN U. S. A.

FIGURE VIII-9

DR. BY J. BENDO
(7/22/70)

EUGENE DIEZELSEN CO.
MADE IN U. S. A.

NO. 34UR-MP DIEZELSEN GRAPH PAPER
MILLIMETER

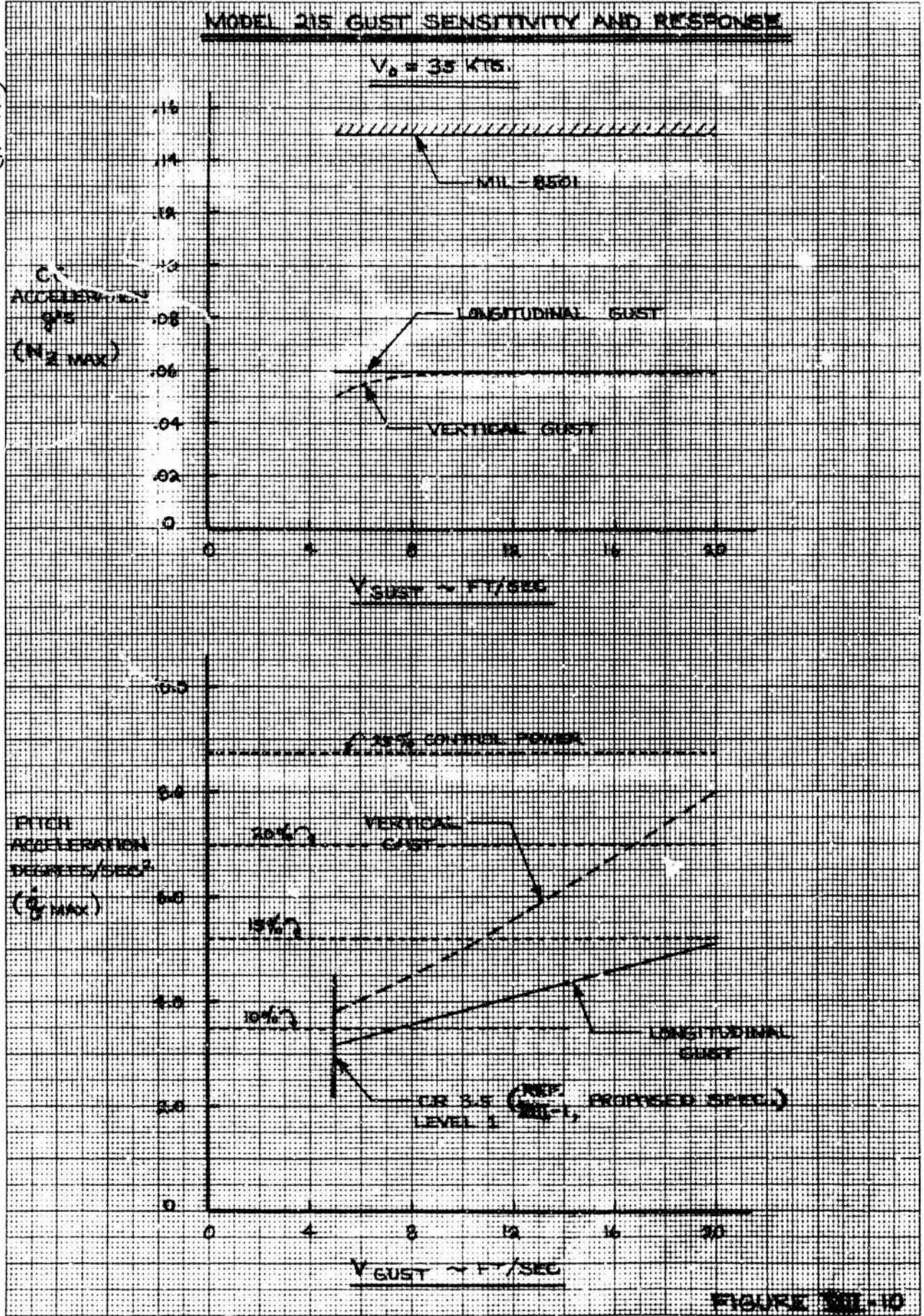


FIGURE 311-10

DR. GY. J. BEARD
(7/22/70)

MODEL 215 GUST SENSITIVITY AND RESPONSE

$V_0 = 35$ KTS.

LATERAL GUST

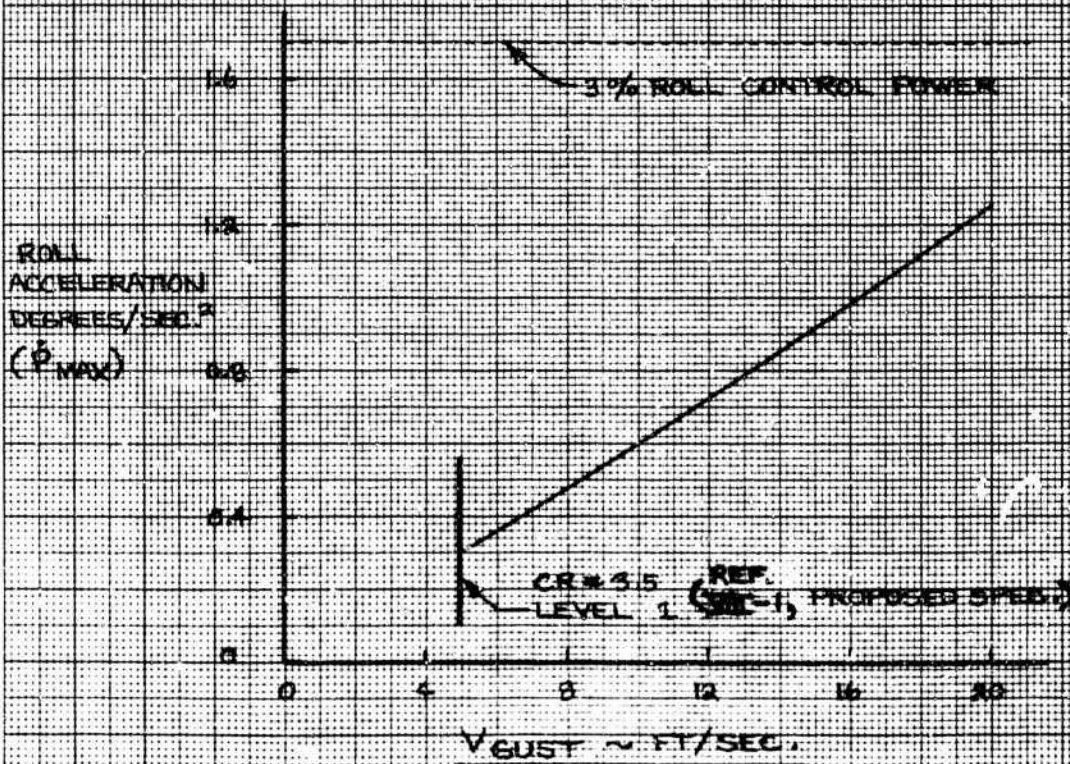
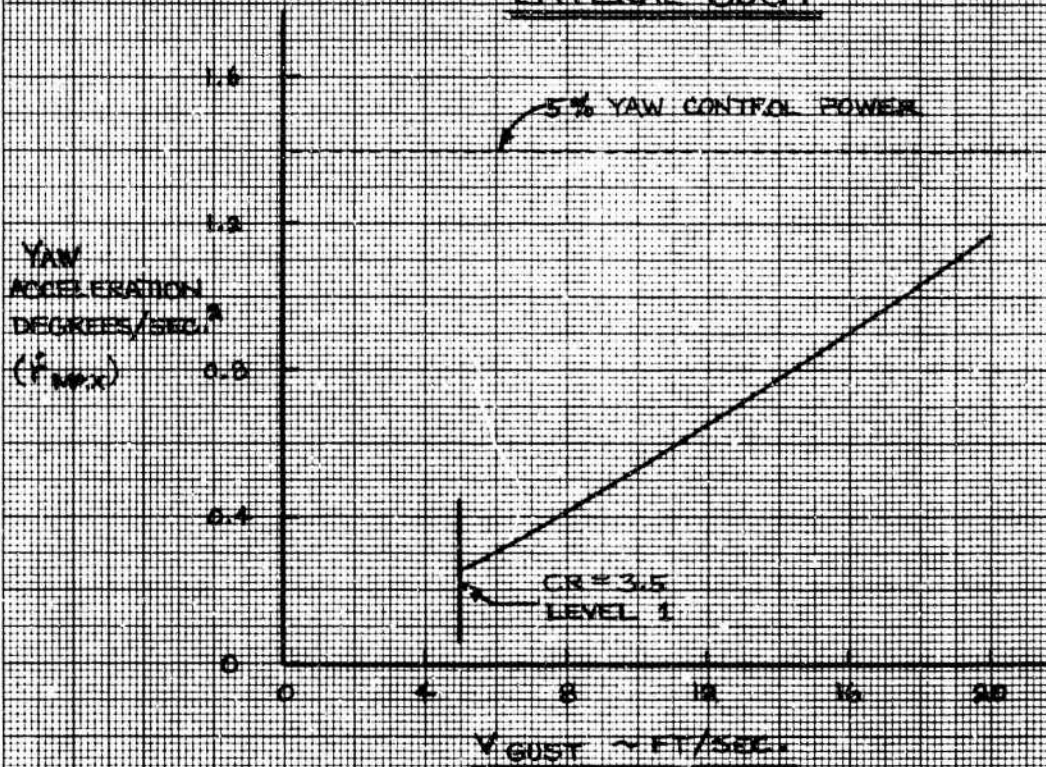


FIGURE 215-11

gust requires approximately 10% of the available control power. This can easily be obtained from the rotor feedback system. Similarly, the roll and yaw control authority required for a feedback system is approximately 5%.

Von Karman-type turbulence spectra with intensities for storm and nonstorm conditions from Reference VIII-8 were used to calculate the resulting incremental acceleration levels in the cruise mode. Longitudinal, lateral and vertical turbulence spectra were used in terms of the RMS gust velocities. For this preliminary calculation the assumption of a rigid airframe with gust velocities effecting only the rotor angle of attack was used. Incremental C.G. accelerations per unit gust velocity using the above assumptions are shown in Figure VIII-12. This analysis was extended to show the distribution of the aircraft vertical acceleration shown in Figure VIII-13. From these figures, it can be seen that the rotor has a significant contribution and can not be ignored. Further studies are required, however, to determine the attenuating effects of rotor elastic flapping and wing flexibility since these were not included in this simple analysis.

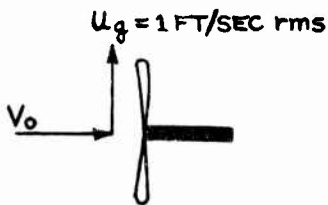
2.5 CONTROL MIXING IN TRANSITION

The use of rotor forces and moments to provide roll control from hover through transition was investigated. Control mixing is simplified and aileron controls and the associated system weight can be eliminated if roll control in cruise flight mode can be accomplished by differential longitudinal cyclic. The rolling moment generated from propeller normal force was calculated by

EFFECTS OF GUST LOADING ON THE MODEL 215 AIRCRAFT

CRUISE MODE
 WEIGHT = 67000 LB.
 M = 0.63
 10000 FT.

VERTICAL GUST

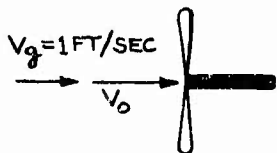


CG "q's" / FT/SEC GUST	
AIRFRAME	ROTOR

.0265

.0112 VERTICAL

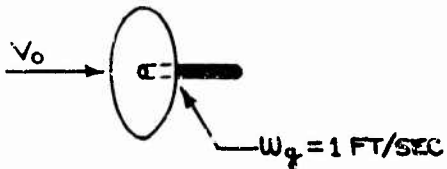
LONGITUDINAL GUST



.00033

.00518 LONGITUDINAL

LATERAL GUST

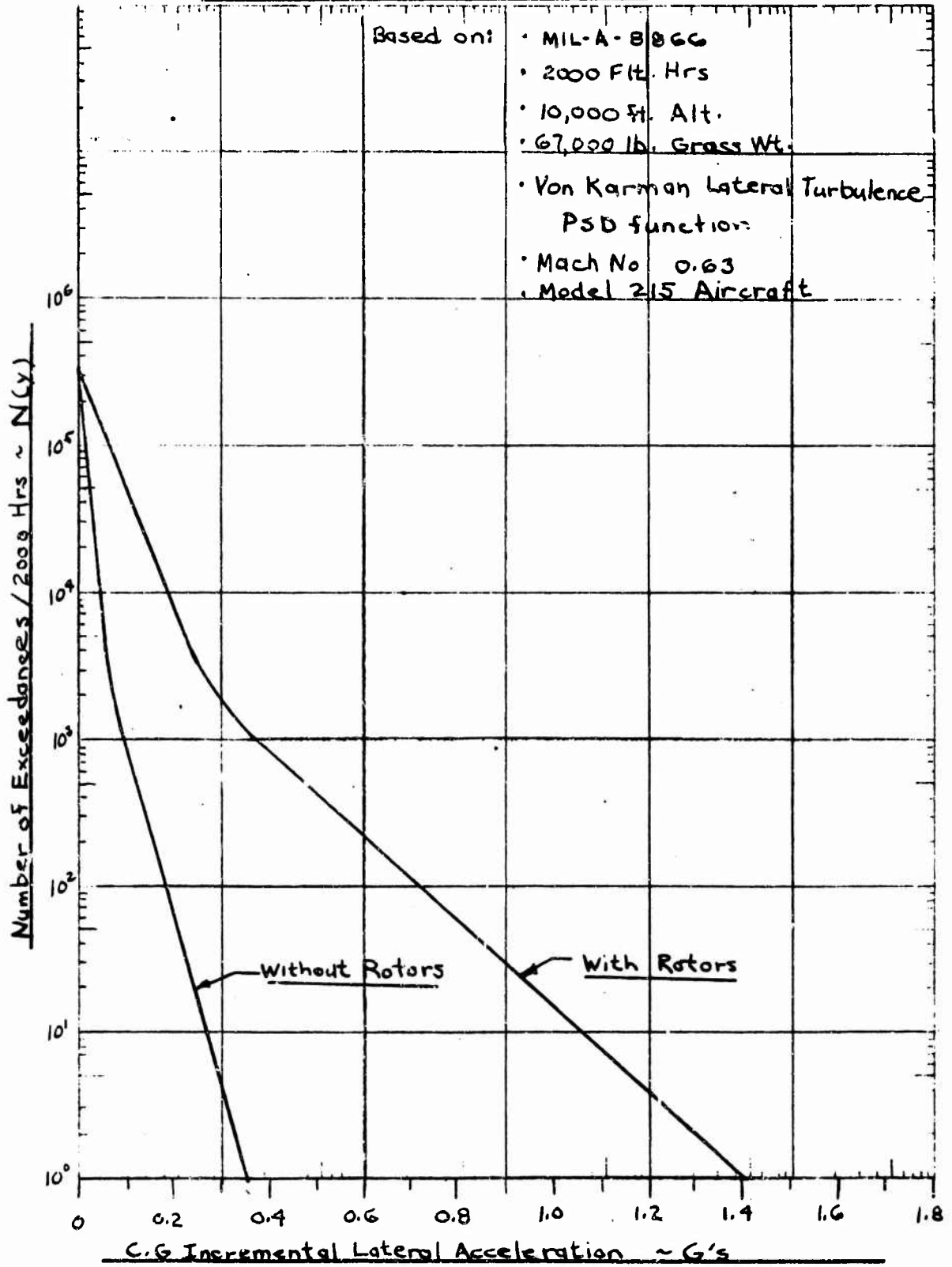


.0036

.0112 LATERAL

EFFECT OF TURBULENCE ENCOUNTER ON THE MODEL 215

AIRCRAFT IN THE CRUISE MODE



VIII-21

FIGURE VIII-13

using the methods of Reference VIII-7. As can be seen from Figure 14, adequate roll control power is available in hovering and in the cruise flight mode. Further analyses are needed to investigate other flight conditions such as the transition flight corridor for restraints to the use of rotor controls.

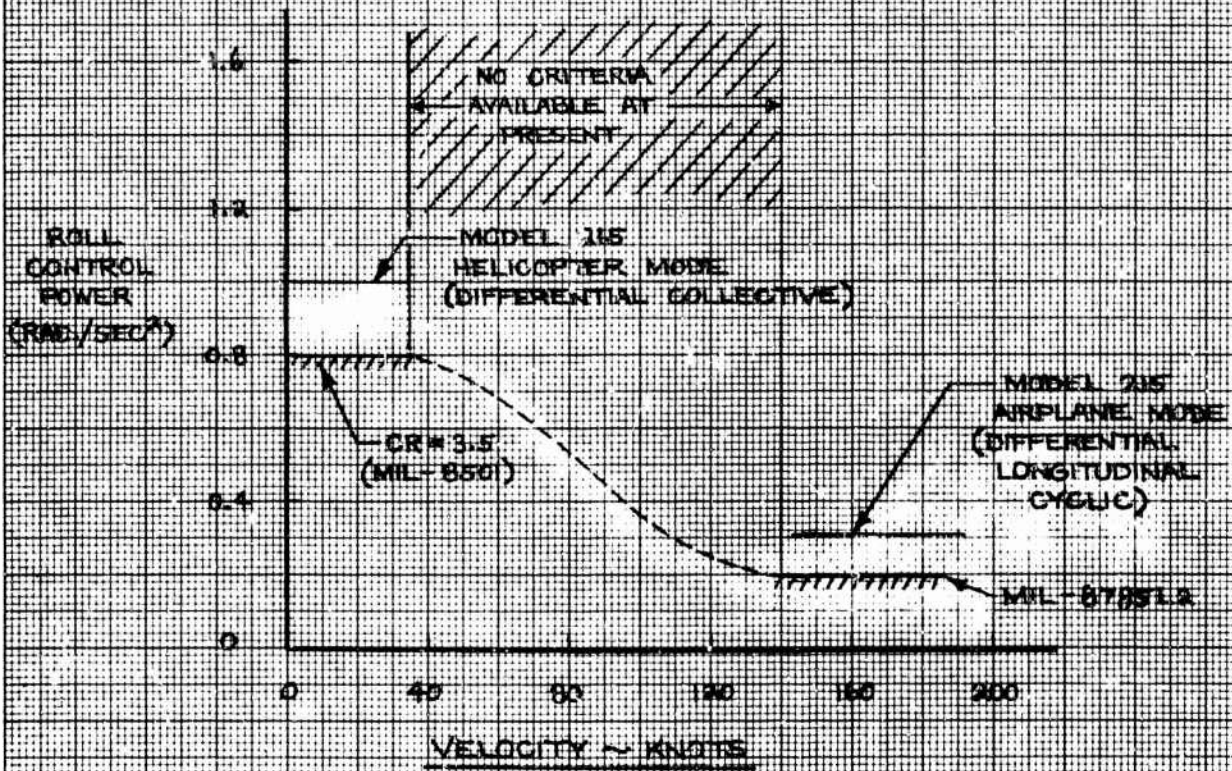
2.6 POWER MANAGEMENT SYSTEM

The thrust management system provides constant speed operation by governing rotor blade collective pitch. Due to the cross shafting, constant speed governing in flight is provided by a single governor controlling the pitch of both rotors. A second governor (redundant) is provided for fail-operational use at the pilot's discretion. A system schematic is shown in Figure VIII-15. The master governor provides input signals to both rotors for pitch changes. The redundant governor is passive and is only brought into operation in the event of a failure. Overspeeding is prevented by automatic switching using an independent RPM pickup to provide a monitor source.

During helicopter operation, governing is provided by the engine fuel controls to provide constant RPM. The propeller governors are locked out so that the pilot and SAS system is given direct mechanical blade authority. The pilot can feed differential collective pitch to each rotor for roll control while the fuel control maintains RPM by increasing or decreasing fuel flow. Power management to provide a balance between the four engines involved requires further study.

DR. BY J. BENDO
(7/22/70)

ROLL CONTROL MIXING IN TRANSITION



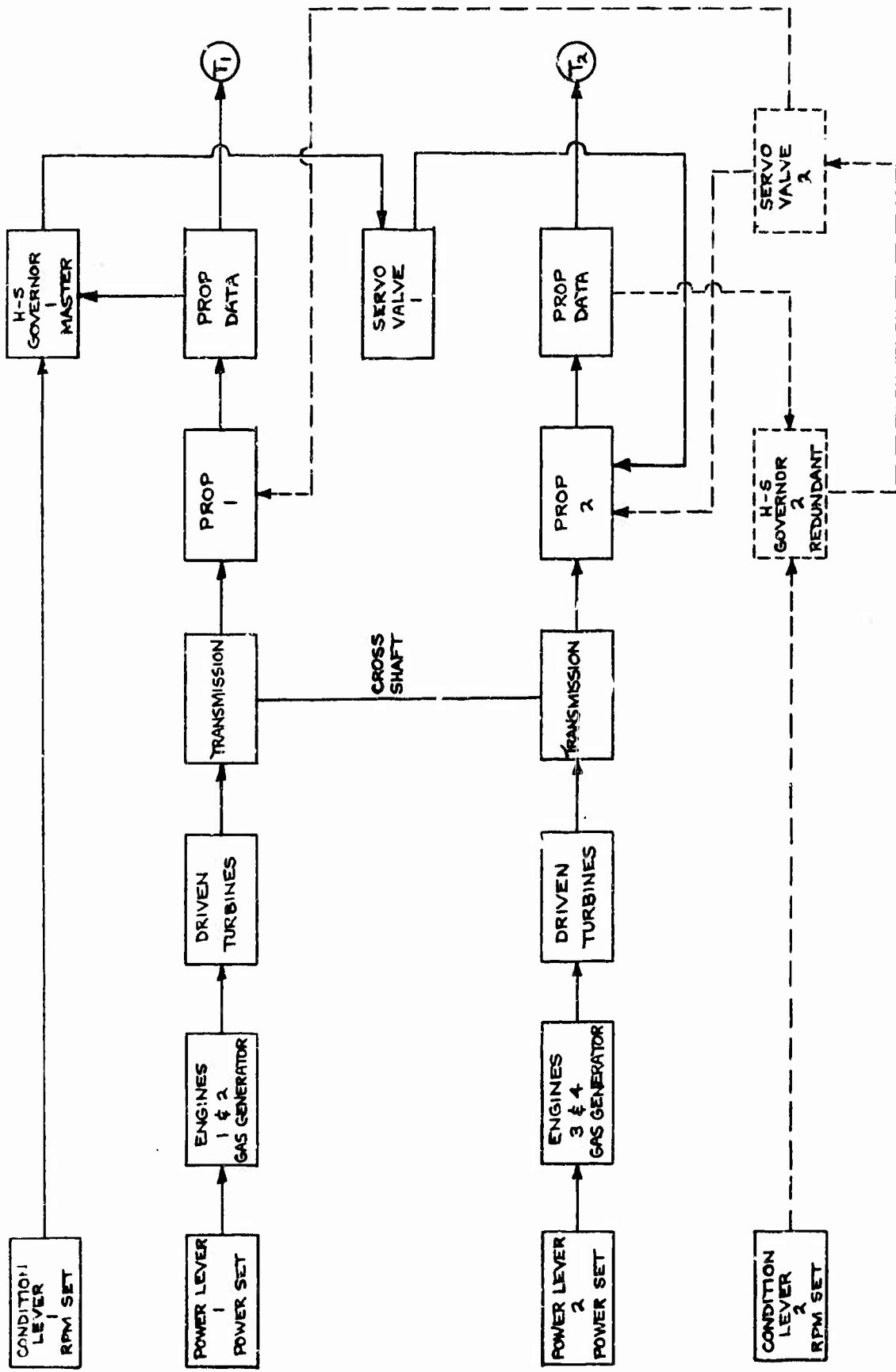
EUGENE DIETZGEN CO.
MADE IN U. S. A.

NO. 340R-MP DIETZGEN GRAPH PAPER
MILLIMETER

FIGURE VIII-14

DR. BY J. BEINDG
(7/24/76)

MODEL 215 POWER MANAGEMENT SYSTEM



VIII-24

FIGURE VIII-15

2.7 WING TORSIONAL EFFECTS

As has been shown in Section VI, control moments in yaw can produce 3.5° of wing torsion. During certain high g maneuvers, the effects of wing torsion on flying qualities and control must be considered. Although no wing stiffness criteria are specifically mentioned in Reference VIII-2, the items to be considered are as follows:

- a. Short period natural frequency
- b. Wing transient twisting
- c. Control coupling
- d. Loop stability with SAS
- e. Ground operations

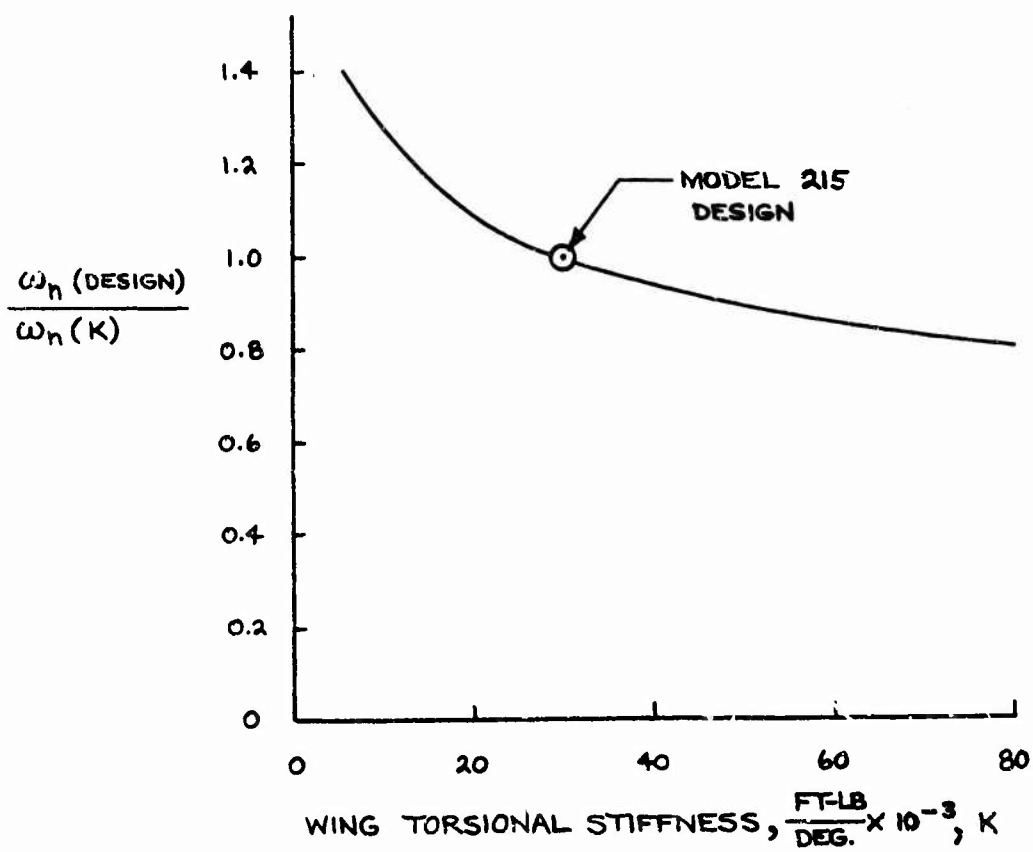
Wing transient twisting causes changes in wing and rotor angle of attack which in turn affect not only aircraft stability derivatives but also flying qualities. Wing twisting also affects flying qualities through damping. The low sensitivity of the short period mode to wing torsional stiffness is shown in Figure VIII-16.

2.8 ROTOR FEEDBACK SYSTEM

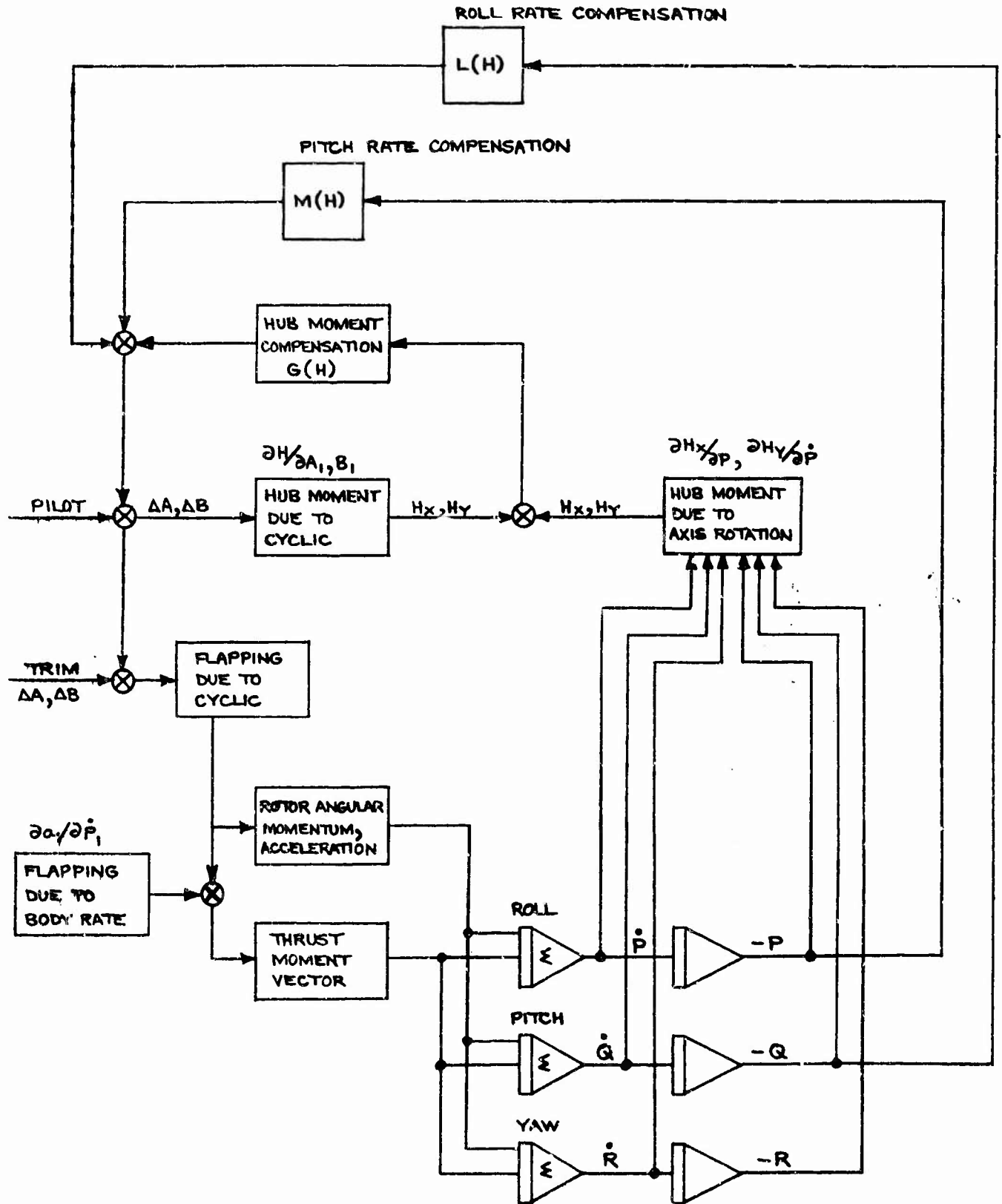
The requirements for the design of the rotor feedback system are discussed in Reference I-1. Based on these requirements, an analog computer simulation shown in Figure VIII-17 was developed. The analog model considers the first rotor flapping mode and rigid airframe rotational degrees of freedom. The model includes an aircraft rate and hub moment feedback system.

This model will be used in Phase III to determine feedback gain schedules and mixing of rate and hub moment feedbacks.

EFFECT OF WING TORSION ON
SHORT PERIOD FREQUENCY



ROTOR ANALOG SCHEMATIC



3. AEROELASTIC STABILITY

An analysis of the aeroelastic stability of the baseline Model 215 aircraft has been made to define those areas which could need increased stiffening or mass balancing. The dynamic properties of Model 215 have changed from the preliminary values shown in Table VII-8, Reference I-1, especially in the areas of wing frequencies and rotor blade characteristics. The new values developed from the detailed designs in this report are shown in Table VIII-2. All calculations in this report are based on the values in Table VIII-2 and supercede those in Reference I-1. It was found that the baseline aircraft is adequately stable in all of the dynamic modes involved.

3.1 WHIRL FLUTTER

The aircraft has been analyzed assuming the rotor feedback system is inoperative. Results shown in Figure VIII-18 indicate that the aircraft will have greater than the required 3% of critical damping in all important flutter and vibration modes up to V_L (450 knots). In addition it is seen that the whirl flutter mode does not go unstable until 538 knots, which is well over the $1.15 \times V_L = 517$ knots.

Adequate stability margins at low power settings with the rotor feedback system inoperative is shown by Figure VIII-19. The results shown supercede the results appearing in Figure VII-12 of Reference I-1 which were wrong due to calculation errors.

Parameters of the aircraft used in this analysis are listed in Table VIII-2. Wing natural frequencies for the normal and damaged wing are given in Table VIII-3. A sketch of the damage assumed is shown in Figure VIII-20. This damage would result in the stiffness losses shown in Figure VIII-21.

The analysis of the M-215 wing (using computer program D-46) was performed to obtain the wing-nacelle uncoupled frequencies and mode shapes. These frequencies and mode shapes along with rotor/nacelle properties were input into the C-26 prop/whirl program which determines the stability characteristics of the system. Several parametric

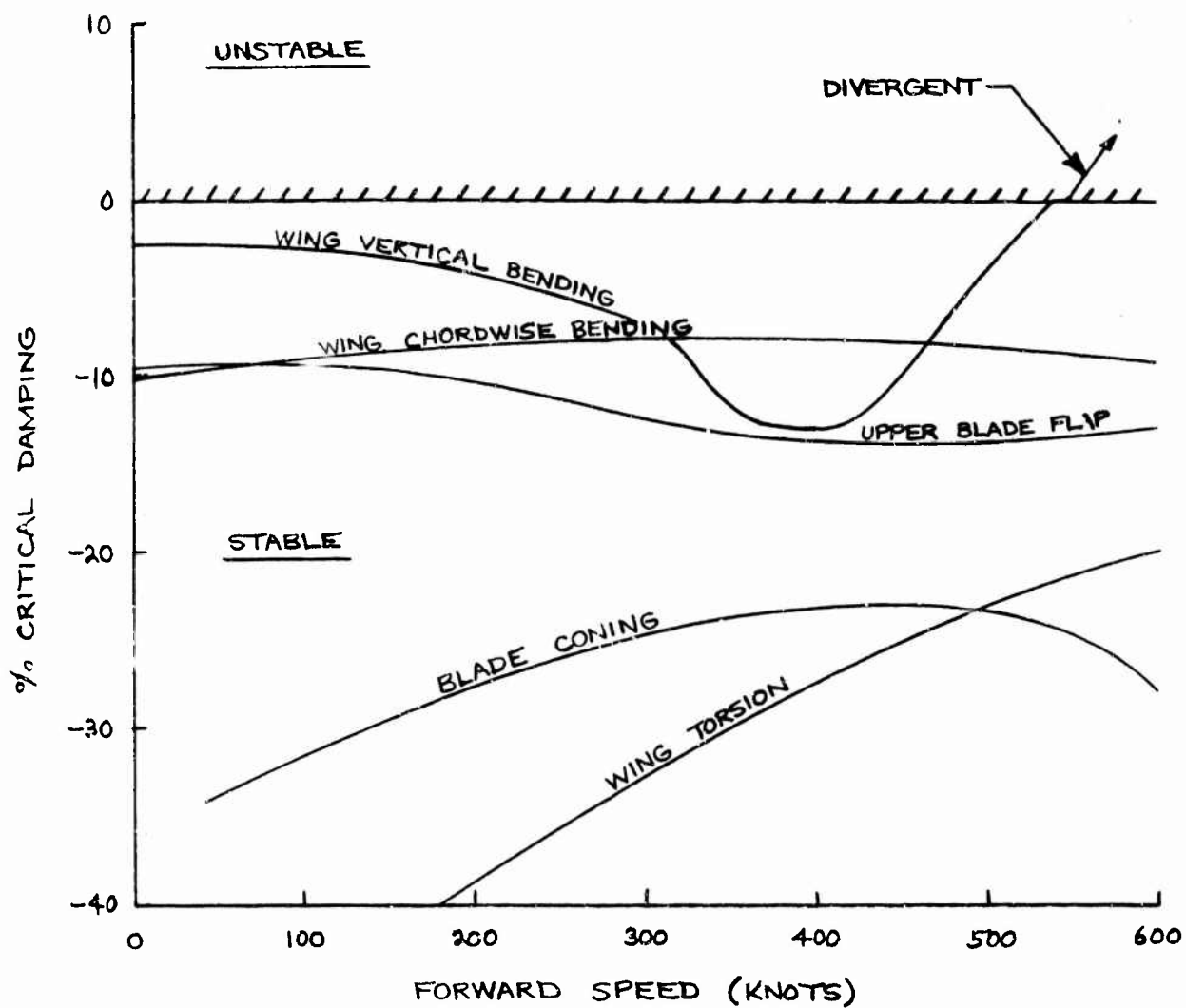


FIGURE VIII-18. DAMPING OF 215 AIRCRAFT WHIRL FLUTTER MODES AT SEA LEVEL WITH 267 RPM.

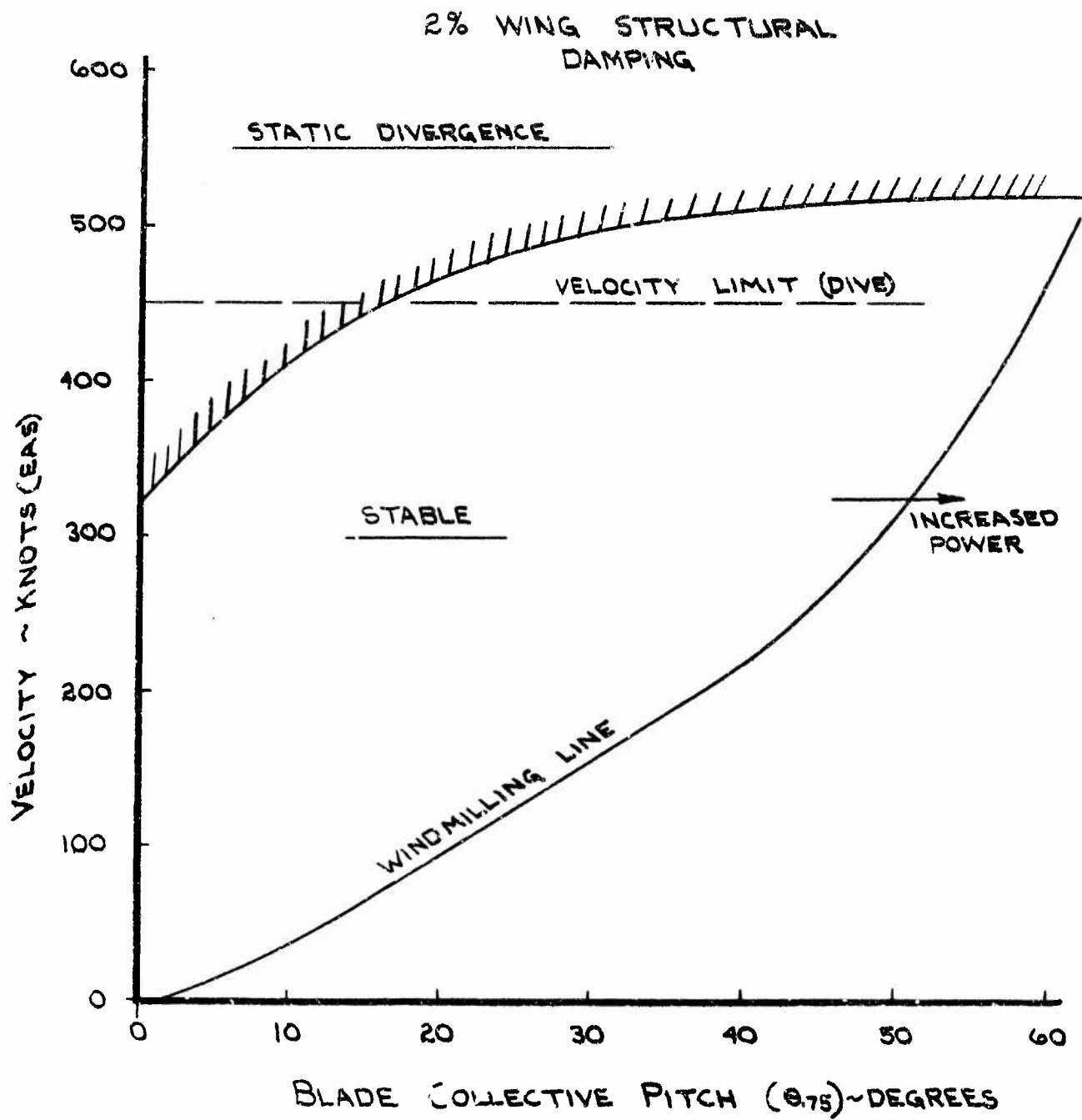


FIGURE VIII-19 : ADEQUATE STABILITY MARGINS AT LOW POWER SETTINGS WITH CYCLIC FREEDOM SYSTEM INOPERATIVE.

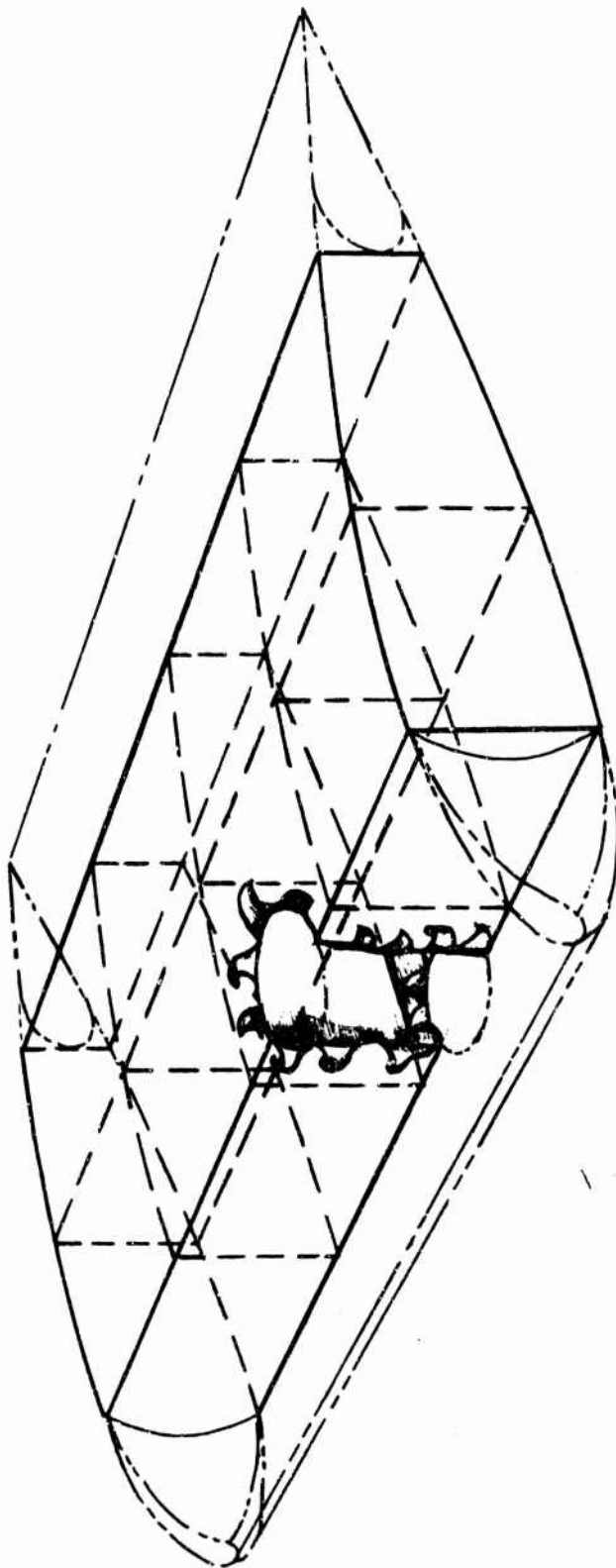


FIGURE VIII-60. SKETCH OF DAMAGE TO WING CONSIDERED
IN WHIRL FLUTTER ANALYSIS.

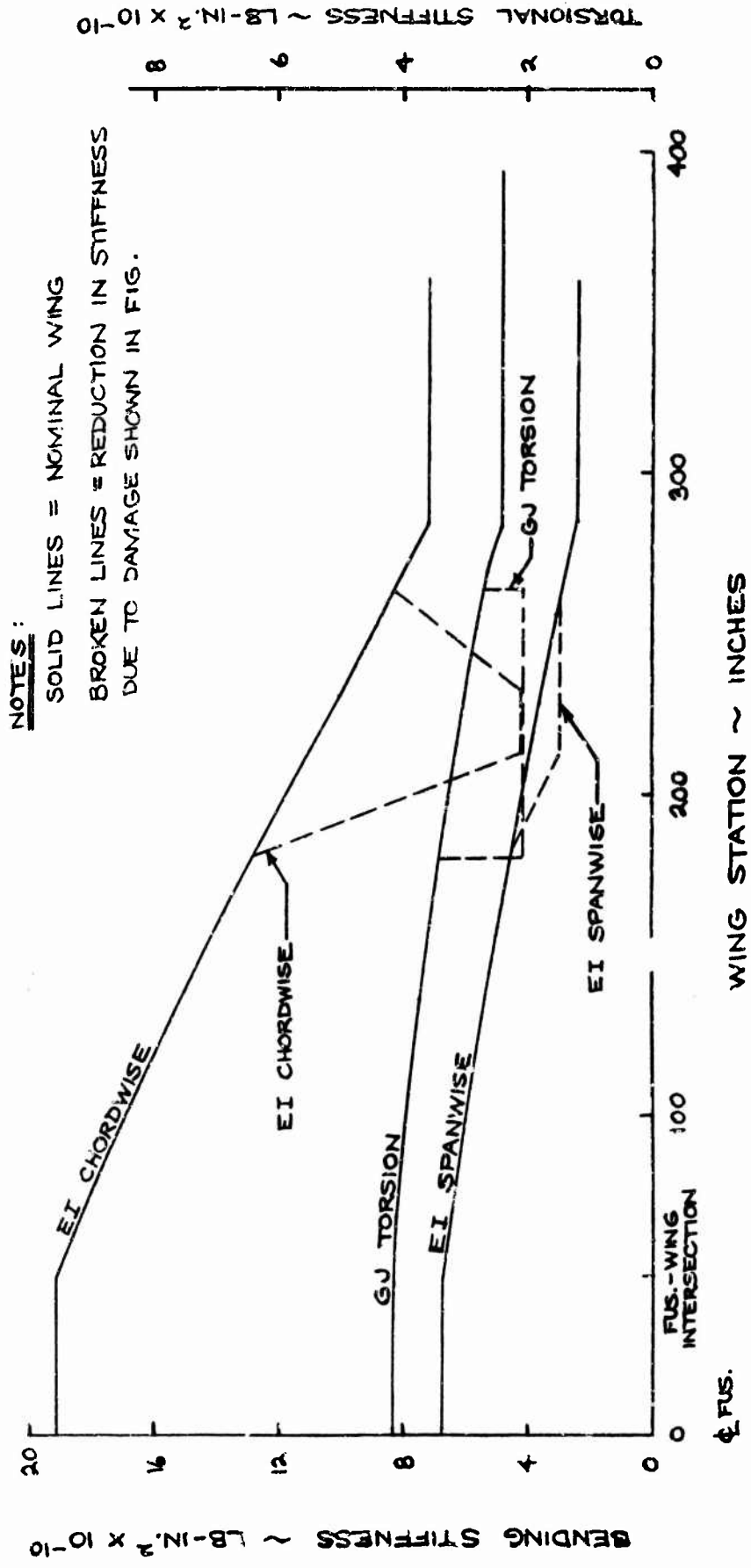


FIGURE VIII-21. LOSS OF WING STIFFNESS OF DAMAGED WING.

TABLE VIII-2

AIRCRAFT GEOMETRIC PARAMETERS USED IN PROP WHIRL ANALYSIS

<u>SYMBOL</u>	<u>DESCRIPTION</u>	<u>VALUE</u>	<u>UNITS</u>
R	Radius of rotor	330.	inches
n	Number of blades	3.	N.D.
M_1	1st moment of inertia - one blade	110.69	lb-sec ²
I_b	Blade flap inertia - one blade	21711.0	lb-sec ² -in.
X_c	Blade cutout to rotor radius ratio (rc/R)	.075	N.D.
θ_{t75}	Blade twist at 75% radius	-35.5	deg.
C_M	Blade mean chord	36.75	inches
a	Lift slope coefficient	5.73	1/rad.
h	Distance between nacelle pivot point and center of rotation of rotor	112.0	inches
λ	Distance between nacelle center-line and modal effective wing root	207.5	inches
e	Distance between nacelle pivot and rotor/nacelle C.G.	67.4	inches
I_X	Nacelle pitching inertia about pivot (including rotor wt. assumed lumped at C.R.)	139570.	lb-sec ² -in
W_n	Weight of nacelle plus rotor	11097.	lb
Ω	Rotor speed - cruise	207	RPM
V	Velocity cruise	350	knots

TABLE VIII-3
UNCOUPLED FREE-FREE WING MODE NATURAL
FREQUENCIES OF THE 215 AIRCRAFT

<u>SYMBOL</u>	<u>DESCRIPTION</u>	<u>VALUE</u>	<u>UNITS</u>
	Wing Frequencies (including mass of normal fuel)		
W_Y	Chordwise, Normal	2.4	CPS
W_P	Torsion, Normal	3.5	CPS
W_V	Vertical, Normal	1.4	CPS
W_Y	Chordwise, Damaged	2.2	CPS
W_P	Torsion, Damaged	3.5	CPS
W_V	Vertical, Damaged	1.4	CPS

- NOTES: 1. Mass of normal fuel is included in wing
2. Calculations of damaged wing frequencies was based on projectile penetration at Station 222 in Area of Front Spar and Extended Aft through Forward Torque Box.

studies were made including the varying of wing pitch and yaw frequencies, rotor speed, forward speed and blade pitch angle.

A parametric study of the effects of wing chordwise bending variations illustrates the effect of the wing damage shown in Figure VIII-20 on whirl flutter. This damage causes about a 10% change in the wing chordwise bending frequency but no other significant changes as shown in Table VIII-3. Results of such a study are shown for a constant airspeed in Figure VIII-22. These results show that the damaged wing is slightly closer to the region of whirl flutter. Loss in damping of the whirl flutter modes has not been calculated but would be expected to be small.

3.2 AIR/GROUND RESONANCE

The frequency spectrum of the three blade flap modes and the three blade lag modes is shown as a function of rotor speed in Figure VIII-23. Bands of wing-nacelle bending frequencies have been superimposed for reference. The lower frequency boundary of each band represents the cantilever wing frequency and the upper frequency boundary and the free-free symmetric wing-nacelle frequency. Results shown indicate the following:

- a. There is no coalescence of the lower blade lag mode with any of the wing modes over the operating rotor speed range which indicates that energy will not be fed into the system and no instability will be produced.
- b. Near cruise rotor speed there can be coupling between the upper blade flap mode, the upper blade lag mode and the wing torsional freedoms. This should not produce an

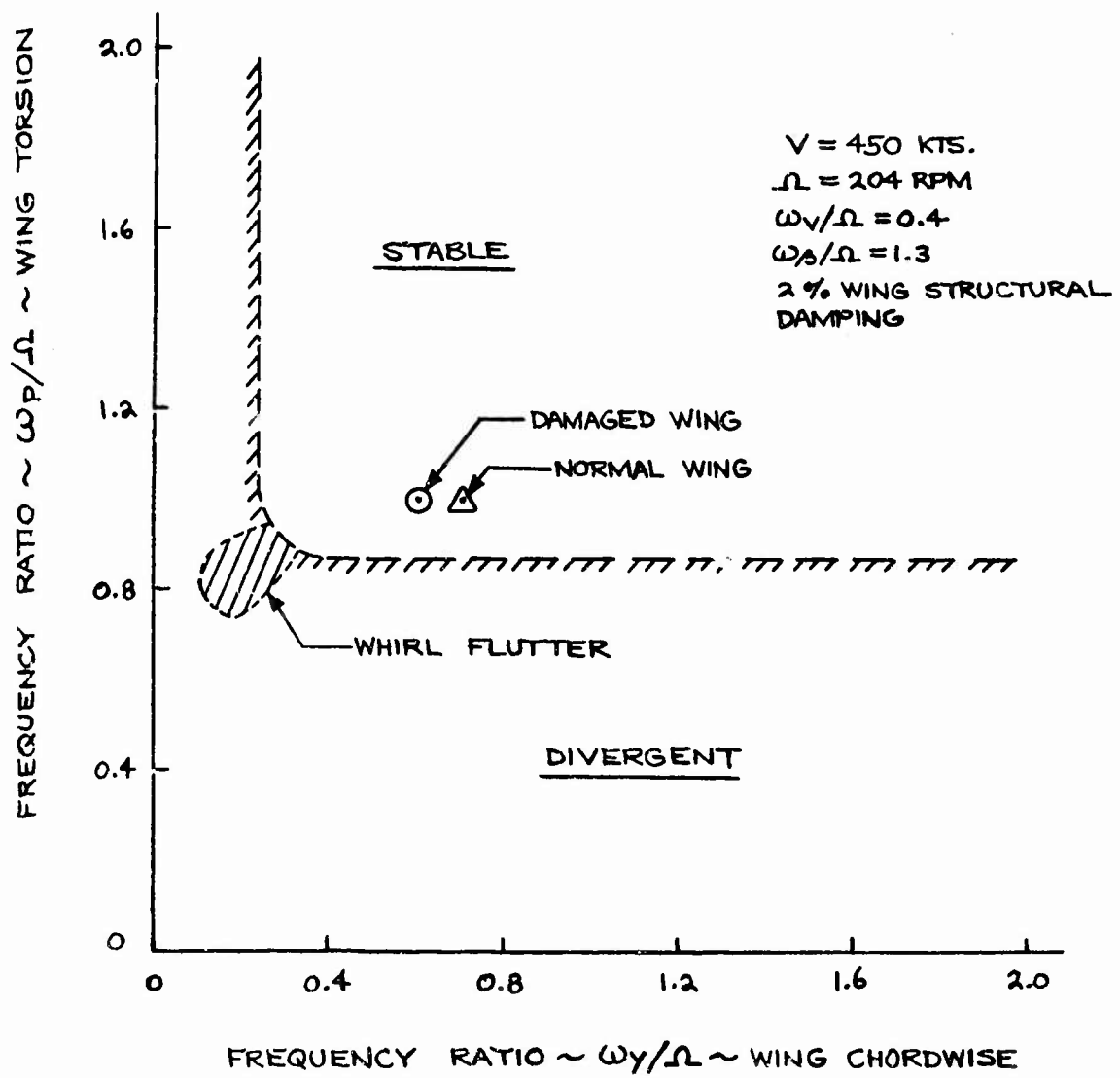


FIGURE VIII-22. WING DAMAGE SLIGHTLY INCREASES TENDENCY TO WHIRL FLUTTER.

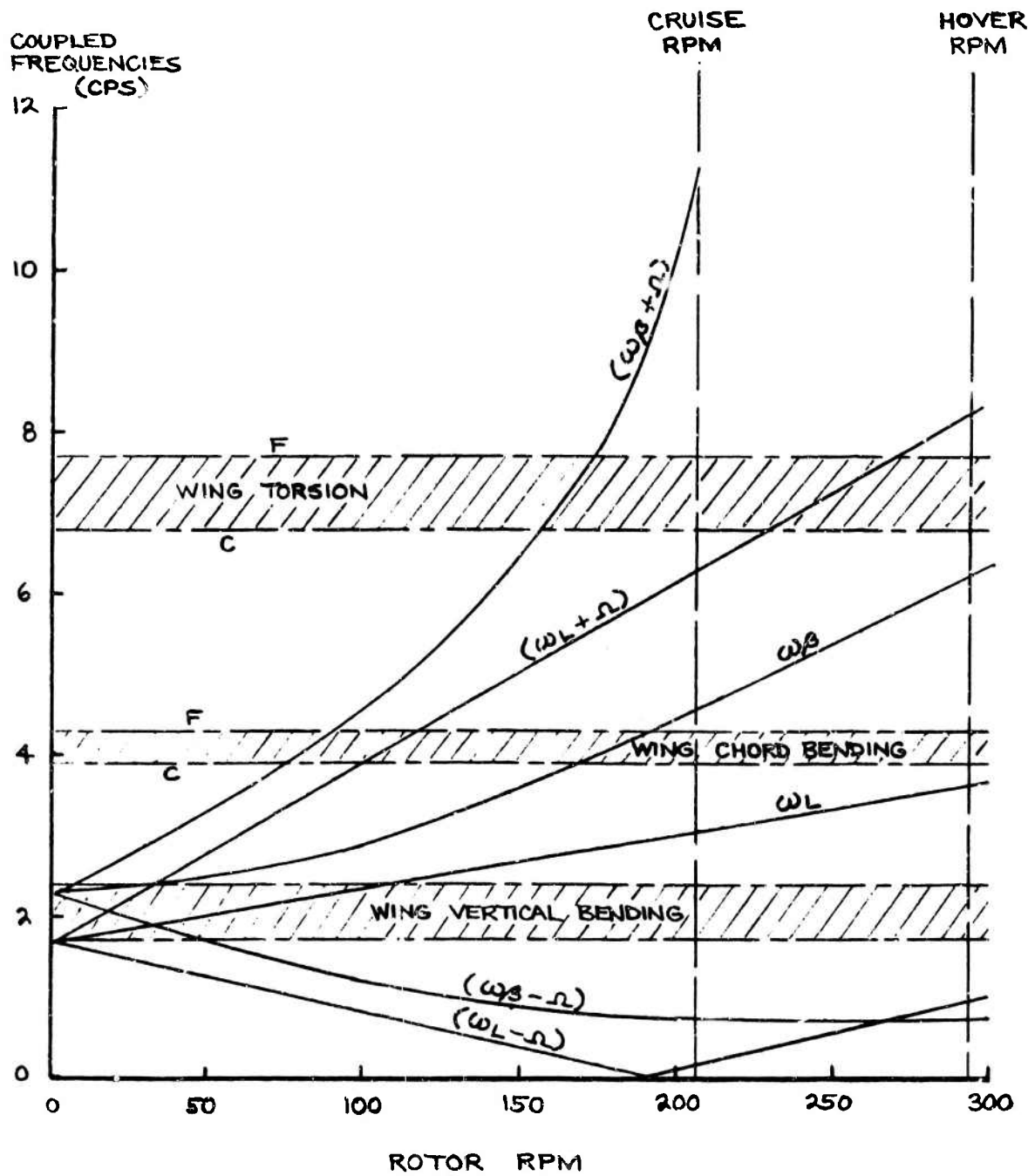


FIGURE VIII-23 . FREQUENCY SPECTRUM OF ROTOR AIR/GROUND RESONANCE MODES RELATIVE TO UNCOUPLED WING MODES . VIII-38

instability, but could adversely affect the aircraft response and blade loads. This area needs a thorough investigation. It may be necessary to adjust the wing torsional frequency such that this coupling occurs at an RPM further removed from steady operating speeds.

The baseline design is believed to be adequately stable from air/ground resonance.

3.3 CLASSICAL FLUTTER

Properly mass balanced structures are not prone to the coupled vertical bending - torsional oscillations of classical flutter. The wing analysis shows freedom from such flutter to speeds in excess of 600 knots.

The rotor blade was found, by conservative calculations, to be free of classical flutter at all rotor speeds up to 1.25 times the design speed for all aircraft speeds up to 1.15 the maximum aircraft speed.

3.4 STALL FLUTTER

The rotor blades of a tilt rotor aircraft are susceptible to stall flutter in near hover flight. Prediction of this phenomena is presently based on empirical techniques. Evaluation of the 215 design is presented previously.

3.5 PITCH-LAG INSTABILITY

A linear two-degree of freedom blade flap and lag analysis was used to study this stability. The results of the analysis showed stability for normal operating conditions with approximately 2% critical damping in the blade lag mode for a pitch-lag coupling value of 1.0. This analysis involved several simplifying assumptions and the results need verifying with more sophisticated methods of analysis soon to be available. The matched-stiffness root flexure of the 215 blade design is expected to give much smaller coupling so this design is believed adequate.

4. VIBRATION SUPPRESSION CONSIDERATIONS

The need for tuning of the aircraft structure to achieve a vibration level of 0.05g in the occupied areas has been considered. The analysis of the wing dynamics has shown the strength designed wing to act as a vibration isolator for 3 per rev excitations. It therefore appears that no weight penalty needs to be taken for vibration tuning on the 215 aircraft.

Analysis of vibration considered a high speed transition condition which is believed to be critical. This condition causes the largest edgewise flow component and is expected from helicopter experience to cause the largest vibration. As shown in the Phase I analysis the empirical vibration prediction would indicate a vibration level of 0.106g for this condition. In the present study a rotor loads analysis was made including wing lift interference but a 3/rev excitation of only 0.013g at the rotor hub was predicted. This result is lower than expected but predicted vibration levels

characteristically neglect the small variations between blades, etc, and therefore usually show low vibration predictions. The important result of this analysis is the isolation of the excitation from the fuselage. As shown in Figure VIII-24 the acceleration of the rotor and nacelle is greater than the rigid response to the excitation. Acceleration at the wing root is about half of the rigid response indicating that even if the excitation is as large as the empirical value, the design will meet the objective without special tuning.

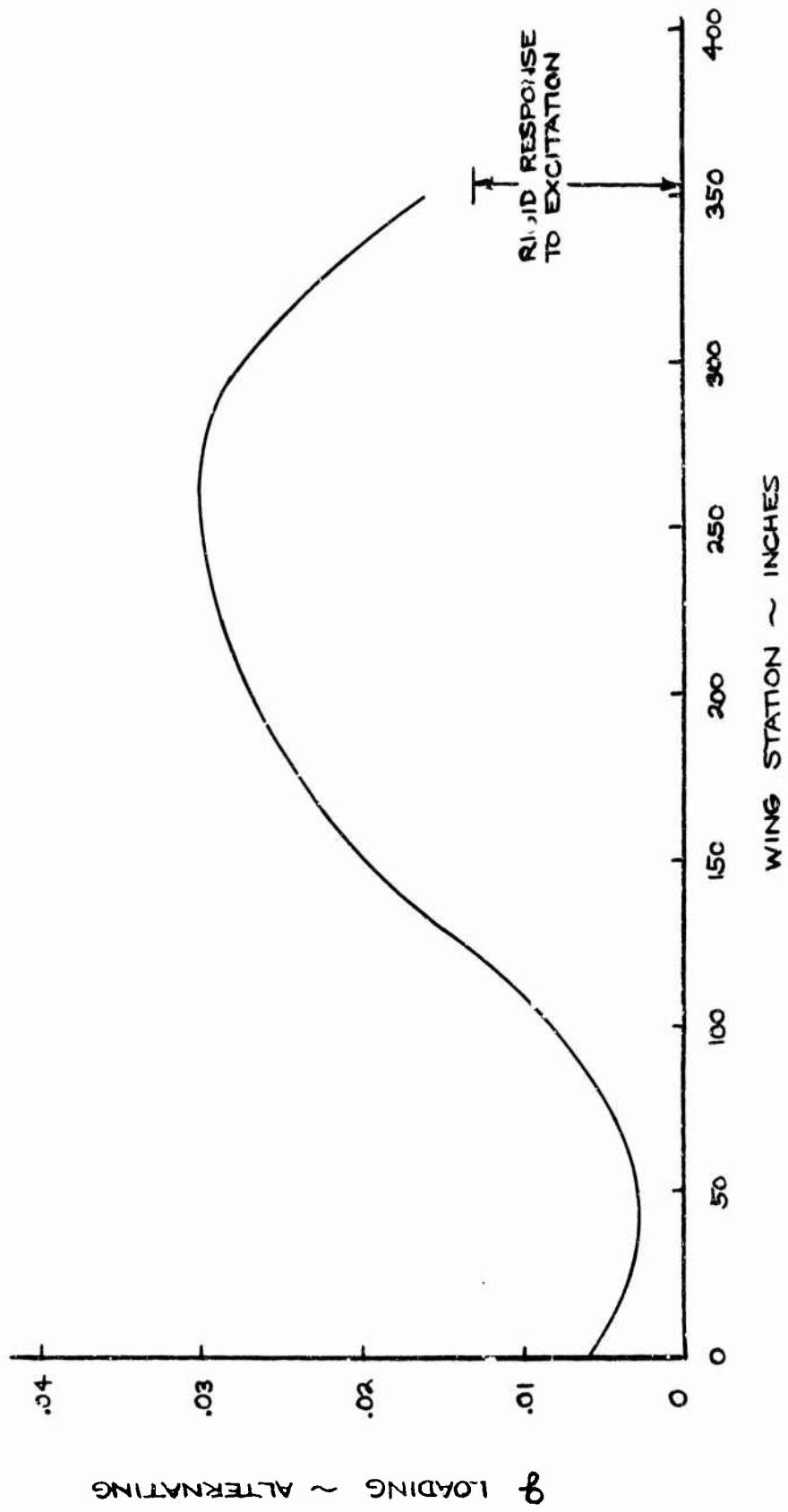


FIGURE VIII-24. VIBRATION ISOLATION PROVIDED BY 215 WING DESIGN FOR 3/REV ROTOR FORCES.

REFERENCES

- I-1 D. A. Richardson and J. Liiva, Configuration Design Analysis of a Prop/Rotor Aircraft, AFFDL-TR-70-44, April 1970.
- I-2 Proposal to Determine Design Criteria and Demonstrate Technology of a Prop/Rotor Aircraft, Boeing Report D8-2367-1, February 1969.
- III-1 Boeing-Vertol Structural Design Manual
- III-2 Boeing-Vertol Report SRR-7
- IV-1 R. Baier and J. Mack, Design and Test Evaluation of a Supercritical Speed Shaft, USAAVLABS TR66-49, June 1966.
- IV-2 Proceedings of the Fifth Weight Prediction Workshop for Advanced Aerospace Design Projects, Paper No. V, Estimation of Wing Non-Optimum and Secondary Structure Weight by R. W. Patterson, 20 October 1969.
- VI-1 U.S. Army Transportation Research Command, Wind Tunnel Tests of an Optimized Matched-Stiffness Rigid Rotor, TRECOM TR64-56, November 1964.
- VI-2 Ward, J.F., Exploratory Flight Investigation and Analysis of Structural Loads Encountered by a Helicopter Hingeless Rotor System, NASA TN D-3676, November 1966.
- VI-3 G. Miliziano and R. Sanford, Results of Model 160 Tilt Rotor Blade Structural Analysis Accomplished in 1969. Boeing Document D160-10004-1, May 1970.
- VIII-1 Chalk, C. R., et al., A Proposed Military Specification for V/STOL Flying Qualities, Cornell Aero. Lab., November 1969 (R-3)
- VIII-2 Anon, Military Specification, Flying Qualities of Piloted Airplanes, MIL-F-8785B, 1969.
- VIII-3 Davis, J. M., Flight Control Design Objectives and Criteria, Boeing Vertol Report D8-2334-1, December 1968.

REFERENCES (continued)

- VIII-4 Anon, Military Specification, Helicopter Handling Qualities, General Specification For, MILH-8501A
- VIII-5 Bird, B. J., et al, A Stability and Control Prediction Method for Helicopters and Stoppable Rotor Aircraft, AFFDL TR-69-123, February 1970.
- VIII-6 Anon, AFSC Design Handbook, Series 2-0, AFSC DH2-2, May 1969.
- VIII-7 Magee, J. F. and Pruyn, R. R., Prediction of the Stability Derivatives of Large Flexible Prop/Rotors By a Simplified Analysis, Paper presented at the 26th Annual National Forum, AHS-443, June 1970.
- VIII-8 Anon, Military Specification, Airplane Strength and Rigidity Reliability Requirements, Repeated Loads, and Fatigue, MIL-A-886C, May 1960.

APPENDIX 1

INTEGRAL SPAR INSPECTION SYSTEM (ISIS)

An inspection system has been developed to detect cracks in rotor blade spars prior to catastrophic failure. The system was developed primarily for the CH-46 blade spar; however, the ISIS may be utilized to monitor any critically stressed structural member. The system is a visual, ground inspectable indicating system which provides an early warning of impending catastrophic failure.

The system consists of a mylar-aluminum laminate liner with a dacron bleeder cloth which contours the member to be monitored as shown in Figure 1. The periphery of the liner/structural member interface is sealed against leakage.

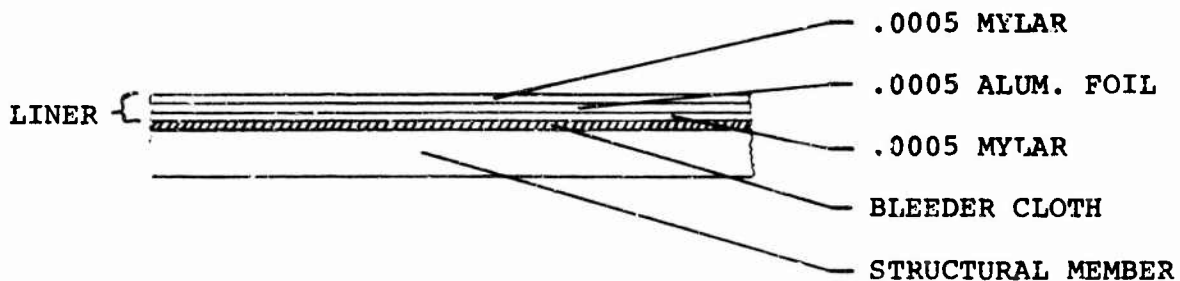


FIGURE 1

DESCRIPTION OF ISIS

A vacuum is drawn between the liner and the structural member and monitored by a pressure indication device to sense a change in the vacuum level caused by air leaking into the vacuum chamber through cracks or holes in the structural member.

Figure 2 represents the indicator design concept. If a crack developed in the structural member being monitored, the pressure between the liner and the structural member and in the pressure sensor evacuating chamber around the bellows increases above the reference pressure inside the bellows. The bellows will contract until the visual indicator, connected to the bellows, bottoms on its stop. This indicator mechanism is held in position by the stop after a crack develops in the structural member and the system loses its vacuum.

The ISIS indicator incorporates a push-to-test feature. Therefore, the operation of the system can be checked by pushing in the plunger attached to the visual indicator. If there has been no crack in the spar and the system is operating, the plunger will be forced back to its "safe" position. If there has been a failure in the system the plunger will remain depressed.

Inasmuch as the system depends on differential pressure between the liner/structural member cavity and the atmosphere, it is desirable to evacuate the interface to the lowest practical pressure level. It was determined that 1 psia be the desired level. Although the mylar/aluminum liner permeability rate would result in a leakage of 1.0 psi per year, a safety margin allows for permeability losses up to a delta of 2 psi. An additional pressure increase could result due to solar heating. Taking these considerations into account, the indicator is set to 4.0 psia for the start of an unsafe indication. This pressure is called the reference pressure and is sealed into the bellows. When the absolute pressure within the liner/structural member cavity reaches 4.0 psia, the indicator begins to move. The full unsafe position will be reached when the cavity pressure reaches 5.5 psia. The setting of this level is predicated on always maintaining a positive pressure differential.

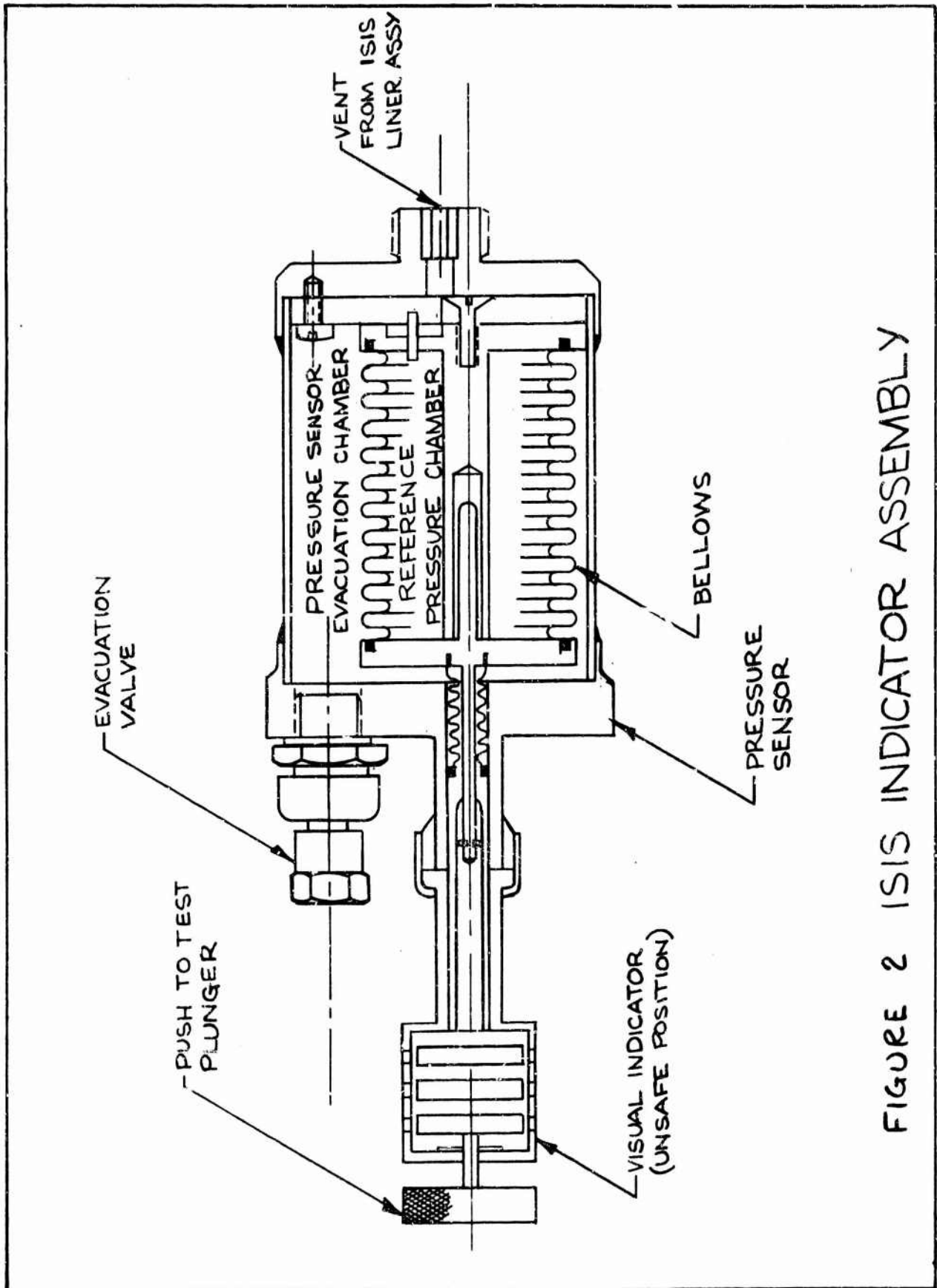


FIGURE 2 ISIS INDICATOR ASSEMBLY

APPENDIX 2

DESCRIPTION OF COMPUTER PROGRAMS

The Boeing-Vertol developed computer programs used in the Phase II analyses are tabulated in this section. Table B-1 describes the whirl flutter and Divergence Computer Programs, Table B-2 the Vibration and Classical Flutter Programs, Table B-3 the Blade Loads Programs and Table B-4 the Flying Qualities Programs.

TABLE B-I. DESCRIPTION OF PROP WHIRL FLUTTER AND DIVERGENCE COMPUTER PROGRAMS

PROGRAM	DESCRIPTION	COMMENTS
C-27	Nine degrees of freedom treats hingeless rotor blade as 2 coupled flap-lag elastic modes of each blade. Wing-nacelle representation in pitch and yaw is same as C-26. Wing bending is equivalent flapping about pivot point which is coincident with equivalent yaw pivot point.	Increments advance ratio, nacelle pitch, yaw, and wing vertical bending natural frequencies to determine stability boundaries. Time history of hub whirl is in work.

TABLE B-II. DESCRIPTION OF VIBRATION AND CLASSICAL FLUTTER PROGRAMS

D-46, Solution For Eigenvalues and Eigenvectors	The complex aircraft structure is considered as simple structural elements (beam, axial, and skin) meeting at structural nodes. The e stiffness parameters together with the mass distribution provide the program input. The IBM 360 generates a dynamic matrix from the stiffness and mass properties which is solved for natural frequencies and modes.	The solution provides for 2750 structural elements, connecting a maximum of 600 structural nodes. The computer performs a double precision natural frequency and mode solution for 139 degrees of freedom.
---	--	--

TABLE B-II. (Continued)

PROGRAM	DESCRIPTION	COMMENTS
D-96, Forced Response	The damped forced response of the aircraft structure is computed utilizing the natural modes computed in the D-46 program. Excitation loads required for the response are obtainable experimentally (model and/or flight testing) or analytically from the L-22 program, which compute rotor hub shaking forces and moment.	The solution provides for 30 modes each having 139 degrees of freedom and structural damping variation between modes.

TABLE B-III. DESCRIPTION OF BLADE LOADS PROGRAMS

TYPE	PROGRAM	DESCRIPTION	COMMENTS
Rotor Blade Analysis	L-01	Computes the natural frequencies and mode shapes for the uncoupled flap bending, chord bending and torsion-free vibrations of stationary and rotating wings.	Utilizes the lumped parameter method of analysis employing finite difference equations to relate the dynamic aeroelastic quantities of adjacent wing stations, whose maximum number is fifty.
	L-02	Computes the uncoupled flap bending, chord bending and torsion-forced response of stationary and rotating wings to dynamics and aerodynamic excitations. The results include the steady and vibratory flap bending, chord bending and torsional moments and rotor hub forces and moments.	Utilizes the lumped parameter method of analysis employing finite difference equations to relate the dynamic aeroelastic quantities of adjacent wing stations, whose maximum number is fifty (50).
	L-21	Computes the coupled flap and chord bending, natural frequencies and mode shapes of a highly twisted propeller blade for both pinned and cantilevered root-end boundary conditions.	Utilizes the lumped parameter method of analysis employing finite difference equations to relate the dynamic aeroelastic quantities of adjacent propeller station, whose maximum number is forty (40).

TABLE B-III. (Continued)

TYPE	PROGRAM	DESCRIPTION	COMMENTS
Rotor Blade Analysis	D88	Computes coupled flap bending and torsion and uncoupled chord bending response of rotating wings to dynamic and aerodynamic excitations. The results include the steady and vibratory blade and hubs loads.	Utilizes the lumped parameter method of analysis and hyperbolic section deflections. The maximum number of stations is 15. The program utilizes non-linear, compressible and unsteady aerodynamics.

TABLE B-IV. DESCRIPTION OF FLYING QUALITIES PROGRAMS

PROGRAM	DESCRIPTION	COMMENTS
Y-62, Stability and Control Prediction of Stopable Rotor Aircraft	10 degrees of freedom, computes stability derivations and calculates trim conditions for flight modes from helicopter through transition to cruise in airplane mode.	Analysis includes maneuvers in both accelerated and non-accelerated flight conditions. Methods developed to investigate all control coupling and phasing throughout all flight modes.
SWISH-096, Rotor Analogs Feedback Control System	Considers rigid body aircraft with rotor flapping effects, feed-back loops consider hub moments and body rates.	Includes integration of rotors in solution. Gyro-coupling and thrust inclination effects are simulated.

Unclassified
Security Classification.

DOCUMENT CONTROL DATA - R&D		
<i>(Security classification of title, body of abstract and indexing annotation must be entered when the overall report is classified)</i>		
1. ORIGINATING ACTIVITY (Corporate author) The Boeing Company Vertol Division Philadelphia, Pa.		2a. REPORT SECURITY CLASSIFICATION Unclassified
		2b. GROUP
3. REPORT TITLE Detail Design of Critical Components for a Prop/Rotor Aircraft		
4. DESCRIPTIVE NOTES (Type of report and inclusive dates)		
5. AUTHOR (Last name, first name, initial) Richardson, David A., Liiva, Jaan (NMN), Pruyn, Richard R., et al		
6. REPORT DATE 31 July 1970	7a. TOTAL NO. OF PAGES	7b. NO. OF REFS
8a. CONTRACT OR GRANT NO. F33615-69-C-1570	8a. ORIGINATOR'S REPORT NUMBER(S) D215-10001-1	
b. PROJECT NO.	8b. OTHER REPORT NO(S) (Any other numbers that may be assigned this report)	
c.		
d.		
10. AVAILABILITY/LIMITATION NOTICES This document is subject to special export controls and each transmittal to foreign government or foreign nationals may be made only with prior approval of AFFDL (FDV), Wright-Patterson Air Force Base, Ohio 45433		
11. SUPPLEMENTARY NOTES	12. SPONSORING MILITARY ACTIVITY Air Force Flight Dynamics Laboratory Air Force Systems Command Wright-Patterson Air Force Base, Ohio	
13. ABSTRACT Detail design studies of critical prop/rotor aircraft components are summarized in this interim report as a second phase of the four-phase USAF Contract F33615-69-C-1570. The program objective is to determine design criteria and demonstrate the adequacy of technology by designing a full-scale prop/rotor aircraft and by designing, manufacturing and testing scaled models. Thirty percent of the weight empty components of the aircraft consisting of the wing, nacelle support and tilt mechanism, nacelle truss, prop/rotor hub, controls and blades has been designed in this phase. The weight empty of the aircraft has decreased by one to five percent from the target value established in the Phase I studies. Weight increases in the nacelle and tilting mechanism components were offset by substantial weight decreases in the rotor and hub components. Supporting technology studies in the areas of stability and control and aeroelastic stability requirements are also included. Discussed are the primary control system, rotor feedback system and power management system and aircraft flutter and vibration suppression considerations.		

DD FORM 1473
1 JAN 64

Unclassified
Security Classification

14. KEY WORDS	LINK A		LINK B		LINK C	
	ROLE	WT	ROLE	WT	ROLE	WT
Aircraft Prop/Rotor Tilt Rotor Wing Design Nacelle Design Prop/Rotor Design Prop/Rotor Dynamics Prop/Rotor Flying Qualities						

INSTRUCTIONS

1. **ORIGINATING ACTIVITY:** Enter the name and address of the contractor, subcontractor, grantee, Department of Defense activity or other organization (*corporate author*) issuing the report.

2a. **REPORT SECURITY CLASSIFICATION:** Enter the overall security classification of the report. Indicate whether "Restricted Data" is included. Marking is to be in accordance with appropriate security regulations.

2b. **GROUP:** Automatic downgrading is specified in DoD Directive 5200.10 and Armed Forces Industrial Manual. Enter the group number. Also, when applicable, show that optional markings have been used for Group 3 and Group 4 as authorized.

3. **REPORT TITLE:** Enter the complete report title in all capital letters. Titles in all cases should be unclassified. If a meaningful title cannot be selected without classification, show title classification in all capitals in parenthesis immediately following the title.

4. **DESCRIPTIVE NOTES:** If appropriate, enter the type of report, e.g., interim, progress, summary, annual, or final. Give the inclusive dates when a specific reporting period is covered.

5. **AUTHOR(S):** Enter the name(s) of author(s) as shown on or in the report. Enter last name, first name, middle initial. If military, show rank and branch of service. The name of the principal author is an absolute minimum requirement.

6. **REPORT DATE:** Enter the date of the report as day, month, year, or month, year. If more than one date appears on the report, use date of publication.

7a. **TOTAL NUMBER OF PAGES:** The total page count should follow normal pagination procedures, i.e., enter the number of pages containing information.

7b. **NUMBER OF REFERENCES:** Enter the total number of references cited in the report.

8a. **CONTRACT OR GRANT NUMBER:** If appropriate, enter the applicable number of the contract or grant under which the report was written.

8b, 8c, & 8d. **PROJECT NUMBER:** Enter the appropriate military department identification, such as project number, subproject number, system numbers, task number, etc.

9a. **ORIGINATOR'S REPORT NUMBER(S):** Enter the official report number by which the document will be identified and controlled by the originating activity. This number must be unique to this report.

9b. **OTHER REPORT NUMBER(S):** If the report has been assigned any other report numbers (*either by the originator or by the sponsor*), also enter this number(s).

10. **AVAILABILITY/LIMITATION NOTICES:** Enter any limitations on further dissemination of the report, other than those

imposed by security classification, using standard statements such as:

- (1) "Qualified requesters may obtain copies of this report from DDC."
- (2) "Foreign announcement and dissemination of this report by DDC is not authorized."
- (3) "U. S. Government agencies may obtain copies of this report directly from DDC. Other qualified DDC users shall request through _____."
- (4) "U. S. military agencies may obtain copies of this report directly from DDC. Other qualified users shall request through _____."
- (5) "All distribution of this report is controlled. Qualified DDC users shall request through _____."

If the report has been furnished to the Office of Technical Services, Department of Commerce, for sale to the public, indicate this fact and enter the price, if known.

11. **SUPPLEMENTARY NOTES:** Use for additional explanatory notes.

12. **SPONSORING MILITARY ACTIVITY:** Enter the name of the departmental project office or laboratory sponsoring (*paying for*) the research and development. Include address.

13. **ABSTRACT:** Enter an abstract giving a brief and factual summary of the document indicative of the report, even though it may also appear elsewhere in the body of the technical report. If additional space is required, a continuation sheet shall be attached.

It is highly desirable that the abstract of classified reports be unclassified. Each paragraph of the abstract shall end with an indication of the military security classification of the information in the paragraph, represented as (TS), (S), (C), or (U).

There is no limitation on the length of the abstract. However, the suggested length is from 150 to 225 words.

14. **KEY WORDS:** Key words are technically meaningful terms or short phrases that characterize a report and may be used as index entries for cataloging the report. Key words must be selected so that no security classification is required. Identifiers, such as equipment model designation, trade name, military project code name, geographic location, may be used as key words but will be followed by an indication of technical context. The assignment of links, rules, and weights is optional.